The dynamics of pharmacometrics
to personalize the treatment of inborn bleeding disorders

Michael Emanuel Cloesmeijer

The dynamics of pharmacometrics
to personalize the treatment of inborn bleeding disorders

ACADEMISCH PROEFSCHRIFT

Ter verkrijging van de graad van doctor
aan de Universiteit van Amsterdam
op gezag van de Rector Magnificus
prof. dr. ir. P.P.C.C. Verbeek
ten overstaan van een door het College voor Promoties ingestelde commissie,
in het openbaar te verdedigen in de Aula der Universiteit
op woensdag 18 december 2024, te 14.00 uur

door Michael Emanuel Cloesmeijer
geboren te Rotterdam

Promotiecommissie

Promotores:	prof. dr. R.A.A. Mathôt	AMC-UvA
	prof. dr. M.H. Cnossen	Erasmus Universiteit Rotterdam
Overige leden:	prof. dr. D.J. Touw	Rijksuniversiteit Groningen
	prof. dr. J.G.C. van Hasselt	Universiteit Leiden
	prof. dr. M.G.W. Dijkgraaf	AMC-UvA
	prof. dr. C.J. Fijnvandraat	AMC-UvA
	dr. R.M. van Hest	AMC-UvA
	prof. dr. J.C.M. Meijers	AMC-UvA

Faculteit der Geneeskunde
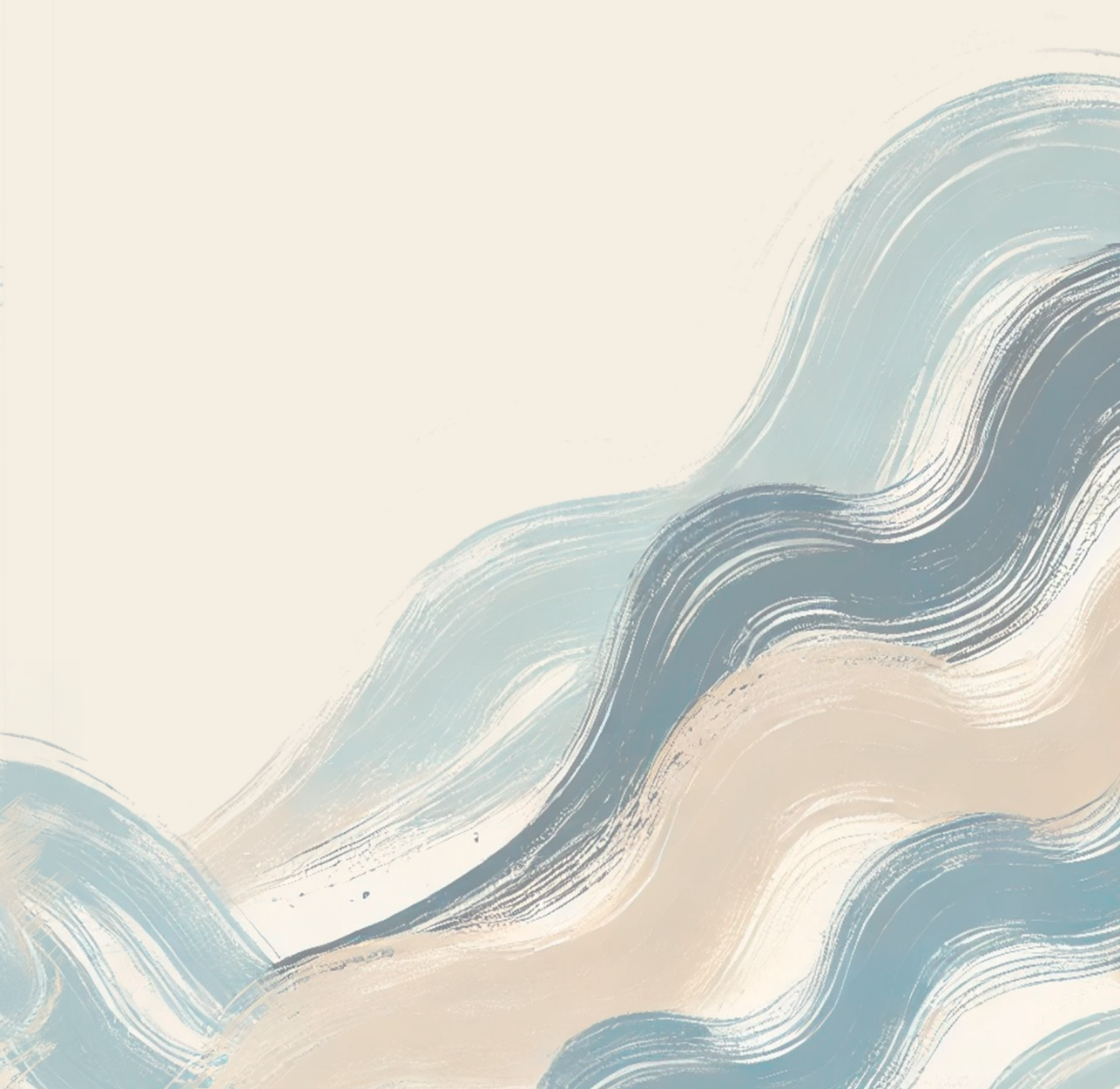
TABLE OF CONTENTS

1
2
3
4
5
6
7
8
9
10

CHAPTER 1

General introduction

GENERAL INTRODUCTION

Inborn bleeding disorders constitute a heterogeneous group of hematological disorders characterized by abnormalities in the coagulation process, leading to prolonged bleeding. Among these bleeding disorders, hemophilia A, hemophilia B, and von Willebrand disease (VWD) are the most well-known [1,2].
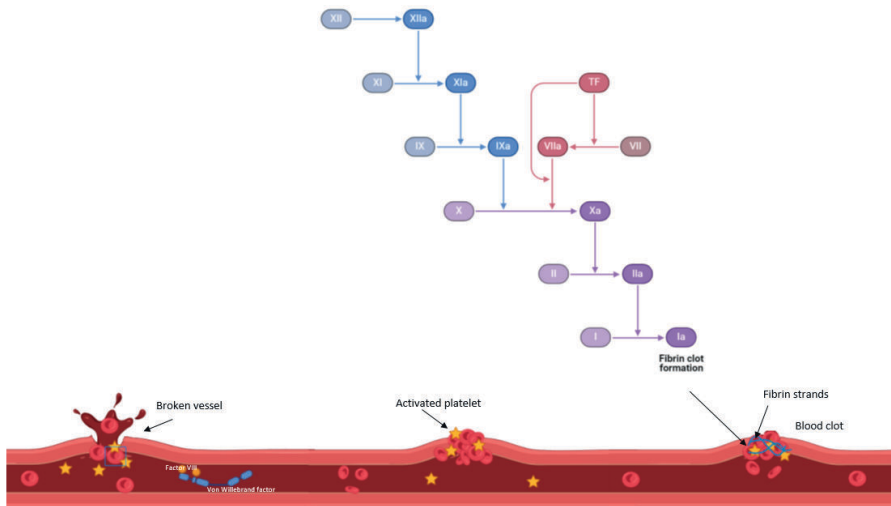
Figure 1. The blood coagulation cascade. This figure illustrates the coagulation cascade and the process of blood clot formation in response to a damaged blood vessel wall. The top section depicts the intrinsic, extrinsic, and common pathways of the coagulation cascade. The intrinsic pathway (blue arrows) involves the activation of Factors XII, XI, IX, and VIII. The extrinsic pathway (red arrows) involves Tissue Factor (TF) and the activation of Factor VII. Both pathways converge at the activation of Factor X (Xa), leading to the common pathway (purple arrows), where thrombin (IIa) converts fibrinogen (I) to fibrin (Ia), forming the hemostatic clot. The bottom section shows the sequence of events at a damaged blood vessel: platelets are activated and accumulate at the injury site, von Willebrand factor stabilizes Factor VIII, and fibrin strands form a meshwork to stabilize the platelet plug, resulting in the stable blood clot. Subsequently, the third phase of the coagulation cascade takes place, known as fibrinolysis (not depicted here). This phase involves the breakdown and removal of the fibrin clot once the blood vessel is sufficiently healed, ensuring that the clot does not persist longer than necessary.

Characteristics of hemophilia A and B

Hemophilia A and B are both inborn bleeding disorders caused by deficiencies of specific coagulation factors. Hemophilia A results from a deficiency or dysfunction of coagulation factor VIII (FVIII), while hemophilia B is caused by a deficiency or dysfunction of coagulation factor IX (FIX). Both are inherited in an X-linked recessive pattern, predominantly affecting males. Prevalence is 17.1 and 3.8 cases per 100,000 males for all severities of hemophilia A and B[3]. Females are disease carriers and diagnosed as patients when factor levels <0.40 IU/ml.[4]

Disease severity is categorized based on residual coagulation factor activity, often but not always with concomitant clinical symptoms. Patients with severe hemophilia (factor levels <0.01 IU/mL) may suffer from spontaneous and frequent often bleeding, whereas moderate (factor levels 0.01 – 0.05 IU/mL) and mild hemophilia (factor levels 0.06 – 0.40 IU/mL) patients mainly bleed after sometimes only minor trauma or medical procedures such as surgery or dental extractions. Bleeding typically occurs in joints and muscles and when treated inadequately may lead to joint deterioration and persistent pain (hemophilic arthropathy). In clinical practice, severity of bleeding is also differentiated into: *mild bleeding* encompassing among others mucocutaneous bleeding, and first symptoms of a joint or muscle bleed, *severe bleeding* among others including joint and muscle bleeds as well as gastrointestinal and psoas muscle bleeds and *life-threatening bleeding* including (suspected or anticipated) cerebral bleeding and (suspected risk of) severe bleeds necessitating long-term treatment. The various types of bleedings require different dosing regimens of factor concentrates and consequently, different peak and trough factor levels for adequate treatment over time.

Characteristics of von Willebrand disease

VWD is the most common hereditary inborn bleeding disorder in humans with an incidence of 10 cases per 100,000 [5]. VWD patients have a quantitative of qualitative defect of von Willebrand factor (VWF). VWF is a large glycoprotein synthesized by endothelial cells and megakaryocytes, which plays a pivotal role in both the primary and secondary hemostasis. The primary hemostasis is the initial phase of blood clot formation. VWF promotes platelet adhesion and aggregation at sites of vascular injury. Additionally during the secondary hemostasis, VWF protects FVIII by acting as a chaperone protein, preventing its rapid clearance from the circulation and enhancing its availability for blood clot formation[2]. VWD is a heterogeneous disorder, categorized into three different types[6]. Type 1 and 3 VWD are caused by the respective partial and complete absence of VWF, whereas type 2 VWD is caused by qualitative defects of VWF. Type 1 is the most prevalent type of VWD, embodying >75% of cases. Normal VWF levels range from 0.50 to 1.50 IU/mL, whereas type 1 VWD patients present with VWF levels below 0.30 IU/mL or below 0.50 IU/mL with abnormal, excessive bleeding. Type 2 VWD is subdivided in type 2A, 2B, 2N, and 2M, each characterized by distinct molecular abnormalities and clinical features.[2] VWD type 2A is marked by a decreased ability of VWF to form large multimers, leading to reduced platelet adhesion. Type 2B involves an enhanced affinity of VWF for platelets, resulting in increased platelet binding and clearance, potentially leading to thrombocytopenia and also presenting with abnormal multimers. VWD type 2N involves a defect in VWF's ability to bind FVIII, especially lowering FVIII levels in the circulation. Type 2M is characterized by a defect in VWF function due to impaired binding to platelets without significant alterations in VWF levels and normal multimers. Type

3 VWD is the most severe form, characterized by a complete absence of VWF leading to a severe bleeding tendency similar to severe hemophilia[7]. However, type 3 VWD is also the most rare type of VWD with <5% of VWD cases. Overall, the most common symptoms of VWD are hematomas, bleeding from minor wounds, menorrhagia, and bleeding around medical procedures such as surgery, dental interventions and child birth e.g. peri-procedural bleeding[8]. Type 2 and 3 VWD patients however may present with more severe bleeding, as observed in hemophilia.

Treatment of hemophilia A and B

Treatment options for hemophilia A and B have evolved significantly over the years. For severe hemophilia, treatment generally consists of prophylactic therapy to prevent bleeding episodes. This approach maintains a certain level of coagulation factor in the blood persistently over time to reduce the risk of spontaneous bleeding.

However, a subset of patients with moderate hemophilia may also require prophylactic treatment to prevent spontaneous or frequent bleeding, highlighting the variability in treatment needs even among those with similar levels of residual coagulation factors. The mechanisms behind this inter-individual variation in bleeding phenotype, even in patients with the same diagnosis and similar residual coagulation factor levels, are yet to be unraveled. In contrast, overall moderate and mild hemophilia can often be managed on an on-demand basis, where treatment is administered only when bleeding occurs or in anticipation of medical procedures.

In mild and some patients with moderate hemophilia A, desmopressin which is a synthetic vasopressin analog, can be used to prevent and treat bleeding. Desmopressin stimulates the release of stored VWF and FVIII from vascular endothelial cells[9]. Desmopressin effectively increases plasma levels of VWF and FVIII, offering a non-immunological treatment option without risk of developing inhibiting antibodies to therapy as is seen in coagulation factor concentrates. This is an important concern associated with factor concentrate replacement therapy. Other treatments include replacement therapy with recombinant standard half-life (SHL) coagulation factor concentrates, which are administered intravenously to replace deficient FVIII (hemophilia A) or FIX (hemophilia B)[10]. Extended half-life (EHL) coagulation factor concentrates, engineered for longer duration of action, require less frequent dosing while maintaining therapeutic levels[10]. Non-factor replacement therapy for hemophilia A includes emicizumab, a bispecific monoclonal antibody mimicking FVIII's function, that can be administered subcutaneously. But also alternative approaches such as fitusiran and concizumab will probably form a part of the standard treatment landscape for inborn bleeding disorders in the near future [10,11]. Gene therapy aims to introduce functional copies of the deficient coagulation factor gene into

patient liver cells to restore coagulation factor levels for extended periods, potentially indefinitely. In this way, making prophylaxis unnecessary. These options highlight the urgent obligation to tailor therapeutic options in hemophilia, according to patient characteristics and preferences but also bleeding phenotype and economical possibilities[12].

Treatment of von Willebrand disease

On-demand treatment is typical for VWD, while prophylactic treatment is mainly initiated for more severe patients with type 3 VWD presenting with frequent bleeding episodes[13]. Desmopressin also can be used in VWD treatment, demonstrating efficacy in certain subtypes of VWD, particularly type 1 VWD and some cases of type 2 VWD[14,15]. By stimulating the release of stored VWF from vascular endothelial cells. Plasma-derived VWF containing concentrates still play a crucial role in managing of VWD in instances where desmopressin is inadequate for severity of bleed or medical procedure, ineffective or contraindicated[16]. These concentrates are especially vital in treating patients with more severe forms of VWD and those who require surgery or face significant bleeding episodes[16]. It is important to note that the concentrates containing VWF also include FVIII in varying ratios. Additionally, these concentrates contain VWF multimers in varying concentrations[18]. One such product is Haemate P®[19], which is effectively in the treatment of VWD. But recombinant VWF concentrates are also coming to market, still only consisting of recombinant VWF (Vonvendi®)[17]. This concentrate offers an alternative treatment option for individuals with VWD, providing purified VWF without additional FVIII found in plasma-derived concentrates.

The road to more personalized treatment of inborn bleeding disorders

Historically, dosing of FVIII, FIX, combined VWF/FVIII concentrates and desmopressin in patients with hemophilia and VWD has been based on body weight. However, studies show that coagulation factor levels are reported both above and below targeted levels when dosing according to body weight in both the perioperative and prophylactic settings is applied [20–22]. High coagulation factor levels increase the risk of thrombotic events and are excessively costly[23,24], while low coagulation factor levels increase the risk of bleeding. Alternatively, pharmacokinetic-guided dosing, particularly in hemophilia, has emerged in recent years as a promising approach to individualize dosing regimens[25–27]. This method tailors treatment regimens to each patient's unique pharmacokinetic profile, optimizing dosing to achieve better target levels.

Pharmacometrics in bleeding disorders

Pharmacometrics involves the integrating of biology, physiology, and pharmacology to quantify drug-patient interactions through mathematical models, thereby individualizing therapeutic approaches[28]. Pharmacometrics can be categorized into pharmacokinet-

ic, pharmacodynamic, and physiologically-based pharmacokinetic modelling. Through pharmacometric modelling, we can predict how a patient with a bleeding disorder will respond to different treatments, allowing for the optimization of dosing regimens. This approach not only aims to maximize therapeutic efficacy but also to minimize potential adverse effects by tailoring treatment plans to the individual's specific needs. Figure 2 gives an overview of pharmacometric methods applied in quantifying drug treatment effect in bleeding disorders.
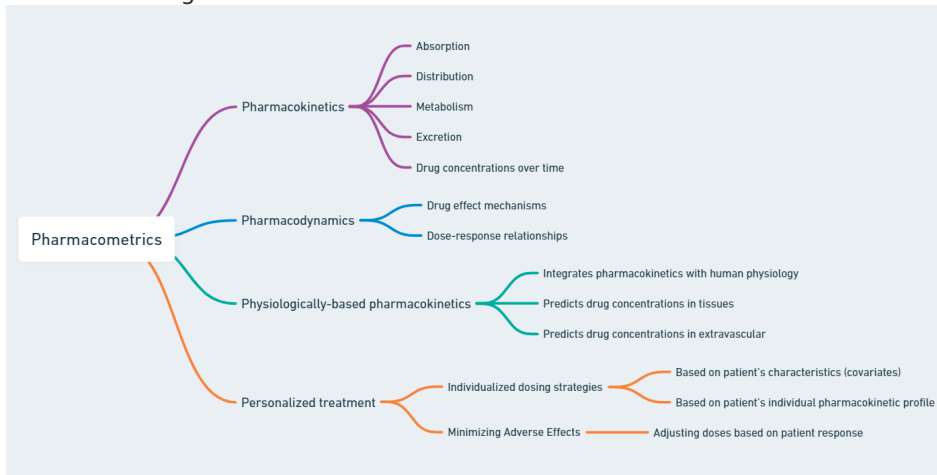
Figure 2. Schematic overview of application of pharmacometrics in the personalization of treatment, which is applied in inborn bleeding disorders within the OPTI-CLOT/To WiN studies.

Pharmacokinetics

Pharmacokinetics describes the relationship between dose and concentration of the drugs over time, in which the processes of absorption, distribution, metabolism and excretion are crucial[29]. Absorption describes how the drug moves from the site of administration into the bloodstream. Distribution refers to how the drug spreads through body fluids and tissues. Metabolism involves the biochemical transformation of the drug, mainly in the liver, into inactive or more active substances. Finally, excretion is the process of removing the drug from the body, which occurs primarily through the kidneys in urine or by the liver in bile.

Pharmacokinetic parameters, such as clearance and volume of distribution, provide quantitative measures of drug disposition[30]. Clearance refers to the volume of plasma or blood from which a drug is removed per unit of time. It indicates the ability of the body to eliminate the drug. Clearance is expressed in terms of volume per time (e.g., liters per hour). Volume of distribution is a theoretical volume representing the apparent space in the body available to contain the drug. It describes how a drug distributes throughout the body relative to its concentration in the bloodstream. These pharmacokinetic parameters

vary among individuals, leading to inter-individual variability. Consequently, pharmacokinetic parameters of blood coagulation factors and desmopressin differ between patients. To account for this variability, a population pharmacokinetic model can be developed, which quantifies the variability in pharmacokinetics within a specific population.

Pharmacokinetic-guided dosing in inborn bleeding disorders

Pharmacokinetic-guided dosing represents a significant advancement in the treatment of hemophilia and VWD, addressing the challenges of inter-individual variability that complicate dosing based solely on body weight. Pharmacokinetic-guided dosing involves the use of individual pharmacokinetic parameters, such as clearance and volume of distribution, to customize the dosage for each patient, aiming to achieve and maintain target peak and trough levels within a therapeutic range.

To characterize the pharmacokinetic profile of an individual patient, numerous samples are typically required. To overcome this problem, a previously developed population pharmacokinetic model combined with *maximum a posteriori* (MAP) Bayesian estimation can be used[31]. This approach enables the estimation of individual pharmacokinetic parameters with fewer samples, combining prior knowledge about the population with individual-specific data samples. Population pharmacokinetic models are comprehensive, incorporating patient characteristics (e.g., age, body weight) and treatment specifics (e.g., type and brand of coagulation factor concentrate or VWF containing concentrate) to account for observed inter-individual variability. By combining this pre-existing population-level data with a small number of FVIII, FIX or VWF level measurements levels from the individual patient, MAP Bayesian estimation can accurately predict the individual pharmacokinetic parameters of a patient with one of these inborn bleeding disorders. This method significantly reduces the patient burden associated with traditional pharmacokinetic profiling while providing the detailed information necessary to individualize dosing[32].

Pharmacodynamics in bleeding disorders

Pharmacodynamics describes the relationship between concentration and effect. Unlike pharmacokinetic-guided dosing that describes the behavior of the drug within the body, pharmacodynamics takes into account the actual effects observed in patients. This distinction is important because individuals may respond differently to a drug even if they share similar pharmacokinetic profiles[33]. In conditions like hemophilia, pharmacodynamic modelling is essential for understanding how varying levels of coagulation factors in the bloodstream correlate with hemostatic outcomes. Similarly, for VWD, pharmacodynamic research is important in determining the efficacy of treatments such as desmopressin in increasing VWF and FVIII levels, thereby guiding optimal therapeutic strategies.

Physiologically based pharmacokinetics in bleeding disorders

Physiologically based pharmacokinetic modelling uses a mechanistic framework that incorporates human anatomy, physiology, and the physicochemical properties of drugs to simulate their pharmacokinetics[34]. Unlike empirical population pharmacokinetic models that rely on drug concentration data from specific populations to develop the model, physiologically based pharmacokinetic modelling can be developed without direct drug concentration measurements. This characteristic makes physiologically based pharmacokinetic an attractive approach in scenarios where developing a population pharmacokinetic model is not feasible or when a more mechanistic insight into drug pharmacokinetics is desired.

The utilization of physiologically based pharmacokinetic modelling in the field of inborn bleeding disorders has been limited, yet it presents notable opportunities for enhancing patient care. For instance, in bleeding disorders like hemophilia B which are treated with FIX concentrates, it is critical to understand not just the presence of these coagulation factors in the plasma compartment but also their distribution in the extravascular spaces[35,36]. Especially as studies have shown that FIX plays a hemostatic role in the extravascular compartment REF. Physiologically based pharmacokinetic modelling has the potential to mechanistically predict the pharmacokinetics and pharmacodynamics of FIX beyond the vascular compartment.

Artificial intelligence and machine learning in pharmacometrics

Traditional pharmacometric modelling relies on statistical and mathematical techniques to describe and predict the effects of drugs, focusing on their pharmacokinetics and pharmacodynamics[37]. This process often involves the use of software like non-linear mixed-effects modelling (NONMEM) to conduct population-based analyses, facilitating the understanding of drug action and variability among individuals[38]. However, the novel integration of artificial intelligence and machine learning into pharmacometrics marks a novel era in the field[39]. These advanced technologies offer the ability to process and analyze vast datasets more efficiently, uncovering relationships that traditional methods are not able to investigate. By applying artificial intelligence and machine learning in a thoughtful manner, also realizing its limitations, we are able to further optimize our models, ultimately leading to tailoring of therapeutic strategies to meet the unique needs of patients.

THESIS OUTLINE

The aim of this thesis is to further optimize treatment of patients with inborn bleeding disorders by using various pharmacometric modelling techniques to personalize dosing. Application of these different techniques will ultimately lead to further personalization of therapeutic approaches in patients.

Part I of this thesis focuses on using pharmacometric modelling within hemophilia A and B. In **chapter 2,** the effects of FVIII gene (F8) missense mutations on the response of desmopressin in non-severe hemophilia A were investigated. A population pharmacokinetic model was developed in order to explain the inter-individual variability of the response of desmopressin in patients with F8 missense variants applying machine learning techniques. In **chapter 3,** the predictive performance of a previously developed pharmacokinetic-pharmacodynamic model of a plasma derived VWF/FVIII concentrate (Haemate P®) on thrombin and plasmin generation was investigated by using an external independent dataset of hemophilia A patients. **Chapter 4** describes the quantification of recombinant factor IX-Fc fusion protein (rFIXFc) in the extravascular spaces by using a physiologically based pharmacokinetic model. Here, we quantify and discuss how rFIXFc distributes outside the plasma compartment and the hemostatic importance of extravascular rFIXFc.

Part II of this thesis focuses on the application of pharmacometrics in VWD. In **chapter 5**, we aim to investigate and assess the relationship between desmopressin concentration and VWF in type 1 VWD patients by developing a population pharmacokinetic-pharmacodynamic model. By using this population pharmacokinetic-pharmacodynamic model, we investigate the feasibility of a capped desmopressin dose. In **chapter 6,** the external validation of a population pharmacokinetic model of desmopressin response in terms of VWF:Act levels is described. **Chapter 7** describes the predictive performance of pharmacokinetic-guided dosing in VWD in the perioperative setting. This prospective study investigates the feasibility and reliability of using pharmacokinetic-guided dosing in VWD. In **Chapter 8**, a previously reported population pharmacokinetic model describing the interaction between VWF/FVIII is refined, using the data from the prospective study presented in chapter 7.

Part III of this thesis focuses on the application of artificial intelligence in pharmacometrics. **Chapter 9** describes the usage of an artificial intelligence tool e.g. ChatGPT, within pharmacometrics. We present an example of how ChatGPT could be used in population pharmacokinetic modelling and its limitations.
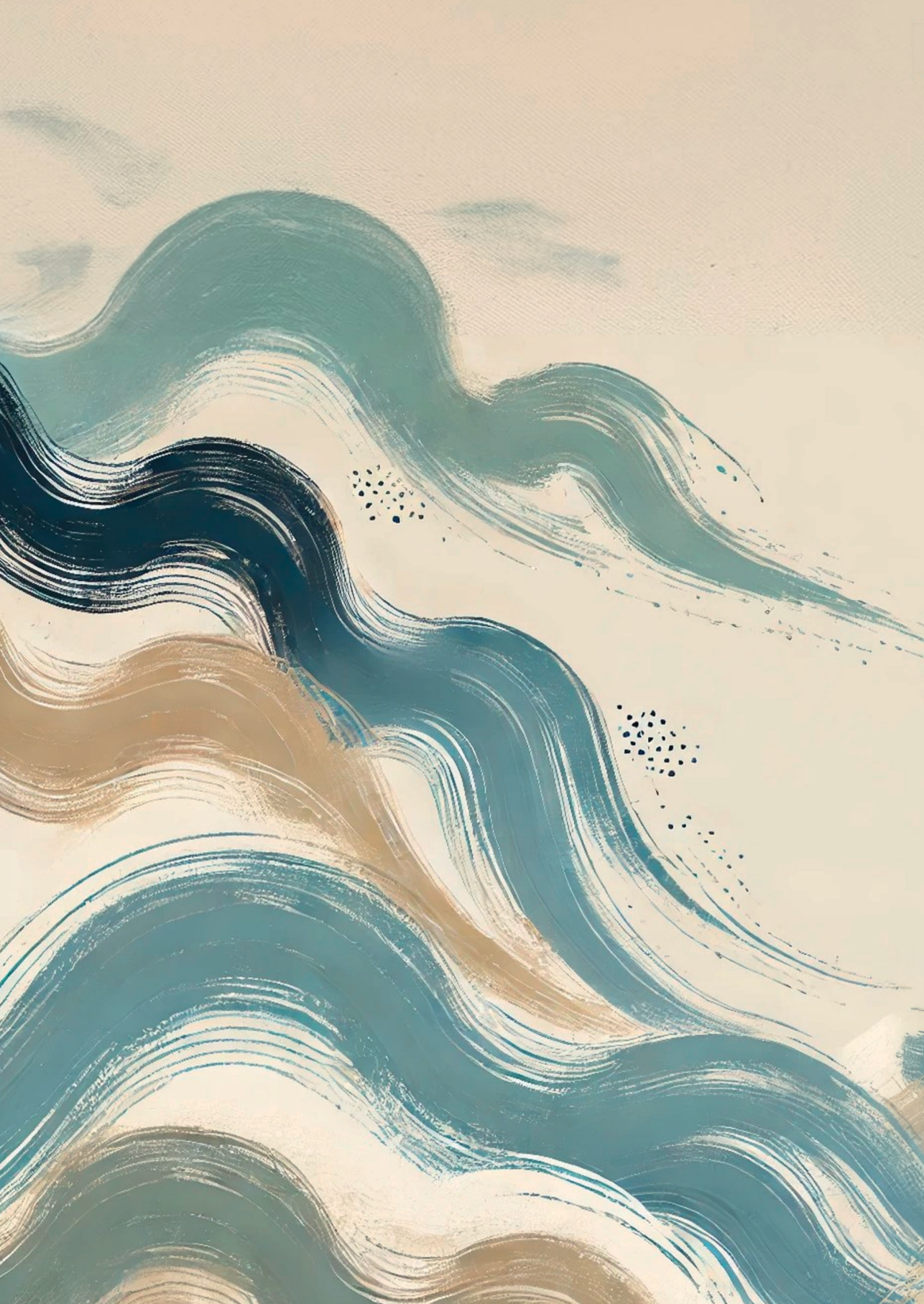
In Part IV, **in Chapter 10** the results of the studies presented in this thesis are discussed in broader context to the literature and different areas of future research are speculated on. Finally, **chapter 11** summarizes the results of the studies presented in this thesis.

REFERENCES

1. Franchini M, Mannucci P. The History of Hemophilia. *Semin Thromb Hemost*. 2014;40(05):571-576. doi:10.1055/s-0034-1381232

2. Leebeek FWG, Eikenboom JCJ. Von Willebrand's Disease. Longo DL, ed. *N Engl J Med*. 2016;375(21):2067-2080. doi:10.1056/NEJMra1601561

3. Iorio A, Stonebraker JS, Chambost H, et al. Establishing the Prevalence and Prevalence at Birth of Hemophilia in Males: A Meta-analytic Approach Using National Registries. *Ann Intern Med*. 2019;171(8):540-546. doi:10.7326/M19-1208

4. van Galen KPM, d'Oiron R, James P, et al. A new hemophilia carrier nomenclature to define hemophilia in women and girls: Communication from the SSC of the ISTH. *J Thromb Haemost*. 2021;19(8):1883-1887. doi:10.1111/jth.15397

5. Ng C, Motto DG, Di Paola J. Diagnostic approach to von Willebrand disease. *Blood*. 2015;125(13):2029-2037. doi:10.1182/blood-2014-08-528398

6. Sadler JE, Budde U, Eikenboom JC E, Favalor. Update on the pathophysiology and classification of vonWillebrand disease a report of the Subcommittee on von Willebrand Factor. *J Thromb Haemost*. 2006.

7. James PD, Connell NT, Ameer B, et al. ASH ISTH NHF WFH 2021 guidelines on the diagnosis of von Willebrand disease. *Blood Adv*. 2021;5(1):280-300. doi:10.1182/BLOODADVANCES.2020003265

8. de Wee EM, Sanders Y V., Mauser-Bunschoten EP, et al. Determinants of bleeding phenotype in adult patients with moderate or severe von Willebrand disease. *Thromb Haemost*. 2012;108(4):683-692. doi:10.1160/TH12-04-0244

9. de la FUENTE B. Response of Patients with Mild and Moderate Hemophilia A and von Willebrand's Disease to Treatment with Desmopressin. *Ann Intern Med*. 1985;103(1):6. doi:10.7326/0003-4819-103-1-6

10. Miesbach W, Schwäble J, Müller MM, Seifried E. Treatment Options in Hemophilia. *Dtsch Arztebl Int*. 2019;116(47):791-798. doi:10.3238/arztebl.2019.0791

11. Gualtierotti R, Pasca S, Ciavarella A, et al. Updates on Novel Non-Replacement Drugs for Hemophilia. *Pharmaceuticals (Basel)*. 2022;15(10). doi:10.3390/ph15101183

12. Cnossen MH, van Moort I, Reitsma SH, et al. SYMPHONY consortium: Orchestrating personalized treatment for patients with bleeding disorders. *J Thromb Haemost*. 2022;20(9):2001-2011. doi:10.1111/jth.15778

13. Berntorp E. Prophylaxis and treatment of bleeding complications in von Willebrand disease type 3. *Semin Thromb Hemost*. 2006;32(6):621-625. doi:10.1055/s-2006-949667

14. De Wee EM, Leebeek FWG, Eikenboom JCJ. Diagnosis and management of von Willebrand Disease in the Netherlands. *Semin Thromb Hemost*. 2011;37(5):480-487. doi:10.1055/s-0031-1281032

15. Connell NT, Flood VH, Brignardello-Petersen R, et al. Ash isth nhf wfh 2021 guidelines on the management of von willebrand disease. *Blood Adv*. 2021;5(1):301-325. doi:10.1182/BLOODADVANCES.2020003264

16. Miesbach W, Krekeler S, Wolf Z, Seifried E. Clinical use of Haemate® P in von Willebrand disease: A 25-year retrospective observational study. *Thromb Res*. 2015;135(3):479-484. doi:10.1016/j.thromres.2014.12.017

17. Franchini M, Mannucci PM. Von Willebrand factor (Vonvendi®): the first recombinant product licensed for the treatment of von Willebrand disease. *Expert Rev Hematol*. 2016;9(9):825-830. doi:10.1080/17474086.2016.1214070

18. Heijdra JM, Cnossen MH, Leebeek FWG. Current and Emerging Options for the Management of Inherited von Willebrand Disease. *Drugs*. 2017;77(14):1531-1547. doi:10.1007/s40265-017-0793-2

19. Berntorp E, Archey W, Auerswald G, et al. A systematic overview of the first pasteurised VWF/FVIII medicinal product, Haemate®P/Humate®-P: History and clinical performance. *Eur J Haematol*. 2008;80(SUPPL. 70):3-35. doi:10.1111/j.1600-0609.2008.01049.x

20. Björkman S. Population pharmacokinetics of recombinant factor IX: Implications for dose tailoring. *Haemophilia*. 2013;19(5):753-757. doi:10.1111/hae.12188

21. Björkman S, Oh M, Spotts G, et al. Population pharmacokinetics of recombinant factor VIII: the relationships of pharmacokinetics to age and body weight. *Blood*. 2012;119(2):612-618. doi:10.1182/blood-2011-07-360594

22. Hazendonk HCAM, Heijdra JM, de Jager NCB, et al. Analysis of current perioperative management with Haemate® P/Humate P® in von Willebrand disease: Identifying the need for personalized treatment. *Haemophilia*. 2018;24(3):460-470. doi:10.1111/hae.13451

23. Martinelli I. von Willebrand factor and factor VIII as risk factors for arterial and venous thrombosis. *Semin Hematol*. 2005;42(1):49-55. doi:https://doi.org/10.1053/j.seminhematol.2004.09.009

24. Mannucci PM. Venous thromboembolism in von Willebrand disease. *Thromb Haemost*. 2002;88(3):378-379.

25. Hazendonk HCAM, van Moort I, Mathôt RAA, et al. Setting the stage for individualized therapy in hemophilia: What role can pharmacokinetics play? *Blood Rev*. 2018;32(4):265-271. doi:10.1016/j.blre.2018.01.001

26. Goedhart TMHJ, Bukkems LH, Michel Zwaan C, Mathôt RAA, Cnossen MH. Population pharmacokinetic modeling of factor concentrates in hemophilia: An overview and evaluation of best practice. *Blood Adv*. 2021;5(20):4314-4325. doi:10.1182/bloodadvances.2021005096

27. Grazzi EF, Sun SX, Burke T, O'hara J. The Impact of Pharmacokinetic-Guided Prophylaxis on Clinical Outcomes and Healthcare Resource Utilization in Hemophilia A Patients: Real-World Evidence from the CHESS II Study. *J Blood Med*. 2022;13:505-516. doi:10.2147/JBM.S363028

28. Standing JF. Understanding and applying pharmacometric modelling and simulation in clinical practice and research. *Br J Clin Pharmacol*. 2017;83(2):247-254. doi:10.1111/bcp.13119

29. Benet LZ, Kroetz D, Sheiner L, Hardman J, Limbird L. Pharmacokinetics: the dynamics of drug absorption, distribution, metabolism, and elimination. *Goodman Gilman's Pharmacol basis Ther*. 1996;3:e27.

30. Rowland M, Benet LZ, Graham GG. Clearance concepts in pharmacokinetics. *J Pharmacokinet Biopharm*. 1973;1(2):123-136.

31. Van Der Meer AF, Marcus MAE, Touw DJ, Proost JH, Neef C. Optimal sampling strategy development methodology using maximum a posteriori Bayesian estimation. *Ther Drug Monit*. 2011;33(2):133-146. doi:10.1097/FTD.0b013e31820f40f8

32. Brocks D, Hamdy D. Bayesian estimation of pharmacokinetic parameters: An important component to include in the teaching of clinical pharmacokinetics and therapeutic drug monitoring. *Res Pharm Sci*. 2020;15(6):503-514. doi:10.4103/1735-5362.301335

33. Bukkems LH, Valke LLFG, Barteling W, et al. Combining factor VIII levels and thrombin/plasmin generation: A population pharmacokinetic-pharmacodynamic model for patients with haemophilia A. *Br J Clin Pharmacol*. 2021;(May 2021):1-12. doi:10.1111/bcp.15185

34. Sager JE, Yu J, Ragueneau-Majlessi I, Isoherranen N. Physiologically based pharmacokinetic (PBPK) modeling and simulation approaches: A systematic review of published models, applications, and model verification. *Drug Metab Dispos*. 2015;43(11):1823-1837. doi:10.1124/dmd.115.065920

35.   Salas J, Van Der Flier A, Hong VP, et al. Extravascular Distribution of Conventional and Ehl FIX Products Using In Vivo SPECT Imaging Analysis in Hemophilia B Mice. *Blood*. 2017;130(Suppl 1):1061 LP - 1061. http://www.bloodjournal.org/content/130/Suppl_1/1061.abstract.

36.   van der Flier A, Hong V, Liu Z, et al. Biodistribution of recombinant factor IX, extended half-life recombinant factor IX Fc fusion protein, and glycoPEGylated recombinant factor IX in hemophilia B mice. *Blood Coagul Fibrinolysis*. 2023;34(6):353-363. doi:10.1097/MBC.0000000000001230

37.   Sheiner LB, Steimer J-L. Pharmacokinetic/Pharmacodynamic Modeling in Drug Development. *Annu Rev Pharmacol Toxicol*. 2000;40(1):67-95. doi:10.1146/annurev.pharmtox.40.1.67

38.   Keizer RJ, Karlsson MO, Hooker A. Modeling and simulation workbench for NONMEM: Tutorial on Pirana, PsN, and Xpose. *CPT Pharmacometrics Syst Pharmacol*. 2013;2(6):1-9. doi:10.1038/psp.2013.24

39.   Janssen A, Bennis FC, Mathôt RAA. Adoption of Machine Learning in Pharmacometrics: An Overview of Recent Implementations and Their Considerations. *Pharmaceutics*. 2022;14(9):1-26. doi:10.3390/pharmaceutics14091814

1

PART I

Pharmacometrics in hemophilia A and B

CHAPTER 2

The effects of F8 missense variants on desmopressin response in non-severe hemophilia A patients investigated using machine learning

M.E. Cloesmeijer*, J. del Castillo Alferez*, A. Janssen, J. Loomans, R.M. van Hest, M.H. Cnossen, A.B. Meijer, R.A.A. Mathôt, K. Fijnvandraat

*Shared first authorship – both equally contributed

ABSTRACT

Observed inter-individual variability in factor VIII (FVIII) response after desmopressin administration to patients with non-severe hemophilia prompts the need for individual testing before clinical application. The FVIII gene (F8) variant is a strong determinant of the desmopressin response. In this multicenter cohort study, a machine learning approach (Shapley Additive exPlanations; SHAP) was applied to investigate the effect of F8 missense variants on desmopressin response in the context of other covariates in a population PK model, using data from 1441 non-severe hemophilia A patients with 55 different F8 variants who underwent desmopressin testing. The reference group included patients who received intravenous desmopressin and had non-significant F8 missense variants, representing the typical responders. After subcutaneous and intranasal administration, the desmopressin response quantified by FVIII peak levels was 88% and 73% compared to peak FVIII levels after intravenous administration(100%). F8 missense variants Pro149Arg, Gly477Val, and Tyr450Asn were associated with a lower FVIII increase of respectively 24%, 25% and 56%, compared to the reference population (100%). Asn637Ser, Phe2146Ser, Glu132Asp, Arg550His, Ser2030Asn, Thr74Met and Arg717Leu were associated with an augmented FVIII increase of respectively 199%, 219%, 231%, 252%, 265%, 296% and 336% compared to the reference population (100%). Inclusion of all covariates reduced desmopressin response variability from 141.6% to 78.1%. This population pharmacokinetic study using machine learning enables a comprehensive analysis of the effect of F8 missense variants on desmopressin response and illustrates the complexity of inter-individual variability. Moreover, these findings provide deeper insights in the underlying molecular mechanisms that influence the response of desmopressin.

INTRODUCTION

Hemophilia A is an x-linked bleeding disorder caused by a reduced functional activity of coagulation factor VIII (FVIII) [1]. Patients are typically classified based on residual FVIII activity levels. Severe hemophilia A is defined as FVIII activity levels <0.01 IU/mL and non-severe hemophilia A as FVIII activity levels between 0.01 – 0.40 IU/mL[2]. These patients are further classified as moderate when FVIII levels are 0.01 – 0.05 IU/mL and as mild when FVIII levels exceed 0.05 IU/mL [2]. Etiologically, non-severe hemophilia A is primarily caused by missense variants in the FVIII gene (F8)[3] . More than 976 missense variants have been reported, making non-severe hemophilia A genetically extremely heterogenous [4]. Baseline FVIII activity levels are determined by the underlying F8 missense variant and age as well as other unknown factors[5].

FVIII circulates in the blood plasma in a complex with Von Willebrand Factor (VWF) that protects FVIII from rapid clearance and proteolytic degradation [6,7]. FVIII is activated after proteolytic cleavage by thrombin enabling its accelerative role in the coagulation cascade[8]. More specifically, activation by thrombin leads to dissociation of the FVIII – VWF complex and formation of the membrane bound complex of both activated FVIII (FVIIIa) and factor IX (FIXa)[9,10]. Subsequently, this leads to activation of FX (FXa), that is required for thrombin and consequent fibrin formation to achieve hemostasis[11]. FVIII variants may affect any aspect of FVIII function, such as protein expression, VWF binding, activation by thrombin, stability of the activated mutant FVIII, and/or its binding to FIXa or phospholipid membranes (Figure 1)[12].
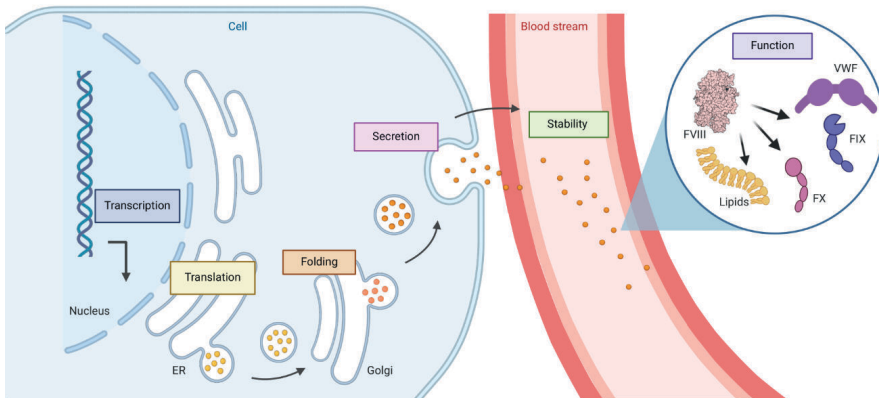
Figure 1. FVIII modification and expression in endothelial cells and associated (coagulation) factors in blood plasma Several steps are necessary for synthesis, secretion and intravascular survival of functional Factor VIII: DNA is first transcribed in the nucleus and translated in the ER (Endoplasmic Reticulum), subsequently the synthesized amino acid sequence is folded in the Golgi Apparatus; the FVIII is secreted into the blood stream. In the circulation, the protein stability and structure of FVIII will determine whether successful interaction with lipids, FX, FIX and VWF can take place. Mutations interfering with any of these processes will also hamper desmopressin response. Figure created with BioRender.

Non-severe hemophilia patients generally suffer from prolonged and/or excessive bleeding after minor trauma and dental or surgical procedures[13,14]. In the majority of non-severe hemophilia A patients bleeding is successfully prevented or treated by administration of desmopressin[15,16]. Desmopressin is a synthetic analogue of vaso-pressin that is physiologically involved in bodily stress responses[17]. Administration of desmopressin results in an increase of circulating VWF and FVIII[18]. A rise in FVIII plasma levels ≥0.50 IU/mL is defined as a complete response whereas a rise to 0.30-0.50 IU/mL is considered a partial response[19,20]. Desmopressin is a safer and less expensive alternative when compared to FVIII concentrates for the treatment of bleeding, as it does not pose the risk of inhibitor development associated with administration of FVIII concentrates[21,22]. However, the widespread clinical implementation of desmopressin use is hampered by a large inter-individual variability in FVIII response, requiring desmopressin testing in patients to obtain certainty about the hemostatic effect that can be expected[23,24]. It has been reported that several factors are associated with desmopressin response, such as FVIII and von Willebrand antigen baseline levels, peak von Willebrand factor activity, body weight and route of administration [25]. The achieved FVIII levels following desmo-pressin administration depend on the availability of sufficiently stored FVIII, efficacy of FVIII release from the endothelial cells and the rate of clearance and/or stability of FVIII in the circulation[26]. F8 variants may impact on one or more of these mechanisms, thereby affecting desmopressin response[25,27]. Yet, the effect of each specific FVIII variant remains largely unknown, as it is challenging to address the large heterogeneity of variants when each occurs in a very limited number of patients.

In the present study, we aim to investigate the effect of F8 missense variants on des-mopressin response in the context of other covariates. To this end, population pharma-cokinetic modelling and machine learning (ML) techniques were employed to identify variants with a strong effect on desmopressin response. Shapley Additive exPlanations (SHAP) was used to interpret the ML model. Recent advances in the application of machine learning tools in pharmacometrics are promising to enable fast screening of covariates, especially when facilitated by ML explainability methods such as SHAP[28]. Particularly, SHAP decomposes a ML model into a simplified additive representation for identifying importance of specific covariates used in ML models[29,30]. Here we used pharmacokinetic (PK) modelling and SHAP to resolve the contribution of specific F8 missense variants on desmopressin response in patients receiving desmopressin from a large multicenter cohort study.

METHODS

Study population

Data from the multicenter RISE (Response to desmopressin in non-severe hemophilia A patients, in Search for determinants) cohort study was used [25]. According to the participating review boards, informed consent was not required as the initial dataset involves retrospective data collection.

Data from desmopressin tests were collected from 1474 non-severe hemophilia patients at 24 Hemophilia Treatment Centers in nine countries in Europe, Canada and Australia. Data from patients who had been treated with medication affecting hemostasis other than desmopressin within 72 hours of desmopressin administration, or patients who had an inhibitor at the time of desmopressin administration were excluded.

Data collection

Demographic and clinical data was extracted from medical records using a standardized electronic case report form. The following data were included: age, weight, and inhibitor status. Presence of inhibitors was an exclusion criterion for this study. Each *F8* variant is reported using the Human Genome Variation Society (HGVS)-type numbering. Upon testing: date of desmopressin response, route of administration and desmopressin dose were recorded. Data were collected on FVIII measured by one-stage clotting assay and VWF antigen and activity before desmopressin administration and at least 1 hour after desmopressin administration. Some patients also had blood samples taken 4 hours and 24 hours after desmopressin administration.

Pharmacokinetic modelling and machine learning

A population pharmacokinetic (PK) model, describing the desmopressin response and FVIII activity levels over time after desmopressin administration was made. For a one-compartment model, the PK parameters were a first-order absorption rate constant (ka), relative amount of released FVIII after desmopressin administration (F), apparent clearance (CL/F) and apparent central volume of distribution (Vd/F). F relates normally to the bioavailability of the drug. In this manuscript bioavailability (F) was adjusted to the relative amount of released FVIII after desmopressin administration. This adjustment aimed to provide a clearer understanding of the effect of depression on FVIII bioavailability. Relative amount of released FVIII after desmopressin administration was fixed as one after IV desmopressin administration. Subsequently, inter-individual variability was attributed on relative amount of released FVIII after desmopressin administration. Patients with a lower relative amount of released FVIII after desmopressin administration, would result in a lower FVIII exposure, whereas patients with a higher relative amount

of released FVIII after desmopressin administration, would result in a higher exposure of FVIII. The dose of FVIII was arbitrarily set to one in all patients, since no actual FVIII was administered [31].

The population PK model was developed using NONMEM (7.4., ICON, Hanover, MD, United States)[33a] and further evaluated using PsN and R studio[33,34]. Development of the model was performed in three steps (i) a structural model including inter-individual variability, (ii) residual error model and (iii) covariate analysis. Details of model development are provided in the supplementary.

Allometric body weight scaling was applied to CL/F and Vd/F in the structural model. The following covariates were evaluated: age, VWF activity (VWF:Act) and VWF antigen baseline, VWF:Act after desmopressin administration, FVIII variant and route of administration. A single variant had to be present in at least three patients to be included in the evaluation of its association with PK parameters. For the remaining covariates, all patients were used. All variants used in our model development are listed in Supplement table 1. Moreover, the relative amount of released FVIII after desmopressin administration was adjusted for body weight with an exponential function, in which the exponent was estimated[35]. This is based on our assumption that the absolute amount of released FVIII is likely correlated exponentially to body weight. In our population PK model, the FVIII baseline was fixed at the level measured before the administration of desmopressin.

For the covariate analysis, we first fit a random forest model to individual PK parameter estimates produced by a baseline population PK model. Covariates for consideration in the final model were determined based on their importance in the random forest model. Next, SHAP analysis was performed to inspect the variants' mean effect on the relative amount of released FVIII after desmopressin administration [30]. The variance of the SHAP values between subjects can be used to evaluate the strength of the effect of variants as previously reported.[30] F VIII variants demonstrating large interindividual variability SHAP values may indicate model overfitting or spurious effects. Therefore, inclusion in the model should be carefully evaluated. Variants were ranked based on their absolute mean SHAP value. The first twenty ranked variants from the SHAP analysis were added to the structural population PK model in a stepwise manner followed by a backward elimination procedure to establish the full and final PK model. More details about the covariate analysis are in the supplementary.

Model evaluation

Visual evaluation methods (goodness-of-fit plots) were applied to evaluate the performance of all models. The precision of the parameter estimates was expressed as relative standard error (RSE, %) and confidence intervals (CI). A RSE value < 30% for fixed effects and < 50% for random effects were considered acceptable [36]. For internal validation, a bootstrap and prediction-corrected visual predictive check (pcVPC) were performed.

Pharmacokinetic simulations

After establishing the final model, simulations up to 24h after desmopressin administration were performed based on the final PK parameter estimations to display the difference in desmopressin response on FVIII levels for specific variants and routes of administration. Typical patients, defined as the average individual within this population PK analysis, were used to perform the simulations. Typical patients presenting each variant were grouped, simulated and compared to the reference population. One typical patient per variant was simulated. The reference population was defined as all individuals with variants that were unknown or did not have a significant impact on the PK parameters.

Simulations were based on the following parameters: baseline FVIII 0.16 IU/mL or as the observed median of the variant group, bodyweight 70 kg, unless stated otherwise. Target levels between 0.30 and 0.50 IU/mL were used, as these target levels were used as partial response.

RESULTS

Patient characteristics: RISE cohort

Data cleaning was performed to eliminate incorrectly observed FVIII levels, thus ensuring the reliability of our analysis. In Table 1, we present the patient characteristics of the 1441 non-severe hemophilia A patients included in this study. The median age was 24 years (IQR 11-42) and the median body weight was 72 kg (IQR 41-82). Baseline FVIII was 0.16 IU/mL (IQ 0.10-0.25). Desmopressin was administered intravenously (IV, 62%), subcutaneously (SC, 35%) and intranasally (IN, 3%). Baseline VWF antigen (VWF:Ag) was 0.97 IU/ml (IQR 0.76-1.19). Altogether, 55 genetic variants were used for the analysis (Supplemental Table 1).

Table 1. Patient population and treatment characteristics

	N = 1441 Number or median (interquartile range) [min-max]
Patients and phenotype	
Age, years	24 (11 – 42) [0.08 - 87]
Body weight, kilogram	72 (41 – 82) [4 - 143]
Route of administration and dose, n [%]	
Intravenous	891 [62]
Subcutaneous	510 [35]
Intranasal	40 [3]
Dose intravenous and subcutaneous, mcg/kg	0.30 (0.29 – 0.31)
Dose intranasal, mcg	150 (150 - 300)
Baseline characteristics, IU/mL	
Baseline (T0) FVIII	0.16 (0.10 – 0.25) [0.01 - 0.80]
Baseline (T0) VWF:Act	0.90 (0.71 - 1.15) [0.21 - 3.00]
Baseline (T0) VWF:Ag	0.98 (0.78 - 1.23) [0.29 - 3.00]
Hemophilia severity, n [%]	
Mild	1351 [94]
Moderate	90 [6]

FVIII: factor VIII, VWF:Act: von Willebrand factor Activity, VWF:Ag: von Willebrand factor Antigen,

Pharmacokinetic analysis

FVIII levels were collected at multiple time points up to 24 hours after desmopressin administration, resulting in 4086 data points (Figure 2a). A one-compartment model could adequately describe the change in FVIII levels over time after IV, SC, and IN administration of desmopressin (Figure 2b).
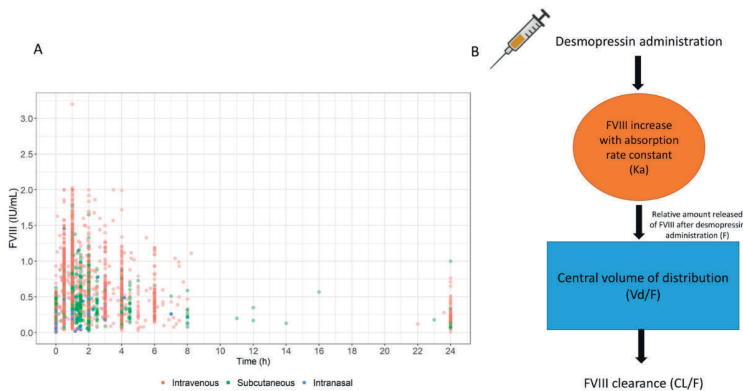

Figure 2. Desmopressin test response 2A) Measured FVIII activity levels over time after intravenous (red), intranasal (blue) or subcutaneous (green) desmopressin administration in study cohort. 2B) Schematic overview of the one-compartment pharmacokinetic model

Table 2. Population pharmacokinetic parameter estimates

Parameter	Structural model values (RSE%) [Shrinkage]	Final model values (RSE%) [Shrinkage %]	Bootstrap Medan value [95% CI]
General characteristics of the PK model			
Ka intravenous	53.1 FIX	53.1 FIX	-
Ka subcutaneous and intranasal	2.43 (19)	2.89 FIX	-
F intravenous (%)	100 FIX	100 FIX	-
Clearance/F (L/h/70 kg)	0.389 (6)	0.299 (6)	0.301 [0.265 – 0.347]
Volume of distribution/F (L/70 kg)	3.12 (4)	2.48 (3)	2.47 [2.30 – 2.64]
Covariates			
Body weight on F			
Exponent body weight	-	1.23 (3)	1.23 [1.15 – 1.32]
Route of administration on F (% compared to intravenous)			
Intravenous	100 FIX	100 FIX	
Subcutaneous	-	88.2 (45)	87.7 [78.9 – 99.9]
Intranasal	-	73.4 (42)	72.7 [50.5 – 98.2]
Mutations on F (% compared to reference population)			
Tyr450Asn	-	24.2 (5)	24.2 [18.9 - 38.0]
Gly477Val	-	25.1 (4)	25.2 [18.2 - 30.2]
Pro149Arg	-	56.0 (27)	57.8 [32.2 - 84.2]
Reference population		100 FIX	
Asn637Ser	-	199 (10)	200 [179 – 219]
Phe2146Ser	-	219 (43)	232 [122 – 358]
Glu132Asp	-	231 (23)	233 [167 – 301]
Arg550His	-	252 (20)	254 [202 – 339]
Ser2030Asn	-	265 (20)	272 [205 – 342]
Thr74Met	-	296 (17)	296 [226 – 393]
Arg717Leu	-	336 (30)	344 [200 – 477]
Inter-individual variability (CV%)			
F	141.6 (3) [4]	78.1 (3) [5]	77.6 [71.7 – 84.4]
Residual variability			
Proportional error (%)	15.5 (5) [18]	14.5 (5) [17]	14.4 [13.0 – 16.2]

Applied formulas to calculate PK parameters

Clearance/F $= \theta_{Clearance} \times (\frac{Body\ weight}{70})^{0.75}$;

Volume of distribution/F $= \theta_{Volume\ of\ distribution} \times (\frac{body\ weight}{70})$;

$F = \theta_{FVIIIr} \times (\frac{Body\ weight}{70})^{1.23} \times 1_{intravenous} \times -0.118_{subcutaenous} \times -0.266_{intranasal} \times -0.440_{Pro149Arg} \times -0.749_{Gly477Val} \times -0.758_{Tyr450Asn} \times 2.36_{Arg717Leu} \times 1.96_{Thr74Met} \times 1.65_{Ser2030Asn} \times 1.52_{Arg550His} \times 1.31_{Glu131Asp} \times 1.19_{Phe2146Ser} \times 0.990_{Asn637Set} \times e^{\eta_{fviiir}}$

The reference population constituted of the remaining variants not included in the final model or unknown mutations in the patients. FIX: parameter was fixed in the model.

Abbreviations: F: Relative amount of released factor VIII (FVIII) after desmopressin administration, FIX: Values were fixed in the model, instead of estimating the parameter, CI: confidence interval, Clearance/F: apparent clearance, CV: coefficient of variation calculated as $\sqrt{e^{\omega^2} - 1} \times 100$, Ka: absorption rate constant, RSE: relative standard error, Volume of distribution/F: apparent volume of distribution

Table 2 shows the estimates of the population PK parameters. The inter-individual variability in relative amount of released FVIII after desmopressin administration was estimated to be 141.6% in the model without covariates. This indicates substantial variation among individuals in their response to desmopressin in terms of FVIII release. Inter-individual variability was not estimated on clearance and volume of distribution to avoid excessive complexity in the model. The absorption rate constant was estimated in the structural model and fixed during covariates analysis. The absorption rate constant was 53.1 1/h and 2.69 1/h after IV and SC/IN administration, respectively. A lower value of the absorption rate indicates the FVIII peak levels occur later, whereas a high value of Ka indicates the FVIII peak levels occurs rapidly. Thus, the lower absorption rate constant observed after subcutaneous and intranasal indicates the peak FVIII occurs later than after intravenous administration. The Ka values for subcutaneous and intranasal were combined in further analysis. Baseline FVIII values were read from the dataset, instead of estimated, since this improved the accuracy of the model. The residual variability was described by a proportional error model. Goodness-of-fit plots showed good agreement between predicted and observed FVIII levels (Supplemental Figure 1). The visual predictive check plots show that most of the observed FVIII levels are within the 95% confidence interval of the model predictions (Supplemental Figure 2). The bootstrap median and confidence intervals were comparable to the parameter estimates. (Table 2). Thus, we concluded that the validity of the final model was adequate.

Investigating missense variant contribution to response variance using machine learning

Results from the SHAP analysis were used to evaluate the contribution of specific FVIII variants to desmopressin response, based on their effect on the relative amount of FVIII released after desmopressin administration. SHAP values were calculated to estimate the additive contribution of each variant to the relative amount of FVIII released after desmopressin administration in the model. These values represent the relative change in FVIII for each specific variant compared to the reference population. In total 55 genetic variants were evaluated (Supplemental Table 1). The missense variants with the strongest effect on relative amount of released FVIII after desmopressin administration and the observed FVIII peak levels after desmopressin administration are displayed in Figure 3.

Table 2 displays all significant covariates included in the final model. Variants Tyr450Asn, Gly477Val and Pro149Arg had a negative association with relative amount of released FVIII, while variants Asn637Ser, Phe2146Ser, Glu132Asp, Arg550His, Ser2030Asn, Thr74Met and Arg717Leu had a positive association with relative amount of released FVIII. All significant variants are mapped to the structure of FVIII in Figure 4 and include domains A1, A2, A3 and C1.
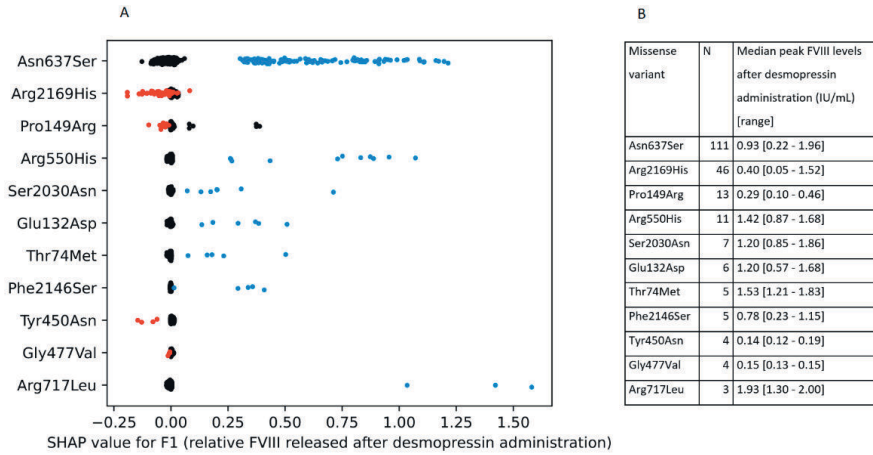
Figure 3. Effect of FVIII variants on the desmopressin response using SHAP analyses. 3A) displays the SHAP analysis. 3B) displays the median peak FVIII levels after desmopressin administration for each variant. Each dot represents an individual patient. Red dots illustrate a negative effect on F (negative mean SHAP value), reflecting lower FVIII levels observed after desmopressin administration when compared to the population median. Blue dots illustrate a positive effect on FVIII (positive mean SHAP value), reflecting higher FVIII levels observed after desmopressin administration compared to the population median. **SHAP =** SHapley Additive exPlanations
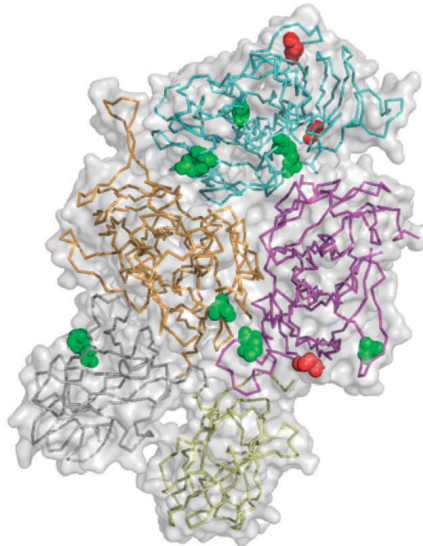
Figure 4. Locations of FVIII variants associated with a decreased or an increased desmopressin response
The structure of FVIII is displayed in grey. Within the transparent surface, the amino acid back bone of the different FVIII domains is depicted in lines with the following colors: A1=magenta, A2=aquamarine, A3=orange, C1=grey, C2=yellow. Mutations of the amino acids that are associated with a decreased (red) or increased (green) desmopressin response are represented by spheres.

Other significant covariates associated with the relative amount of released FVIII after desmopressin administration included route of administration and body weight (Supplemental Figure 3). Relative amount of released FVIII after desmopressin administration was respectively 12% and 27% lower via SC and IN administration compared to IV administration. In addition, relative amount of released FVIII after desmopressin administration increases with body weight using a power function with an estimated exponent of 1.24. We were not able to find a significant effect of VWF levels on relative amount of released FVIII after desmopressin administration. In the structural population PK model, no covariates were included, while the final model incorporated all covariates, resulting in a reduction of inter-individual variability from 141.6% to 78.1% in the relative amount of released FVIII after desmopressin administration. Body weight explained most of the inter-individual variability (53.4%), while the F8 variants explained 7.5% and the remaining covariates explained a further 2.6%.

Simulating the effect of missense Variants on FVIII response using the final PK model

Based on the final model, simulations were performed to display the difference in response for body weight, specific variants, and route of administration (Figure 5). Among the analyzed variants in our population PK model for hemophilia A patients, we identified a subset of variants that demonstrated a significant influence on the PK parameters as shown in table 2, while the remaining variants constituted the reference population with no significant impact on the PK parameters.

The reference population had a FVIII baseline of 0.16 IU/mL, the peak FVIII level was 0.56 IU/mL after desmopressin administration and a FVIII level of >0.30 IU/mL was sustained for 8.8h after desmopressin administration. Supplemental Figure 4 displays the FVIII levels over time after desmopressin administration for the variants that were retained in the final model as they had a significant effect on relative amount of FVIII released after desmopressin administration.

In Figure 5A, variants associated with a lower response compared to the reference population are displayed. Following IV desmopressin administration the presence of variant Pro149Arg (n=13), Gly477Val (n=4) and Tyr450Asn (n=4) resulted in a relative amount of released FVIII after desmopressin administration of respectively 24%, 25% and 56% compared to the reference population (100%). In Figure 5B, variants are displayed with a higher response compared to the reference population The presence of variants Asn637Ser (n=113), Phe2146Ser (n=5), Glu132Asp (n=6), Arg550His (n=11), Ser2030Asn (n=7), Thr74Met (n=5) and Arg717Leu (n=3) resulted in an increased relative amount of released FVIII after desmopressin administration of respectively 199%, 219%, 231%,

252%, 265%, 296% and 336% compared to the response in the reference population (100%). Both route of administration and weight were covariates identified to have a significant effect on relative amount of released FVIII. Figure 5C displays the difference in response between intravenous, subcutaneous, and intranasal administration. Lastly, figure 5D shows the difference in response between various body weights. These data indicated that intravenous administration and a larger body weight were associated with higher FVIII peak levels.
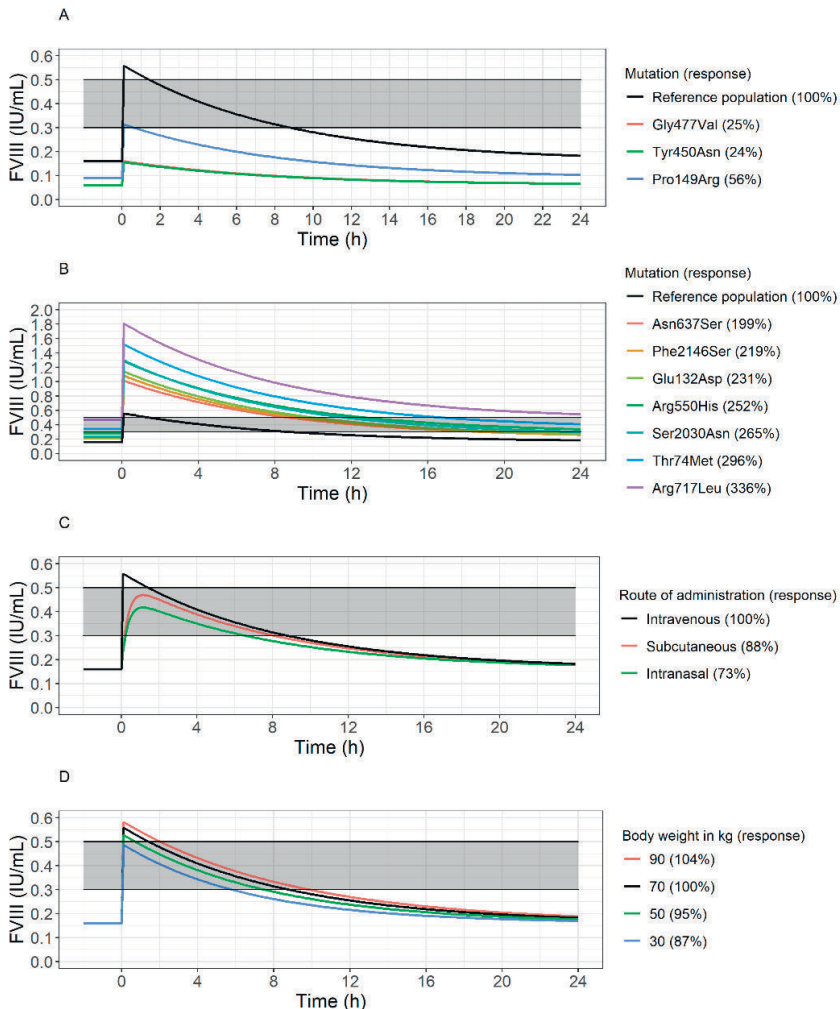
Figure 5. Simulated FVIII plasma levels over time after desmopressin administration in the typical hemophilia A patients. 5A and 5B) display desmopressin response after intravenous desmopressin administration in the reference population and in patients with specific mutations. 5C) displays desmopressin response after intravenous, subcutaneous and intranasal desmopressin administration in the total population. 5D) displays desmopressin response after intravenous desmopressin administration in patients with varying body weights. The shaded grey areas correspond with FVIII levels between 0.30 and 0.50 IU/mL, indicating a partial response to desmopressin.

Discussion

In the present study, we combine population PK analysis with a SHAP analysis to assess the impact of patient characteristics on desmopressin response; in particular the role of the F8 variants. Notably, the utilization of machine learning techniques enabled evaluation of F8 variants that occurred in very few patients, thereby enhancing our insight into the way that these variants affect the pharmacokinetics of desmopressin response. In total, 55 F8 missense variants were evaluated. Of these, ten missense variants had a significant effect on FVIII release after desmopressin administration. Moreover, we observed that IV administration leads to higher responses compared to SC and IN administration. Previously, FVIII levels upon treatment with desmopressin have been reported to correlate to several patient characteristics including route of administration and genetic FVIII variants associated with hemophilia A[26,27,37,38].

Three missense variants (Pro149Arg, Gly477Val and Tyr450Asn) were significantly associated with a reduced relative amount of released FVIII after desmopressin administration compared to the reference population. Pro149Arg and Gly477Val have been reported to lead to a poor desmopressin response [20,39]. Although these three variants have various mechanistic associations, they may be linked to a defect in FVIII synthesis. Pro149Arg is in a highly conserved region in the A1 domain, that is also predicted to be important for maintaining the correct structure of FVIII, while Gly477Val and Tyr450Asn are in the A2 domain[40]. Tyr450Asn may hamper stability of the A2 domain and Gly477Val has been associated with rapid clearance[26]. These variants may therefore reflect misfolding of FVIII thereby reducing FVIII storages.

Conversely, we identified seven missense variants (Thr74Met, Glu132Asp, Arg550His Asn637Ser, Arg717Leu, Ser2030Asn and Phe2146Ser) that were associated with an increased relative amount of released FVIII after desmopressin administration in our final population PK model compared to the reference population. Five of these (Glu132Asp, Arg550His, Asn637Ser, Ser2030Asn, Phe2146Ser) have previously been noted in patients that respond well to desmopressin[26,27]. To our knowledge, the two remaining variants, Thr74Met and Arg717Leu, have not been reported in any study investigating desmopressin response. According to the SHAP analysis, Asn637Ser had the largest effect on the relative amount of released FVIII after desmopressin administration. Interestingly, this variant has been observed to induce intracellular accumulation due to impaired secretion in transfected C127 cells[41]. It is tempting to speculate that this also occurs in vivo, resulting in an increased storage of FVIII in Weibel Palade bodies that is released upon desmopressin treatment.

Variants Ser2030Asn and Glu132Asp have previously been shown to lead to a decreased stability of FVIII in the circulation[42]. Intriguingly, these variants are located at the interface between two domains or a binding partner and may thus be associated with a disruption of interdomain association[43]. For example, Ser2030Asn is a missense variant in the A3 domain that alters the A1/ A3 interface, while variant Glu132Asp is located on the surface of A1, in proximity of A3[4,44,45]. Accordingly, these variants may reduce the ability to support the interaction between the A domains, resulting in a decreased stability of FVIII which may be reflected by a reduction of activity. Although FVIII peak levels may be quite high upon initial release, the activity of FVIII may decrease rapidly. The reason for the other variants to show an increased response to desmopressin remains to be established. We propose that their storage might be intact but upon release, these variants may rapidly become non-functional.

Though Thr74Met is a novel variant that has not been described before, variants in the neighboring positions 72, 73, and 75, have been previously observed in hemophilia A patients[4,45]. Amino acids in this region of the A1 domain are highly conserved across several primate species, implying that they are indeed important for the proper functioning of FVIII. Remarkably, some of these variants are also often associated with a higher FVIII baseline suggesting that these variants have no major hindering effects on the synthesis, storage or release of FVIII[46].

Surprisingly, some substitutions at the same amino acid position presented different SHAP values, e.g. the missense variants in position 550 at the A2 domain. This is normally an Arginine that forms a hydrogen bond with Arginine in position 282 (A1 domain) stabilizing domains A2 and A1. The substitution Arg550Cys had a negative SHAP value, whilst Arg550His had a positive one. Like Arg550Cys, Arg550His also disrupts the hydrogen bonding with Arg282[47], but the substitution for a Cysteine is predicted to have more disruptive consequences by SIFT, PROVEAN and GRANTHAM scores[4]. In addition, two distinct missense variants in position 717 were associated with a positive SHAP value of different magnitude, namely Arg717Leu and Arg717Trp. Notoriously, these two variants have been reported to have an impact on the stability of FVIII as they also lie on the interface of the A2 domain with A1 domain[48].

Consistent with previous literature, the route of administration has a significant impact on the relative amount of released FVIII. IV administration of desmopressin was most effective in increasing FVIII plasma levels[13]. It has previously been shown that VWF protects FVIII from fast clearance from circulation[49]. As desmopressin administration also increases VWF levels, the role of VWF increase as a covariate was also addressed in this study. We were not able to find a significant additional effect of the rise in VWF on the

relative amount of released FVIII after desmopressin administration. This may suggest that the level of VWF prior to desmopressin administration is sufficient to stabilize the increased level of FVIII in the circulation.

Some limitations were experienced when developing the population PK model. Firstly, high variability was observed in response to desmopressin within the variant groups. When we tested the significance of each variant on the PK parameters, many variants had a high relative standard error (>50%) value due to low frequency within the dataset, indicating the imprecision in estimating the effects of certain variants on desmopressin response. As response data of several FVIII variants occurred less than ten times in our data set (Supplement table 1) the effect of variants on the PK parameters is difficult to establish with such low frequency[50]. Secondly, only 77 FVIII samples were measured around 24h after desmopressin administration. The limited data hindered investigating the influence of missense variants on FVIII clearance. Thirdly, only a limited number of patients (n=40) had received IN administration compared to IV (n=891) and SC (n=510) administration. SC and IN routes were utilized as covariates for PK parameter estimation. The discrepancy in sample sizes may have impacted the robustness regarding IN administration. However, despite this smaller IN sample size, population PK models have been successfully developed with fewer than 40 patients. Future studies with a more balanced representation across all administration routes would be essential to strengthen the generalizability and precision of the observed PK relationships.

In conclusion, by using novel ML techniques, we Identified ten missense variants that had a significant effect on the relative amount of released FVIII after desmopressin administration. Moreover, IV administration leads to higher responses compared to SC and IN administration. This information can be utilized to optimize the use of desmopressin in patients with non-severe hemophilia A, as identifying the specific F8 mutation may improve the prediction of a patient's response to desmopressin. Moreover, these insights also contribute to our understanding of the clinical impact of the molecular mechanism associated with these F8 missense variants.

REFERENCES

1.   Franchini M, Mannucci P. Past, present and future of hemophilia: a narrative review. *Orphanet J Rare Dis*. 2012;7(1):24. doi:10.1186/1750-1172-7-24

2.   Blanchette VS, Key NS, Ljung LR, Manco-Johnson MJ, van den Berg HM, Srivastava A. Definitions in hemophilia: communication from the SSC of the ISTH. *J Thromb Haemost*. 2014;12(11):1935-1939. doi:10.1111/JTH.12672

3.   Santagostino E, Mancuso ME, Tripodi A, et al. Severe hemophilia with mild bleeding phenotype: molecular characterization and global coagulation profile. *J Thromb Haemost*. 2010;8(4):737-743. doi:10.1111/J.1538-7836.2010.03767.X

4.   McVey JH, Rallapalli PM, Kemball-Cook G, et al. The European Association for Haemophilia and Allied Disorders (EAHAD) Coagulation Factor Variant Databases: Important resources for haemostasis clinicians and researchers. *Haemophilia*. 2020;26(2):306-313. doi:10.1111/hae.13947

5.   Loomans JI, van Velzen AS, Eckhardt CL, et al. Variation in baseline factor VIII concentration in a retrospective cohort of mild/moderate hemophilia A patients carrying identical F8 mutations. *J Thromb Haemost*. 2017;15(2):246-254. doi:10.1111/jth.13581

6.   Swystun LL, Ogiwara K, Rawley O, et al. *Genetic Determinants of VWF Clearance and FVIII Binding Modify FVIII Pharmacokinetics in Pediatric Hemophilia A Patients*.; 2019.

7.   LOLLAR P. The Association of Factor VIII With von Willebrand Factor. *Mayo Clin Proc*. 1991;66(5):524-534. doi:10.1016/S0025-6196(12)62395-7

8.   Camire RM, Bos MHA. The molecular basis of factor V and VIII procofactor activation. *J Thromb Haemost*. 2009;7(12):1951-1961. doi:10.1111/j.1538-7836.2009.03622.x

9.   Van Galen J, Freato N, Przeradzka MA, et al. Hydrogen-Deuterium Exchange Mass Spectrometry Identifies Activated Factor IX-Induced molecular Changes in Activated Factor VIII. *Thromb Haemost*. 2021;121(5):594-602. doi:10.1055/s-0040-1721422

10. Freato N, Ebberink EHTM, van Galen J, et al. Factor VIII-driven changes in activated Factor IX explored by Hydrogen-Deuterium eXchange Mass Spectrometry. *Blood*. Published online July 2020. doi:10.1182/blood.2020005593

11. Schuijt TJ, Bakhtiari K, Daffre S, et al. Factor XA activation of factor v is of paramount importance in initiating the coagulation system: Lessons from a tick salivary protein. *Circulation*. 2013;128(3):254-266. doi:10.1161/CIRCULATIONAHA.113.003191

12. Jacquemin M, Lavend'homme R, Benhida A, et al. A novel cause of mild/moderate hemophilia A: mutations scattered in the factor VIII C1 domain reduce factor VIII binding to von Willebrand factor. *Blood*. 2000;96(3):958-965. doi:10.1182/blood.v96.3.958

13. Fijnvandraat K, Cnossen MH, Leebeek FWG, Peters M. Diagnosis and management of haemophilia. *BMJ*. 2012;344:e2707-e2707. doi:10.1136/bmj.e2707

14. Kloosterman FR, Zwagemaker AF, Bagot CN, et al. The bleeding phenotype in people with nonsevere hemophilia. *Blood Adv*. 2022;6(14):4256-4265. doi:10.1182/bloodadvances.2022007620

15. Mannucci, Pier M, Pareti FI, Ruggeri ZM, Capitanio A. DDAVP: a new pharmacological approach to the management of haemophilia and von Willebrand's disease. *Lancet*. 1977;(April):869-872.

16. Mannucci PM, Bianchi A, Hemophilia B, Center T. *DESMOPRESSIN (DDAVP) IN THE TREATMENT OF BLEEDING DISORDERS Revised Edition*.; 2012.

17. D.L. DeWald BB. ADMINISTRATION OF DESMOPRESSIN HEMOPHILIACS (DDAVP) TO D . L . Dewald , Division and R . E . Smith of Hematology , University Hospital , The Ohio State University , Columbus , OH 43210 that VIII-C ,. 1980;(c).

18.   Wang HH, Liu M, Portincasa P, Wang DQH. Recent Advances in the Critical Role of the Sterol Efflux Transporters ABCG5/G8 in Health and Disease. *Adv Exp Med Biol*. 2020;1276:105. doi:10.1007/978-981-15-6082-8_8

19.   Stoof SCM, Schütte LM, Leebeek FWG, Cnossen MH, Kruip MJHA. Desmopressin in haemophilia: The need for a standardised clinical response and individualised test regimen. *Haemophilia*. 2017;23(6):861-867. doi:10.1111/hae.13295

20.   Stoof SCM, Sanders Y V., Petrij F, et al. Response to desmopressin is strongly dependent on F8 gene mutation type in mild and moderate haemophilia A. *Thromb Haemost*. 2013;109(3):440-449. doi:10.1160/TH12-06-0383

21.   Levi MM, Vink R, de Jonge E. Management of bleeding disorders by prohemostatic therapy. *Int J Hematol*. 2002;76 Suppl 2:139-144. doi:10.1007/BF03165104

22.   Di Perna C, Riccardi F, Franchini M, Rivolta G, Pattacini C, Tagliaferri A. Clinical efficacy and determinants of response to treatment with desmopressin in mild hemophilia A. *Semin Thromb Hemost*. 2013;39(7):732-739. doi:10.1055/s-0033-1354418

23.   Revel-Vilk S, Blanchette VS, Sparling C, Stain AM, Carcao MD. DDAVP challenge tests in boys with mild/moderate haemophilia A. *Br J Haematol*. 2002;117(4):947-951. doi:10.1046/j.1365-2141.2002.03507.x

24.   Candy V, Whitworth H, Grabell J, et al. A decreased and less sustained desmopressin response in hemophilia A carriers contributes to bleeding. *Blood Adv*. 2018;2(20):2629-2636. doi:10.1182/bloodadvances.2018023713

25.   Loomans JI, Kruip MJHA, Carcao M, et al. Desmopressin in moderate hemophilia a patients: A treatment worth considering. *Haematologica*. 2018;103(3):550-557. doi:10.3324/haematol.2017.180059

26.   Castaman G, Mancuso ME, Giacomelli SH, et al. Molecular and phenotypic determinants of the response to desmopressin in adult patients with mild hemophilia A. *J Thromb Haemost*. 2009;7(11):1824-1831. doi:10.1111/j.1538-7836.2009.03595.x

27.   Stoof S, Sanders Y, Petrij F, et al. Response to desmopressin is strongly dependent on F8 gene mutation type in mild and moderate haemophilia A. *Thromb Haemost*. 2013;109(3):440-449.

28.   Sibieude E, Khandelwal A, Hesthaven JS, Girard P, Terranova N. Fast screening of covariates in population models empowered by machine learning. *J Pharmacokinet Pharmacodyn*. 2021;48(4):597-609. doi:10.1007/s10928-021-09757-w

29.   Lundberg SM, Erion G, Chen H, et al. From local explanations to global understanding with explainable AI for trees. *Nat Mach Intell 2020 21*. 2020;2(1):56-67. doi:10.1038/s42256-019-0138-9

30.   Janssen A, Hoogendoorn M, Cnossen MH, et al. Application of SHAP values for inferring the optimal functional form of covariates in pharmacokinetic modeling. *CPT Pharmacometrics Syst Pharmacol*. 2022;11(8):1100-1110. doi:10.1002/psp4.12828

31.   De Jager NCB, Heijdra JM, Kieboom Q, et al. Population Pharmacokinetic Modeling of von Willebrand Factor Activity in von Willebrand Disease Patients after Desmopressin Administration. *Thromb Haemost*. 2020;120(10):1407-1416. doi:10.1055/s-0040-1714349

32.   Bauer RJ. NONMEM Tutorial Part I: Description of Commands and Options, With Simple Examples of Population Analysis. *CPT Pharmacometrics Syst Pharmacol*. 2019;8(8):525-537. doi:10.1002/psp4.12404

33.   Keizer RJ, Karlsson MO, Hooker A. Modeling and simulation workbench for NONMEM: Tutorial on Pirana, PsN, and Xpose. *CPT Pharmacometrics Syst Pharmacol*. 2013;2(6):1-9. doi:10.1038/psp.2013.24

34. Lindbom L, Ribbing J, Jonsson EN. Perl-speaks-NONMEM (PsN) - A Perl module for NONMEM related programming. *Comput Methods Programs Biomed*. 2004;75(2):85-94. doi:10.1016/j.cmpb.2003.11.003

35. Björkman S, Oh M, Spotts G, et al. Population pharmacokinetics of recombinant factor VIII: the relationships of pharmacokinetics to age and body weight. *Blood*. 2012;119(2):612-618. doi:10.1182/blood-2011-07-360594

36. Nguyen THT, Mouksassi MS, Holford N, et al. Model evaluation of continuous data pharmacometric models: Metrics and graphics. *CPT Pharmacometrics Syst Pharmacol*. 2017;6(2):87-109. doi:10.1002/psp4.12161

37. Seary M, Feldman D, Carcao M. DDAVP responsiveness in children with mild or moderate haemophilia A correlates with age, endogenous FVIII:C level and with haemophilic genotype. *Haemophilia*. 2012;18(1):50-55.

38. Nance D, Fletcher S, Bolgiano D, Thompson A, Josephson N, Konkle B. Factor VIII mutation and desmopressin-responsiveness in 62 patients with mild haemophilia A. *Haemophilia*. 2013;19(5):720-726.

39. Castaman G, Mancuso ME, Giacomelli SH, et al. Molecular and phenotypic determinants of the response to desmopressin in adult patients with mild hemophilia A. *J Thromb Haemost*. 2009;7(11):1824-1831. doi:10.1111/j.1538-7836.2009.03595.x

40. Thompson AR. Structure and function of the factor VIII gene and protein. *Semin Thromb Hemost*. 2003;29(1):11-22. doi:10.1055/s-2003-37935

41. Roelse JC, De Laaf RTM, Timmermans SMH, Peters M, Van Mourik JA, Voorberg J. Intracellular accumulation of factor VIII induced by missense mutations Arg593→Cys and Asn618→Ser explains cross-reacting material-reduced haemophilia A. *Br J Haematol*. 2000;108(2):241-246. doi:10.1046/j.1365-2141.2000.01834.x

42. REPESSÉ Y, SLAOUI M, FERRANDIZ D, et al. Factor VIII (FVIII) gene mutations in 120 patients with hemophilia A: detection of 26 novel mutations and correlation with FVIII inhibitor development. *J Thromb Haemost*. 2007;5(7):1469-1476. doi:10.1111/j.1538-7836.2007.02591.x

43. Pipe SW, Saenko EL, Eickhorst AN, Kemball-Cook G, Kaufman RJ. Hemophilia A mutations associated with 1-stage/2-stage activity discrepancy disrupt protein-protein interactions within the triplicated A domains of thrombin-activated factor VIIIa. *Blood*. 2001;97(3):685-691. doi:10.1182/blood.V97.3.685

44. Liu ML, Murphy MEP, Thompson AR. A domain mutations in 65 haemophilia a families and molecular modelling of dysfunctional factor VIII proteins. *Br J Haematol*. 1998;103(4):1051-1060. doi:10.1046/j.1365-2141.1998.01122.x

45. EAHAD CF DB Factor VIII Gene (F8) Variant Database.

46. Margaglione M, Castaman G, Morfini M, et al. The Italian AICE-Genetics hemophilia a database: Results and correlation with clinical phenotype. *Haematologica*. 2008;93(5):722-728. doi:10.3324/haematol.12427

47. Morichika S, Shima M, Kamisue S, et al. Factor VIII gene analysis in Japanese CRM-positive and CRM-reduced haemophilia A patients by single-strand conformation polymorphism. *Br J Haematol*. 1997;98(4):901-906. doi:10.1046/j.1365-2141.1997.2963113.x

48. Hill M, Deam S, Gordon B, Dolan G. Mutation analysis in 51 patients with haemophilia A: Report of 10 novel mutations and correlations between genotype and clinical phenotype. *Haemophilia*. 2005;11(2):133-141.

2

49. Przeradzka MA, Galen J van, Ebberink EHTM, et al. D' domain region Arg782-Cys799 of von Willebrand factor contributes to factor VIII binding. *Haematologica*. 2020;105(6):1695-1703. doi:10.3324/HAEMATOL.2019.221994

50. Wählby U, Jonsson EN, Karlsson MO. Assessment of actual significance levels for covariate effects in NONMEM. *J Pharmacokinet Pharmacodyn*. 2001;28(3):231-252. doi:10.1023/A:1011527125570

SUPPLEMENT

Supplemental Table 1. Mutation and frequency in dataset

Mutation	n
Asn637Ser	113
Arg612Cys	105
Arg2169His	44
Arg2178Cys	34
Arg550Cys	21
Leu644Val	21
Asp1260Glu	15
Val2035Ala	15
Val181Met	13
Tyr530His	13
Pro149Arg	13
Arg1960Gln	12
Arg550His	11
Arg717Trp	8
Leu1777Phe	8
Ser2030Asn	7
Thr154Ala	6
Ser308Leu	6
Ala563Gly	6
Glu132Asp	6
Ala219Thr	5
Arg391His	5
c.-257T>G	5
Arg2169Cys	5
Tyr2124Cys	5
Tyr1998Cys	5
Thr74Met	5
Phe2146Ser	5
Arg1708His	5
Leu2229Phe	5
Gly498Arg	5
Gln664His	5
Asp186Glu	4
Arg546Trp	4
Ala1834Val	4
Val502Gly	4
Tyr450Asn	4

2

Mutation	n
Pro2319Leu	4
Leu523Leu	4
Ile192Thr	4
Gly477Val	4
Gly1729Glu	4
Glu291Lys	4
Gln2265Arg	4
Arg717Leu	3
Arg2326Gln	3
Trp2248Cys	3
Ser714Leu	3
Pro1873Leu	3
Pro1844Ser	3
Leu562Pro	3
Ala723Thr	3
His1980Tyr	3
Glu72Asp	3
Glu2247Asp	3
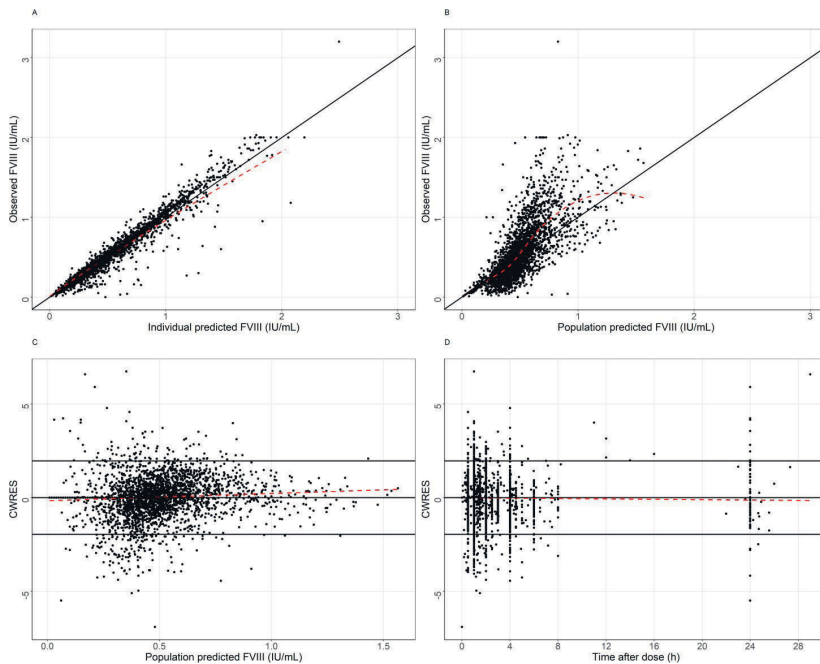
Supplemental Figure 1. Goodness-of-fit plots of the final pharmacokinetic model of FVIII. A) Individual predicted (IPRED) vs observed concentrations, B) Population predicted (PRED) vs observed concentrations, C) Conditional weighted residuals (CWRES) vs PRED, D and H) Time after administration vs CWRES. The solid line is the line of identity. The dashed line represents the local regression smooth line (loess smooth).
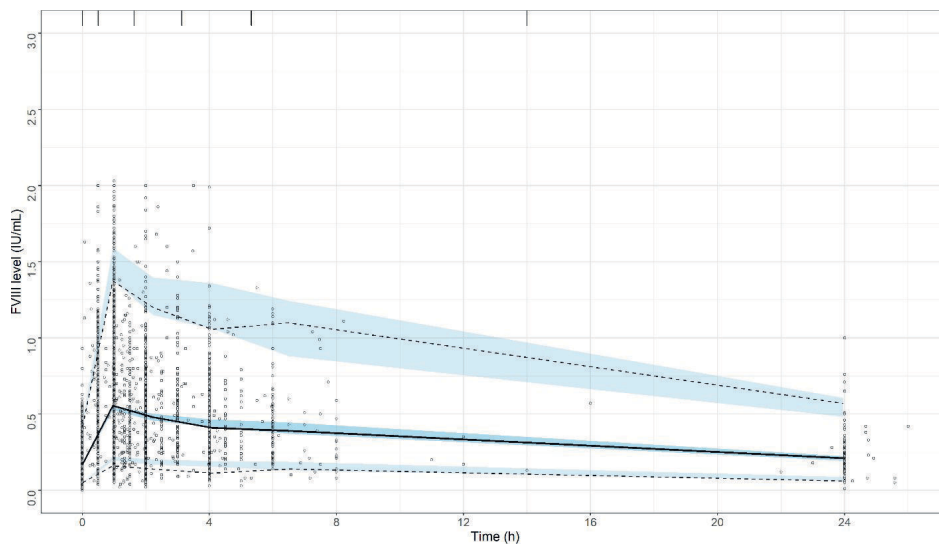
Supplemental Figure 2. Prediction corrected visual predictive (pcVPC) check of the final pharmacokinetic model of FVIII. Dots represent observed FVIII levels; the solid black line represents the 50th percentile of observed data; the dashed black lines represent the 5th and 95th percentiles of the population model. Shaded areas depict the model predicted 95% confidence intervals of the simulated percentiles. Most of the FVIII levels are within the 95% confidence interval.
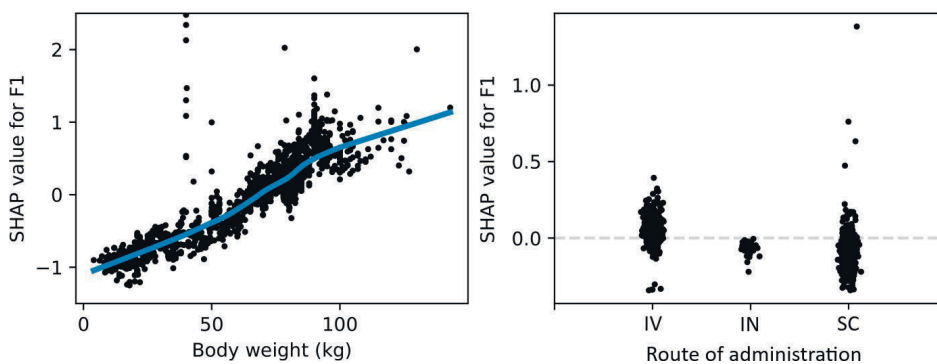
Supplemental Figure 3. Effect of body weight and route of administration on the desmopressin response using SHAP analyses. SHAP values for FVIII increase (F1) Left) on Body weight and Right) Route of administration. IV= Intravenous, IN=Intranasal, SC=Subcutaneous. SHAP = SHapley Additive exPlanations;
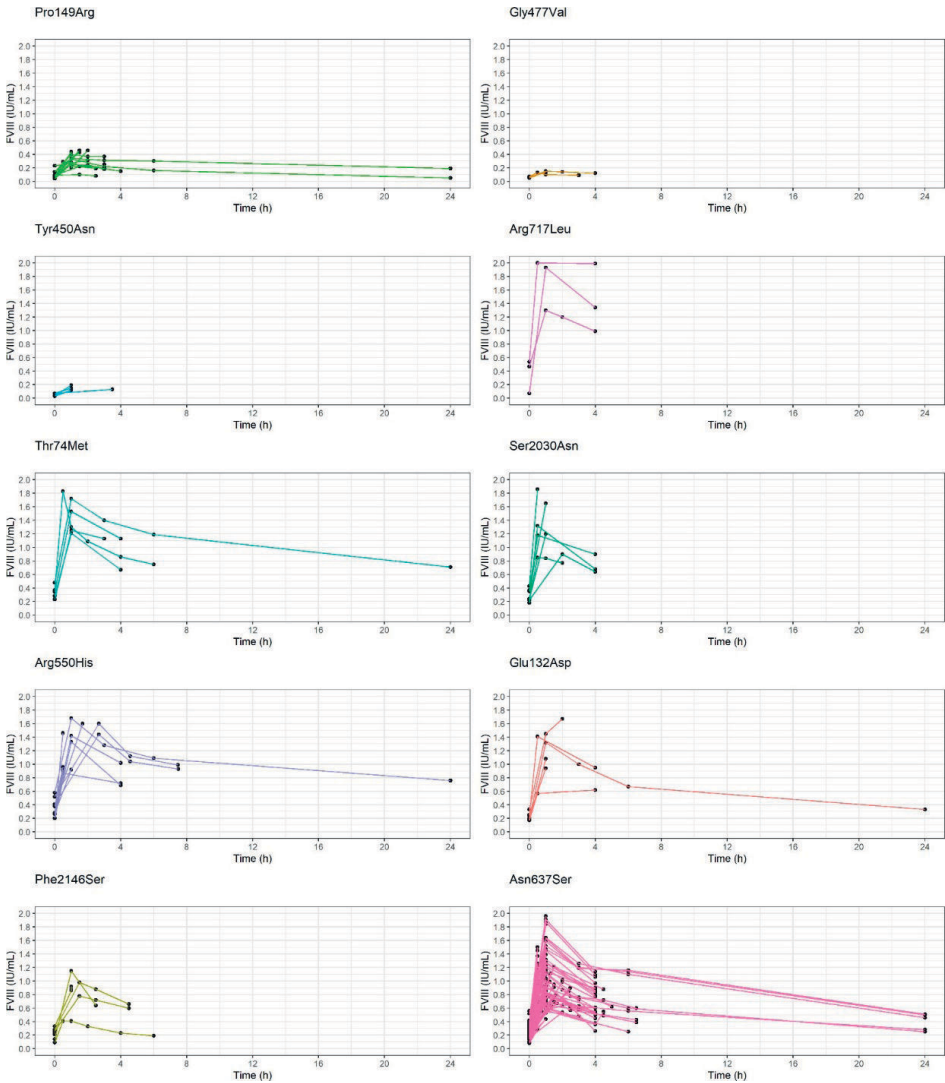
Supplemental Figure 4. Factor VIII levels over time after desmopressin administration. Stratified in the mutation groups that had a significant effect on the response of desmopressin

SUPPLEMENTARY METHODS SECTION

Population PK model development

Development of the model was performed in three steps (i) a structural model with inter-individual variability added, (ii) residual error model and (iii) covariate analysis.

An one and two-compartment model was tested and evaluated. The compartment model with the best fit was selected. Evaluation of the compartment model was based on the goodness-of-fit (GOF) plots, objective function value (OFV) and relative standard error (RSE) of the PK parameters.

GOF plots are graphical representations that allow to visually assess the model's predictions match the observed data. They are used to evaluate the overall performance of the model in describing the data. The OFV is a quantitative measure used in statistical model fitting. It quantifies how well the model fits the observed data. A lower OFV indicates a better fit, as it implies that the model's predictions are closer to the actual data. To assess the significance of the improvement in fit, p-values of 0.05 and 0.01 are commonly used thresholds. A reduction in OFV by a value greater than the critical chi-squared distribution value corresponding to these p-values (i.e., 3.841 for p=0.05 and 6.635 for p=0.01) suggests a statistically significant improvement in model fit.

The RSE is a statistical measure used to assess the precision or reliability of estimated parameters in a model. A lower RSE indicates a more precise estimate, meaning that the parameter's value is well-determined with relatively small uncertainty. Whereas, a higher RSE suggests that the estimate is less precise and may have more uncertainty.

Allometric body weight scaling was included on the PK parameters in the structural model. on clearance (CL) and central volume of distribution (V) (equation 1):

$$\theta_{pop\ PK} = \theta_{pk} \times \left(\frac{Bodyweight}{70} \right)^{\theta_{exp}}$$

$$(1)$$

In which, $\theta_{pop\ PK}$ is the typical population value for a PK parameter dependent on bodyweight, θ_{pk} is the typical PK value for a patient with a body weight of 70 kg, and θ_{exp} is an exponent fixed at 0.75 for CL and 1 for V.

The individual PK parameters were described by using equation 2.

$$\theta_i = \theta_{pop\ PK} \times exp^{\eta i}$$

$$(2)$$

In which, θ_i is the estimated individual PK parameter of the i$^{\text{th}}$ individual, $\theta_{pop\,PK}$ is the typical population value for a PK parameter, ηi is the inter-individual variability from normal distribution with a mean of zero and estimated variance of ω^2 of the i$^{\text{th}}$ individual.

Regarding the residual error model, we explored three different approaches: additive error (described by equation 3), proportional error (as shown in equation 4), and a combined error model (which combines the equations 2 and 3). In these equations, Yij represents the predicted concentration for individual *i* at time *j* $f(\theta,\,\eta i,\,x_{ij})$corresponds to the individual's concentration prediction at time *j*, and ε signifies the residual error arising from a normal distribution with a mean of zero and an estimated variance of σ^2.

$$Y_{ij} = f\left(\theta, \eta i, x_{ij}\right) + \varepsilon_{ij}$$

(3)

$$Y_{ij} = f\left(\theta, \eta_i, x_{ij}\right) \times (1 + \varepsilon_{ij})$$

(4)

Continuous covariates were included by a power model, involving the centering of the covariate around its median value, while the exponent was estimated as indicated in equation 5. On the other hand, categorical covariates were handled using flag variables, where values of 1 and 0 represented "true" and "false" conditions, respectively, as outlined in equation 6.

$$\theta_{pop} = \theta_{pk} \times \left(\frac{Cov}{Cov_{median}}\right)^{\theta_{exp}}$$

(5)

$$\theta_{pop} = \theta_{pk} \times (\theta_1^{Flag1} \times \theta_2^{Flag2} \times \theta_3^{Flag3} \cdots)$$

(6)

A stepwise approach involving both forward inclusion and backward exclusion was used for covariate assessment. During forward inclusion, a reduction in the objective function value (OFV) of 3.84 or more (with a corresponding p-value of 0.05) was considered statistically significant. In the backward exclusion process, an increase in OFV of 6.64 or more (with a corresponding p-value of 0.01) was deemed significant. The covariate that led to the most substantial reduction in OFV was initially incorporated into the model. Subsequently, other covariates that demonstrated significant OFV reductions were systematically added to the covariate model in a sequential manner. This process was repeated iteratively until all relevant covariates exhibiting significant effects were included in the final model.

Internal validation

A nonparametric bootstrap method was used for internal validation. The bootstrap method is a resampling technique that is used to assess the robustness of parameter estimates and the uncertainty associated with them. One thousand bootstrap data sets

were generated by resampling from the original data set. Median parameter values and the 2.5th-97.5th percentile from bootstrap estimates were compared with the final model estimates. Moreover, a prediction-corrected visual predictive check (pcVPC) was also performed by simulating 1,000 patients to evaluate the predictive performance of the final model. Visual checks were performed by overlaying the observed data points with the 95%CI of the simulated 5th, 50th, and 95th percentile curves.

Visualizing learned covariate effects using SHapley Additive exPlanations

Individual estimates of the PK parameters were obtained from the population PK model. Based on the covariates (patient weight, height, age, route of administration and the presence of each of the FVIII variants) a random forest model was fit to predict these PK parameters. Random forest models were also fit to predict the proportional and absolute increase in FVIII levels following DDAVP administration.

K-fold cross validation was performed with K = 10. Models were fit on the training fold and SHAP values were calculated on the test folds and pooled over all the training replicates in order to obtain the SHAP values for all samples. In the case of the prediction of PK parameters, the SHAP values represent the contribution of each of the covariates to the final prediction in an additive fashion:

$$y = E[y] + s1 + s2 + s3 + \ldots + sX \tag{7}$$

Here E[y] represents the expectation of the dependent variable y (e.g. the increase in FVIII levels) over all samples. The SHAP values are specific to one of the covariates indicated by the subscript. X here represents the number of covariates. After calculating the SHAP values, the SHAP value for each of the samples can be collected and visualized to produce the figures in the main manuscript. By pooling this information we can determine the mean effect of each of the covariates, as well as the variance of the effect. The variance between samples comes from the covariate implementation in random forest.

Covariates with high variance SHAP values combined with a low sample size in specific regions of the covariate space (for example, a low number of patients with a specific mutation) might be indicative of the random forest model overfitting to the data. Even though SHAP values can be used to explain model output it does not mean that we can understand how the model produces predictions. It is thus important to carefully evaluate the results of the analysis to prevent including effects that are only important in the model by correlation rather than causation.

CHAPTER 3

Pharmacokinetic-pharmacodynamic modelling in hemophilia A: Relating thrombin and plasmin generation to factor VIII activity after administration of a VWF/FVIII concentrate

Lars L.F.G. Valke* Michael E. Cloesmeijer,* Hassan Mansouritorghabeh, Wideke Barteling, Nicole M.A. Blijlevens, Marjon H. Cnossen, Ron A.A. Mathôt, Saskia E.M. Schols and Waander L. van Heerde

*Shared first authorship – both equally contributed

ABSTRACT

Background Hemophilia A patients are treated with factor (F) VIII prophylactically to prevent bleeding. In general, dosage and frequency are based on pharmacokinetic measurements. Ideally, an alternative dose adjustment could be based on the hemostatic potential, measured with a thrombin generation assay (TGA), like the Nijmegen Hemostasis Assay.

Objective Investigate the predicted performance of a previously developed pharmacokinetic-pharmacodynamic model for FVIII replacement therapy, relating FVIII dose and FVIII activity levels with thrombin and plasmin generation parameters.

Methods Pharmacokinetic and pharmacodynamic measurements were obtained from 29 severe hemophilia A patients treated with pdVWF/FVIII concentrate (Haemate P®). The predictive performance of the previously developed pharmacokinetic-pharmacodynamic model was evaluated using nonlinear mixed-effects modelling (NONMEM). When predictions of FVIII activity or TGA parameters were inadequate (median prediction error (MPE) >20%), a new model was developed.

Results The original pharmacokinetic -model underestimated clearance and was refined based on a two-compartment model. The pharmacodynamic model display no bias in the observed normalized thrombin peak height and normalized thrombin potential (MPE of 6.83% and 7.46%). After re-estimating pharmacodynamic parameters, EC50 and Emax values were relatively comparable between the original model and this group. Prediction of normalized plasmin peak height was inaccurate (MPE 58.9%).

Conclusion Our predictive performance displayed adequate thrombin pharmacodynamic predictions of the original model, while a new pharmacokinetic model was required. The pharmacodynamic model is not factor specific and applicable for multiple factor concentrates. A prospective study is needed to validate the impact of the FVIII dosing pharmacodynamic model on bleeding reduction in patients.

INTRODUCTION

Hemophilia A is characterized by a deficiency of coagulation factor (F) VIII leading to re-current spontaneous and trauma-induced bleeding.[1] Current guidelines recommend treatment with prophylactic FVIII replacement therapy,[2] bypassing agents (BPAs) in case of inhibitors, [3] and non-factor replacement therapies, such as emicizumab,[4] for hemophilia A patients (FVIII activity level of <1 IU/dL) with the goal to reduce bleeding. [5] Prophylactic or on-demand FVIII replacement therapy is still the mainstay of treat-ment in large parts of the world, as other, more expensive therapies, are not available.[5]

Prophylactic FVIII replacement therapy can be dosed according to body weight and subsequently adjusted based on bleeding episodes or can be pharmacokinetic-based. [3] Increasingly pharmacokinetic guidance is applied using population pharmacokinetic models to individualize dosing and to relate FVIII activity levels to bleeding, as bleeding risk varies significantly between persons with hemophilia.[6, 7] Both strategies exhibit disadvantages as additional bleeding episodes may occur before adequate dosing is achieved.[2] Bayesian forecasting analysis is used to apply limited sampling and to overcome a factor concentrate wash-out period.[8-10] However, this approach relies on plasma factor activity monitoring and does not consider the effect of factor replacement therapy on hemostasis (hemostatic potential or pharmacodynamics) and the inter-individual variation in bleeding tendency is not taken into account.[11]

The thrombin generation assay (TGA) measures the amount of thrombin generated over time and is able to assess hemostasis globally.[12] It has been suggested that throm-bin generation parameters are a better representation of the bleeding phenotype in hemophilia A patients than measurement of FVIII activity level.[13-15] In addition, FVIII replacement therapy can be monitored by TGA and this global hemostatic assay may better reflect the patients bleeding risk in the presence of similar FVIII activity levels after dosing.[14] To date, only two pharmacokinetic-pharmacodynamic models for FVIII replacement therapy have been described in literature,[16, 17] of which one suggests that bleeding can be decreased by intensifying treatment in patients presenting with low thrombin generation parameters.[17]

The previously developed model [16] is based on the Nijmegen Hemostasis Assay (NHA) which incorporates thrombin generation with plasmin generation in one assay. [18] Multiple standard half-life (SHL) FVIII replacement concentrates were used in this model,[16] but the results have not yet been replicated. In the current study, we per-formed a combined pharmacokinetic-pharmacodynamic analysis with the NHA of he-mophilia A patients treated with only plasma-derived von Willebrand factor (VWF)/FVIII

3

(pdVWF/FVIII) concentrate (Haemate P®). Here, we describe the thrombin and plasmin generation parameters of these patients after a single bolus. These data were used to investigate the predictive performance, and eventually adapt, the previously developed pharmacokinetic-pharmacodynamic model by Bukkems et al.[16]

METHODS

Patients

Twenty-nine severe (FVIII activity level <1 IU/dL) adult hemophilia A patients were included in this study between August 1st 2011 and December 20th 2012 in the Ghaem Hospital, Mashhad University of Medical Sciences, Mashhad, Iran. This project was a sub-study of the IMPALA study (registered at the Dutch Trial Register, number NL2808) and it was approved by the Medical Ethical Committee of the Radboud university medical center and of the regional ethics committee of Mashhad University of Medical Sciences (number 89-88215). All patients gave written informed consent and the study was conducted in accordance with the Declaration of Helsinki. Only adult patients (≥18 years) with severe hemophilia A were included. Exclusion criteria were: active bleeding, known allergy to plasma proteins, liver cirrhosis, hepatitis C treated with interferon within six months before inclusion, HIV infection, hemoglobin level <8.0 mmol/l, platelet count <50×10^9/l, difficult venous access, and specific medications known to interact with hemostasis (non-steroidal anti-inflammatory drugs (NSAIDs), platelet aggregation inhibitors, antimicrobials, thyroid inhibitors and selective serotine reuptake inhibitors (SSRIs)).

The pharmacokinetic-pharmacodynamic study was performed with a single bolus of 25 IU/kg pdVWF/FVIII (Haemate P®, CSL Behring, King of Prussia, PA, USA). A standard wash-out period of 72 hours was issued. Plasma samples were obtained before the bolus and at nine time points until 24 hours after the bolus, as described before.[19] Blood samples were collected by venipuncture in 3.2% buffered sodium citrate siliconize blood collection tubes (Becton Dickenson, Plymouth, UK). At baseline hemoglobin, hematocrit, and blood platelets were determined locally and an additional samples were collected for FVIII activity and VWF activity level and inhibitor level determination.

Sample preparation

All blood samples were processed immediately after collection. Platelet poor plasma (PPP) was obtained for NHA measurement by centrifuging the sample at 4200 *g* for 15 minutes at 4°C. The PPP was aliquoted into multiple 1.5 mL tubes for long-term freezer storage. All samples were frozen in liquid nitrogen, stored at -80°C and shipped to the Radboud university medical center, Nijmegen, the Netherlands on dry ice. Samples were

stored at -80°C and were defrosted only once to measure FVIII activity level, VWF activity level, inhibitor levels and the NHA.

FVIII activity level and inhibitor measurement

FVIII activity level was measured with the one-stage (OSA) Cephascreen reagent at the STA Evolution (Stago Group, Asnières sur Seine, France) and chromogenic (CSA) assay (Biophen FVIII:C assay, HYPHEN Biomed SAS, Neuville-sur-Oise, France), according to the manufacturer's instructions at the STA Evolution (Stago Group).

Inhibitor titers were determined with the Nijmegen-modified Bethesda Assay (NBA; cut-off for positivity ≥0.60 NBU/mL),[20, 21] and Nijmegen Low Titer Inhibitor Assay (NLTIA, cut-off for positivity ≥0.04 NLTIU/mL),[22] as previously described.

Nijmegen Hemostasis Assay measurement

The NHA was measured as described before and is described in detail in the supplementary methods.[18, 19] The essential parameters obtained with the NHA are shown in supplementary figure 1. All NHA measurements were performed in batches between 30th September until 23rd November 2015. For all results, the mean of two measurements was used. Normal pooled plasma (NPP) was used as control measurement and to normalize the NHA parameter to the percentage of normal. The absolute NHA parameter of the patient was divided by the mean of the NPP samples that were used in the same run as the patient samples. The reference values of the NHA based on healthy controls (n=20), healthy men and women not using medication interfering with coagulation, are shown in supplementary table 1 and are shown as a gray area in the figures.

Model development

The previously described population pharmacokinetic-pharmacodynamic model was developed by Bukkems et al.[16] The population pharmacokinetic-pharmacodynamic model was developed using nonlinear mixed-effect modelling (NONMEM, version 7.4). Their original pharmacokinetic analysis used 466 samples from 30 patients, while the pharmacodynamic analysis used 252 samples from 24 patients.

To investigate the predictive performance of the previous model in this replication study, two sequential steps were performed using the first-order estimation method in NONMEM. Firstly, the performance in predicting the FVIII activity levels was assessed by the population pharmacokinetic model of Bukkems et al. The relative prediction error (PE%, Eq. 1) was estimated by comparing the predicted population concentrations and the corresponding observations for each subject in the dataset.[23] In which, Cpred is the model predicted value and Cobs is observed value. VWF activity was not measured

after pdVWF/FVIII administration, therefore this covariate effect was not included in evaluating the population pharmacokinetic model. The median prediction error (MPE) and median absolute prediction error (MAPE) were used for the evaluate bias and precision of the models. Model appropriateness was confirmed when the MPE was below 20% with the 95% CI including zero and the MAPE was below 30%.[23]

$$PE\% = \frac{c_{PRED} - c_{OBS}}{c_{OBS}} \times 100$$

(equation 1)

Secondly, if the population model failed to adequately predict the observations, then a novel population model was developed. During the population pharmacokinetic model development, both one and two-compartment models were evaluated. *A priori* allometric scaling of pharmacokinetic parameters by body weight was included in the structural pharmacokinetic model. Inter-individual variability (IIV) was estimated and evaluated for each population pharmacokinetic model parameter. For residual error models, a proportional, an additive and a combined error model were evaluated. Next, associations between covariates and pharmacokinetic parameters were tested to explain the IIV in the pharmacokinetic parameters. The following covariates were tested: age, NLTIA and NBA. During the covariate analysis, stepwise forward inclusion and backward elimination approaches were used. A reduction in the objective function value (OFV) of at least 3.84 ($p < 0.05$, chi-square distribution with 1 degree of freedom) and greater than 6.64 ($p < 0.01$, chi-square distribution with 1 degree of freedom) were required for a covariate to be considered significant in the forward inclusion and backward elimination steps, respectively. The supplement provides further details about the development of the pharmacokinetic model. The individual pharmacokinetic parameters obtained from the pharmacokinetic model were used as input for the population pharmacodynamic model.

To investigate the predictive performance of the pharmacodynamic model by Bukkems et al., a similar approach was used as for the pharmacokinetic part of the model. When the population pharmacodynamic model failed to adequately predict observations, a novel population pharmacodynamic model was developed by using the external pharmacodynamic dataset. A maximum effect (Emax) and a sigmoidal Emax model were tested to describe the relationship between FVIII activity levels and normalized thrombin peak height, normalized thrombin potential and normalized plasmin peak height. Evaluation of the residual error models, addition of IIV to the pharmacodynamic parameters and performance of the covariate analysis were similar to those for the pharmacokinetic model part.

Model evaluations criteria included the change in the OFV, goodness-of-fit (GOF) plots, precision of parameter estimates, decreases in IIV and residual variability, condition number, shrinkage and a successful convergence step.[24] Prediction-corrected visual predictive checks (pcVPCs) were used to assess the predictive performance of the model. The supplement contains more details on the evaluation and development of the models. A schematic overview of the predictive performance of the population pharmacokinetic-pharmacodynamic models is displayed in figure 1.
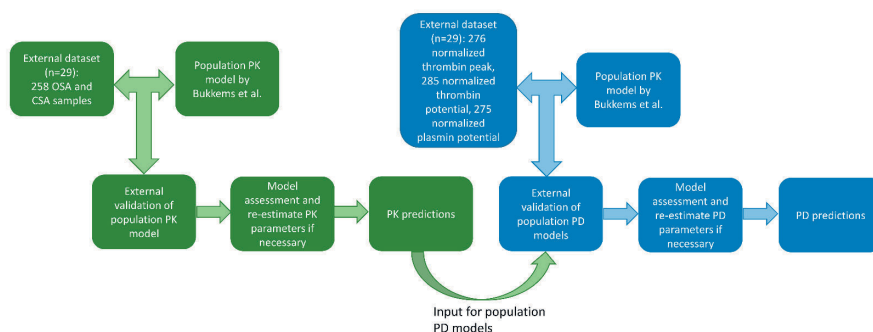
Figure 1: Schematic workflow of predictive performance of population pharmacokinetic-pharmacodynamic models.
CSA, chromogenic substrate assay; OSA, one-stage assay; PD, pharmacodynamic; PK, pharmacokinetic

Statistical analysis

The reported parameters are shown as median (interquartile range; IQR) unless otherwise stated. Descriptive statistics were used for demographic parameters and NHA parameters. Spearman correlation was used for the correlation between FVIII OSA and CSA assay, and for the correlation between FVIII activity level and thrombin generation parameters. For the analysis of differences before and after the FVIII bolus, the Wilcoxon matched-pairs signed ranked tests were used.

Statistical analyses were performed using Prism GraphPad, version 9.4. All *p*-values are two-sided and a *p*-value of less than 0.05 was considered statistically significant.

RESULTS

Patient characteristics

A total of 29 male severe hemophilia A patients were included in the study. The baseline patient characteristics are described in table 1. The median age was 27 years (range 19-53), the mean body weight was 62 kg (SD: 7) and median body weight was 62 kg (range 48-73 kg). The median pre-bolus FVIII activity level was <1 IU/dL, as measured by both the OSA and CSA assay. The correlation of FVIII activity level measured by the OSA and CSA assay was excellent (r=0.96, 95%-confidence interval (95%-CI): 0.95-0.97, *p*<0.0001, see figure 2A). Eight patients had a detectable FVIII activity level pre-bolus with the CSA (5 patients 1 IU/dL and 3 patients 2 IU/dL), while 4 were detectable with the OSA (3 patients 1 IU/dL and 1 patient 2 IU/dL).

Table 1: Baseline characteristics of the 29 included patients

Characteristic	Value
Age, median (range), in years	27 (19-53)
Body weight, in kg Mean (SD) Median (range)	 62 (7) 62 (48-73)
Baseline values	
Baseline one stage FVIII concentration in IU/dL, median (range)	<1 (<1-2)
Baseline chromogenic FVIII concentration in IU/dL, median (range)	<1 (<1-3)
Baseline VWF concentration in %, mean (SD)	117 (46)
Total pharmacokinetic number samples	
OSA	258
CSA	258
Total pharmacodynamic number samples[a]	287
FVIII product and dosage	
Haemate P, n (%)	29 (100)
Dosage FVIII replacement therapy, median (IQR)	1600 (1500-1700)
Dosage FVIII/kg, median (IQR), in IU/kg	25.0 (24.6-25.4)
FVIII half-life in hours, median (IQR)	10.6 (8.3-12.9)
Inhibitor positivity	
NBA, n (%)	1 (3)
NLTIA, n (%)	7 (24)

Abbreviations: CSA, chromogenic substrate assay; FVIII, factor VIII; IQR, interquartile range; NBA, Nijmegen Bethesda Assay; NLTIA, Nijmegen Low Titer Inhibitor Assay; OSA, one-stage assay; SD, standard deviation.
[a] Of the normalized thrombin peak height and normalized plasmin potential, 9 and 10 measurements were not detectable, respectively.

The mean VWF activity level before the bolus was 117% (SD 43%). All 29 patients received the same pdVWF/FVIII concentrate, with a median bolus of 1600 IU FVIII (IQR 1500-1700 IU), corresponding to 25 IU/kg FVIII (24.6-25.4). One patient had an inhibitor detected with the NBA (titer 1.1 NBU/mL), while six additional patients had an inhibitor measured with the NLTIA (titer 0.04-0.05 NLTIU/mL), all patients were included in the analysis. For the population pharmacokinetic -analysis, all 258 FVIII activity levels measured with OSA and CSA were used. The FVIII activity level measured before pdVWF/FVIII concentrate administration was considered to be the endogenous baseline and subtracted from the observed FVIII activity levels during model development. One patient had a FVIII activity level that was not detectable at 24 hours after administration. In one patient, 3 samples at 3, 5 and 15 min were missing. In the full dataset 5.2% (OSA) and 4.2% (CSA) of the samples were below the detection limit of the assay, mostly samples taken before pdVWF/FVIII administration. These samples were excluded in the pharmacokinetic data analysis.
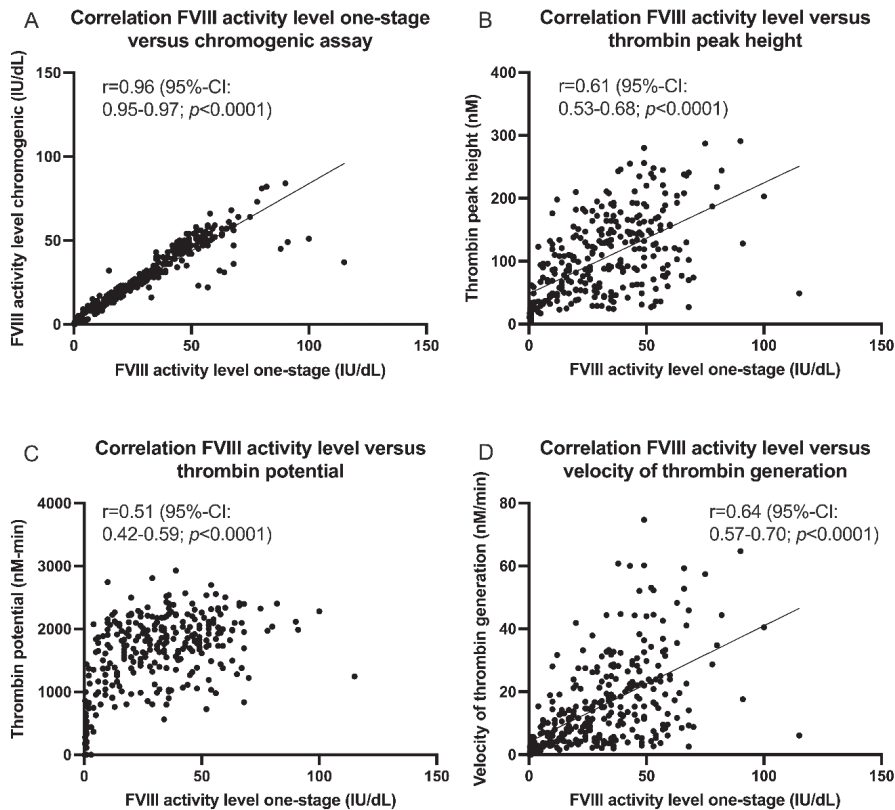
3

Figure 2: Correlations of factor VIII activity level with thrombin generation parameters. (A) Correlation between factor VIII activity level determined with the one stage assay and chromogenic assay. Correlation of factor VIII activity level with (B) thrombin peak height, (C) thrombin potential and (D) velocity of thrombin generation.

Pharmacokinetic measurements

After the bolus injection, FVIII activity level increased to 52 IU/dL (42-62; see figure 3A and supplementary table 2) after 15 minutes, which was the anticipated increase with the amount of infused FVIII concentrate. At 1 hour FVIII activity level was 46 IU/dL (35-53), at 6 hours 29 IU/dL (19-35) and 7 IU/dL (4-10) at 24 hours post the bolus. This led to a median FVIII half-life of 10.6 hours (8.3-12.9).
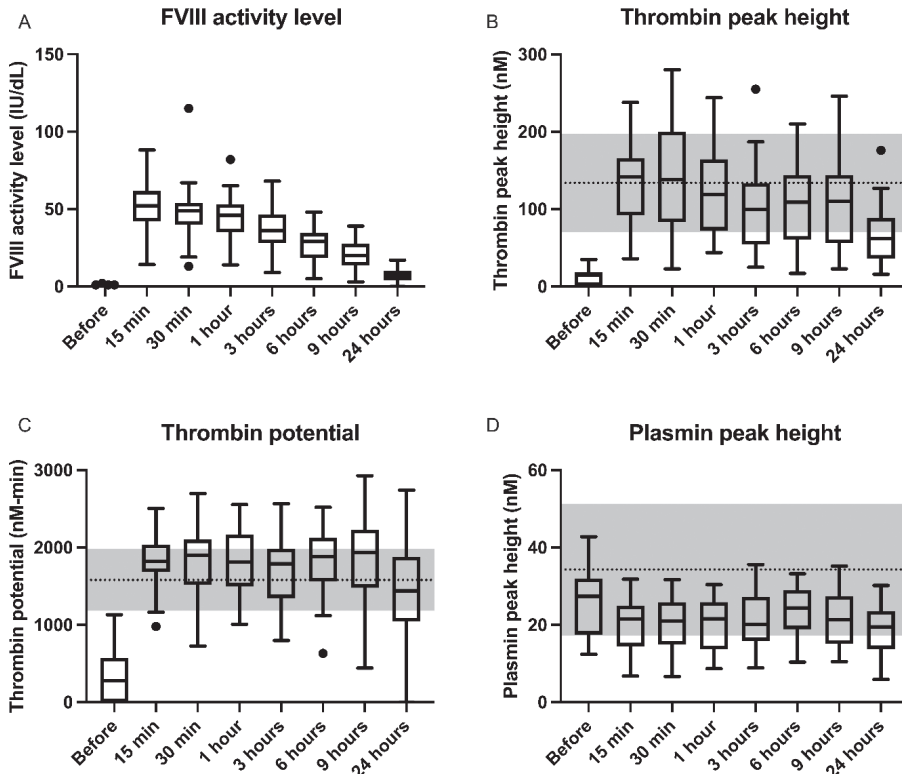
Figure 3: Factor VIII activity level, thrombin peak height, thrombin potential and plasmin peak height after a bolus of factor VIII replacement therapy.

Thrombin and plasmin generation

Thrombin generation parameters were low at baseline but differed between patients as illustrated by the large range of obtained results (figure 3B, 3C). At baseline, thrombin peak height was 15 nM (undetectable-19; figure 3B), thrombin potential was 280 nM-min (undetectable-280; figure 3C) and plasmin peak height was within the normal range despite the low thrombin generation (median 27.4 (IQR 17.5-32.0); figure 3D). The other parameters are shown in supplementary figure 2 and supplementary table 2.

After the FVIII bolus, parameters increased rapidly to near normal values (figure 3, supplementary figure 3 and supplementary table 2). Thrombin peak height rose to 142 nM (92-166) at 15 minutes and decreased slowly to 109 nM (61-144) at 6 hours and to 62 nM (37-89) after 24 hours. The increase in thrombin potential persisted even longer, with 1823 nM-min (1683-2028) at 15 minutes, 1886 nM-min (1565-2128) at 6 hours and 1440 nM-min (1044-1878) after 24 hours. This is best illustrated with plasmin peak height which was 21.5 nM (14.5-25.0) at 15 minutes after the bolus and persisted at this low level with higher thrombin generation (plasmin peak height 24.4 nM (18.9-29.0) at 6 hours and 19.5 nM (13.8-23.6) after 24 hours). With the increase in thrombin generation, plasmin generation decreased (figure 3D).

3

A

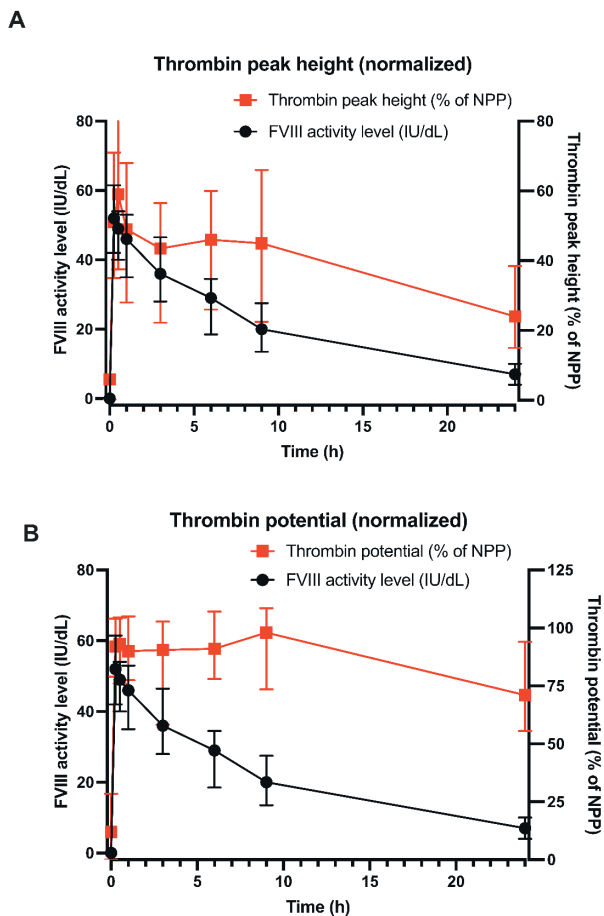Thrombin peak height (normalized)

B

Thrombin potential (normalized)

Figure 4: Factor VIII activity level and normalized thrombin peak height and thrombin potential after a bolus of factor VIII replacement therapy.

Previously, it was reported that velocity of thrombin generation is a better representation of the effect of factor supplementation in hemophilia patients.[25] The correlation between FVIII activity level and velocity of thrombin generation (r=0.64 (95%-CI 0.57-0.70); figure 2D) was equal to the correlation of FVIII activity level and thrombin peak height (r=0.61 (95%-CI 0.53-0.68); figure 2B) and thrombin potential (r=0.51 (95%-CI 0.41-0.59); figure 2C). Furthermore, differences in velocity of thrombin generation between patients were significant (as illustrated by the large range in supplementary figure 2C).

Normalized thrombin generation parameters are preferred above absolute parameters according to guidelines of the ISTH[26] to compare results at different laboratories. In figure 4 the normalized thrombin peak height and normalized thrombin potential are

Table 2: Comparison population pharmacokinetic parameter estimates of Bukkems et al. and external dataset in patients of this replication study.

Parameter	External dataset		Bukkems et al.	
Pharmacokinetic model	Parameter estimation (RSE%)	Inter-individual variability (RSE%) [Shr%]	Parameter estimation (RSE%)	Inter-individual variability (RSE%) [Shr%]
CL (dL/h/70 kg)	3.07 (10)	57.3 (15) [1.4]	1.69 (11.1)	41.2 (18.9) [2.1]
V1 (dL/70 kg)	39.1 (7.7)	38.2 (15) [0.1]	27.7 (5.80)	15.6 (16.5) [2.8]
Q (dL/h/70 kg)	1.09 (35.5)		2.27 (44.5)	-
V2 (dL/70 kg)	9.16 (32.3)		5.63 (19.2)	-
Correction factor CSA	0.939 (2.2)		1.20 (3.50)	18.1 (13.3) [4.7]
Correlation IIV CL and V1 (%)		77.0		43.6
Covariates				
Positive NLTIA on V1 (%)	-		114 (3.9)	
Full-length recombinant product on V1(%)	-		117 (6.8)	
VWF exponent on CL	-		-0.52 (26.6)	
Positive NLTIA on CL (%)	-		149 (11.1)	
Full-length recombinant product on CL (%)	-		127 (10.3)	
Positive NBA on CL (%)	153		-	
Residual variability				
Proportional error OSA (%)	25.0 (6.6)		11.2 (21.6)	
Additive error OSA (IU/dL)	0.854 (26.5)		4.15 (14.9)	
Proportional error CSA (%)	21.0 (17.5)		10.5 (17.5)	
Additive error CSA (IU/dL)	4.28 (9.7)		2.69 (49.8)	

Abbreviations: CL, clearance; CSA, chromogenic FVIII activity assay; CV, coefficient of variation calculated as $\sqrt{(\exp[\omega2]-1)} \times 100$; IIV, inter-individual variability; NBA, Nijmegen-modified Bethesda Assay; NLTIA, Nijmegen Low Titer Inhibitor Assay; OSA, one-stage FVIII activity assay; Q, intercompartment clearance; RSE, relative standard error; Shr, shrinkage; V1, central volume of distribution; VWF, von Willebrand factor activity level (%); V2, peripheral volume of distribution.

shown. The results in figure 4 illustrates that Tmax is identical for FVIII activity level, normalized thrombin peak height(normalized thrombin peak height 51% (35-71)), but it remains higher compared to FVIII activity level (at 6 hours 29 IU/dL (19-35) versus 46% (26-60) and at 24 hours 7 IU/dL (4-10) versus 24% (15-39), respectively). The same holds true for normalized thrombin potential, which is 92% (79-104) after 15 minutes, and remains 91% (78-107) at 6 hours, but the Tmax occurred at 9 hours post dose with 98% (74-109) and 71% (56-94) at 24 hours(see figure 4 and supplementary table 3).

Re-estimation of the population pharmacokinetic model

The predictive performance of the population pharmacokinetic model by Bukkems et al. was evaluated with the current data.[16] The observed FVIII activity was lower than the predicted activity (supplementary figure 4) with a MPE and MAPE value of 60.9 and 61.3% (figure 5). Therefore, a novel population pharmacokinetic model was developed. An one- and two-compartment model were tested. The data was best described with a two-compartment model with IIV attributed on clearance and central volume of distribution. For the residual error, a combined proportional and additive error model was used. Since FVIII activity levels were measured with both OSA and CSA, a correction factor was included to correct for the difference in assay methods. Samples measured with CSA were 0.939 times lower compared to samples measured with OSA. IIV was tested on the correction factor, but including IIV on the correction factor did not significantly improve the model fit.
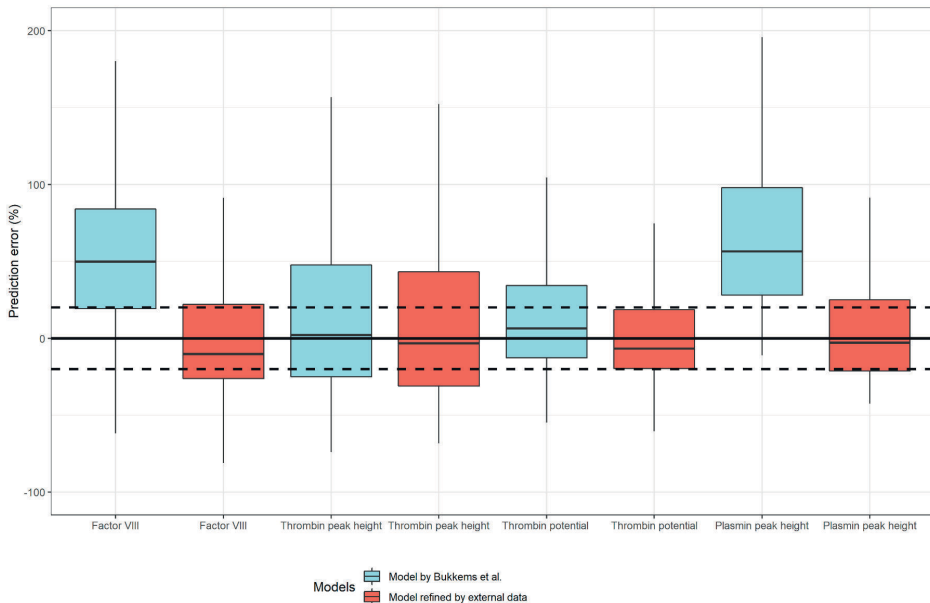

Figure 5: Box plots of the prediction error (PE%) of the novel models vs Bukkems et al.

During the covariate analysis, a relationship was found between FVIII clearance and the presence of an NBA inhibitor leading to a 153% increase in clearance. The NLTIA did not have an effect on FVIII clearance. The final pharmacokinetic parameter estimates are displayed in table 2. The GOF plots and pcVPC of the final pharmacokinetic model are presented in supplementary figure 4 and 5.

Re-estimation of the population pharmacodynamic models

For the population pharmacodynamic analysis, 285 values of normalized thrombin peak height and potential, and normalized plasmin peak were measured. Of the normalized thrombin peak height and normalized plasmin potential, 9 and 10 measurements were undetectable, respectively. These were excluded from the pharmacodynamic data analysis, since only a small portion of the samples (<4%) were undetectable.

The individual pharmacokinetic parameters obtained from the pharmacokinetic model were used for estimation of the pharmacodynamic part of the model. The predictive performance of the previously published FVIII population pharmacodynamic models was tested. As shown in figure 5, differences in the predictive performance of different models were observed. For the models of Bukkems et al. the MPE and MAPE was 6.83 and 38.6 , 7.46 and 18.6, 58.9 and 58.9% for normalized thrombin peak height, normalized thrombin potential, and normalized plasmin peak, respectively. This indicates that the final pharmacodynamic parameters by Bukkems et al. for the normalized thrombin potential adequately predict our external dataset. There is no bias in prediction of the normalized thrombin peak height, however the prediction is not accurate since the MAPE is 38.6%. Moreover, the normalized plasmin peak pharmacodynamic model showed over prediction. It should also be noted that the models have a high IIV, therefore a high MAPE is expected. The MPE and MAPE of all models are summarized in supplement table 4.

Afterwards, re-estimations of pharmacodynamic parameters were performed by using the external pharmacodynamic dataset. The final pharmacodynamic parameter estimates are displayed in table 3. As expected, similar pharmacodynamic parameters for normalized peak height and normalized thrombin potential were obtained. For the normalized thrombin peak height an EC50 of 51.6 IU/dL and an Emax (factor of baseline) of 8.06 was obtained (supplement equation 9), while previously the EC50 and Emax was 50.1 IU/dL and 7.05, respectively. For the normalized thrombin potential an EC50 of 1.93 IU/dL and an Emax (percentage of NPP) of 65.3 was obtained (supplement equation 10), while in Bukkems et al. the EC50 and Emax was 13.9 IU/dL and 72.5 respectively. For the normalized plasmin peak height a baseline and EC50 of 81.2 IU/dL and 256 IU/dL was obtained (supplement equation 9), while in the original model the baseline was 125 IU/dL and EC50 was 614 IU/dL. In our novel pharmacodynamic models, IIV was only added

to one pharmacodynamic parameter. Adding IIV to more than one pharmacodynamic parameter did not result in a significant improvement (*p*=0.05) in model fit. Therefore, in the re-estimated pharmacodynamic models, IIV was included on the pharmacodynamic parameter with the largest drop in OFV (<3.84, *p*=0.05). Afterwards, a covariate analysis was performed, in which age and body weight were tested. However, none of the co-variates had significant effect on the pharmacodynamic parameters. GOF plots using models of Bukkems et al. and the re-estimated models are displayed in supplementary figure 6-8. The pcVPC of the plasmin peak height in which parameters are re-estimated,

Table 3: Comparison population pharmacodynamics parameter estimates of Bukkems et al. and external dataset in patients of this replication study.

Parameter	External dataset		Bukkems et al.	
Pharmacodynamic model	Parameter estimation (RSE%)	Inter-individual variability (RSE%) [Shr%]	Parameter estimation (RSE%)	Inter-individual variability (RSE%) [Shr%]
Normalized thrombin peak height				
Baseline effect (% of NPP)	11.2 (26.3)	34.7 (33.6) [7.5]	15.6 (18.8)	-
EC50 (IU/dL)	51.6 (13.2)		50.1 (24.4)	55.1 (26.8) [12.5]
Maximal effect (factor of baseline)	8.06 (32.6)		7.05 (33.6)	37.3 (25.8) [16.8]
Hill coefficient	1 FIX		1.85 (25.7)	-
Additive error (% of NPP)	17.4 (7.4)		11.2 (8.0)	-
Normalized thrombin potential				
Baseline effect (% of NPP)	21.9 (13.6)	-	37.5 (13.1)	41.8 (25.2) [15.7]
EC50 (IU/dL)	1.93 (46.4)	-	13.9 (21.2)	88.0 (16.9) [15.5]
Maximal effect (Emax) (% of NPP)	65.3 (6.7)	33.1 (37.0) [4]	72.5 (9.5)	22.9 (23.9) [17.5]
Mild haemophilia on Emax (% of severe)	-		70.9 (15.9)	-
Coefficient bodyweight on Emax	-		-0.28 (21.0)	-
Hill coefficient	1 FIX		1.62 (20.8)	-
Additive error (% of NPP)	16.2 (6.7)		8.62 (12.2)	-
Normalized plasmin peak height				
Baseline effect (% of NPP)	81.2 (4.5)	26.4 (12.9) [0.1]	125 (8.2)	32.1 (19.0) [1.0]
EC50 (IU/dL)	256 (49.9)	-	614 (47.7)	
Maximal effect (% of NPP)	1 FIX	-	1 FIX	-
Hill coefficient	1 FIX	-	1 FIX	-
Proportional error (%)	16.3 (5.8)	-	26.8 (6.6)	-

Abbreviations: CV, coefficient of variation calculated as $\sqrt{(\exp[\omega2]-1)} \times 100$; EC50, the FVIII activity level which produces 50% of the maximal effect; IIV, inter-individual variability; NPP, normal pooled plasma; RSE, relative standard error; Shr, shrinkage

Pharmacodynamic formula external dataset:

Normalized thrombin peak height: $E = E_{base} \times (1 + \frac{E_{max} * C^n}{(EC50^n + C^n)})$

Normalized thrombin potential: $E = E_{base} \times (1 + \frac{E_{max} * C^n}{(EC50^n + C^n)})$

Normalized plasmin peak height: $E = E_{base} \times (1 + \frac{E_{max} * C^n}{(EC50^n + C^n)})$

is displayed in supplementary figure 9.The GOF plots and pcVPC show that the final models adequately described the observed data. The pcVPC using the thrombin peak height and thrombin potential models of Bukkems et al. with the external dataset is displayed in supplementary figure 10-11.

Figure 6 displays patients with similar pharmacokinetic profiles, but have a different normalized thrombin potential profile, which is caused by the IIV in the baseline, EC50 and Emax. The third patient has longer effect of the normalized thrombin potential due to a lower EC50 compared to the other patients. In this figure, the model of Bukkems et al. further displays sufficient predictive performance in an external dataset. Supplementary figure 12 displays the normalized thrombin potential response after factor VIII administration in a patient with inhibitor.
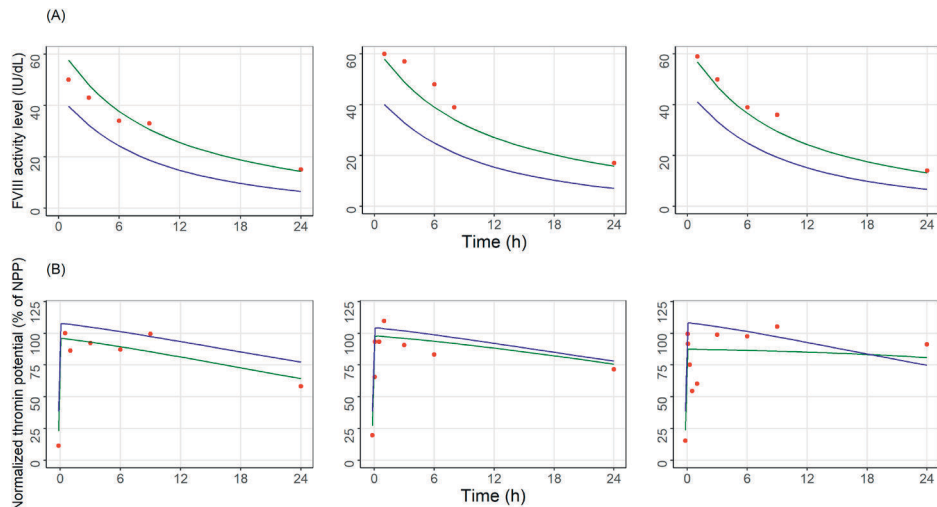
Figure 6: Three patients from the external dataset with a similar pharmacokinetic profile displaying a different normalized thrombin potential response after factor VIII administration using the model by Bukkems et al.

DISCUSSION

In this replication study, we show that our previously developed pharmacodynamic model for dosing of SHL FVIII concentrates was able to adequately describe the relationship between FVIII activity level and normalized thrombin peak height and normalized thrombin potential in another factor concentrate containing VWF e.g. pdVWF/FVIII concentrate (Haemate P®). This finding underscores the additive value of measuring pharmacodynamics by TGA in hemophilia A patients, as thrombin generation measured by NHA subsequent to prophylactic FVIII administration, was able to predict the hemo-

static potential of FVIII in an individual patient. The original developed pharmacokinetic-pharmacodynamic FVIII concentrate dosing model included a wide range of plasma derived and recombinant FVIII concentrates, as to secure the generalization of the model.[16] As this study shows, thrombin generation remains equal despite differences in administered factor concentrates, while the pharmacokinetic model was unable to describe the pharmacokinetic of this pdVWF/FVIII product.

In the previous study, it was difficult to compare pharmacokinetic-pharmacodynamic profiles of different patients, as it was unknown whether differences in the pharma-cokinetic-pharmacodynamic profile were caused by patient-related factors or were dependent on the factor VIII concentrate administered. Both recombinant and plasma derived FVIII concentrates were used, and some patients (n=3) also received pdVWF/FVIII concentrate. Therefore, the use of only one FVIII/VWF product in this replication study enabled the comparability of the generated pharmacokinetic-pharmacodynamic profiles. Subsequently, differences found between patients will be caused by patient-related factors, like body weight, pre-existent VWF concentration and the presence of (very) low-titer inhibitors.

Our data show that thrombin generation remained increased after replacement of FVIII activity during the first 24 hours, even though FVIII activity levels decrease rapidly. This is clearly illustrated by the normalized thrombin potential which remained at 71% of normal (IQR 56-94) after 24 hours while FVIII activity level was only 7 IU/dL (4-10). This is comparable with our previous study, in which normalized thrombin potential was 75% of normal (59-87) with an associated FVIII activity level of 15 IU/dL (10-26).[19] It should be noted that the FVIII activity level in the prior study was twice as high as observed in this current study because of higher dosage in the prior study, while normalized thrombin potential remained roughly equal. This indicates that FVIII stimulated thrombin generation has a maximum capacity and only little FVIII is necessary to stimulate thrombin generation (i.e. FVIII supplementation has a low EC50 for thrombin generation). Moreover, plasmin generation may not be suitable as a pharmacodynamic target, because of little difference in plasmin generation between healthy and hemophilia A patients.

In the current study, we observed a plasmin peak height that was within normal range compared to healthy controls. Nonetheless, plasmin peak height decreased after FVIII replacement therapy, and this decrease was present until 24 hours after the bolus. This apparent hyperfibrinolysis in patients has been observed earlier and is possibly due to the reduced activation of thrombin activated fibrinolytic inhibitor (TAFI), for which a higher amount of thrombin is required than can be produced when amplification is insufficient.[27, 28] Because the NHA is the only assay that measures thrombin and plas-

min generation simultaneously in a single well,[29, 30] the interplay between thrombin and plasmin generation can only be investigated using this assay.[18] This observation was in accordance with our previous study, in which we also observed hyperfibrinolysis before the FVIII bolus in patients with HA, which was resolved after normalization of FVIII activity level.[19]

Previously, the velocity of thrombin generation was suggested to correspond better with factor activity levels in both HA and hemophilia B (HB).[25, 31] The correlation between FVIII activity level and velocity of thrombin generation was slightly better than the correlation with thrombin potential and thrombin peak height. Also, the curve of FVIII activity and velocity of thrombin generation corresponds better with each other than the curve of thrombin potential (supplementary figure 3). However, it remains questionable whether a thrombin generation parameter that corresponds better with FVIII activity level also reflects the hemostatic potential of the patient. Especially since previous studies have shown that thrombin potential could better identify patients with an increased bleeding risk.[14] Furthermore, velocity of thrombin generation is calculated with a formula that consists of three components of the thrombin generation assay (lag time, time to thrombin peak, and thrombin peak height) and is therefore vulnerable for artefacts when one or more of these parameters are slightly aberrant. Therefore, thrombin potential could be a better parameter to adjust dosage of FVIII replacement therapy upon. It has a better correlation with bleeding phenotype, where it is able to differentiate patients between and mild and severe bleeding phonotype, based on the ABR.[32, 33] Furthermore, it can improve identification of patients who will bleed while treated compared to FVIII activity level.[14] The main difficulty, however, is that trough levels of thrombin generation are not known yet. A prospective study investigating the optimal amount of thrombin generation to prevent bleeding is highly needed.

The previously developed population pharmacokinetic model by Bukkems et al. could not sufficiently predict the FVIII activity levels in the current study, since the predictions were higher compared to the observed FVIII activity levels. Therefore, a novel population pharmacokinetic model was developed which estimated a higher clearance (3.07 dL/h) compared to clearance of Bukkems et al. (1.69 dL/h). The volume of distribution is larger as well (39.1 dL versus 27.7 dL).[16] Bukkems et al. previously published also a population pharmacokinetic model describing the interaction between FVIII and VWF in von Willebrand disease, in which patients received pdVWF/FVIII. The volume of distribution was estimated as 44.4 dL which was similar as to our estimate (39.1 dL), whereas the clearance was estimated as 1.17 dL/h, which was different compared to our estimate (3.07 dL/h).[31] It is known that VWF protects FVIII from proteolysis[5], therefore we expected a lower clearance in the novel population. In this study all 29 patients received

pdVWF/FVIII whereas in Bukkems et al. only 3 received pdVWF/FVIII. Hence the influence of pdVWF/FVIII could be underestimated in the population pharmacokinetic of Bukkems et al. Moreover, the interindividual-variability on the clearance was 41.2% in Bukkems et al. In the previous population pharmacokinetic model, a significant effect between a very low-titer inhibitor and clearance and volume of distribution was found. Patients with a very low-titer inhibitor have 149% increase in the clearance. In the current study, only a significant effect between a positive NBA and clearance was found.

The predictive performance of the previously developed pharmacodynamic models was also evaluated with the current dataset. Predictive performance was adequate when using the normalized thrombin potential models, but overprediction was observed when using the normalized thrombin peak height and plasmin peak height model. However, there was no bias in the predictions of the normalized thrombin peak height (MPE <20%), but the MAPE was slightly >30% which shows inaccurate predictions. A reason for the overprediction in plasmin peak height model could be that the estimated baseline was different in our dataset (81.2% of NPP) compared to Bukkems et al. (125% of NPP). This difference is probably caused by an assay artefact in plasmin peak height determination. Re-estimations of the pharmacodynamic parameters for normalized thrombin peak height and normalized thrombin potential models displayed similar parameter estimation, further enhancing the adequate predictive performance of the previously developed models. In the normalized thrombin potential we estimated an EC50 of 1.93 IU/dL, whereas Bukkems et al. estimated an EC50 of 13.9 IU/dL. In both models, a low level of FVIII was already sufficient to produce a higher normalized thrombin potential. As a result, the normalized thrombin potential displays a sustained effect after 24 hours (Figure 4C). Moreover, the pharmacodynamic models have a high IIV and residual error. Even after improving the models, there is still considerable inter-patient and residual variability. In this study, we did not opt to use Bayesian approaches because we wanted to investigate the predictive performance of the previous models and re-estimate parameters if no adequate predictions were made. However, Bayesian approaches can be a valuable tool for improving predictive performance by individualizing models and incorporating prior knowledge.

This study has a number of limitations. First, patients were included in Iran and samples were handled, frozen and afterwards collectively shipped to Nijmegen, the Netherlands on dry ice. It is unknown whether this could have influenced the quality of the samples and if results are impacted by this. For example, the 3 hour sample showed lower than expected results in some patients, possibly due to pre-analytical disturbances. To prevent further deterioration by repeated thaw-freeze cycles, all samples were defrosted only once to measure FVIII activity levels, inhibitor titers and NHA at one occasion. However,

lack of standardization or pre-analytical and analytical procedures is still a major. Second, samples for the pharmacokinetic-pharmacodynamic study were only collected for the first 24 hours. Therefore, we were unable to identify the course of thrombin generation after 24 hours, which would be highly interesting, as FVIII activity levels had not reached the baseline level corresponding to the grade of hemophilia severity while thrombin potential was still increased. To overcome this difficulty with the model development, the pre-bolus sample was also used as if it was determined after 72 hours, which was equal to the washout period. Thirdly, numerous studies have previously shown a clear association between thrombin generation and bleeding phenotype as determined with the annual bleeding rate (ABR). Here, the ABR was not systematically determined when patients were included and it was not possible to determine the ABR retrospectively. Because this is associated with reporting and recall bias, we were not able to include an analysis between ABR and as such the bleeding phenotype and pharmacokinetic-pharmacodynamic parameters. Lastly, VWF was only measured before pdVWF/FVIII concentrate administration. It is known that VWF acts as a protector and chaperone of FVIII. In the previously developed population pharmacokinetic -model, VWF had an effect on the clearance of FVIII. Unfortunately, the effect of VWF could not be tested in the external dataset because samples after administration did not include measurements of VWF due to insufficient sample volumes.

Despite the development of non-factor replacement therapies for HA (like emicizumab), FVIII concentrate will remain an important part of the treatment. FVIII concentrates are still used for bleeding episodes and during the peri-operative period during prophylactic therapy with non-factor concentrates. Therefore, it remains important to measure and improve dosing of FVIII concentrates. Furthermore, expensive non-factor concentrates will remain out of reach for large parts of the world while the decreasing price of FVIII concentrates enforces them to remain an important corner stone in the treatment of HA. This study adds to the knowledge of optimal dosing FVIII concentrates on the basis of pharmacokinetic-pharmacodynamic measurements which can become available to larger parts of the world due to point of care measurement techniques and digital powered devices.

CONCLUSION

The previously developed population pharmacodynamic models of normalized thrombin peak height and normalized thrombin potential were able to adequately predict the observations in our external dataset. These thrombin generation models can be used to guide the application of pharmacokinetic-pharmacodynamic guided dosing of FVIII concentrates in patients with hemophilia A. A prospective study in which this thrombin generation pharmacodynamic based dosing model is used and combined with bleeding phenotype data to individualize prophylactic therapy with FVIII concentrate will answer the question whether the current prophylactic HA management can be further individualized and improved.

3

REFERENCES

1. Mannucci, P.M. and E.G. Tuddenham, *The hemophilias--from royal genes to gene therapy.* N Engl J Med, 2001. **344**(23): p. 1773-9.

2. Oldenburg, J., *Optimal treatment strategies for hemophilia: achievements and limitations of current prophylactic regimens.* Blood, 2015. **125**(13): p. 2038-44.

3. Srivastava, A., et al., *WFH Guidelines for the Management of Hemophilia, 3rd edition.* Haemophilia, 2020. **26 Suppl 6**: p. 1-158.

4. Oldenburg, J., et al., *Emicizumab Prophylaxis in Hemophilia A with Inhibitors.* N Engl J Med, 2017. **377**(9): p. 809-818.

5. Franchini, M. and P.M. Mannucci, *Hemophilia A in the third millennium.* Blood Rev, 2013. **27**(4): p. 179-84.

6. Iorio, A., *Using pharmacokinetics to individualize hemophilia therapy.* Hematology Am Soc Hematol Educ Program, 2017. **2017**(1): p. 595-604.

7. Iorio, A., et al., *Target plasma factor levels for personalized treatment in haemophilia: a Delphi consensus statement.* Haemophilia, 2017. **23**(3): p. e170-e179.

8. Iorio, A., et al., *Development of a Web-Accessible Population Pharmacokinetic Service-Hemophilia (WAPPS-Hemo): Study Protocol.* JMIR Res Protoc, 2016. **5**(4): p. e239.

9. Stemberger, M., et al., *Impact of Adopting Population Pharmacokinetics for Tailoring Prophylaxis in Haemophilia A Patients: A Historically Controlled Observational Study.* Thromb Haemost, 2019. **119**(3): p. 368-376.

10. Yu, J.K., et al., *Using pharmacokinetics for tailoring prophylaxis in people with hemophilia switching between clotting factor products: A scoping review.* Res Pract Thromb Haemost, 2019. **3**(3): p. 528-541.

11. Zhou, J.Y., et al., *Joint Bleeding Tendencies in Adult Patients With Hemophilia: It's Not All Pharmacokinetics.* Clin Appl Thromb Hemost, 2019. **25**: p. 1076029619862052.

12. van Geffen, M. and W.L. van Heerde, *Global haemostasis assays, from bench to bedside.* Thromb Res, 2012. **129**(6): p. 681-7.

13. Dargaud, Y., et al., *Evaluation of thrombin generating capacity in plasma from patients with haemophilia A and B.* Thromb Haemost, 2005. **93**(3): p. 475-80.

14. Dargaud, Y., et al., *Individual thrombin generation and spontaneous bleeding rate during personalized prophylaxis with Nuwiq((R)) (human-cl rhFVIII) in previously treated patients with severe haemophilia A.* Haemophilia, 2018. **24**(4): p. 619-627.

15. Beltran-Miranda, C.P., et al., *Thrombin generation and phenotypic correlation in haemophilia A.* Haemophilia, 2005. **11**(4): p. 326-34.

16. Bukkems, L.H., et al., *Combining factor VIII levels and thrombin/plasmin generation: A population pharmacokinetic-pharmacodynamic model for patients with haemophilia A.* Br J Clin Pharmacol, 2022. **88**(6): p. 2757-2768.

17. Delavenne, X., et al., *A new paradigm for personalized prophylaxis for patients with severe haemophilia A.* Haemophilia, 2020. **26**(2): p. 228-235.

18. van Geffen, M., et al., *A novel hemostasis assay for the simultaneous measurement of coagulation and fibrinolysis.* Hematology, 2011. **16**(6): p. 327-36.

19. Valke, L., et al., *Pharmacodynamic monitoring of factor VIII replacement therapy in hemophilia A: Combining thrombin and plasmin generation.* J Thromb Haemost, 2020. **18**(12): p. 3222-3231.

20. Verbruggen, B., et al., *The Nijmegen modification of the Bethesda assay for factor VIII:C inhibitors: improved specificity and reliability.* Thromb Haemost, 1995. **73**(2): p. 247-51.

21. Ketteler, C., et al., *Impact of different factor VIII inhibitor kinetic profiles on the inhibitor titer quantification using the modified Nijmegen-Bethesda assay.* Res Pract Thromb Haemost, 2022. **6**(8): p. e12799.

22. Dardikh, M., et al., *Low-titre inhibitors, undetectable by the Nijmegen assay, reduce factor VIII half-life after immune tolerance induction.* J Thromb Haemost, 2012. **10**(4): p. 706-8.

23. Sheiner, L.B. and S.L. Beal, *Some suggestions for measuring predictive performance.* J Pharmacokinet Biopharm, 1981. **9**(4): p. 503-12.

24. Nguyen, T.H., et al., *Model Evaluation of Continuous Data Pharmacometric Models: Metrics and Graphics.* CPT Pharmacometrics Syst Pharmacol, 2017. **6**(2): p. 87-109.

25. Takeyama, M., K. Nogami, and M. Shima, *A new parameter in the thrombin generation assay, mean velocity to peak thrombin, reflects factor VIII activity in patients with haemophilia A.* Haemophilia, 2016. **22**(5): p. e474-7.

26. Dargaud, Y., et al., *Proposal for standardized preanalytical and analytical conditions for measuring thrombin generation in hemophilia: communication from the SSC of the ISTH.* J Thromb Haemost, 2017. **15**(8): p. 1704-1707.

27. Broze, G.J., Jr. and D.A. Higuchi, *Coagulation-dependent inhibition of fibrinolysis: role of carboxypeptidase-U and the premature lysis of clots from hemophilic plasma.* Blood, 1996. **88**(10): p. 3815-23.

28. Mosnier, L.O., et al., *The defective down regulation of fibrinolysis in haemophilia A can be restored by increasing the TAFI plasma concentration.* Thromb Haemost, 2001. **86**(4): p. 1035-9.

29. Simpson, M.L., et al., *Simultaneous thrombin and plasmin generation capacities in normal and abnormal states of coagulation and fibrinolysis in children and adults.* Thromb Res, 2011. **127**(4): p. 317-23.

30. Matsumoto, T., K. Nogami, and M. Shima, *Simultaneous measurement of thrombin and plasmin generation to assess the interplay between coagulation and fibrinolysis.* Thromb Haemost, 2013. **110**(4): p. 761-8.

31. Atsou, S., et al., *Pharmacodynamics of eftrenonacog-alfa (rFIX-Fc) in severe hemophilia B patients: A real-life study.* Eur J Pharmacol, 2021. **891**: p. 173764.

32. Verhagen, M.J.A., L. Valke, and S.E.M. Schols, *Thrombin generation for monitoring hemostatic therapy in hemophilia A: A narrative review.* J Thromb Haemost, 2022. **20**(4): p. 794-805.

33. Verhagen, M.J.A., et al., *In patients with hemophilia, a decreased thrombin generation profile is associated with a severe bleeding phenotype.* Res Pract Thromb Haemost, 2023. **7**(2): p. 100062.

3

SUPPLEMENT

Detailed execution of the Nijmegen Hemostasis Assay

The NHA was performed by mixing 80 μL of patient plasma with 2 μL crude cephalin (Roche), 2 μL tissue factor (Innovin®, Healthcare Diagnostics, final concentration corresponding to approximately 0.3 pM), 4 μL fluorescent thrombin-specific substrate Bz-β-Ala-Gly-Arg-7-amino-4-methylcoumarin (final concentration 833 μmol/L) and 2 μL fluorescent plasmin-specific substrate (Cbz-L-phenylalanyl-L-arginyl)-rhodamine-morpholino urea (final concentration 33 μmol/L). Substrates (Symeres) were dissolved in Tris Buffered Saline (TBS, 50 mmol/L Tris, 150 mmol/L NaCl, buffer pH 7.4). The reaction was started with 18 μL TBS buffer containing tissue plasminogen activator (tPA; Actilyse®, Boehringer Ingelheim, with a final concentration of 193 IU/mL) and 4 μL CaCl$_2$ (Merck, final concentration 16.7 mmol/L), which resulted in a total volume of 120 μL. Prewarmed black polystyrene Fluotrac microtiter plates (Greiner Bio-One) were used and fluorescence was measured alternately every 30 seconds for 70 minutes in a 37°C thermo-stated fluorometer (Fluostar Optima Fluorometer, BMG Labtechnologies). The thrombin-specific substrate was excited at 355 nm and measured at an emission wavelength of 460 nm. The plasmin-specific substrate was excited at 485 nm and measured at an emission wavelength of 520 nm. A calibration curve prepared with known amounts of human α-thrombin and human plasmin was used to calculate thrombin and plasmin proteolytic activities, respectively. The calibration curve demonstrated linear substrate cleavage throughout the reaction. The first derivative of the calibration curve was used to convert the fluorescence tracing to thrombin and plasmin concentrations. This first derivative was calculated from the fluorescent cumulative signal and all parameters of the NHA were determined by a Microsoft Excel macro program in Microsoft Visual Basic (version 11.1.1 (Microsoft Corporation)), as described before.[1] The obtained parameters are shown in supplementary figure 1.

Control measurements were obtained with normal pooled plasma (NPP) which consisted of equal amount of platelet poor plasma, collected from 10 healthy donors, representing males and females equally, in the age range 18-70 years. Females were not pregnant, nor on oral contraceptives. The negative control measurements were obtained with plasma deficient of FVIII (HRF Inc, NC, USA).

Additional details of the modelling process

A sequential PK-PD analysis method was performed. A population PK model was developed using NONMEM subroutines ADVAN3, TRANS4 with the FOCE method.

A priori allometric scaling of bodyweight on clearance (CL), central volume of distribution (V1), intercompartmental clearance (Q) and peripheral volume of distribution (V2) was included in the structural model (equation 1):

$$\theta_{pop\ PK} = \theta_{pk} \times \left(\frac{Bodyweight}{70}\right)^{\theta_{exp}}$$

(1)

In which, $\theta_{pop\ PK}$ is the typical population value for a PK parameter dependent on bodyweight, θ_{pk} is the typical PK value for a patient with a body weight of 70 kg, and θ_{epx} is an exponent fixed at 0.75 for CL and Q and 1 for V1 and V2.

The individual PK parameters were described by using equation 2.

$$\theta_i = \theta_{pop\ PK} \times exp^{ni}$$

(2)

In which, θ_i is the estimated individual PK parameter of the ith individual, $\theta_{pop\ PK}$ is the typical population value for a PK parameter, ηi is the inter-individual variability from normal distribution with a mean of zero and estimated variance of ω^2 of the ith individual.

For the residual error model, an additive (equation 3), proportional (equation 4) and combined error models (combination of equation 2 and 3) were tested, in which Y_{ij} is the prediction of the concentration of individual *i* at time *j* $f(\theta,\eta i,x_{ij})$ is the individual concentration prediction at time *j* and ε is the residual error originating from a normal distribution with a mean of zero and estimated variance of σ^2.

$$Y_{ij} = f(\theta, \eta i, x_{ij}) + \varepsilon_{ij}$$

(3)

$$Y_{ij} = f(\theta, \eta_i, x_{ij}) \times (1 + \varepsilon_{ij})$$

(4)

Continuous covariates were included by a power model, in which the covariate was centred around its median value and the exponent was estimated (equation 5). Categorical covariates were modelled with the use of flag variables (1 and 0 for "true" and "false"; equation 6).

$$\theta_{pop} = \theta_{pk} \times \left(\frac{Cov}{Cov_{median}}\right)^{\theta_{exp}}$$

(5)

$$\theta_{pop} = \theta_{pk} \times (\theta_1^{Flag1} \times \theta_2^{Flag2} \times \theta_3^{Flag3} \cdots)$$

(6)

A stepwise forward inclusion and backward exclusion process was used to evaluate covariates, in which a reduction in the objective function value (OFV) of 3.84 ($p = 0.05$) or more was considered significant during forward inclusion and a reduction in OFV of 6.64 ($p = 0.01$) or more in the backward exclusion process.

3

Pharmacodynamic model

The relationship between FVIII activity level and hemostatic effect defined by normalized thrombin peak height, normalized thrombin potential and normalized plasmin peak was described by a maximal effect (Emax; equation 7) or sigmoid Emax (equation 8) relation.

$$E_{drug} = \frac{E_{max} * C}{(EC_{50} + C)} \tag{7}$$

$$E_{drug} = \frac{E_{max} * C^n}{(EC_{50}^n + C^n)} \tag{8}$$

In which. Emax is the maximal effect, C the FVIII activity level, Slope the slope of the linear relation, EC_{50} the FVIII activity level that is associated with 50% of the maximal effect and n the hill factor that determines the steepness of the sigmoidal concentration-effect curve.
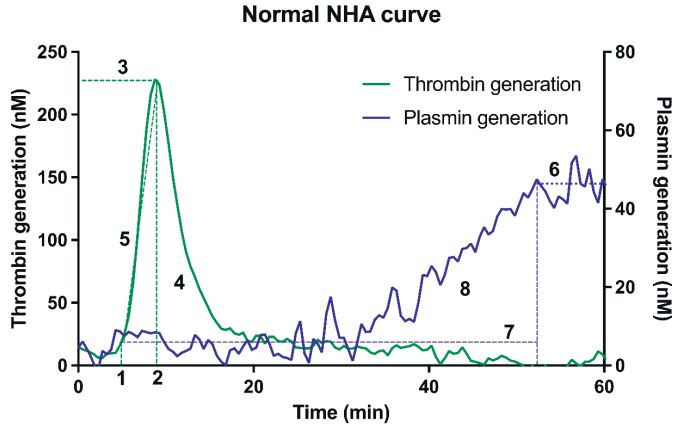
Both an proportional (equation 9) and additive(equation 10) relation between the baseline effect and drug effect were investigated.

$$E = E_{base} * (1 + or - E_{drug}) \tag{9}$$

$$E = E_{base} + (1 + E_{drug}) \tag{10}$$

Afterwards, IIV was estimated for the PD parameters to obtain individual PD parameters by using equation 11.

$$\theta_i = \theta_{pop\ PD} \times exp^{\eta i} \tag{11}$$

Normal NHA curve

Supplementary figure 1: Standard curve and essential parameters of the Nijmegen Hemostasis Assay (NHA). The following parameters are obtained with the NHA: 1. lag time: the time after initiation at which thrombin generation is initiated; 2. time to thrombin peak: the time after initiation when thrombin production reaches maximal velocity; 3. thrombin peak height; the maximal concentration of thrombin generation; 4. the area under the curve (AUC, also called thrombin potential), the total amount of thrombin generated; 5. velocity of thrombin generation, the amount of thrombin formed in the acceleration phase; 6. plasmin peak height: the maximal concentration of plasmin production; 7. fibrin lysis time (FLT): the time between the initiation of thrombin generation and the time plasmin generation reaches maximal velocity, and: 8. plasmin potential: area under the curve that represents the total amount of plasmin generated.
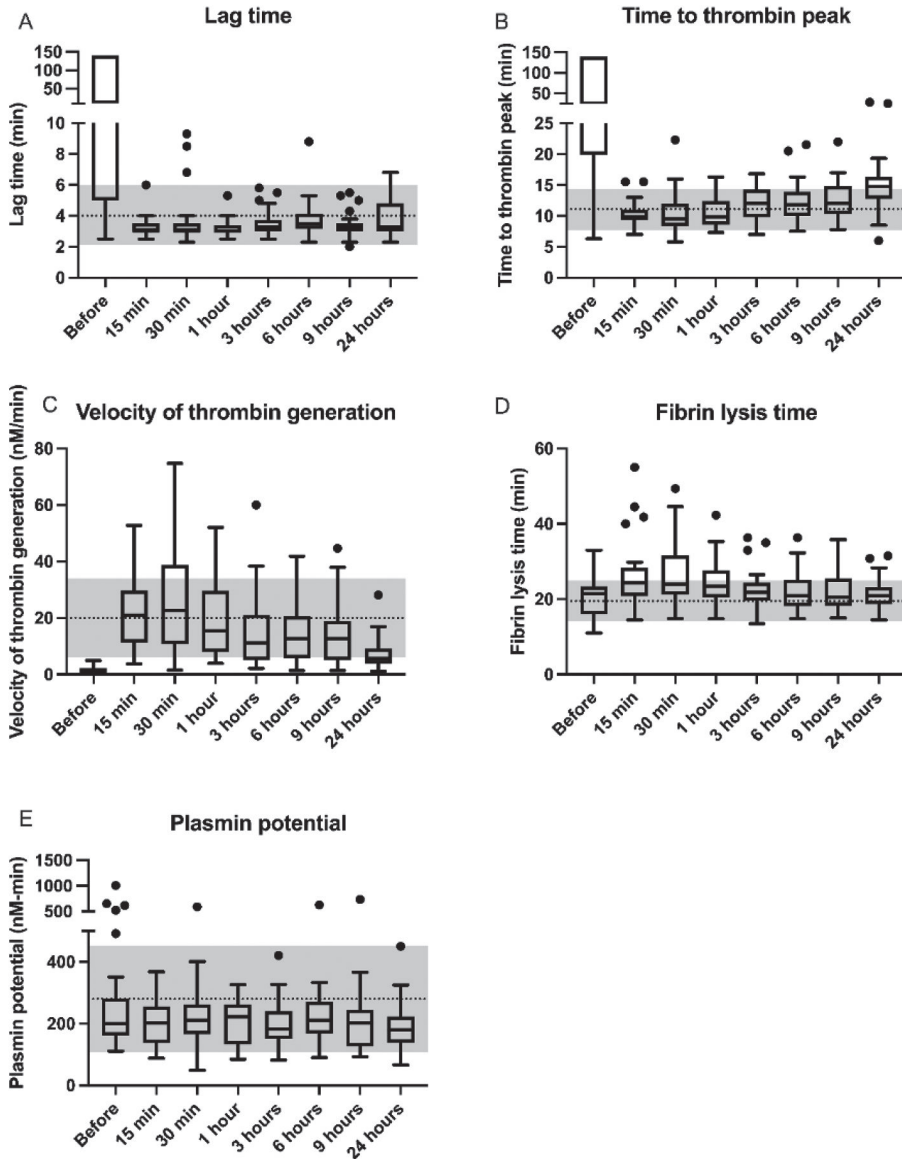
Supplementary figure 2: Additional parameters measured with the Nijmegen Hemostasis Assay after a bolus of factor VIII replacement therapy. (A) Lag time, (B) time to thrombin peak, (C) velocity of thrombin generation, (D) fibrin lysis time, and (E) plasmin potential prior and after a standardized bolus of plasma derived von Willebrand factor / factor VIII concentrate. Box represents median with interquartile range, whiskers indicate minimum and maximum, dots are outliers. Dotted line represents mean of individual healthy control Nijmegen Hemostasis Assay measurements, gray area ± 2 standard deviations.
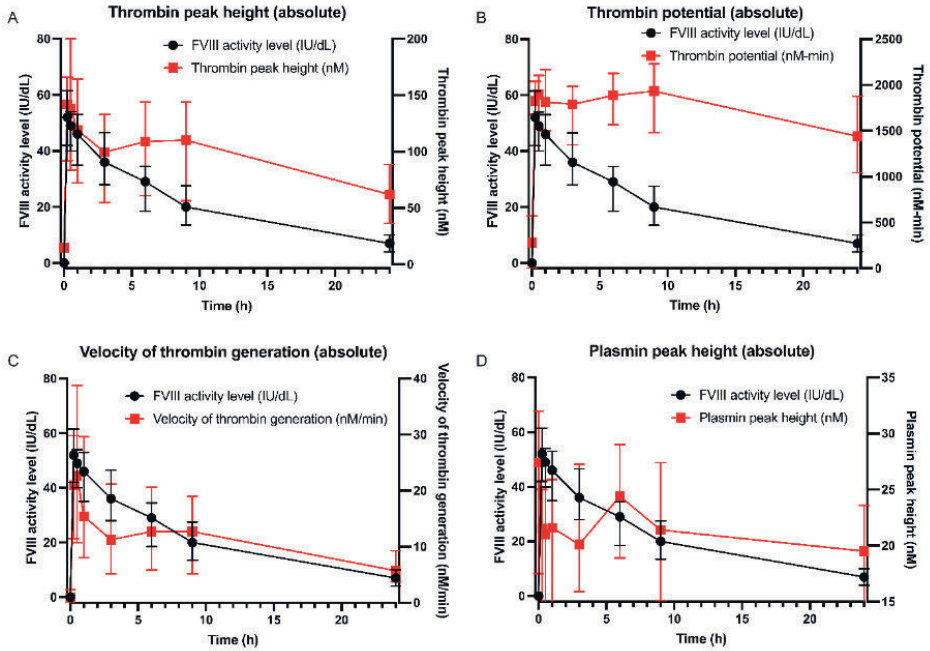
Supplementary figure 3: Absolute thrombin peak height, thrombin potential, velocity of thrombin generation and plasmin peak height after a bolus of factor VIII replacement therapy. Reached factor VIII activity level (left y-axis, in black) and (A) thrombin peak height, (B) thrombin potential, (C) velocity of thrombin generation, and (D) plasmin peak height, all on right y-axis in red, before and after a standardized bolus of plasma derived von Willebrand factor / factor VIII concentrate.

3
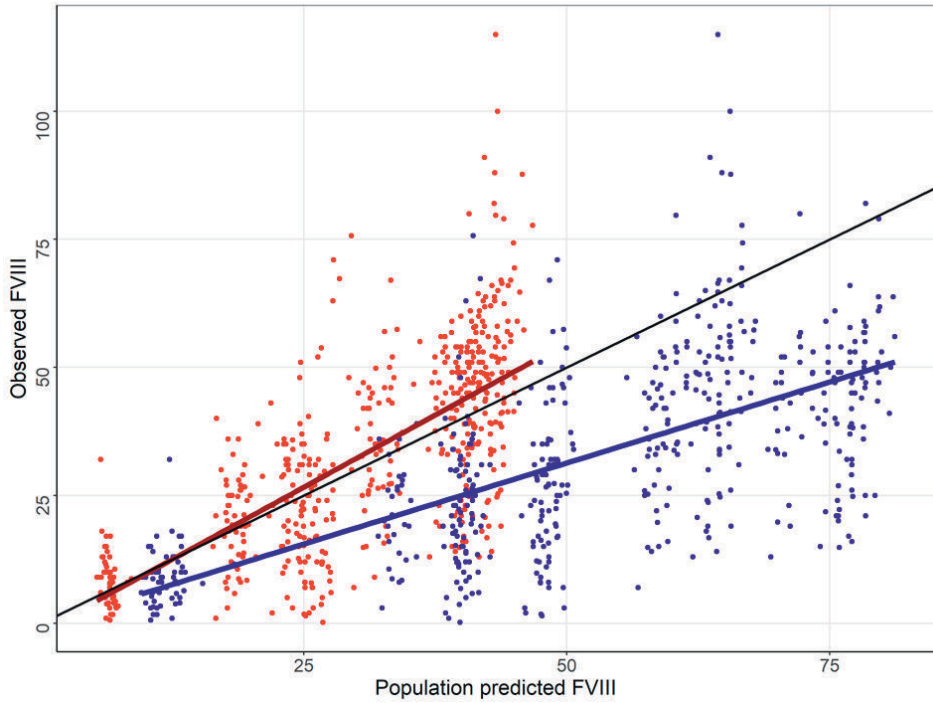
Supplementary figure 4: Predictive performance of novel population PK model vs Bukkems et al.[2]
Population predicted (PRED) vs observed concentrations The black solid line is the line of identity. The blue and red solid line represents the linear regression line. Blue lines and dots represents predictions based on the PK model of Bukkems et al. Red lines and dots represents predictions based on the novel PK model.
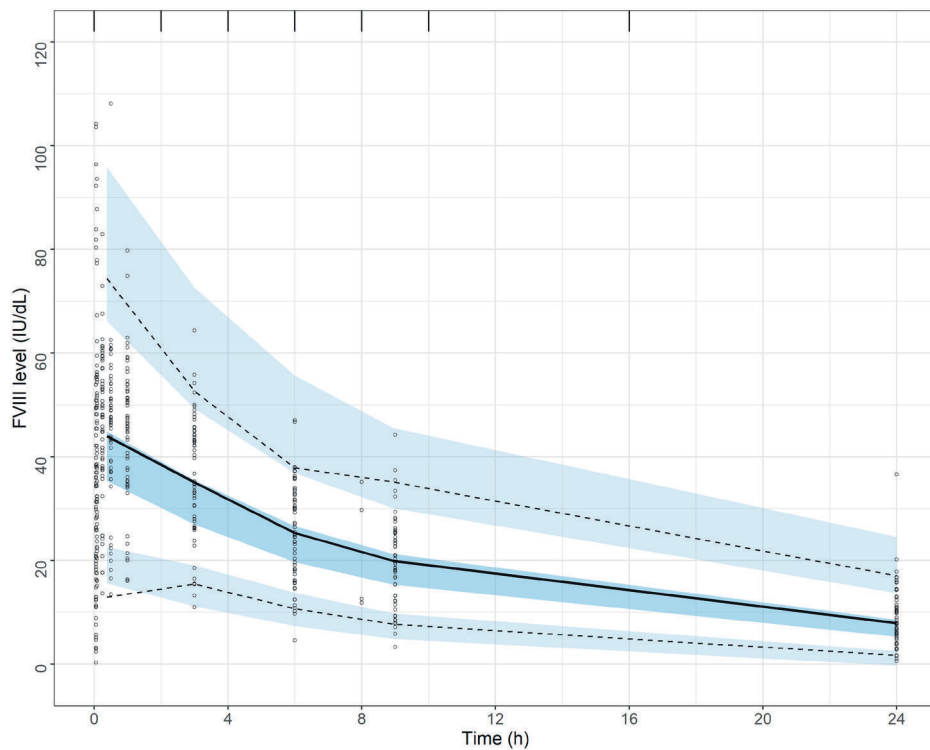
Supplementary figure 5: Prediction-corrected visual predictive check of the novel population PK model. Dots represent observed FVIII levels; the solid black line represents the 50th percentile of observed data; the dashed black lines represent the 5th and 95th percentiles of the population model. Shaded areas depict the model predicted 95% confidence intervals of the simulated percentiles.
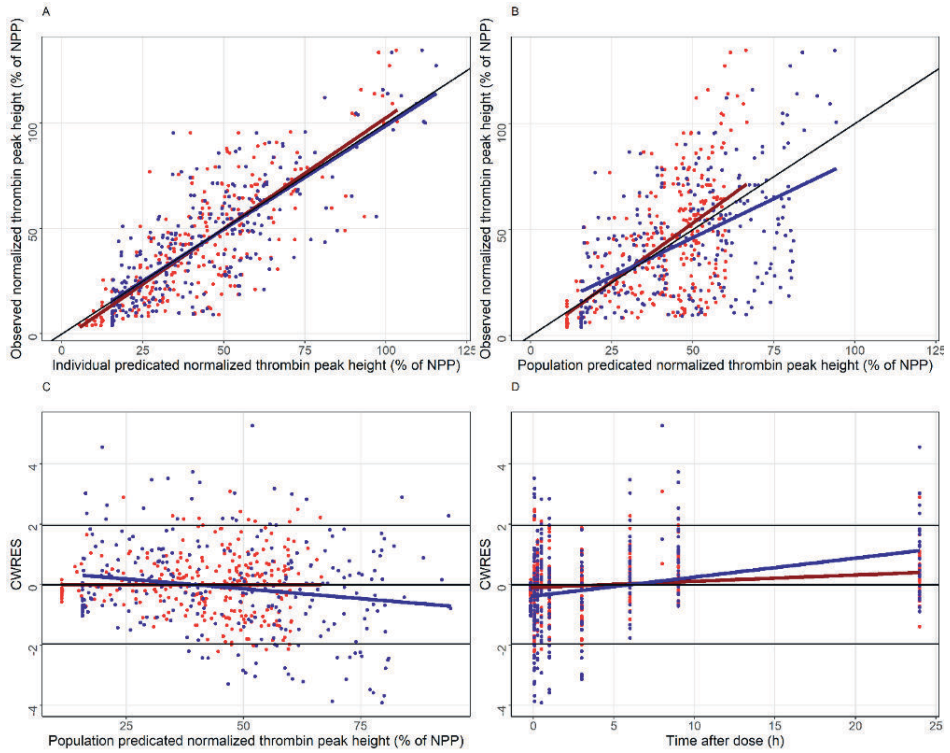
Supplementary figure 6: Goodness-of-fit plots of novel population normalized thrombin peak height vs Bukkems et al.[2] (A) Individual predicted (IPRED) vs observed concentrations, (B) Population predicted (PRED) vs observed concentrations, (C) Conditional weighted residuals (CWRES) vs PRED, (D) Time after dose vs CWRES. The black solid line is the line of identity. The blue and red solid line represents the linear regression line. Blue lines and dots represents predictions based on the PD model of Bukkems et al. Red lines and dots represents predictions based on the novel PD model.
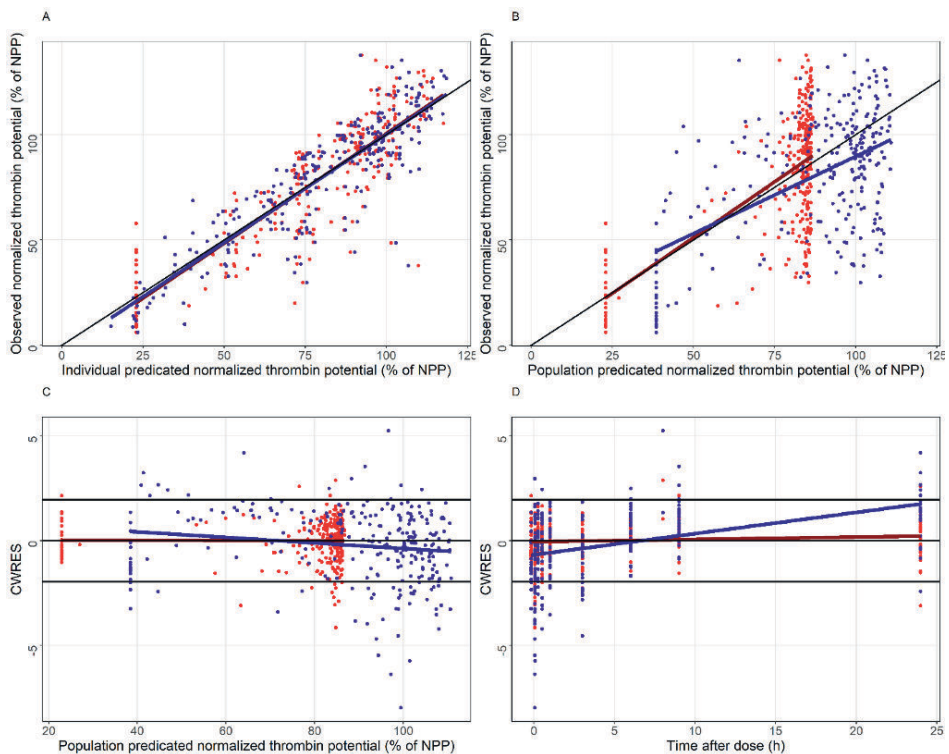
Supplementary figure 7: Goodness-of-fit plots of novel population normalized thrombin potential vs Bukkems et al.[2] (A) Individual predicted (IPRED) vs observed concentrations, (B) Population predicted (PRED) vs observed concentrations, (C) Conditional weighted residuals (CWRES) vs PRED, (D) Time after dose vs CWRES. The black solid line is the line of identity. The blue and red solid line represents the linear regression line . Blue lines and dots represents predictions based on the PD model of Bukkems et al. Red lines and dots represents predictions based on the novel PD model.
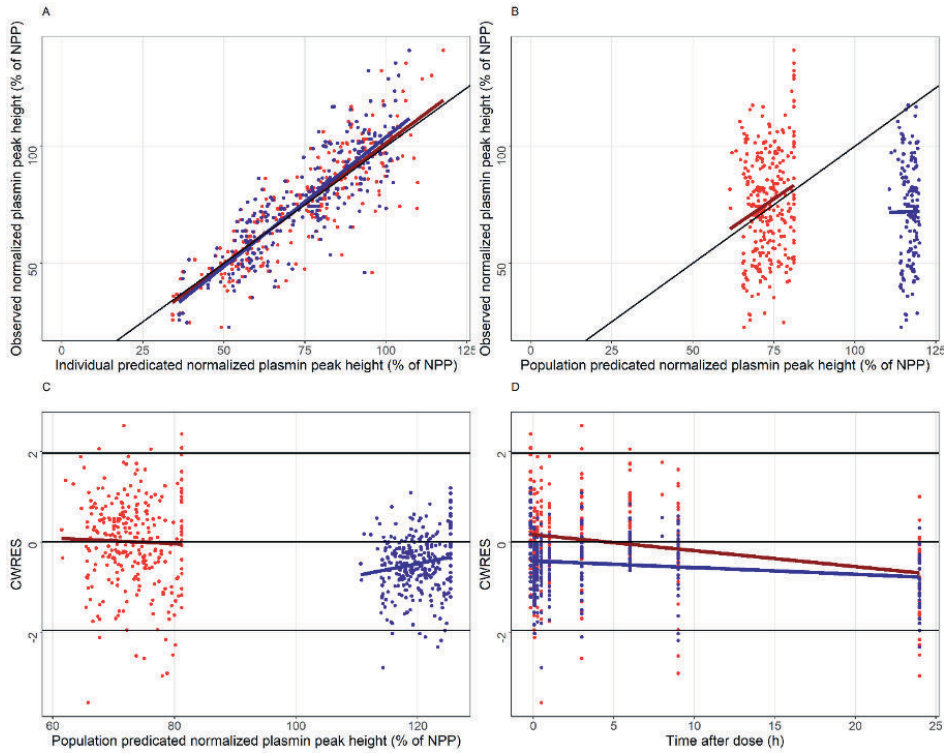
Supplementary figure 8: Goodness-of-fit plots of novel population normalized plasmin peak height vs Bukkems et al.[2] (A) Individual predicted (IPRED) vs observed concentrations, (B) Population predicted (PRED) vs observed concentrations, (C) Conditional weighted residuals (CWRES) vs PRED, (D) Time after dose vs CWRES. The black solid line is the line of identity. The blue and red solid line represents the linear regression line. Blue lines and dots represents predictions based on the PD model of Bukkems et al. Red lines and dots represents predictions based on the novel PD model.

Supplementary figure 9: Prediction-corrected visual predictive check of the novel plasmin peak height model. Dots represent observed plasmin peak height levels; the solid black line represents the 50th percentile of observed data; the dashed black lines represent the 5th and 95th percentiles of the population model. Shaded areas depict the model predicted 95% confidence intervals of the simulated percentiles.
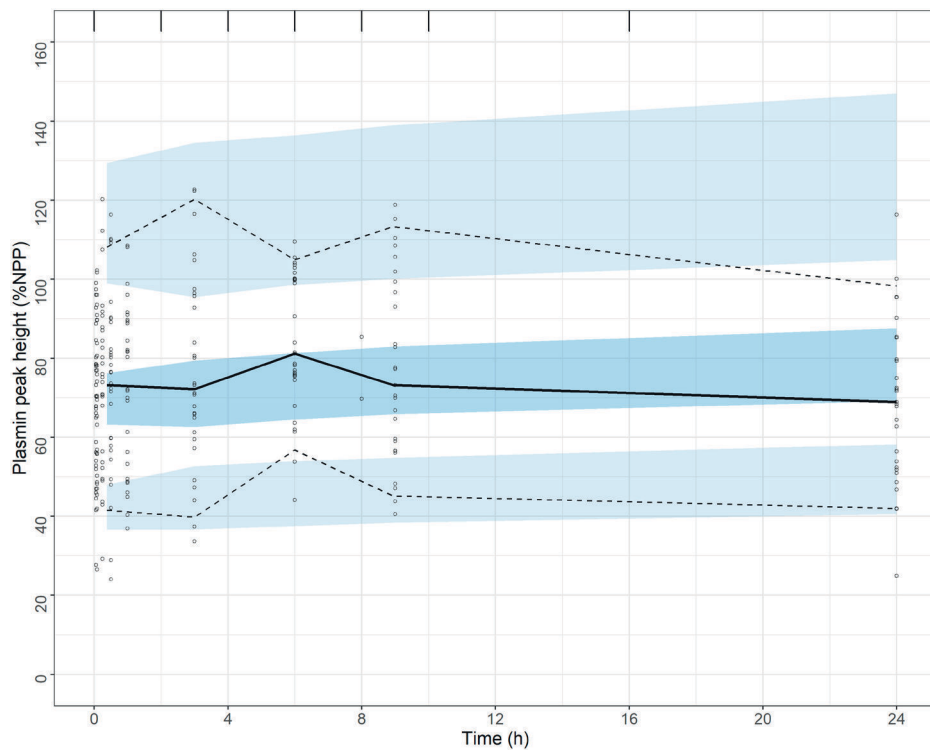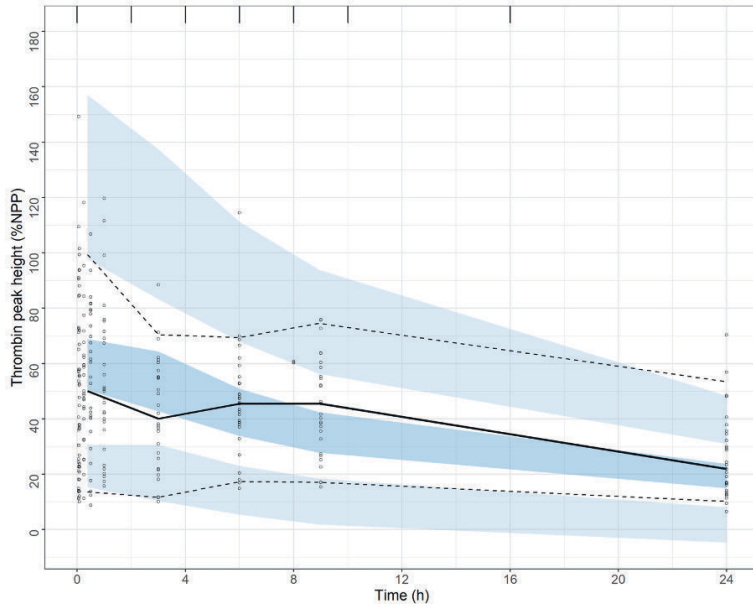
Supplementary figure 10: Prediction-corrected visual predictive check of the thrombin peak height model by Buk-kems et al. Dots represent observed plasmin peak height levels; the solid black line represents the 50th percentile of observed data; the dashed black lines represent the 5th and 95th percentiles of the population model. Shaded areas depict the model predicted 95% confidence intervals of the simulated percentiles.
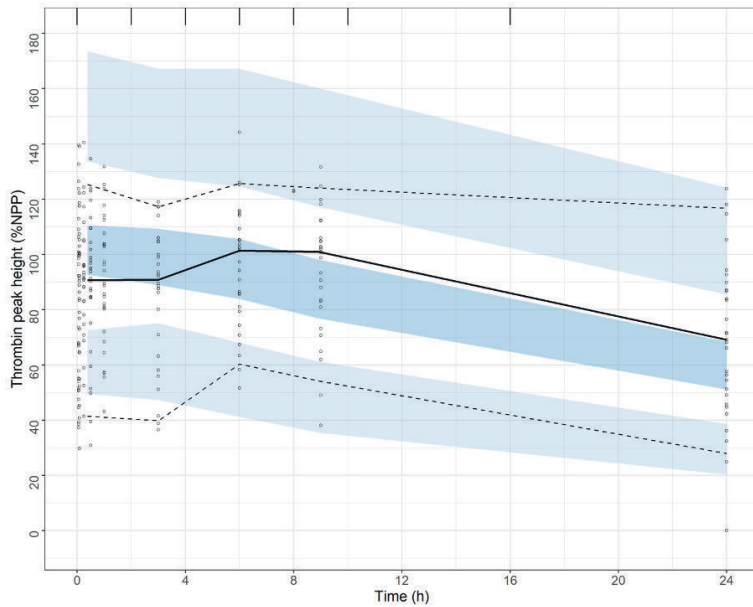
Supplementary figure 11: Prediction-corrected visual predictive check of the thrombin potential model by Buk-kems et al. Dots represent observed plasmin peak height levels; the solid black line represents the 50th percentile of observed data; the dashed black lines represent the 5th and 95th percentiles of the population model. Shaded areas depict the model predicted 95% confidence intervals of the simulated percentiles.
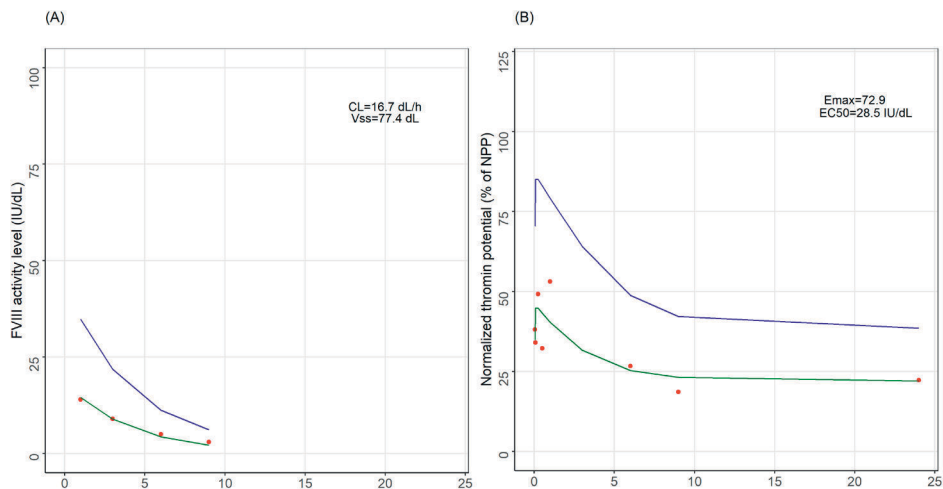
Supplement figure 12: Patient with inhibitor from the external validation dataset displaying its pharmacokinetic profile (A) and normalized thrombin potential response after factor VIII administration using the model by Bukkems et al (B). The green lines display the individual prediction, the blue lines display the population prediction, the red dots display the observed data. CL; individual predicted clearance, Vss; individual predicted volume of distribution at steady state., Emax; maximum effect of the normalized thrombin potential as a percentage of the normal pooled plasma, EC50; the factor VIII level that is associated with the half maximum effect.

SUPPLEMENTARY TABLES

Supplementary table 1: Reference values of the Nijmegen Hemostasis Assay based on the results of healthy individuals (n=20).

Parameter	Value, mean (SD)
Lag time (min)	4.0 (1.0)
Time to thrombin peak (min)	11.1 (1.7)
Thrombin peak height (nM)	134 (32)
Thrombin potential (nM-min)	1580 (199)
Velocity of thrombin generation (nM/min)	20.0 (7.0)
Plasmin peak height (nM)	17.2 (8.5)
Fibrin lysis time (min)	19.5 (2.7)
Plasmin potential (nM-min)	280 (86)

Supplementary table 2: Pre- and post-infusion values of factor VIII activity level and Nijmegen Hemostasis Assay parameters. The median and interquartile range (IQR) are given for each time point.

		Baseline	15 min	30 min	1 hour	3 hours	6 hours	9 hours	24 hours
FVIII activity level (IU/dL)	Median	<1.0	52	49	46	36	29	20	7
	IQR	<1.0-<1.0	42-62	40-54	35-53	28-47	19-35	14-28	4-10
Lag time (min)	Median	12.5	3.0	3.0	3.0	3.3	3.5	3.5	3.3
	IQR	5.0-140	3.0-3.5	3.0-3.5	2.9-3.4	3.0-3.7	3.2-4.2	3.0-3.5	3.0-4.8
Time to thrombin peak (min)	Median	26.0	9.8	9.5	9.8	12.1	11.8	12.0	14.8
	IQR	19.9-140	9.3-11.0	8.4-12.0	8.6-12.4	9.8-14.3	10.0-13.9	10.3-14.8	12.8-16.3
Thrombin peak height (nM)	Median	15	142	138	119	100	109	110	62
	IQR	undetectable-19	92-166	84-200	73-165	55-133	61-144	57-144	37-89
Thrombin potential (nM-min)	Median	280	1823	1897	1814	1790	1886	1933	1440
	IQR	undetectable-574	1683-2038	1520-2103	1498-2167	1348-1985	1565-2128	1480-2129	1044-1878
Velocity of thrombin generation (nM/min)	Median	0.9	21.0	22.6	15.4	11.3	12.7	12.7	5.7
	IQR	undetectable-2.3	11.4-29.8	10.7-38.8	8.1-29.6	5.2-21.2	5.8-20.7	5.2-19.0	3.8-9.3
Plasmin peak (nM)	Median	27.4	21.5	21.0	21.6	20.1	24.4	21.4	19.5
	IQR	17.5-32.0	14.5-25.0	14.9-25.8	13.7-25.9	15.9-27.3	18.9-29.0	15.1-27.4	13.8-23.6
Fibrin lysis time (min)	Median	21.5	24.3	24.0	23.5	21.8	21.0	20.5	21.0
	IQR	16.0-23.4	20.8-28.3	21.2-31.6	20.5-27.7	19.6-23.4	18.2-25.2	18.3-25.5	18.7-23.2
Plasmin potential (nM-min)	Median	201	103	211	223	184	210	202	180
	IQR	163-282	137-255	167-255	133-263	150-240	168-271	127-244	139-223

3

Supplementary table 3: Pre- and post-infusion values of normalized thrombin peak and thrombin potential. The median and interquartile range (IQR) are given for each time point.

		Baseline	15 min	30 min	1 hour	3 hours	6 hours	9 hours	24 hours
Thrombin peak height (% of NPP)	Median	6	51	59	49	44	46	45	24
	IQR	undetectable-8	35-71	38-84	28-68	22-57	26-60	23-66	15-39
Thrombin potential (% of NPP)	Median	12	92	93	90	91	91	98	71
	IQR	undetectable-29	79-104	76-105	78-105	58-103	78-107	74-109	56-94
Plasmin peak height (% of NPP)	Median	95	74	74	79	74	82	74	70
	IQR	69-112	51-85	57-88	53-90	61-95	73-102	59-98	52-85

Supplementary table 4: Precision and accuracy assessment of the published and re-estimated PK-PD models

Model reference	MPE (%)	MAPE (%)
Factor VIII Bukkems et al.	60.9	61.3
Factor VIII re-estimated	-8.47	26.3
Thrombin peak height Bukkems et al.	6.83	38.6
Thrombin peak height re-estimated	2.92	37.7
Thrombin potential Bukkems et al.	7.46	18.6
Thrombin potential re-estimated	-6.49	19.9
Plasmin peak height Bukkems et al.	58.9	58.9
Plasmin peak height re-estimated	-2.72	22.1

3

SUPPLEMENTARY REFERENCES
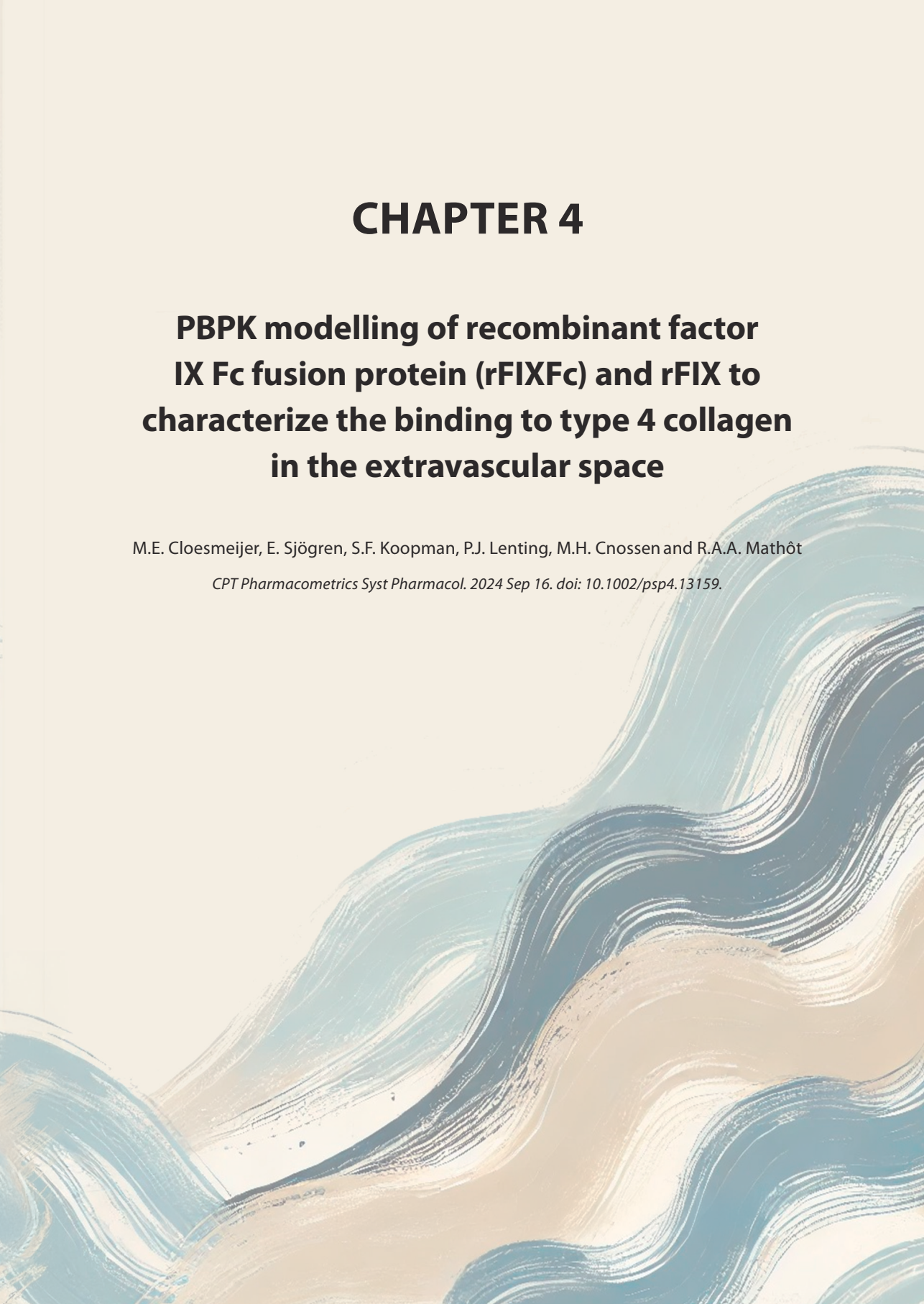
1.   van Geffen, M., et al., *A novel hemostasis assay for the simultaneous measurement of coagulation and fibrinolysis.* Hematology, 2011. **16**(6): p. 327-36.
2.   Bukkems, L.H., et al., *Combining factor VIII levels and thrombin/plasmin generation: A population pharmacokinetic-pharmacodynamic model for patients with haemophilia A.* Br J Clin Pharmacol, 2022. **88**(6): p. 2757-2768.

CHAPTER 4

PBPK modelling of recombinant factor IX Fc fusion protein (rFIXFc) and rFIX to characterize the binding to type 4 collagen in the extravascular space

M.E. Cloesmeijer, E. Sjögren, S.F. Koopman, P.J. Lenting, M.H. Cnossen and R.A.A. Mathôt

ABSTRACT

Patients with severe and sometimes moderate hemophilia B are prophylactically treated with factor IX concentrates to prevent bleeding. For some time now, various extended terminal half-life (EHL) recombinant factor IX concentrates are available allowing less frequent administration during prophylaxis in comparison to standard half-life recombinant FIX (rFIX). Especially recombinant FIX-Fc fusion protein (rFIXFc; Alprolix®) exhibits a rapid distribution phase, potentially due to binding to type IV collagen (Col4) in the extravascular space. Studies suggest that the presence of extravascular rFIXFc is protective against bleeding as without measurable FIX activity in plasma, no extra bleeding seems to occur. The physiologically-based pharmacokinetic (PBPK) model for rFIXFc which we describe in this study, is able to accurately predict the observed concentration-time profiles of rFIXFc in plasma and is able to quantify the binding of rFIXFc to Col4 in the extravascular space after an intravenous dose of 50 IU/kg rFIXFc in a male population. Our model predicts that the total AUC of rFIXFc bound to Col4 in the extravascular space is approximately 19 times higher compared to the AUC of rFIXFc in plasma. This suggests that rFIXFc present in the extravascular compartment may play an important role in achieving hemostasis after rFIXFc administration. Further studies on extravascular distribution of rFIXFc and the distribution profile of other EHL-FIX concentrates are needed to evaluate the predictions of our PBPK model and to investigate its clinical relevance.

INTRODUCTION

Hemophilia B patients are characterized by a deficiency of coagulation factor IX (FIX) resulting in bleeding, typically in joints and muscles[1]. Patients with severe and sometimes moderate hemophilia B receive FIX prophylaxis to prevent bleeding by maintaining a plasma FIX trough level of at least >1 IU/dL[2]. For some time now, biochemically modified FIX concentrates with extended terminal half-lives (EHL-FIX concentrates) are available for prophylaxis [3]. One of these concentrates consists of recombinant FIX coupled to the human IgG1 Fc domain (rFIXFc; Alprolix). Compared to standard terminal half-life recombinant FIX concentrate (rFIX; Benefix), rFIXFc has been shown to have a four to five times longer terminal half-life[3], resulting in less frequent dosing to maintain target FIX trough concentrations, thereby improving patient burden of administration frequency and quality of life.

Especially rFIXFc has been demonstrated to exhibit a rapid distribution phase, which is possibly due to binding to the neonatal Fc-receptor (FcRn) and to type IV collagen (Col4) in the extravascular space (Figure 1). Col4 is a major component of the basement membrane, which is a differentiated extravascular space that provides support and structural integrity to various tissues and organs, including blood vessels[4]. Endothelial cells line the inner surface of blood vessels and form a continuous layer known as the endothelium. The basement membrane, which lies beneath the endothelium, is composed
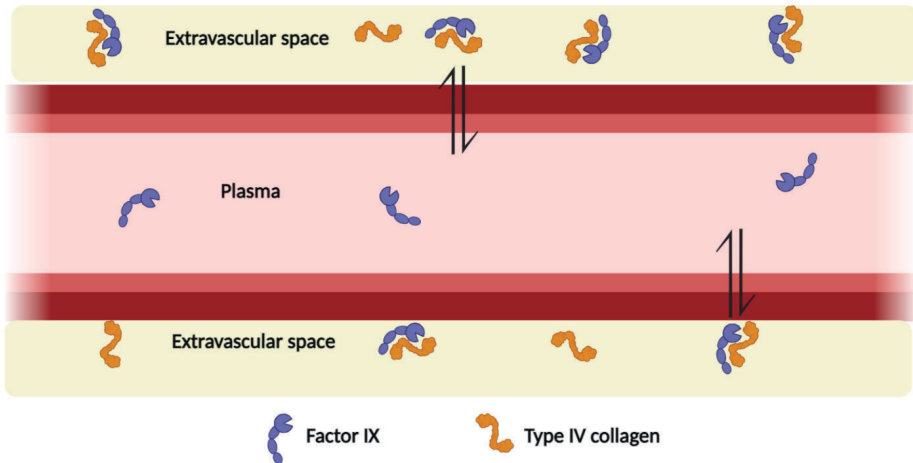

Figure 1. Schematic representation of a blood vessel showing the distribution of Factor IX (FIX) in plasma and the extravascular space. FIX circulates in plasma. In the extravascular space, FIX binds to Type 4 collagen in the extracellular matrix.

of various components, including Col4[5]. The extravascular concentration pool of both rFIX and rFIXFc is approximately 17-20 times greater compared to plasma according to studies[6,7] Studies suggest that the presence of extravascular rFIXFc is protective against bleeding as without measurable FIX activity in plasma, no extra bleeding seems to occur[7]. Despite these findings, current empirical population pharmacokinetic (PK) models for FIX only describe FIX concentrations over time in plasma, as FIX concentrations are typically measured in the blood and not in the extravascular space[3]. Therefore, a better understanding of the distribution and PK of rFIXFc in the extravascular space is important for optimization of the treatment of hemophilia B patients with this and other EHL-concentrates.

Physiologically-based pharmacokinetic (PBPK) modelling is a powerful tool that allows for the prediction of drug distribution and PK in various tissues, including the extravascular space[8]. Unlike empirical population PK models, PBPK models are based on mechanistic understanding of drug absorption, distribution, metabolism, and elimination in the body, and can take into account physiological factors and physicochemical characteristics of the drug. Therefore, PBPK modelling offers a potential solution to the current limitations of FIX PK modelling, allowing for the prediction of rFIXFc distribution and PK in both plasma and extravascular space.

In this study, we aim to develop a PBPK model for rFIXFc using the PK-Sim platform. Our goal is to predict the PK of rFIXFc in plasma and investigate the distribution and binding of rFIXFc to Col4 in the extravascular space of various tissues. By exploring the distribution and PK of rFIXFc in the extravascular space, we will gain new insights into the potential impact of these factors on the hemostatic characteristics of the drug. Additionally, we aim to assess the applicability of the developed PBPK model for other FIX concentrates such as rFIX . With this study, we hope to begin to acquire a better understanding of the most optimal use of EHL-FIX concentrates in people living with hemophilia B.

METHODS

Software
The whole-body scale PBPK modelling of rFIXFc and rFIX was performed using PK-Sim (version 11 – build 150, Open Systems Pharmacology)[9]. Plasma concentration-time curve data for rFIX were obtained from literature using GetData Graph Digitizer (Version 2.26.0.20). Data analysis and graphics were performed with the R (Version 4.1.1) and R Studio (version 1.4.1717).

PBPK model development of rFIXFc

The base model for large molecule drugs in the software package has been described previously[8]. Fifteen organs were included in the model structure to represent a virtual human. Each tissue compartment is subdivided into a plasma compartment, vascular endothelium compartment, an endosomal compartment, an interstitial fluid or extra-vascular compartment, and an intracellular space compartment (figure 2). In the endo-somal compartment, a generic mechanistic model for FcRn-drug binding and complex recycling was included. The transit of drugs around the body and between organs is mediated via plasma flow into tissues and then returned via plasma flow except for the portion undergoing lymphatic drainage into a lymph node compartment, which then returns back to plasma. More details about the PBPK model and mass transfer process can be found in the supplementary.

For development of the PBPK model for rFIXFc, physicochemical properties and clinical observations of rFIXFc were collected from published literature and the European public assessment report (EPAR)[10].
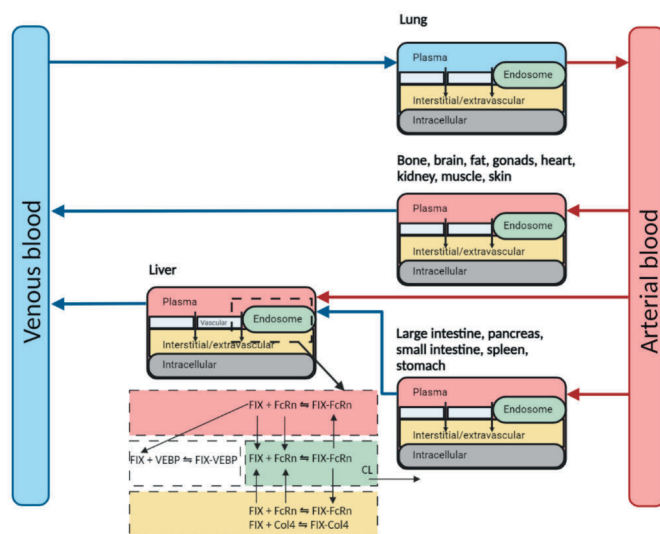
Figure 2. Schematic overview of the physiologically-based pharmacokinetic model. Each of the organ compartments consist of a vascular space (red or blue), containing blood serum and blood cells, an endothelial barrier (white, interrupted by small and large pores), interstitial/extravascular space (yellow), which contains the type 4 collagen (Col4). Factor IX (FIX) is able to bind reversibly to the Col4 in the extravascular space and FIX has binding partner in the vascular endothelium (VEBP). In the endosomal space (green) the reversible binding of rFIXFc to the neonatal Fc receptor (FcRn) is included.

Using the PK-Sim software, we developed a PBPK model for rFIXFc in a virtual Caucasian male patient of 30 years with a height of 176 cm and body weight of 73 kg receiving an intravenous (IV) dose of 50 IU/kg rFIXFc (approximately 0.6 mg/kg)[10]. According to the EPAR specification, 1 mg of rFIXFc contains 55-84 IU rFIXFc activity. In our model, we used 1 IU of rFIXFc activity corresponding with 12 µg of protein. Concentrations of rFIXFc activity are expressed in nanomolar (nM); molecular weight of rFIXFc is 98 kDa, Therefore, in our model we used 1 IU/mL of rFIXFc is equal to 122 nM. However, FIX has a normal activity of 90 nM[11], therefore we opted for the conversion of 1 IU/mL of rFIXFc is equal to 122 nM, as this was the closest to the FIX activity of 90 nM.

To account for the rapid distribution phase of rFIXFc, we incorporated binding to Col4 in the extravascular space. The tissue expression distribution of Col4 (relative expression amount) in the model was informed by the PK-Sim® expression database based on array profiles[12]. It has been reported that FIX may also bind to the vascular endothelium[13]. Therefore, we also included a binding site for rFIXFc in the vascular space as a vascular endothelium binding partner (VEBP) to replicate the mechanics of binding to vascular endothelium. A generic enzyme was added to the model to simulate the degradation of rFIXFc in plasma. The reaction was implemented as first-order reaction described by the catalytic rate constant Kcat. Moreover, we incorporated the FcRn pathway into our model to account for the recycling of rFIXFc through these receptors. The model parameters related to the binding of rFIXFc to Col4 and VEBP, available Col4 and VEBP in tissues, enzymatic degradation, and recycling through FcRn receptors were calibrated using observed clinical data of rFIXFc in plasma. Functionalities provided in PK-Sim for model parameter estimation (Monte-Carlo optimization method) and local sensitivity analysis were applied. A detailed description of the sensitivity analysis is provided in the supplement.

Model verification

To verify the accuracy of our PBPK model, we compared the simulated rFIXFc PK profiles with the observed clinical data from the EPAR[10]. A virtual male population was generated, consisting of 1000 subjects ranging in age from 12 to 60 years. Each individual in the population was characterized by their height, weight and BMI. The population predictions were plotted as the median with a 95% prediction interval. If the observed concentrations and its standard deviation fall within the 95% prediction interval in the majority of calculations, it indicates that the model provides a reasonable estimate of the observed data variability.

Applicability of developed PBPK model for rFIX

To assess the applicability of the developed PBPK model for other FIX concentrates such as rFIX, we predict plasma rFIX concentrations after IV administration of rFIX. In the rFIXFc model the FcRn pathway was disabled and the molecular weight was adjusted to 55 kDa for rFIX[14]. Here, we aim to understand the impact of FcRn-mediated recycling to the PK of rFIXFc. If the model accurately predicts the PK of rFIX when disabling FcRn recycling, then it indicates that other parameters and mechanisms incorporated in the model (aside from FcRn recycling) are sufficient to predict the PK of rFIXFc.

The predicted rFIX plasma concentrations were then compared by using observed clinical data provided by Suzuki et al[15] where patients received a median dose of 55 IU/kg of rFIX (approximately 0.25 mg/kg, since 1 mg of rFIX contains at least 200 IU/dL rFIX activity)[16]. The model performance was assessed in which the observed clinical data had to be within a two-fold error of the PBPK model prediction.

Prediction of extravascular rFIXFc concentration in major tissues

To further understand the PK behavioral characteristics of rFIXFc in the extravascular tissues, we simulated the extravascular rFIXFc binding to Col4 over time of 50 IU/kg rFIXFc in major organs in a Caucasian male patient of 30 years with a height of 176cm and body weight of 73kg. The extravascular tissues concentrations of major organs in the human body were simulated, including bone, brain, gonads, heart, intestinal mucosa, (small and large) intestines, kidney, liver, lung, muscle, pancreas, skin, spleen and stomach.

RESULTS

PBPK modelling and model evaluation

A PBPK model was developed for rFIXFc using the base model for large molecules in PK-Sim with modifications to feature the binding of rFIXFc to Col4. Supplement figure 1 displays a schematic overview of the model development. The model was optimized by fitting the model to the reference plasma concentration-time profiles through estimation of drug specific parameters relevant for the elimination and distribution.

Parameter sensitivity analysis

A sensitivity analysis was performed to evaluate model parameters that influence the PK of rFIXFc in plasma. In summary, total body clearance was most sensitive to Kcat and to a lesser degree the binding to FcRn, while the hydrodynamic radius was the most influential on the volume of distribution. Albeit important for the overall model performance, the binding to Col4 and VEBP was identified to have less influence on the plasma PK of

rFIXFc. Further information and details on the sensitivity analysis method and results are displayed in the supplement and supplement figure 2.

Simulations of rFIXFc and rFIX in plasma

Observations and simulated rFIXFc plasma concentration-time profiles using the final model are shown in Figure 3. We simulated 1000 virtual males with ages ranging from 12 to 60 years that matched the population of the observed clinical trial[10]. In Figure 3A the observed rFIXFc and predicted rFIXFc concentrations in plasma over time after single bolus dose of 50 IU/kg (0.6 mg/kg) in a virtual male population are displayed. After refining the model, the observed rFIXFc concentrations were adequately predicted by the model.
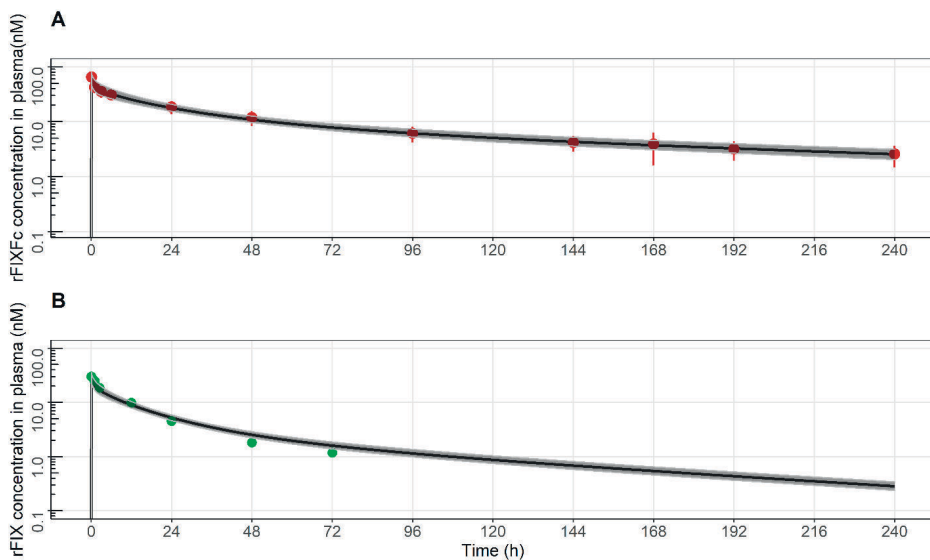
Figure 3: Population predicted of rFIXFc and rFIX concentrations in plasma over time. A) Observed rFIXFc and pre-dicted rFIXFc concentrations in plasma over time in a virtual male population of 12-60 years old after single bolus dose of 50 IU/kg (0.6 mg/kg). Observations were obtained from the EPAR[10] B) Observed rFIX and predicted rFIX concentrations in plasma over time in a virtual male population 12-60 years old on after single bolus dose of 50 IU/kg (0.25 mg/kg). Observations were obtained from Suzuki et al.[15]V Black solid line: population predictions, red circles: median observed rFIXFc concentrations and standard deviation, green circles: median observed rFIX concentrations, grey shaded area: 95% prediction interval.

Table 1 summarizes the model parameters that were used and estimated in the final PBPK model. The observed rFIXFc concentrations and most of its standard deviations are within the 95% prediction interval. This shows that the PBPK model is able to the predict rFIXFc concentrations in a male population between 12 and 60 years old. For rFIXFc a CL of 2.49 mL/h/kg and a Vss of 370 mL/kg was obtained. The calculated terminal half-life

Table 1. Parameters of the final PBPK model

Parameter	Final value	Reference
rFIXFc		
Molecular weight	98 kDa	Drugbank
Hydrodynamic radius	3.6 nm	Estimated
K_D^{FcRn}	1.42 nM	Estimated
K_D^{Col4}	5.26 µM	Estimated
K_D^{VEBP}	0.04 µM	Estimated
rFIX[1]		
Molecular weight	55 kDa	Drugbank
Hydrodynamic radius	3.4 nm	Estimated with inbuild calculator
Binding partners (concentration)		
Collagen IV extravascular	3.83 µM	Estimated
Endothelium vascular	20.0 µM	Estimated
Enzyme		
Enzymatic activity (Kcat)	0.061 1/day	Estimated

K_D^{FcRn} : Dissociation constant for FcRn binding in endosomal space; K_D^{Col4}: Dissociation constant for binding in extravascular space, K_D^{VEBP}: Dissociation constant for vascular endothelium binding partner (VEBP) The K_D^{FcRn} for rFIX was set to 9999 M, indicating no binding to the FcRn receptor. Values for K_D^{Col4} and K_D^{VEBP} were the same as for rFIXFc. rFIXFc = Alprolix®

was 142h. The binding of rFIXFc to the FcRn receptor played a crucial role in accurately characterizing the concentration profiles of rFIXFc in plasma, as the Kd to Fc-Rn receptor was estimated as 1.42 nM.

To assess the applicability of the developed PBPK model for rFIX, we disabled the FcRn recycling mechanism and used the molecular weight to rFIX (55 kDa), in all other respect the same parameterization was applied. In Figure 3B, the median observed rFIX and predicted rFIX concentrations in plasma over time in a virtual male population of 12-60 years is displayed. Most median observed rFIX concentrations are within the 95% prediction interval, although the median observed rFIX concentrations at t=48 and 72h are somewhat lower compared to the model prediction. For rFIX we obtained a CL of 7.51 mL/h/kg and a Vss of 339 mL/kg, while the terminal half-life was 44h.

PBPK model predictions of rFIXFc concentrations in tissues of extravascular space

The rFIXFc PBPK model quantified the binding of rFIXFc to Col4 in the extravascular space. Figure 4 displays the extravascular rFIXFc concentrations in tissues and Table 2 displayed the PK parameters in plasma and tissues. The results showed that area under the curve (AUC) of rFIXFc to Col4 in the extravascular space was approximately 19 times higher compared to the plasma concentration. The highest concentrations
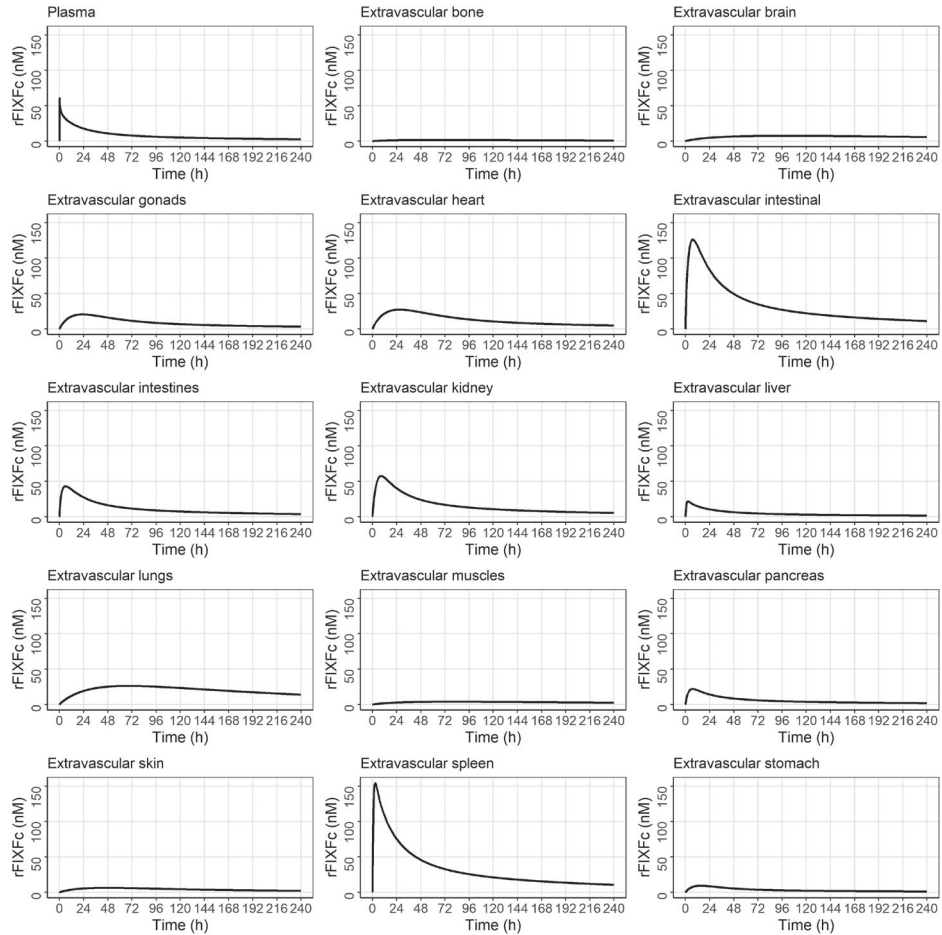
Figure 4: Predicted rFIXFc concentration over time in plasma and extravascular tissues after an intravenous bolus of 50 IU/kg rFIXFc. Black solid line: predicted population median curve.

of extravascular rFIXFc bound to Col4 were found in the spleen and lungs. The peak rFIXFc concentrations and AUC in the extravascular spleen and lungs were 154 and 26.2 nmol, and 10.1 and 7.9 mmol*h/L, respectively. The peak rFIXFc concentrations in the extravascular lungs were lower compared in the extravascular spleen. It is important to note that the concentration of rFIXFc in the extravascular space of the lungs decreased very slowly over time, resulting in a high AUC. Moreover, the extravascular rFIXFc peak in the spleen is higher (154 nmol) compared to the plasma rFIXFc peak (61 nmol).

Table 2. Plasma and tissue exposure after 50 IU/kg rFIXFc

Parameter	AUC (0->240h) (nmol × h/L)	Peak rFIXFc (nM)	Tmax (h)
rFIXFc intravascular			
Plasma	2455	60.9	0.05
rFIXFc extravascular			
Bone	431.5	1.557	76.5
Brain	3601	7.430	94.00
Gonads	2715	20.46	20.50
Heart	3996	27.28	26.50
Intestinal mucosa	17549	27.28	8.00
Intestines	3996	210.6	5.75
Kidney	4952	57.55	9.50
Liver	1402	21.84	2.25
Lungs	7933	26.22	79.50
Muscles	1421	3.921	81.25
Pancreas	1785	22.05	6.75
Skin	1340	6.247	47.50
Spleen	10131	154.4	2.25
Stomach	998.2	9.320	14.75
Total rFIXFc in extravascular tissues	49052	-	-

AUC: area under the concentration versus time curve, Cmax: maximum concentration, Tmax: time to reach maximum concentration; rFIXFc = Alprolix®

4

DISCUSSION

PBPK modelling is a valuable tool for assessing drug distribution in various tissues and organs. It can be applied to predict drug distribution in previously unexplored scenarios, such as binding in extravascular spaces of tissues, with the aim of enhancing our understanding of potential associations between extravascular concentrations and drug effects. In this study, we developed a PBPK model for rFIXFc. Our model was able to predict the PK of rFIXFc in plasma. We also quantified the binding of rFIXFc to Col4 in the extravascular space of various tissues. Moreover, the rFIXFc model was able to predict the plasma concentration-time profile of rFIX.

Previous studies have acknowledged the potential importance of extravascular rFIXFc for hemostasis and protection form bleeding [17,18]. However, to our knowledge, no studies have quantified the concentration of rFIXFc in the extravascular space of tissues in a human population. Our study provides novel insights in this area by predicting that

the AUC of rFIXFc in the extravascular space of tissues is approximately 19 times higher than in plasma, suggesting that extravascular rFIXFc plays a significant role in the local control of bleeding. Our study also revealed the highest AUC of extravascular rFIXFc to be present in the spleen, lungs, intestinal mucosa, and kidney. These higher tissue concentrations of rFIXFc suggests that they may be particularly responsive to treatment with rFIXFc, and that the drug may have a more pronounced effect on hemostasis in these tissues compared to other organs with lower concentrations of extravascular rFIXFc.

Previous studies investigated the distribution of rFIX and rFIXFc concentrations in animals. Van der Flier et al. observed that both rFIX and rFIXFc distributes outside the plasma compartment in certain tissues at higher plasma levels, indicating that rFIX and rFIXFc act similar[19].They found highly perfused tissues such as the heart, liver and lungs signaled a high extravascular level of rFIXFc. While Herrmann et al. found that the highest homogenate plasma FIX level was in the liver, kidney, and lungs in rodents, with a high homogenate plasma FIX level also observed in the lungs after 72h[20]. Our study similarly describes a high level of rFIXFc in the extravascular space of the lungs, not only supporting the potential importance of extravascular rFIXFc for local hemostatic control but also verifying the accuracy and applicability of our PBPK model. However, our PBPK model also predicted the highest extravascular rFIXFc concentration in the spleen. Contrastingly, Herzog et al. found the highest distribution of rFIX to be in the liver, while the distribution to the spleen was much lower compared to the liver.[21]

In our PBPK model for rFIXFc, the distribution to the extravascular space in the liver was much lower compared to the distribution to other organs. The expression distribution of Col4 (relative expression amount) was provided by the PK-Sim® expression database based on array profiles.

The relative expression of Col4 was widely distributed in most organs of humans, with highest expression occurs in the spleen, followed by the lungs, which is reflected by the predictions made by the PBPK model. However, clinical measurements were only obtained from human plasma and not from human extravascular space. Van der Flier et al. used single-photon emission computed tomography/computed tomography (SPECT/CT) technique to investigate the bio distribution of rFIXFc in mice. These SPECT/CT images show the distribution of rFIXFc in various organs. However, we cannot quantify these SPECT/CT images to molar concentrations[19]. Our PBPK model therefore seems to be the only tool now available to estimate the binding of rFIXFc to Col4. Further studies may be needed to investigate the impact of tissue-specific PK on the efficacy and safety of rFIXFc. At low rFIXFc plasma concentrations, extravascular rFIXFc may be particularly

important for achieving hemostasis, since it may provide a local source of the drug that can rapidly be available at the site of injury.

The simulated terminal half-life for rFIXFc and rFIX in plasma was calculated as respectively 142 h and 44 h. Our PBPK model considered the binding of rFIXFc to FcRn receptors, which enabled us to capture the prolonged half-life effect. This modelling approach allowed us to simulate the PK behavior of rFIXFc and rFIX in a dynamic and mechanistic manner, taking into account relevant physiological processes and receptor interactions[22]. When comparing our findings with the study by Diao et al., Koopman et al. and Björkman et al., half-lives of respectively 82, 88 h for rFIXFc and 22 h for rFIX[23–25] were reported, which are notably lower than our calculations. Tardy et al. observed a median half-life of 50h for rFIX in a group of patients aged 13-75 years. This half-life closely aligns with our own findings of 44h. Notably, their study extended the sampling period beyond 72 h, while Björkman et al. restricted sampling to a maximum of 72 h. This divergence in sampling duration may account for the disparity in reported half-life values. Moreover, in our study PK-Sim calculated the half-life based on the terminal 10% of the data points, which might also have contributed to the observed discrepancy compared to other reported half-lives.[26]. While the previous mentioned studies determined the half-life based on the elimination rate, which provides a different perspective on the PK of rFIXFc and rFIX. As our model accurately describes the dynamics of the terminal phase of the plasma profile it is obvious that this discrepancy between the simulated and observed half-lives is caused by the different approaches for calculation. Furthermore, it is important to consider the complexity of the PK profile of rFIXFc and the potential limitations of the population PK models used in previous studies[23,27,28]. Many existing population PK models for rFIXFc are based on two- or three-compartment models, which assume distinct phases in the drug concentration-time profile. However, our findings suggest that a three-compartment model may not adequately capture the complete PK behavior of rFIXFc. As it was necessarily to include an extra binding partner site for rFIXFc to adequately describe the rFIXFc plasma levels. Our PBPK modelling approach allowed us to simulate the PK behavior of rFIXFc and rFIX in a more mechanistic manner. By considering relevant physiological processes and receptor interactions, our model successfully captured the prolonged half-life effect of rFIXFc through its binding to FcRn receptors.

In our PBPK model, we estimated the (Kd of rFIXFc to Col4 as 5.3 µM in the extravascular compartment, while the available Col4 concentration in the extravascular compartment was estimated as 3.8 µM. It is important to consider other studies that have investigated the binding affinity of rFIXFc to Col4. One study focused on mice and reported a Kd of 40 nM for rFIXFc, with an available Col4 concentration of 574 nM[7]. We obtained differ-

ent values regarding the Kd for rFIXFc and the available Col4 concentration, although a direct comparison of mice data to human data is challenging due to species differences. However, an extra binding site of rFIXFc was necessarily to implement in order to describe the rFIXFc over time in plasma adequately. Machado et al. concluded that there might be other binding partners besides Col4 for rFIXFc[29]. In our PBPK model, we included a binding partner in the vascular endothelium site (concentration 13.6 µM) and a Kd of 0.03 µM, which suggested a strong binding of rFIXFc to this binding partner in the vascular endothelium.

Although the developed model shows overall good performance, there are several limitations. Firstly, the model adopts a tissue expression pattern of Col4 binding sites to the extravascular space according to the array profile included in the PK-Sim database, while the actual distribution of Col4 may be slightly different from what is predicted by the array profiles. Secondly, our study did not include a direct comparison of our model predictions with experimental data from the extravascular space of tissues, since only plasma observations were available. Therefore, further validation of our predictions in these tissues is needed. Finally, the binding affinity of rFIXFc to Col4 and the available concentration of Col4 in the tissues was estimated in our PBPK model based on plasma rFIXFc observations. It was notable that the Kd constant for rFIXFc to Col4 was found to be higher compared to the available Col4 in the tissues. Nonetheless, we observed high concentrations of rFIXFc in the extravascular tissues based on parameter estimations. We refined the PBPK model by fitting it to observed data, enabling us to estimate the Kd constant and the available concentration of Col4. It is important to note that the estimation of binding parameters in PBPK models involves simplifications and assumptions. Furthermore, conducting a sensitivity analysis to investigate the parameters that significantly impact predictions is a crucial step in validating a PBPK model. A model is considered reliable if small variations in parameter values result in prediction changes for a dose metric that are within the expected range of its experimental measurement variability[30]. The PBPK model here was shown to be sensitive to parameter changes. The hydronymic radius significantly influences the rate of extravasation, affecting the distribution of the drug between the plasma and extravascular spaces.. K_D^{FcRn} showed a medium sensitivity on the clearance. The K_D^{FcRn} has an inverse effect on the clearance as this processes protects the entities from the generic implementation of endosomal clearance[8]. Not including this binding would result in higher clearance. K_D^{VEBP} and K_D^{Col4} showed respectively, medium and low sensitivity. The binding to Col4 and VEBP facilitates a localized distribution in the respective biophases, impacting not only the extravascular but also the intravascular dynamics of the drug. Despite low sensitivity for overall plasma PK, binding processes were necessary to capture the full dynamics in the plasma concentration-time profile. This is also in line with literature highlighting the

importance of the binding of rFIXFc to Col4[6,31,32]. Overall, in addition to the biological rationale, these processes improve model performance in terms of capturing plasma concentration dynamics. PBPK models aim to capture the overall behavior of drugs within the body, considering multiple physiological factors and interactions. However, the accuracy and reliability of specific parameter estimates, such as binding affinity, can be influenced by the availability and quality of data, as well as the model assumptions.

In conclusion, our study demonstrates the utility of PBPK modelling for predicting the PK of rFIXFc in plasma and for quantifying the binding of rFIXFc to Col4 in the extravascular space of various tissues. Furthermore, our study highlights the potential importance of extravascular rFIXFc for achieving hemostasis and optimizing treatment in people living with hemophilia B. Future studies should focus on further characterizing the distribution and PK of rFIXFc in the extravascular space of tissues, as well as the potential impact of these factors on the hemostatic effects of the drug. In addition, future studies should investigate other EHL FIX concentrates and their potential binding to Col4.

4

REFERENCES

1. Franchini, M., Frattini, F., Crestani, S. & Bonfanti, C. Haemophilia B: Current pharmacotherapy and future directions. *Expert Opin. Pharmacother.* **13**, 2053–2063 (2012).

2. Srivastava, A. *et al.* WFH Guidelines for the Management of Hemophilia, 3rd edition. *Haemophilia* **26**, 1–158 (2020).

3. Preijers, T. *et al.* In silico comparison of pharmacokinetic properties of three extended half-life factor IX concentrates. *Eur. J. Clin. Pharmacol.* **77**, 1193–1200 (2021).

4. Boudko, S. P., Danylevych, N., Hudson, B. G. & Pedchenko, V. K. Basement membrane collagen IV: Isolation of functional domains. In *Physiol. Behav.* 171–185 (2018).doi:10.1016/bs.mcb.2017.08.010

5. Loscertales, M. *et al.* Type IV collagen drives alveolar epithelial-endothelial association and the morphogenetic movements of septation. *BMC Biol.* **14**, 1–21 (2016).

6. Stafford, D. W. Extravascular FIX and coagulation. *Thromb. J.* **14**, (2016).

7. Mann, D. M., Stafford, K. A., Poon, M. C., Matino, D. & Stafford, D. W. The Function of extravascular coagulation factor IX in haemostasis. *Haemophilia* **27**, 332–339 (2021).

8. Niederalt, C. *et al.* A generic whole body physiologically based pharmacokinetic model for therapeutic proteins in PK-Sim. *J. Pharmacokinet. Pharmacodyn.* **45**, 235–257 (2018).

9. Lippert, J. *et al.* Open Systems Pharmacology Community—An Open Access, Open Source, Open Science Approach to Modeling and Simulation in Pharmaceutical Sciences. *CPT Pharmacometrics Syst. Pharmacol.* **8**, 878–882 (2019).

10. European Medicines Agency Alprolix product information. (2021).at <https://www.ema.europa.eu/en/documents/product-information/alprolix-epar-product-information_en.pdf>

11. Orlova, N. A., Kovnir, S. V., Vorobiev, I. I. & Gabibov, A. G. Coagulation Factor IX for Hemophilia B Therapy. *Acta Naturae* **4**, 62–73 (2012).

12. Cordes, H. & Rapp, H. Gene expression databases for physiologically based pharmacokinetic modeling of humans and animal species. *CPT Pharmacometrics Syst. Pharmacol.* 311–319 (2023). doi:10.1002/psp4.12904

13. Machado, S. K. *et al.* Modulation of Extravascular Binding of Recombinant Factor IX Impacts the Duration of Efficacy in Mouse Models. *Thromb. Haemost.* **123**, 751–762 (2022).

14. Liu, J., Jonebring, A., Hagström, J., Nyström, A. C. & Lövgren, A. Improved expression of recombinant human factor IX by co-expression of GGCX, VKOR and furin. *Protein J.* **33**, 174–183 (2014).

15. Suzuki, A., Tomono, Y. & Korth-Bradley, J. M. Population pharmacokinetic modelling of factor IX activity after administration of recombinant factor IX in patients with haemophilia B. *Haemophilia* **22**, e359–e366 (2016).

16. European Medicines Agency Benefix product information. (2015).

17. Feng, D. & , Katherine A. Stafford, George J. Broze, and D. W. S. Evidence of clinically significant extravascular stores of Factor IX. *Bone* **23**, 1–7 (2013).

18. GUI, T. *et al.* Abnormal hemostasis in a knock-in mouse carrying a variant of factor IX with impaired binding to collagen type IV. *J. Thromb. Haemost.* **7**, 1843–1851 (2009).

19. Flier, A. van der *et al.* Biodistribution of recombinant factor IX, extended half-life recombinant factor IX Fc fusion protein, and glycoPEGylated recombinant factor IX in hemophilia B mice. *Blood Coagul. Fibrinolysis* **34**, 353–363 (2023).

20. Herrmann, S. *et al.* Tissue distribution of rIX-FP after intravenous application to rodents. *J. Thromb. Haemost.* **18**, 3194–3202 (2020).

21. Herzog, E. *et al.* Biodistribution of the recombinant fusion protein linking coagulation factor IX with albumin (rIX-FP) in rats. *Thromb. Res.* **133**, 900–907 (2014).

22. Peters, R. T. *et al.* Prolonged activity of factor IX as a monomeric Fc fusion protein. *Blood* **115**, 2057–2064 (2010).

23. Diao, L. *et al.* Population pharmacokinetic modelling of recombinant factor IX Fc fusion protein (rFIXFc) in patients with haemophilia B. *Clin. Pharmacokinet.* **53**, 467–477 (2014).

24. Koopman, S. F. *et al.* A new population pharmacokinetic model for recombinant factor IX-Fc fusion concentrate including young children with haemophilia B. *Br. J. Clin. Pharmacol.* 1–12 (2023). doi:10.1111/BCP.15881

25. Björkman, S. Population pharmacokinetics of recombinant factor IX: Implications for dose tailoring. *Haemophilia* **19**, 753–757 (2013).

26. Simulations - Open Systems Pharmacology. at <https://docs.open-systems-pharmacology.org/working-with-pk-sim/pk-sim-documentation/pk-sim-simulations>

27. Simpson, M. L. *et al.* Population pharmacokinetic modeling of on-demand and surgical use of nonacog beta pegol (N9-gp) and rfixfc based upon the paradigm 7 comparative pharmacokinetic study. *J. Blood Med.* **10**, 391–398 (2019).

28. Bukkems, L. H. *et al.* A Novel, Enriched Population Pharmacokinetic Model for Recombinant Factor VIII-Fc Fusion Protein Concentrate in Hemophilia A Patients. *Thromb. Haemost.* **120**, 747–757 (2020).

29. Knoll Machado, S. *et al.* Modulation of Extravascular Binding of Recombinant Factor IX Impacts Hemostatic Efficacy in Mouse Models. *Blood* **140**, 2701–2702 (2022).

30. WHO Characterization and Application of Physiologically Based Pharmacokinetic Models. *Ipcs - WHO* (2010).

31. Leuci, A. *et al.* Extravascular factor IX pool fed by prophylaxis is a true hemostatic barrier against bleeding. *J. Thromb. Haemost.* **22**, 700–708 (2024).

32. Salas, J. *et al.* Extravascular Distribution of Conventional and Ehl FIX Products Using In Vivo SPECT Imaging Analysis in Hemophilia B Mice. *Blood* **130**, 1061 LP – 1061 (2017).

33. Cnossen, M. H. *et al.* SYMPHONY consortium: Orchestrating personalized treatment for patients with bleeding disorders. *J. Thromb. Haemost.* **20**, 2001–2011 (2022).

4
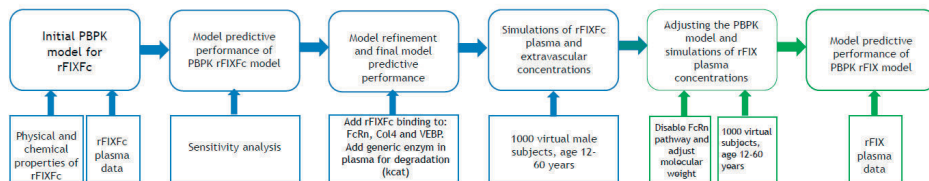
SUPPLEMENT

Supplement figure 1. Schematic overview of model development Col4: type 4 collagen, rFIX: recombinant factor IX, rFIXFc: Alprolix®, VEBP: vascular endothelium binding partner.

Mass transfer flow in physiologically-based pharmacokinetic modelling

Physiologically-based pharmacokinetic (PBPK) modelling is a mechanistic approach to describe how a substance behaves in the body by considering substance-specific properties and the underlying mammalian physiology. This approach relies on the of biological information for model development.

The fundamental concept involves dividing the body into physiologically relevant compartments, primarily vital organs. Each compartment has a mass balance equation, describing the substance's fate within it. PK-Sim® facilitates this by providing a physiological framework model, dividing the mammalian body into 15 organs, along with arterial and venous blood pools connecting these organs through blood flow. Within organs, further subdivisions occur to describe the vascular space in terms of plasma and (red) blood cells, as well as the vascular space divided into interstitial and cellular spaces[1]. This detailed compartmental model serves as the structural foundation for understanding substance behavior.

To simulate the entire body, a system of interdependent differential equations combines all mass balance equations. In this system, all organs are connected in parallel between arterial and venous blood pools, enabling blood to flow from arteries to veins. However, in the lungs, a closed circulation occurs due to blood flow in the opposite direction.

For the simulation of the whole body, all mass balance equations are combined in a system of interdependent differential equations. In the simplest version of this system, all organs are connected in parallel between the arterial and venous blood pools such that blood flows from arteries to veins, except in the lung where the circulation is closed by a blood flow in the opposite direction. The basic passive processes, which determine the behavior of a substance in an organ, are mass transport via the blood flow, permeation from vascular space into organ tissue and partitioning between blood plasma and organ tissue.

For details on the generic large molecule PBPK model implementation in PK-Sim we refer to Niederalt et al. 2018[1]. In brief, equations for the mass transfer of the rFIXFc from plasma (equation 1) and interstitial space (equation 2) to the endosomal space are displayed below, in which $F_{up,vas}$ is the fraction of endosomal uptake from plasma, k_{up} is the endosomal uptake rate constant, V_{end} is the endosomal volume, C^{comp}_{plasma} is the concentration of rFIXFc in plasma, and $C^{comp}_{extravascular}$ is the concentration of rFIXFc in interstitial (extravascular) space.

Equation 1)
$$\frac{d^{comp}}{dt} = F_{up} \times K_{up} \times V_{end} \times C^{comp}_{plasma}$$

Equation 2)
$$\frac{d^{comp}}{dt} = (1 - F_{up}) \times K_{up} \times V_{end} \times C^{comp}_{extravascular}$$

The recycling of the FcRn complex from the endosomal space going back to plasma (equation 3) and interstitial space (equation 4) is described below, in which $n_{rcomp\text{-}FcRn}$ is the amount of rFIXFc with FcRn complex, $F_{rec,end\text{->}plasma}$ is the fraction of recycling of the FcRn complex from the endosomal space to plasma, K_{rec} is the recycling rate constant, and $C_{comp\text{-}FcRn,\,end}$ is the concentration of the rFIXFc in the endosomal space.

Equation 3)
$$\frac{dn^{comp-FcRn}}{dt} = F_{rec,end\rightarrow plasma} \times K_{rec} \times V_{end} \times C_{comp-FcRn,end}$$

Equation 4)
$$\frac{d^{comp-FcRn}}{dt} = (1 - F_{rec,end\rightarrow plasma}) \times K_{rec} \times V_{end} \times C_{comp-FcRn,end}$$

The FcRn binding reaction for rFIXFc in plasma, interstitial (extravascular), or endosomal space is displayed in equation 5, in which K_{ass} is the association rate constant for FcRn binding, C_{comp} is the concentration of the rFIXFc in different organs, C_{FcRn} is the concentration of FcRn, K_d is the dissociation constant for FcRn binding and $C_{comp\text{-}FcRn}$ is the concentration of the FcRn complex with rFIXFc

Equation 5)
$$\frac{d^{comp-FcRn}}{dt} = K_{ass} \times C_{comp} \times C_{FcRn} - K_d \times K_{ass} \times C_{comp-FcRn}$$

Sensitivity Analysis

A sensitivity analysis was performed on the developed model to investigate how parameter adjustments (conducted as a local sensitivity analysis) affect the predicted values for half-life, total body clearance, and volume of distribution (plasma) following intravenous administration of a single 50 IU/kg dose of rFIXFc. In accordance with equation 6, we calculated the relative change in pharmacokinetic (PK) parameters in response to variations in model input parameters. This analysis included all optimized parameters and parameters that could significantly impact the results due to the modelling techniques employed. We applied a relative perturbation of 10% for this analysis.

Equation 6)
$$S = \frac{\Delta\ PK\ parameter}{\Delta p} \times \frac{p}{PK\ parameter}$$

S is the sensitivity of the PK parameter to the examined model parameter, ΔPK parameter is the change of the PK parameter (half-life, total body clearance, volume of distribution (plasma)), PK parameter represents the simulated PK parameter with the original parameter value, p is the original model parameter value and Δp the variation of the model parameter value. For example, a sensitivity value of +1.0 signifies that a 10% increase of the examined parameter causes a 10% increase of the simulated PK parameter. According to the WHO guidelines (WHO, 2010), sensitivity levels were defined as high (absolute value ≥ 0.5), medium (absolute value ≥ 0.2 but less than 0.5) or low (absolute value ≥ 0.1 but < 0.2)[2].
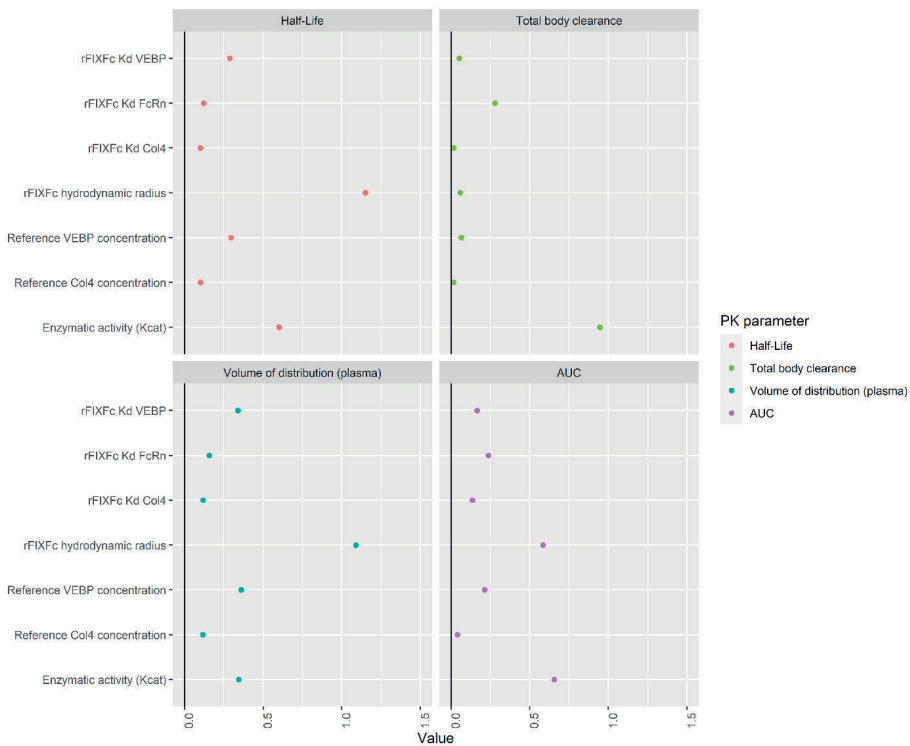
Supplement figure 2. Sensitivity analysis of half-life, total body clearance, volume of distribution (plasma) and area under the curve (AUC) of the PBPK model for Recombinant factor IX-Fc fusion protein (rFIXFc). Absolute sensitivity values are displayed. AUC: Area under the curve, Col4: type 4 collagen, FcRn: Neonatal Fc Receptor, Kd: dissociation constant, PK: pharmacokinetic, VEBP: vascular endothelium binding partner

SUPPLEMENTARY REFERENCES

1. Niederalt C, Kuepfer L, Solodenko J, et al. A generic whole body physiologically based pharmaco-kinetic model for therapeutic proteins in PK-Sim.*J Pharmacokinet Pharmacodyn*. 2018;45(2):235-57.
2. WHO. Characterization and Application of Physiologically Based Pharmacokinetic Models.*Ipcs - WHO*. 2010.

4
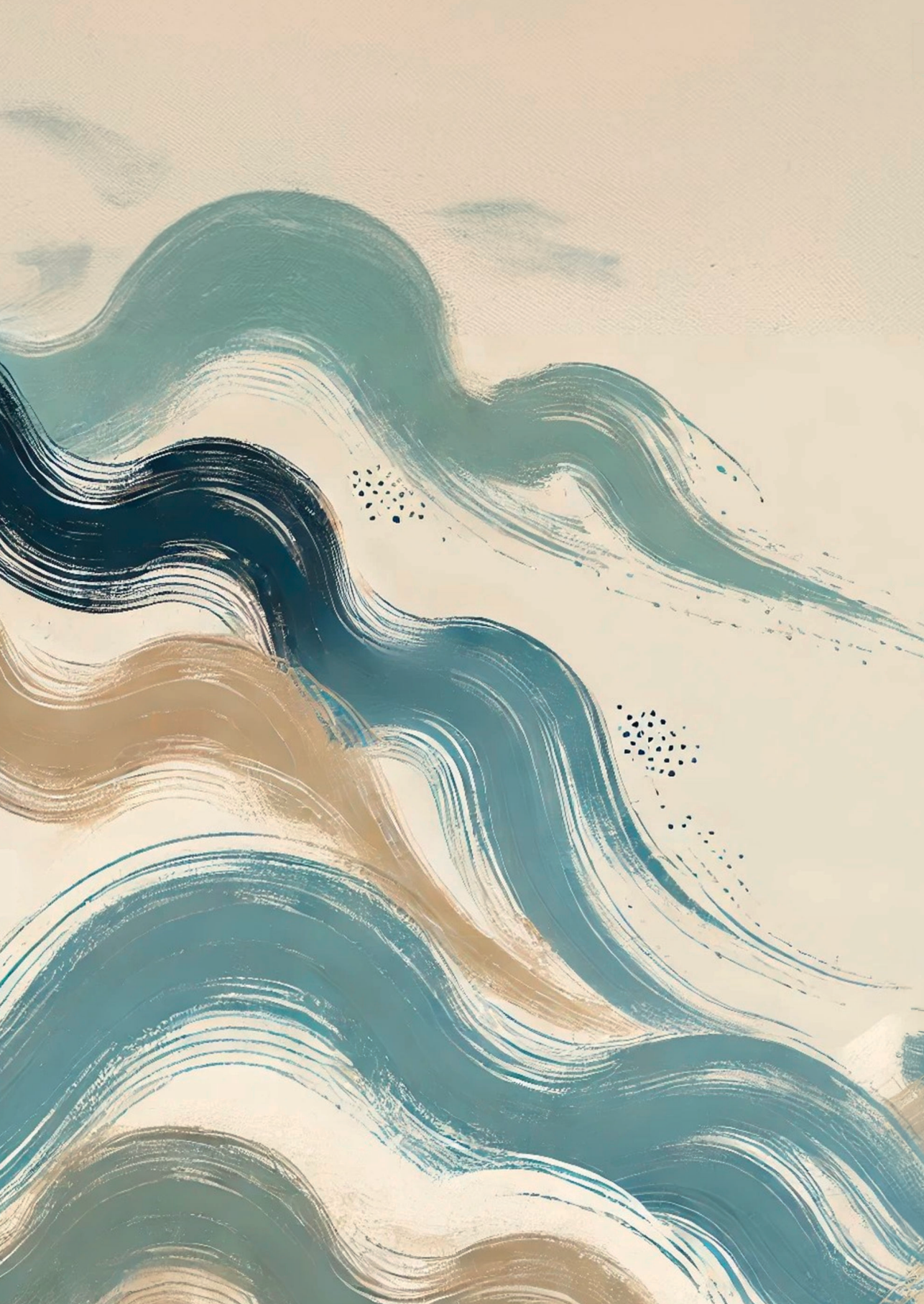
PART II:

Pharmacometrics in von Willebrand disease

CHAPTER 5
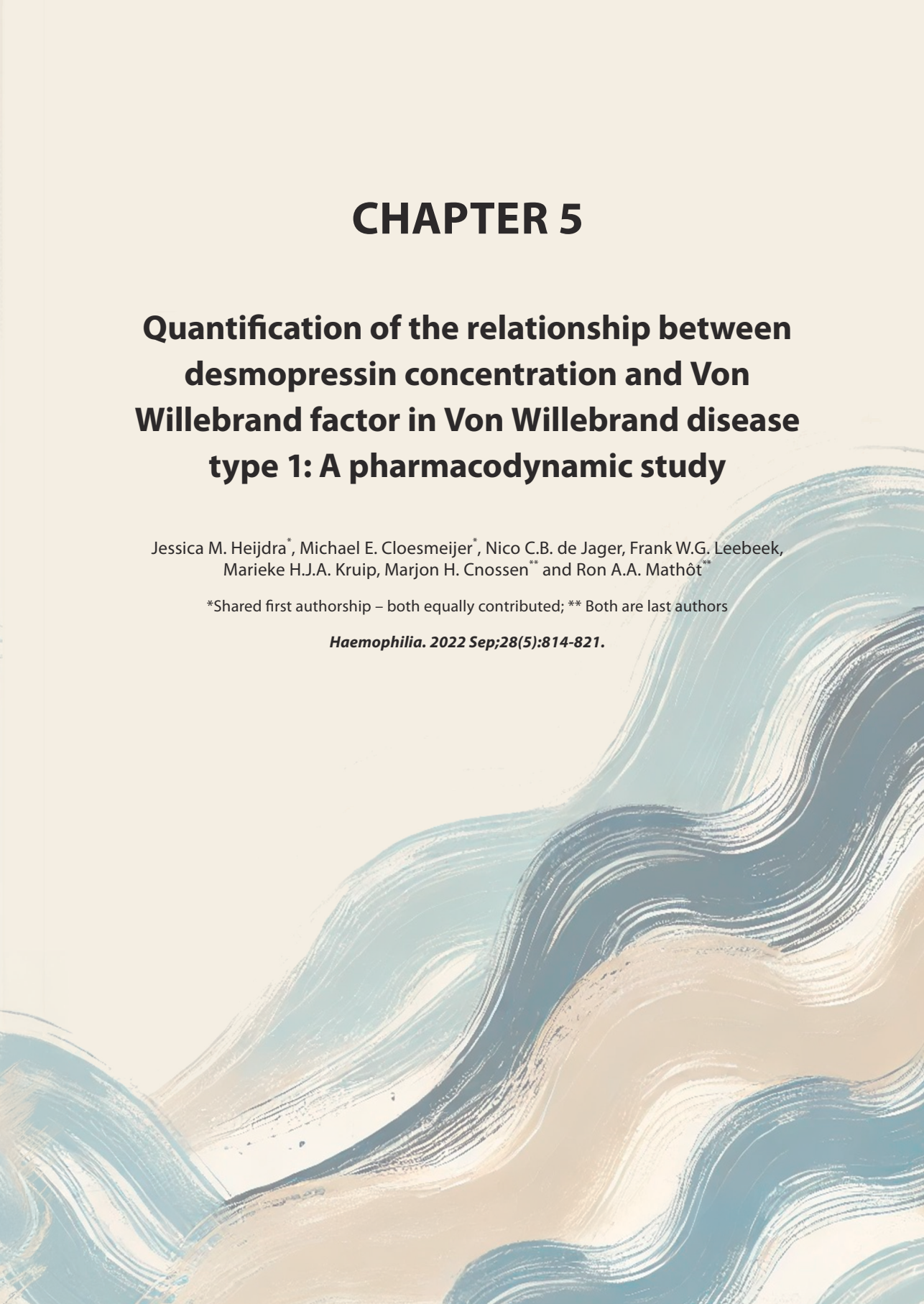
Quantification of the relationship between desmopressin concentration and Von Willebrand factor in Von Willebrand disease type 1: A pharmacodynamic study

Jessica M. Heijdra[*], Michael E. Cloesmeijer[*], Nico C.B. de Jager, Frank W.G. Leebeek, Marieke H.J.A. Kruip, Marjon H. Cnossen[**] and Ron A.A. Mathôt[**]

*Shared first authorship – both equally contributed; ** Both are last authors

ABSTRACT

Introduction: Desmopressin can be used to prevent bleeding in von Willebrand disease (VWD), but the relationship between desmopressin and von Willebrand factor activity (VWF:Act) has yet to be quantified.

Aim: To quantify the relationship between desmopressin dose, its plasma concentration and the VWF:Act response in type 1 VWD patients.

Methods: Forty-seven VWD patients (median age 25 years, IQR: 19-37; median body weight 71 kg, IQR: 59-86) received an IV desmopressin dose of 0.3 mcg/kg. In total, 177 blood samples were available for analysis. We developed an integrated population pharmacokinetic-pharmacodynamic (PK-PD) model using nonlinear mixed effect modelling. Subsequently, we performed Monte Carlo simulations to investigate the efficacy of the current dosing regimen.

Results: A one-compartment PK model best described the time profile of the desmopressin concentrations. In the PD turnover model, the relationship between desmopressin plasma concentration and release of VWF:Act from the vascular endothelium was best described with an Emax model. Typically, VWF:Act increased 452% with an EC50 of 0.174 ng/ml. Simulations demonstrated that after 0.3 mcg/kg desmopressin intravenously, >90% patients with a VWF:Act baseline of ≥0.20 IU/mL attain a VWF:Act >0.5 IU/mL up to ≥4 hours after administration. A capped dose of 30 mcg was sufficient in patients weighing over 100 kg.

Conclusion: The relationship between desmopressin and VWF:Act was quantified in a PK-PD model. The simulations provide evidence that recently published international guidelines advising an intravenous desmopressin dose of 0.3 mcg/kg with a capped dose of 30 mcg >100 kg gives a sufficient desmopressin response.

Keywords: Desmopressin, PK-PD desmopressin, von Willebrand factor, Von Willebrand disease, turn-over model.

INTRODUCTION

Von Willebrand disease (VWD) is the most common inherited bleeding disorder and is caused by a deficiency or qualitative defect of von Willebrand factor (VWF)[1]. VWF is a plasma glycoprotein which plays a crucial role in primary haemostasis by promoting platelet adhesion to the subendothelium at sites of vascular injury and by initiating platelet aggregation. Subsequently it also plays a role in secondary haemostasis by protecting factor VIII (FVIII) from proteolysis in the circulation, safeguarding thrombin and fibrin generation[2]. VWD is classified into three main types based on a partial or complete quantitative defect of VWF (type 1 and 3) or a qualitative defect in VWF (Type 2)[2]. Type 1 consists of patients with VWF lower than 0.30 IU/mL or between 0.30 and 0.50 IU/mL, with abnormal bleeding[3].Type 2 is further divided into the subtypes 2A, 2B, 2M and 2N. Risk of bleeding as well as treatment choice depends on VWD type, although inter-individual variation in bleeding tendency and response to treatment is notably large in VWD.

Desmopressin (1-deamino-8-d-arginine vasopressin) is a synthetic analogue of the antidiuretic hormone l-arginine vasopressin[4]. Desmopressin binds to V2 receptors and thereby induces the release of endogenous VWF from vascular endothelial cells [5,6]. Desmopressin can be used to prevent bleeding during surgical procedures in most type 1 VWD patients and in some patients with type 2A, 2M, and 2N VWD[7]. The most recent advice is to always perform a desmopressin test in VWD patients with baseline VWF activity <0.30 IU/mL, in order to quantify the VWF response[3]. The use of desmopressin is contraindicated in type 2B VWD as it may induce thrombocytopenia. Desmopressin is not effective in type 3 VWD.

Recently published international guidelines recommend an intravenous desmopressin dose of 0.3 mcg/kg, with a capped dose of 20-30 mcg[3,8]. This recommendation is, however, solely based on empirical evidence. It is unclear if the variability in pharmacokinetics (PK) of desmopressin contributes to the consecutive observed variability in VWF response, or pharmacodynamic (PD) effect. Furthermore, proposed capping of dosing, i.e. applying a fixed dose independent of body weight when 0.3 mcg/kg exceeds 20-30 mcg, has never been substantiated by pharmacological evidence. Population PK-PD modelling can be used to establish this concentration-effect relationship[9,10]. We developed a population PK-PD model to evaluate and quantify the concentration-effect relation of desmopressin on the VWF activity (VWF:Act) response in type 1 VWD. The aim of this study was to investigate if current treatment guidelines -including capped dosing- can be substantiated with this novel PK-PD model.

PATIENTS AND METHODS

Patients

VWD patients (historical lowest VWF antigen (VWF:Ag) and/or VWF:Act < 0.50 IU/mL) with abnormal bleeding and/or a family history of VWD were included if a desmopressin test was performed at the Erasmus MC or Erasmus MC - Sophia Children's Hospital Rotterdam, the Netherlands, between April 1st 2011 and July 1st 2014. The study was not subject to the Medical Research Involving Human Subjects Act (WMO) and was approved by the Medical Ethics Committee of the Erasmus University Medical Centre Rotterdam. All patients provided written informed consent.

Blood sampling

Residual stored plasma samples from a prospective single-center cohort study, investigating desmopressin side effects, were obtained[11]. All patients signed informed consent before data and samples were collected.

Desmopressin test protocol

In all patients, desmopressin was administered intravenously in a dose of 0.3 µg/kg dissolved in 30 or 50 mL of NaCl 0.9% in children and adults respectively and infused in 30 minutes. In children, blood was sampled prior to (T0) desmopressin infusion, and at 1 (T1), 2 (T2), 4 (T4) and 6 (T6) hours after infusion. In adults, blood was sampled at T0, T1, T3, T6 and T24.

Laboratory measurements

Venous whole blood was collected in 0.105M sodium citrate tubes and centrifuged twice at 2.200 g for 10 minutes at room temperature and stored at -80°C. Coagulation factor measurements were performed within a few days after sample collection. VWF:Ag was measured by ELISA and VWF:Act was measured by GpIbα binding assay (HemosIL™ von Willebrand Factor Activity; Instrumentation Laboratory BV, Breda, the Netherlands). FVIII activity (FVIII:C) was measured by one-stage clotting assay. Desmopressin plasma concentrations were assessed in the Amsterdam UMC using LC-MS/MS in positive ionisation mode on a Shimadzu LC-30 (Nishinokyo-Kuwabaracho, Japan) UPLC system coupled to an ABSciex (Framingham, MA, USA) API5500Q LC-MS[12]. The method was validated over a range of 0.0200 – 4.00 ng/mL. The accuracy ranged from 89.2% to 111.8% across the validated range, with intra-day and inter-day imprecision below 17.6% and 13.8%, respectively.

Software

Nonlinear mixed-effects modelling software (NONMEM 7.3 ICON Development Solutions, Hanover, MD, USA) and Pirana (version 2.9.4), R (version 3.6.1) and PsN version (version 4.6.0) were used for PK-PD analysis.

Pharmacokinetic modelling

We performed a sequential PK-PD analysis. During PK model development, both one- and two-compartment models were evaluated. *A priori* allometric scaling of PK parameters by body weight was included in the structural PK model. Inter-individual variability (IIV) was estimated for each population PK model parameter. Various residual error models were evaluated. Next, associations between specific covariates and PK parameters were tested in order to explain the IIV in these parameters, by using a stepwise approach. The following covariates were evaluated: age, sex, height, baseline FVIII, baseline VWF:Act, baseline VWF:Ag and blood group (O, non-O). The supplement contains more details about the development of the PK model.

Pharmacodynamic modelling

We used individual post-hoc PK parameter estimates as input for the PD model. In literature, the maximum effect of desmopressin occurs approximately 1 hour after the end of intravenous administration[13]. We modelled the time lag using a turn-over model (Figure 1)[14]. The turn-over model consists of a zero-order rate constant describing the constant release of VWF from the vascular endothelium (K*in*) and a first-order rate constant for loss of VWF (K*out*) from plasma. The baseline VWF:Act (BASE) of each patient is determined by the equilibrium of K*in* and K*out* and was fixed at the VWF:Act level as determined before the desmopressin administration.
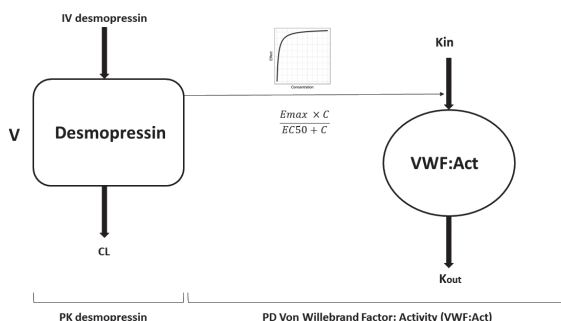
Figure 1. A schematic representation of the PK-PD model relating desmopressin concentration to VWF:Act. V represents the volume of distribution, CL represents the clearance, C the plasma concentration of desmopressin, Emax the maximum effect, EC50 the concentration at half maximal effect, K*in*, the zero-order constant for release of VWF:Act by the endothelium and K*out* the first-order rate constant for loss of VWF:Act, IV = intravenous.

In the PD analysis, the relationship between the increase in VWF release (K_{in}) and desmopressin plasma concentration was quantified by a linear function, Emax function and sigmoidal Emax function. IIV was estimated for the PD parameters, and various residual error models were evaluated. The covariates as mentioned under the PK analysis were tested for correlation with the PD parameters.

The supplement contains more details on the development of the PD model.

Pharmacokinetic-pharmacodynamic model evaluation

Model selection criteria were based on the change in the objective function value (OFV), goodness-of-fit (GOF) plots, precision of parameter estimates, decreases in IIV and residual variability, condition number, shrinkage and a successful convergence step, with at least three significant digits in parameter estimates[16].

Visual predictive checks (VPCs) with 1000 simulated data sets were used to assess the predictive performance of the model. The 5th, 50th, and 95th percentiles of the predictions from the simulations and observations from the original dataset were derived and plotted against time. A non-parametric bootstrap was performed to assess parameter precision and to calculate confidence intervals (CI) for both the population PK and PD parameters. The 5th and 95th percentiles of the bootstrap parameter distribution constitute the 90% CI.

Monte Carlo simulations

Using the final population PK and PD models, Monte Carlo simulations were performed for 1000 patients (females and males) with body weights of 50, 70, 100 and 130 kg to investigate if recently published international desmopressin guidelines[3] can be substantiated by the constructed PK-PD model. Moreover, we investigated whether dosing can be simplified by capping of desmopressin dosing when 0.3 mcg/kg dosing exceeds the 20-30 mcg cap in patients >100 kg.

All virtual patients had a baseline VWF:Act of 0.20 IU/mL. VWF:Act time profiles were simulated and desmopressin doses of 5, 10, 15, 21, 25, 30, 35 and 39 mcg were administered in all patients. A patient was considered a responder if VWF:Act levels were greater than 0.50 IU/mL at 4 hours after desmopressin administration. For each body weight and dose, the percentage of responders was calculated. Treatment was considered effective when >90% of the simulated patients of each body weight were responders.

RESULTS

Patients

The study population consisted of 47 patients, 15 males and 32 females with type 1 VWD. The median age was 25 years and body weight was 71 kg. Further characteristics are summarized in Table 1.

Table 1. Patient characteristics

	N=47 Number or median (interquartile range)
Sex (female)	32
Age, years	25 (19 – 37)
Body weight, kg	71 (59 – 86)
Height, cm	167 (160 – 177)
Historical lowest VWF:Act , IU/mL Historical lowest VWF:Ag, IU/mL Baseline (T0) VWF:Act, IU/mL	0.46 (0.34 – 0.51) 0.43 (0.35 – 0.49) 0.48 (0.41 – 0.60)
Baseline (T0) FVIII, IU/mL	0.59 (0.51 – 0.71)
Baseline (T0) VWF:Ag, IU/mL	0.45 (0.39 – 0.0.59)
Blood group (n)a Non O O	 13 32
Bleeding score (ISTH-BAT) at diagnosis Blood group non O Blood group O	 5 (2 – 6) 4 (1 – 6)

VWD= Von Willebrand disease; VWF=Von Willebrand factor; FVIII = factor VIII.
[a] Blood group data were unknown in 2 patients

Pharmacokinetic analysis

A total of 177 desmopressin plasma concentrations were available. A one-compartment model adequately described the PK of desmopressin. IIV could be estimated for clearance (CL) and volume of distribution (V), which resulted in a significant (p <0.05) decrease in OFV. The residual variability was described by a combined (proportional + additive) error model.

During covariate model selection, inclusion of the following covariates significantly improved the fit of the PK model to the data (p <0.05): sex on CL and sex, baseline FVIII, baseline VWF:Ag and baseline VWF:Act on V. The association between sex and V produced the largest improvement in model fit (p < 0.001): V was 22% higher in females compared to males. After inclusion of sex in the model, the remaining significant covariates were added one-by-one. However, no improvement of the model was observed (p > 0.05).

5

The goodness-of-fit plots showed sufficient agreement between predicted and observed desmopressin concentrations (Figure S1). The VPC of the final model is presented in Figure S2. Overall, the 2.5th, 50th and 97.5th percentiles of observed concentrations were mostly within the predicted 95% confidence interval (CI) of the predicted percentiles. The median values of the parameter estimations of the bootstraps were approximately equal to the final model's respective values. (Table 2)

Table 2. Desmopressin population pharmacokinetic parameters

Parameter	Final model Values (RSE%) [Shrinkage %]	Bootstrap Median value [95% CI]
CL (L/h/70 kg)	9.43 (5)	9.48 [8.48 – 10.3]
V (L/70 kg)	25.9 (11)	26.1 [21.1 – 32.5]
(%) Increase V in females	22.0 (10)	20.6 [4.11 – 49.2]
Inter-individual variability		
CL (CV%)	31.7 (16) [4]	30.7 [21.3 – 41.7]
V (CV%)	36.3 (18) [11]	35.0 [20.4 – 46.7]
Covariance CL~V	0.0705	0.0683 [0.0128 – 0.0131]
Residual variability		
Proportional error (CV%)	1.22 (12)	1.18 [0.869 – 2.00]
Additive error (ng/mL)	0.146 (13)	0.145 [0.0890 – 0.184]

CL = clearance; V= central volume of distribution; CV= coefficient of variation; RSE= relative standard error; CI= confidence interval; CV was calculated as: CV = sqrt(exp(variance)-1) x 100%; RSE was calculated as: RSE = 100 × standard error/parameter estimate.

Pharmacodynamic analysis

A total of 177 VWF:Act levels were available. The time profile of VWF:Act was described using the turn-over model shown in Figure 1. In the modelling procedure BASE (baseline VWF:Act) was fixed to individual baseline VWF:Act values (Table 1). The performance of several PD functions describing the relationship between VWF release and desmopressin concentration was tested (i.e. a linear function, Emax function, and sigmoid Emax function): The relationship between the VWF release and desmopressin concentration was best described with an Emax function (supplement eq. 10). We attempted to estimate the value of BASE, but this did not result in successful convergence of the model. Implementation of IIV on Emax significantly improved the model (p <0.001). Residual variability was best described by an additive error model. No significant relationship was found between covariates and PD parameters. Baseline VWF release (Kin) was typically increased by 452% with an EC50 of 0.174 ng/ml (Table 3). The IIV of Emax was modest with a value of 29.1%. In the concentration-effect curve, the EC90 was reached at a desmopressin concentration of 0.314 ng/mL. Figure 2 displays the time profile of the

desmopressin plasma concentration, PD effect and VWF:Act for a typical patient of 70 kg receiving 0.3 mcg/kg desmopressin.

Goodness-of-fit plots showed good agreement between predicted and observed VWF:Act concentrations (Figure S1). The VPC plots in Figure S2 show that the observed VWF:Act values are well-centred around the predicted median of the PD model. The bootstrap median and confidence intervals are comparable to the parameter estimates (Table 3).

Table 3. Population pharmacodynamic parameters

Parameter	Final parameter Values (RSE%) [Shrinkage %]	Bootstrap median [95% CI] of parameter value
$Kout$ (h^{-1})	5.66 (4)	5.66 [4.71 – 6.81]
EC50 (ng/mL)	0.174 (26)	0.178 [0.107 – 0.277]
Emax	4.52 (10)	4.54 [3.80 – 5.55]
Inter-individual variability		
Emax (CV%)	29.1 (10) [11]	28.8 [22.2 – 34.1]
Residual variability		
Additive error (IU/mL)	0.238 (11)	0.235 [0.183 – 0.282]

$Kout$ = first-order rate constant for loss of VWF:Act; Emax = maximum effect; EC50= drug concentration which produces 50% of the maximal effect; CV, coefficient of variation; RSE =, relative standard error; CI= confidence interval; CV was calculated as: CV = sqrt(exp(variance)-1) x 100%; RSE was calculated as: RSE = 100 × standard error/parameter estimate.

Monte Carlo simulations

The simulated dosage regimens targeting VWF:Act levels above 0.50 IU/mL at 4 hours after desmopressin administration are shown in Figure 3. Figure 3 displays the percentage responders against various dosage regimens for patients with a body weight of 50, 70, 100 and 130 kg. For patients weighing 50 kg, a dose of 15 mcg was necessary to attain a sufficient response in 92% of patients. For patients weighing 70 kg, a dose of 21 mcg was necessary to attain a sufficient response in 93% of patients. Patients with a body weight of 100 kg needed a dose of 25 mcg to attain a sufficient response in 92% of patients. Finally, Patients with a body weight of 130 kg needed a dose of 30 mcg to attain a sufficient response in 91% of patients.
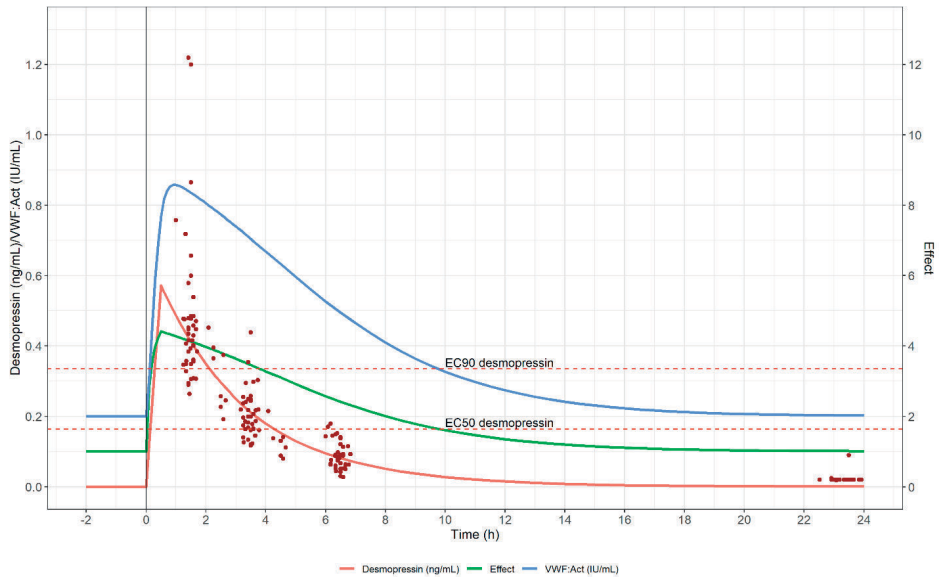
5

Figure 2. Time profiles of desmopressin plasma concentration, the PD effect and VWF:Act for a typical patient weighing 70kg with a VWF:Act baseline of 0.20 IU/mL. The red line represents the typical plasma desmopressin concentration, the red dots represent the observed concentration in all individual patients. The green line depicts the effect of desmopressin starting at unity (no effect) with a maximum value of 5.8. The blue line depicts the VWF:Act response on basis of the turnover model.

DISCUSSION

An innovative and novel turn-over PK-PD model was developed characterizing the relationship between desmopressin dose, desmopressin plasma concentration and VWF:Act response. We demonstrate that a maximum increase in VWF:Act can be established by capped dosing with a fixed dose when body weight exceeds a certain maximum. By performing simulations based on the developed PK-PD model, we confirm the feasibility and efficacy of the recently published guidelines for treatment of VWD with desmopressin of the ASH ISTH NHF WFH 2021[3].

Our simulations demonstrate that an adequate response is reached when patients weighing 50 to 100 kg receive a dose of 0.3 mcg/kg desmopressin intravenously. Although administration of 25 mcg resulted in an adequate response in patients weighing 100 kg, this dose may be insufficient for patients over 100 kg (Figure 3). For practical considerations we therefore suggest a capped dose of 30 mcg desmopressin in all patients above 100 kg and 0.3 mcg/kg for all patients below 100 kg, to ensure an adequate VWF:Act response.
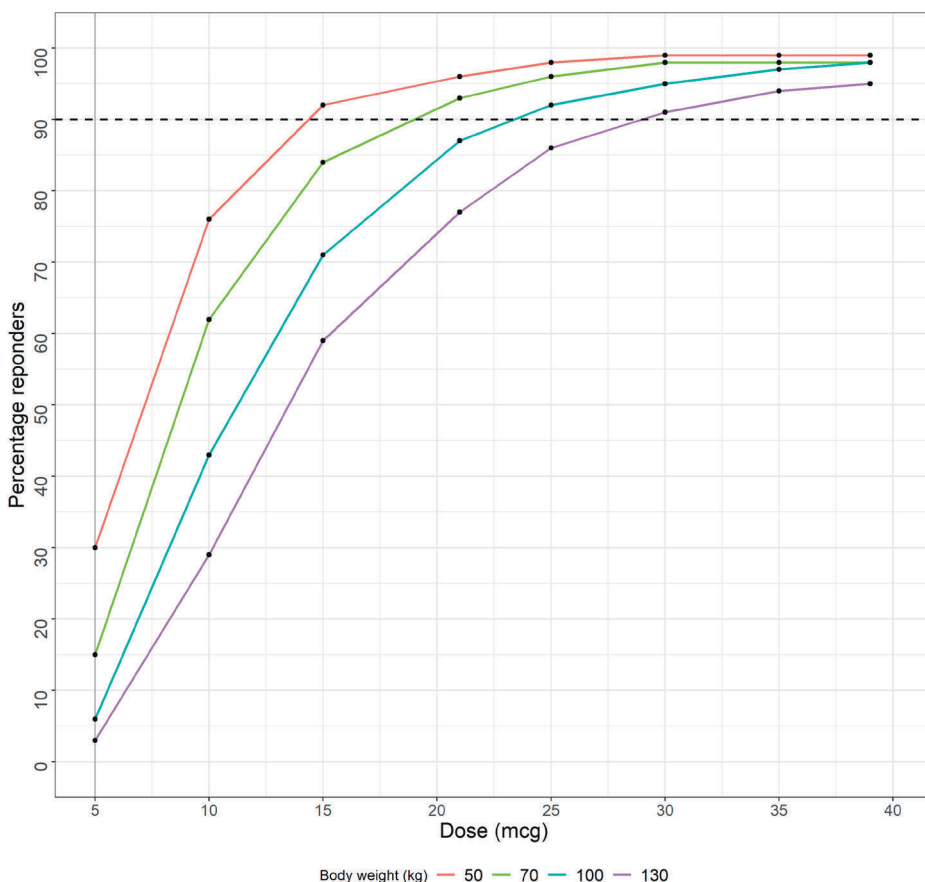
Figure 3. Percentage of VWF:Act responders 4 hours (T4) after desmopressin administration. Desmopressin dosages (5, 10, 15, 21, 25, 30, 35, 39 mcg) given to virtual patients with various body weights (50, 70, 100 or 130 kg). Responders demonstrated VWF:Act greater than 0.50 IU/mL at 4 hours after desmopressin administration. The y-axis denotes the percentage of virtual patients that demonstrated a response. The dashed horizontal black line denotes the 90% responders threshold.

In our PK model describing desmopressin concentrations, the volume of distribution (V) was 22% higher in females compared to males. V was 25.9 L/70kg in males which may reflect limited distribution of desmopressin to other tissues other than plasma, which could be explained by the higher body fat percentage in females compared to males[15]. Due to a higher V, females exhibited lower peak concentrations than males. When we stratified our simulations for sex, a slightly higher peak in desmopressin concentration in males was observed in comparison to females [data not shown]. However, this has no implications for the attained VWF:Act levels, as VWF:Act levels at T1 and T4 were similar in both males and females. The median peak desmopressin concentration for females

is 0.52 ng/mL and for males 0.63 ng/mL, which is more than adequate to produce the maximum effect, as the EC50 is 0.174 ng/mL. Therefore, dose adjustments based on sex are not necessary. In addition, simulations were performed for patients with a VWF:Act baseline of 0.20 IU/mL. Patients with either a higher or lower baseline will attain higher and lower VWF:Act values after receiving 0.3 mcg/kg. Nevertheless, in our study population, only four patients had a baseline lower than 0.20 IU/ml. In usual clinical practice, patients with a VWF:Act baseline lower than 0.30 IU/mL always undergo a desmopressin test to check their responsiveness. If a patient fails to achieve an adequate VWF:Act response, a VWF-containing factor concentrate should be administered to achieve sufficient VWF:Act levels[16].

Based on figure 2, desmopressin is eliminated from the body after approximately 14h in a typical patient of 70kg. Still, in most patients, it is advised to administer a subsequent desmopressin dose only after 24h due to potential side effects, such as fluid retention due to its antidiuretic effects.[17]

It is well known that patients with blood group O have lower VWF:Act levels[18]. During population PK-PD model development, we tested blood group O and non-O as a covariate. In our PD model, K*out* reflects the CL of VWF:Act. We investigated if the K*out* differs between blood group O and non-O, but this did not improve the model. Therefore, we did not include blood group O as a covariate in our models.

Argenti et al. explored the relationship between desmopressin concentrations and VWF:Act in healthy volunteers[6]. In this study, the temporary delay in VWF response was described by a hypothetical effect compartment model. A value of 0.237 ng/mL was reported for EC50 and 367% for Emax, which is comparable to the values observed for VWD patients in our study. Furthermore, this study reported a value of 2.16 h^{-1} for rate constant K*e0*, which corresponds to a half-life of ca. 20 minutes and a delay of ca. 80 minutes before desmopressin changes in plasma are completely reflected in VWF:Act. This also corresponds with the results of our simulations.

A strength of this study is that we have included patients from a real-life population, including a wide range of ages. We included patients in our study if they had abnormal bleeding symptoms and either a historical lowest VWF:Ag or VWF:Act below 0.50 IU/mL. In some patients, there was a difference between historical lowest VWF:Act and VWF:Act at T0. A few patients were diagnosed with VWD 10-30 years before the desmopressin test. In these patients, the higher VWF:Act at T0 could be explained by an age-related increase of VWF[19]. We however also observed differences in some patients who underwent a desmopressin

test shortly after diagnosis. It is well known that VWF may also increase due to stress[1] and a desmopressin test can be a stressful event for some patients, especially children.

We acknowledge some limitations of our study. Our analysis was limited to only type 1 VWD. Therefore, the concentration-effect relationship could not be established for other types of VWD. Also, we did not observe extremely fast clearance as observed in type 1 Vicenza in any of the patients. Furthermore, our dataset contained only six patients with a body weight over 100 kg. Therefore, simulations may be less precise in this category of patients. V of desmopressin was 25.9 L/70kg and we assumed that desmopressin has a limited distribution to the other tissues. This is important for obese patients, since they have more adipose tissue compared to non-obese patients. The total body weight in obese patients is mainly increased because of the adipose tissue, but lean body weight would increase much less[20]. Based on this, we assumed that 30 mcg would be adequate for more severely obese patients based the finding for the 130 kg patients.

In conclusion, our novel turn-over PK-PD model successfully characterized the relationship between desmopressin dose, desmopressin plasma concentration and VWF:Act response. Simulations confirm that current international desmopressin dosing guidelines in which an intravenous dose of 0.3 mcg/kg and a capped dose of 30 mcg desmopressin is recommended are effective for the treatment of VWD patients. The developed PK-PD model can be applied to further investigate the relationship between specific patient characteristics and VWF response, thereby potentially eliminating the necessity of desmopressin testing in the near future.

5

REFERENCES

1. Leebeek FWG, Eikenboom JCJ. Von Willebrand's Disease.*N Engl J Med*. 2016;375(21):2067-80.
2. Sadler JE, Budde U, Eikenboom JCJ, et al. Update on the pathophysiology and classification of von Willebrand disease: a report of the Subcommittee on von Willebrand Factor.*J Thromb Haemost*. 2006;4(10):2103-14.
3. Connell NT, Flood VH, Brignardello-Petersen R, et al. ASH ISTH NHF WFH 2021 guidelines on the management of von Willebrand disease.*Blood Adv*. 2021;5(1):301-25.
4. Lethagen S. Desmopressin - a haemostatic drug: state-of-the-art review.*Eur J Anaesthesiol | EJA*. 1997;14.
5. Mannucci PM, Aberg M, Nilsson IM, et al. Mechanism of plasminogen activator and factor VIII increase after vasoactive drugs.*Br J Haematol*. 1975;30(1):81-93.
6. Argenti D, Jensen BK, Heald D. The pharmacokinetics and pharmacodynamics of desmopressin: effect on plasma factor VIII:C and von Willebrand factor.*Am J Ther*. 1997;4(1):3-8.
7. Heijdra JM, Cnossen MH, Leebeek FWG. Current and Emerging Options for the Management of Inherited von Willebrand Disease.*Drugs*. 2017;77(14):1531-47.
8. Furqan F, Sham R, Kouides P. Efficacy and safety of half-dose desmopressin for bleeding prophylaxis in bleeding disorder patients undergoing predominantly low to moderate risk invasive procedures.*Am J Hematol*. 2020;95(10):E285-87.
9. Mould DR, Upton RN. Basic concepts in population modeling, simulation, and model-based drug development.*CPT pharmacometrics Syst Pharmacol*. 2012;1(9):e6-e6.
10. Upton RN, Mould DR. Basic concepts in population modeling, simulation, and model-based drug development: part 3-introduction to pharmacodynamic modeling methods.*CPT pharmacometrics Syst Pharmacol*. 2014;3(1):e88-e88.
11. Stoof SCM, Cnossen MH, de Maat MPM, et al. Side effects of desmopressin in patients with bleeding disorders.*Haemophilia*. 2016;22(1):39-45.
12. de Jager NCB, Heijdra JM, Kieboom Q, et al. Population Pharmacokinetic Modeling of von Willebrand Factor Activity in von Willebrand Disease Patients after Desmopressin Administration. *Thromb Haemost*. 2020;120(10):1407-16.
13. Mannucci PM, Vicente V, Alberca I, et al. Intravenous and subcutaneous administration of desmopressin (DDAVP) to hemophiliacs: pharmacokinetics and factor VIII responses.*Thromb Haemost*. 1987;58(4):1037-39.
14. Dayneka NL, Garg V, Jusko WJ. Comparison of four basic models of indirect pharmacodynamic responses.*J Pharmacokinet Biopharm*. 1993;21(4):457-78.
15. Whitley H, Lindsey W. Sex-based differences in drug activity.*Am Fam Physician*. 2009;80(11):1254-58.
16. Castaman G. Treatment of von Willebrand disease with FVIII/VWF concentrates.*Blood Transfus*. 2011;9 Suppl 2(Suppl 2):s9-13.
17. Neff AT. Current controversies in the diagnosis and management of von Willebrand disease.*Ther Adv Hematol*. 2015;6(4):209-16.
18. Gallinaro L, Cattini MG, Sztukowska M, et al. A shorter von willebrand factor survival in O blood group subjects explains how ABO determinants influence plasma von willebrand factor.*Blood*. 2008;111(7):3540-45.
19. Sanders Y V., Giezenaar MA, Laros-van Gorkom BAP, et al. Von Willebrand disease and aging: An evolving phenotype.*J Thromb Haemost*. 2014;12(7):1066-75.
20. Hebbes CP, Thompson JP. Pharmacokinetics of anaesthetic drugs at extremes of body weight.*BJA Educ*. 2018;18(12):364-70.

SUPPLEMENT
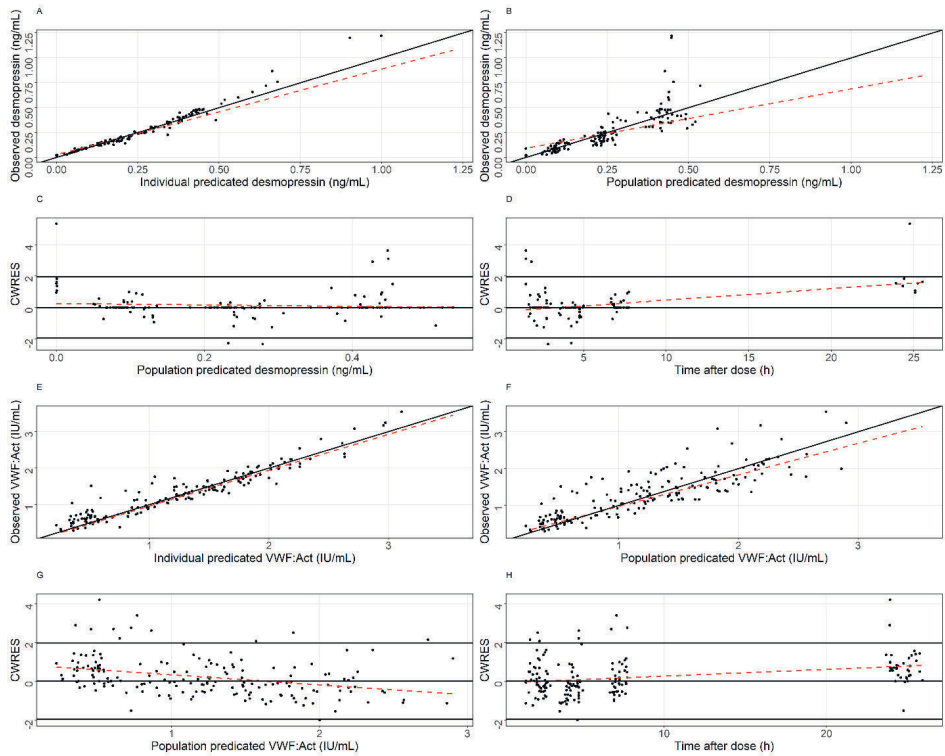
Supplement figure 1. Goodness-of-fit plots of the final pharmacokinetic model of desmopressin (top) and population model of VWF:Act (bottom). A and E) Individual predicted (IPRED) vs observed concentrations, B and F) Population predicted (PRED) vs observed concentrations, C and G) Conditional weighted residuals (CWRES) vs PRED, D and H) Time after administration vs CWRES. The solid line is the line of identity. The dashed line represents the local regression smooth line (loess smooth).
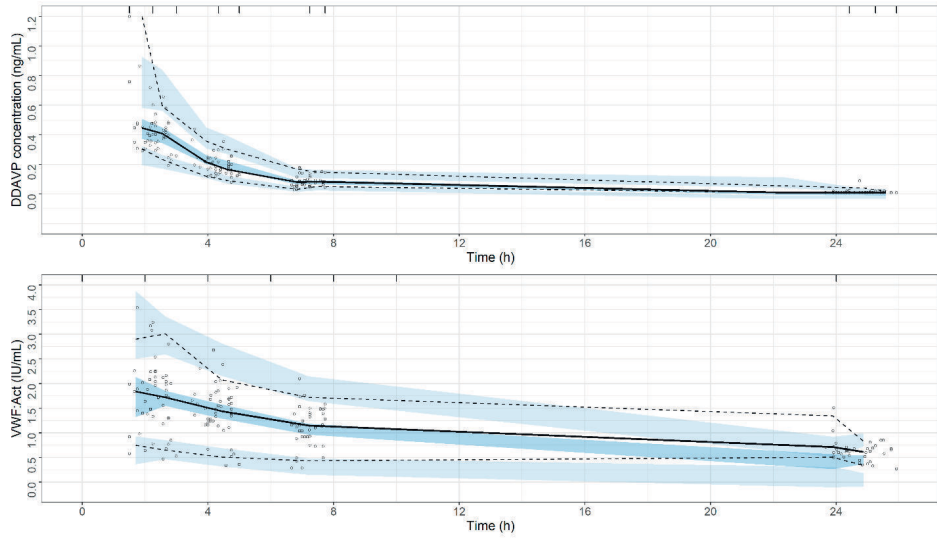
Supplement figure 2. Visual predictive check of the final pharmacokinetic model of desmopressin and pharmaco-dynamic model of VWF:Act. Dots represent observed desmopressin concentrations (top) and VWF:Act (bottom); the solid black line represents the 50th percentile of observed data; the dashed black lines represent the 5th and 95th percentiles of the population model. Shaded areas depict the model predicted 95% confidence intervals of the simulated percentiles.

Supplementary methods section

Population PK model development

A sequential PK-PD analysis method was performed. A population PK model was developed using NONMEM subroutines ADVAN1, TRANS2 and the Laplacian estimation method.

A priori allometric scaling of bodyweight on clearance (CL) and central volume of distribution (V) was included in the structural model (equation 1):

$$\theta_{pop\,PK} = \theta_{pk} \times \left(\frac{Bodyweight}{70}\right)^{\theta_{exp}} \tag{1}$$

In which, $\theta_{pop\,PK}$ is the typical population value for a PK parameter dependent on bodyweight, θ_{pk} is the typical PK value for a patient with a body weight of 70 kg, and θ_{epx} is an exponent fixed at 0.75 for CL and 1 for V.

The individual PK parameters were described by using equation 2.

$$\theta_i = \theta_{pop\,PK} \times exp^{\eta i} \tag{2}$$

In which, θ_i is the estimated individual PK parameter of the ith individual, $\theta_{pop\,PK}$ is the typical population value for a PK parameter, ηi is the inter-individual variability from normal distribution with a mean of zero and estimated variance of ω^2 of the ith individual. A full omega variance−covariance block matrix was tested on the PK parameters

For the residual error model, an additive (equation 3), proportional (equation 4) and combined error models (combination of equation 2 and 3) were tested, in which Y_{ij} is the prediction of the concentration of individual *i* at time *j* , $f(\theta,\eta i,x_{ij})$ is the individual concentration prediction at time *j* and ε is the residual error originating from a normal distribution with a mean of zero and estimated variance of σ^2.

$$Y_{ij} = f\big(\theta,\eta i, x_{ij}\big) + \varepsilon_{ij} \tag{3}$$

$$Y_{ij} = f\big(\theta,\eta_i, x_{ij}\big) \times (1 + \varepsilon_{ij}) \tag{4}$$

The following covariates were evaluated: age, sex, height, baseline FVIII, baseline VWF:Act, baseline VWF:Ag and blood group (O, non-O). Blood groups of two patients were missing, which were excluded during covariate analysis. Continuous covariates were included by a power model, in which the covariate was centred around its median value and the exponent was estimated (equation 5). Categorical covariates were modelled with the use of flag variables (1 and 0 for "true" and "false"; equation 6).

$$\theta_{pop} = \theta_{pk} \times \left(\frac{Cov}{Cov_{median}}\right)^{\theta_{exp}} \tag{5}$$

$$\theta_{pop} = \theta_{pk} \times (\theta_1^{Flag1} \times \theta_2^{Flag2} \times \theta_3^{Flag3} \cdots) \tag{6}$$

A stepwise forward inclusion and backward exclusion process was used to evaluate covariates, in which a reduction in the objective function value (OFV) of 3.84 ($p = 0.05$) or more was considered significant during forward inclusion and a reduction in OFV of 7.88 ($p = 0.005$) or more in the backward exclusion process. The covariate that resulted in the largest decrease in OFV was first implemented in the model. The remaining covariates that significantly decreased OFV were then sequentially added to the covariate model, and repeated until all significant covariates were included.

Plasma concentrations below the lower limit of quantification (LLOQ) were taken in consideration in the analysis, but were flagged and treated as categorical data in the population PK analysis using the M3 method; a likelihood-based approach which maximizes the likelihood of the data being below LLOQ with respect to the model parameters[1]

Population PD modelling

For the population PD model development, the first-order estimation method with the interaction option (FOCE-I) and NONMEM subroutine ADVAN6, TOL3 was used.

A turnover model was used to describe the release of VWF:Act. The turnover model consists of a zero-order constant describing release of VWF:Act from the vascular endothelium (Kin) and a first-order rate constant for loss of VWF:Act (Kout). The baseline VWF:Act (BASE) is determined by the equilibrium of Kin and Kout (equation 7).

$$BASE = \frac{K_{in}}{K_{out}} \tag{7}$$

The differential equation for the turnover-model is displayed in equation 8.

$$\frac{dVWF:Act}{dT} = BASE \times K_{out} \times E - K_{out} \times VWF:Act \tag{8}$$

where E is the effect as a function of the individual predicted desmopressin concentration. A linear and a sigmoidal Emax concentration-effect relationship were tested (equation 9,10).

$$E = 1 + \theta_{slope} \times C \tag{9}$$

$$E = 1 + \frac{\theta_{Emax} \times C^n}{\theta_{ECso} + C^n} \tag{10}$$

where *C* is the desmopressin plasma concentration and *slope* is the change of effect per ng/mL of desmopressin, *Emax* is the maximum effect, *EC50* is the desmopressin concentration which produces 50 % of the maximal effect, *n* is the hill coefficient which was both estimated and fixed at 1. The hill coefficient determines the steepness of the sigmoidal concentration-effect curve. Model comparison using equation 9 and 10 was done using the Bayesian information criterion (BIC). Afterwards, IIV was estimated for the PD parameters to obtain individual PD parameters by using equation 11.

$$\theta_i = \theta_{pop\ PD} \times exp^{\eta i}$$

(11)
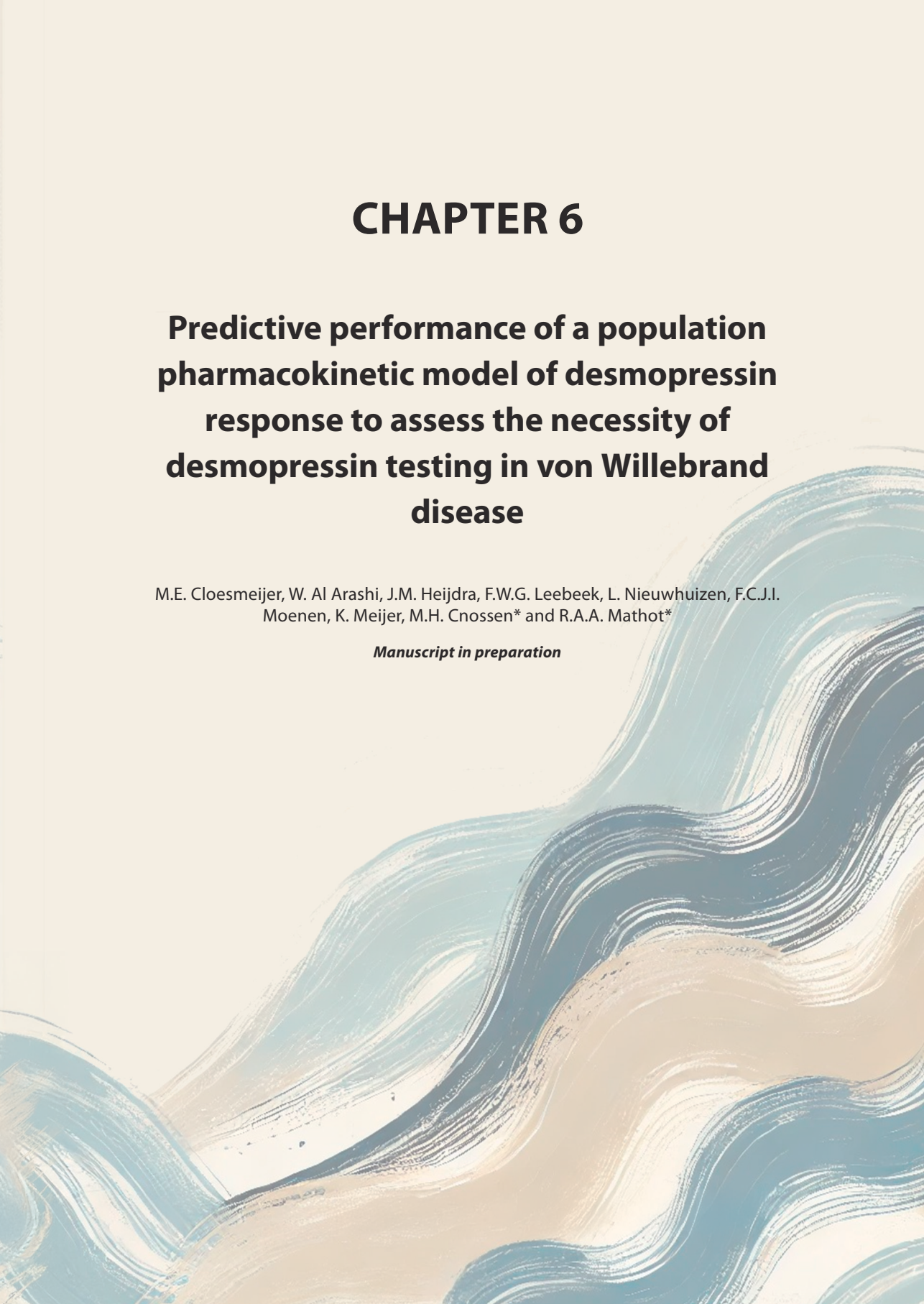
The following covariates were tested for correlation with the PD parameters: bodyweight, age, sex, height, VWD type, baseline FVIII, baseline VWF:Act, baseline von Willebrand factor antigen, von Willebrand factor-multimers and blood group (equations 5 and 6).

5

CHAPTER 6

Predictive performance of a population pharmacokinetic model of desmopressin response to assess the necessity of desmopressin testing in von Willebrand disease

M.E. Cloesmeijer, W. Al Arashi, J.M. Heijdra, F.W.G. Leebeek, L. Nieuwhuizen, F.C.J.I. Moenen, K. Meijer, M.H. Cnossen* and R.A.A. Mathot*

ABSTRACT

Aims

Patients with Von Willebrand disease (VWD) are treated with desmopressin to prevent or treat bleeding. Previously, we developed a population pharmacokinetic (PK) model that described von Willebrand factor activity (VWF:Act) after intravenous desmopressin administration. This population PK model aimed to predict desmopressin response in VWD patients, potentially eliminating the need for a desmopressin test. The aim of this subsequent study is to prospectively investigate the predictive performance of the population PK model with regard to VWF:Act levels using an independent validation dataset.

Methods

The predictive performance was evaluated using nonlinear mixed-effects modelling (NONMEM). The performance was determined using prediction-based and simulation-based diagnostics. In the prediction-based method median prediction error (MPE) and median absolute prediction error (MAPE) determine bias and precision of the VWF:Act prediction. Criteria applied for model acceptance were: MPE of above -20% , reflecting a tolerance for a maximum 20% over-prediction, where the observed value is 80% of the predicted value and a MAPE below 30%.

Results

Sixty-one patients with VWD type 1, 2 and low VWF and 284 VWF:Act samples were included from the prospective To-WiN study. Analyses demonstrated that the earlier model displayed an adequate bias, as the MPE for all patients was 27.2% [interquartile range (IQR) 18.5 – 47.6%] but was not considered sufficiently precise as MAPE was 39.8% [IQR 22.7 – 60.4]. Predictive performances varied per sub-group, with type 1 VWD demonstrating the best predictive performance (MPE=8.0% IQR[-31.7 – 33.6%], MAPE=33.6% IQR[19.0 – 54.7%]. With exception of VWD patients with a baseline VWF:Act <0.30 IU/mL, as this group generally displayed an over-prediction of VWF:Act levels with MPE= -35.0% IQR[-55.0 – 39.9] and MAPE=51.6% IQR[37.4 – 64.4].

Conclusion

This study shows that the previously developed population PK model demonstrates adequate bias, meaning it does not consistently overestimate or underestimate values

significantly, but it leads to less precise predictions when tested with our independent dataset.Importantly, the over-prediction observed , meaning lower actual VWF:Act and FVIII levels than predicted, in patients with a baseline VWF:Act before desmopressin administration <0.30 IU/mL underscores that desmopressin testing is still warranted in the clinical setting to safeguard outcomes.

INTRODUCTION

Von Willebrand disease (VWD) is the most common inherited bleeding disorder[1]. This autosomally inherited disease is characterized by quantitative or qualitative defects of von Willebrand factor (VWF) [2]. VWF is essential for primary hemostasis as it is responsible for platelet adhesion and aggregation[2]. Additionally, it plays a role in the secondary hemostasis, as VWF serves as a carrier protein for coagulation factor VIII (FVIII), protecting it from proteolysis in the bloodstream. Therefore, patients with VWD often also present with reduced FVIII levels. Clinical manifestations of VWD characteristically include mucosa-associated bleeding, such as menorrhagia, gingival bleeding, and postsurgical bleeding[3].

VWD can be divided into different types. These include type 1 (partial quantitative deficiency), type 3 (complete quantitative deficiency), and type 2, which is further categorized into VWF: 2A (decreased platelet adhesion with absence of high-molecular-weight VWF multimers), 2B (increased platelet glycoprotein Ib affinity), 2M (decreased platelet adhesion with presence of high-molecular-weight VWF multimers), and 2N (decreased FVIII affinity)[4] VWD. There are also patients with a VWF activity (VWF:Act) between 0.30-0.50 IU/mL, sometimes referred to as low VWF[5].

Clinical management of VWD includes treatment that increases the levels of VWF/FVIII, such as desmopressin[6] or by replacement of deficient factors with VWF containing concentrates when bleeding occurs or when prevention of bleeding is indicated. Desmopressin stimulates the release of VWF from the vascular endothelial cells. Desmopressin testing is routinely performed in patients to assess their desmopressin response in terms of VWF and FVIII bioavailability, as described by their levels[7]. Definitions of this response vary[8–11], but generally a complete response is defined as a twofold increase in VWF:Act levels from baseline, observed one hour after desmopressin administration (known as peak level), and clinically more relevant, persistence of VWF:Act and FVIII levels above 0.50 IU/mL for up to four hours post-administration[7]. Achieving VWF:Act peak levels above 0.80 or 1.0 IU/mL is particularly desirable for medical procedures such as surgery [12]. It has been reported that patients with a historically VWF:Act baseline ≥0.30 IU/ml

6

do not require desmopressin testing, as they will present with a complete response[5]. Importantly in current guidelines, individuals with VWF levels ≤0.30 IU/mL before desmopressin administration are recommended to undergo desmopressin testing to confirm their response[13].

Previously, a population PK model was developed describing VWF:Act levels after desmopressin administration[14]. With this population PK model we aimed to predict VWF:Act levels after desmopressin administration based on patient characteristics (covariates)[15]. FVIII levels were not included in this population PK model. The following characteristics were associated with the desmopressin response: VWD type, age and sex. An accurate predictive performance of this model is essential [16] in determining whether a desmopressin test is warranted, especially for patients with VWF:Act levels below 0.30 IU/mL. If the model is able to accurately predict VWF:Act and FVIII levels post-desmopressin administration, conducting a desmopressin test may become redundant, unburdening the patient and caregivers of this laborious intervention. This study therefore aims to investigate the predictive performance of the previously developed population PK model by using an independent validation dataset of prospectively included VWD patients undergoing desmopressin testing.

PATIENTS AND METHODS

Patients

Patients included in the OPTI-CLOT/ To WiN study, diagnosed with VWD or low VWF (historically lowest VWF antigen or VWF activity level of 0.30–0.50 IU/mL) were analyzed. OPTI-CLOT/ To WiN is a prospective multicenter, non-randomized, multi-arm intervention, cohort study. The cohort study is divided into four different arms. Arm A: patients who will undergo a desmopressin test, Arm B: patients who will undergo an elective medical procedure, Arm C: patients with a bleeding episode, Arm D: patients receiving or requiring prophylaxis[17]. The study was approved by the Medical Ethics Committee of the Erasmus MC, University Medical Center Rotterdam, Rotterdam the Netherlands, and registered at the Netherlands Trial Register "OMON", as NL-OMON54546 and in EudraCT as 2018-001631-46. The study was conducted according to good clinical practice guidelines and the Declaration of Helsinki, and in accordance with the Dutch Medical Research Involving Humans Act. All patients provided written informed consent.

Sixty-one patients were analyzed from Arm A of the OPTI-CLOT: To WiN trial, described as patients who were prospectively included and underwent desmopressin testing. Patients were recruited from hemophilia treatment centers in the Netherlands between

June 18th, 2019 and May 9th, 2023. During desmopressin testing, VWF:Act and FVIII were measured directly before desmopressin administration to establish baseline VWF:Act and FVIII levels for each patient. Each patient received 0.3 μg/kg intravenously desmopressin with VWF:Act and FVIII sampling at approximately 1.5h, 3h or 4h (some patients also at 5h or 7h) after desmopressin administration to assess desmopressin response in each patient. VWF:Act was measured by GpIbα (VWF:GP1bM) binding assay in all hemophilia treatment centers (HemosIL™ von Willebrand Factor Activity; Instrumentation Laboratory BV, Breda, the Netherlands). FVIII was measured by one-stage clotting assay. More detailed information about the study protocol has been published[17].

External validation of the population PK model

The external validation using prospectively collected data was performed using the nonlinear mixed-effects modelling, NONMEM 7.4 (ICON Development Solutions, United States). Statistical analyses and graphical representations of the results were performed with R version 4.0.2. Prediction-based diagnostics and simulation-based diagnostics were performed in NONMEM and the results were processed in R to evaluate the predictive performance of the population PK model. As mentioned earlier the previously developed population PK model only described the VWF:Act levels after desmopressin response[14] and not FVIII levels.

Prediction-based diagnostics and definitions

The relative prediction error (PE%, Equation 1) was estimated by comparing the population predicted VWF:Act levels ($C_{prediction}$) and the corresponding observed VWF:Act levels ($C_{observation}$) for each subject in the independent dataset. The population predicted VWF:Act levels were estimated by fixing the parameters in the final model, including covariate relationships. The model parameters are displayed in the supplement. The following covariates relationships were included in the final model explaining the interindividual variability: VWD type and sex on clearance (CL) of VWF:Act and age on the response of desmopressin (F).

In assessing the predictive performance of the population PK model within clinical setting, we focused on three primary criteria: bias, precision, and the ability to accurately predict peak levels of VWF:Act in response to desmopressin. Generally, bias refers to the discrepancy between the predictions by the model and actual measurements, with an unbiased model having an even distribution between underestimations and overestimations, resulting in a mean prediction error (MPE) close to zero (equation 1). Positive values indicate a tendency of the model to underestimate the actual measurements, which is deemed clinically tolerable. Conversely, a negative value suggests the model overestimates measurements, a scenario considered undesirable in clinical settings due

to the risk of predicting higher than observed measurements. However, for our model to be considered valid and clinically applicable, it had to meet the following criteria: an MPE of no less than -20%[18], reflecting a tolerance for maximal 20% over-prediction. Under-prediction was acceptable regardless of its magnitude. Precision, on the other hand, indicates the reproducibility of the predictions by the model, measured by the variability of its estimates, with a lower mean absolute prediction error (MAPE) indicating higher precision (equation 2); a MAPE of less than 30%, ensuring a high degree of precision in predictions; and a median absolute difference in predicted versus observed VWF:Act peak levels of less than 0.15 IU/mL, deemed clinically acceptable according to Goedhart et al. models that satisfied these thresholds have satisfactory predictive performance and were deemed clinically acceptable.

$$PE\ (\%) = \frac{C_{observation} - C_{prediction}}{C_{prediction}} \times 100$$

(Equation 1)

$$MAPE\ (\%) = median\ of\ |PE|$$

(Equation 2)

Simulation-based diagnostics

Prediction-corrected visual prediction checks (pcVPC) were performed based on 1,000 Monte Carlo simulated datasets generated using the population PK model and displayed using the "vpc" R package (version 1.2.2, https://cran.r-project.org/package = vpc.). The overall fit of the model was visually assessed by overlaying the 90% confidence interval of 5th, 50th, and 95th quantiles for the simulations with the corresponding quantiles for the VWF:Act levels.

Model predictability in clinical practice

The bias and precision of the predictions of the population PK model is important to ensure that real world measured VWF:Act levels align with the predicted values. We therefore focused on investigating the predictive performance regarding VWF:Act peak levels. Adequate response to desmopressin is crucial. There are different definitions of desmopressin response[7]. We differentiated results into four groups based on measure-ments and predictions VWF:Act levels that were clinically relevant. We evaluated three different thresholds of VWF:Act ≥0.50, ≥0.80 or ≥1.0 IU/mL:
1) both measured and predicted ≥threshold (true positive);
2) both measured and predicted <threshold (true negative);
3) VWF:Act measured ≥threshold but predicted <threshold (false negative);
4) VWF:Act measured <threshold but predicted ≥threshold (false positive).

The last group is of particular clinical interest as this is the group at greatest risk for bleeding.

The predictive performance was further analyzed by receiver operating characteristic (ROC) analysis. A peak VWF:Act level of 0.50, 0.80 or 1.0 IU/mL was used to separate observations into the binary outcome of achieving versus not achieving the set target level. The ROC analysis determines how well the model predicts above or below the target of 0.50, 0.80 or 1.0 IU/mL. The departure of the ROC curve from the diagonal line to the upper left corner indicates an improvement in predictive performance for the dichotomous outcomes. Area under the curve of the ROC curve quantifies the performance of the prediction, ranging from 0.5 (random) to 1 (optimal).

RESULTS

A total of 247 VWF:Act samples from 61 patients with VWD were prospectively collected from June 1st 2016 to July 1st 2023. A summary of the baseline demographic and clinical characteristics of the independent validation dataset is shown in Table 1.

6

Table 1. Patient characteristics

Patient characteristic	Number or median (and interquartile range) (n=61)	Range
Male/female	23/38	
Age, years	17 (10 – 35)	6 – 78
Body weight, kg	59 (36 – 77)	20 – 109
Von Willebrand disease type		
Low VWF	24	
Type 1	26	
Type 2A, M, N, unspecified	6, 4, - , 1	
Total historically lowest VWF:Act, IU/mL	0.33 (0.19 – 0.43)	0.04 – 0.68
Low VWF	0.46 (0.41 – 0.50)	0.34 – 0.68
Type 1	0.25 (0.16 – 0.33)	0.05 – 0.46
Type 2	0.18 (0.08 – 0.21)	0.04 – 0.31
Total historical lowest FVIII, IU/mL	0.65 (0.47 – 0.75)	0.08 – 1.42
Low VWF	0.75 (0.65 – 0.80)	0.38 – 1.12
Type 1	0.56 (0.38 – 0.66)	0.08 – 1.42
Type 2	0.48 (0.28 – 0.73)	0.11 – 1.04
Dose (mcg)	18 (10 – 22)	5 – 31
Dose (mcg/kg)	0.30 (0.29 – 0.30)	0.23 – 0.31

Prediction-based diagnostics

The results of the model performance based on prediction-based diagnostics using the population PK model by de Jager et al. are shown in Table 2 and 3. The model parameters of de Jager et al. are displayed in the supplement. VWD type 1 patients displayed the best predictive performance, as the bias was below 20% and (peak) median absolute was below 0.15 IU/mL.

Table 2. Summary of prediction based diagnostics

Stratification	MPE (%)	IQR PE (%)	MAPE (%)	IQR MAPE (%)
All patients (n=61)	27.2	-18.5 – 47.6	39.8	22.7 – 60.4
Von Willebrand disease type				
Low VWF (n=24)	39.5	19.0 – 60.9	39.5	20.3 – 60.9
Type 1 (n=26)	8.04	-31.7 – 33.6	33.6	19.0 – 54.7
Type 2 (n=11)	3.32	-52.8 – 58.7	56.9	39.2 – 71.1
Baseline VWF:Act				
≥0.30 IU/mL (n=41)	32.2	8.97 – 54.9	33.5	17.7 – 56.7
<0.30 IU/mL (n=20)	-35.0	-55.0 – 39.9	51.6	37.4 – 64.4

IQR: interquartile range, MAPE: median absolute prediction error, MPE: median prediction error, VWF:Act: von Willebrand factor activity

Table 3. Summary of absolute difference between measurements and predictions

Stratification	Median absolute difference (IU/mL)	IQR absolute difference (IU/mL)	Peak median absolute difference (IU/mL)	IQR peak absolute difference (IU/mL)
All patients (n=61)	0.24	0.12 – 0.51	0.31	-0.18 – 0.71
Von Willebrand disease type				
Low VWF (n=24)	0.44	0.24 – 0.63	0.54	0.32 – 0.91
Type 1 (n=26)	0.086	-0.23 – 0.34	0.015	-0.32 – 0.49
Type 2 (n=11)	-0.0049	-0.19 – 0.30	-0.13	-0.41 – 0.36
Baseline VWF:Act				
≥0.30 IU/mL (n=41)	0.34	0.11 – 0.57	0.50	0.13 – 0.77
<0.30 IU/mL (n=20)	-0.18	-0.31 – 0.23	-0.18	-0.44 – 0.25

IQR: interquartile range, VWF:Act: von Willebrand factor activity

The bias of the population PK model evaluated is shown in Table 2 and Figure 1. Positive values indicate the model tends to underestimate actual measurements, which is clinically tolerable. Conversely, negative values suggest the model overestimates measurements, an undesirable scenario due to the risk of predicting higher than observed measurements. In Figure 1a, the PE is depicted for all patients. The observed
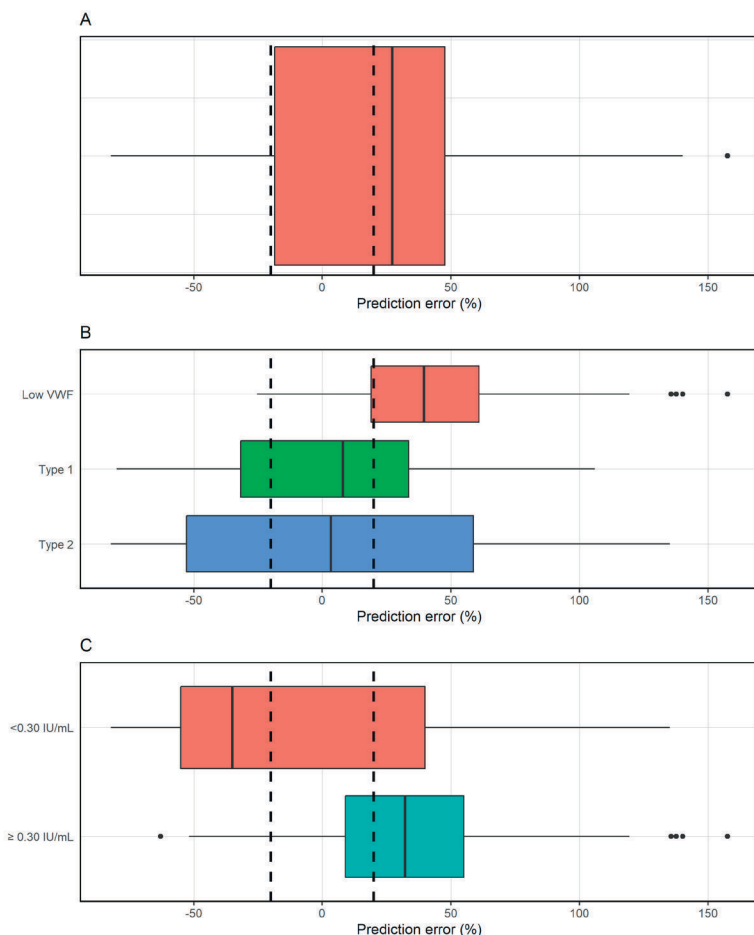
Figure 1. Box plots of the prediction error (PE, %) for VWF:Act levels. A) PE of all patients, B) PE of patients stratified on von Willebrand disease type, C) PE of patients stratified on baseline VWF:Act <0.30 IU/mL or ≥0.30 IU/mL. Black dashed lines are reference lines indicating PE% ±20. The median of the box plot is shown as the solid line within each box, the box represents the interquartile range (IQR), and the whiskers indicate the range of the data.

bias is acceptable with a MPE of 27.2%, as indicated by a higher under-prediction of VWF:Act levels in patients. However, there is a large range in MPE. Figure 1b stratifies patients according to VWD type. For patients with type 1 and type 2 an acceptable MPE of 8.04% and 3.32% was observed, meaning there is no significant under- prediction. For patients with low VWF large over-prediction was observed; the MPE was 39.5%. Figure 1c stratifies patients with a VWF:Act baseline of <0.30 IU/mL and ≥0.30 IU/mL. Patients with a VWF:Act baseline of ≥0.30 IU/mL and <0.30 IU/mL had a MPE of 32.2% and -35.0%, indicative of under-prediction and over-prediction, respectively.

The results of overall precision of the evaluated population PK model are shown in Table 2. When considering all patients, the precision of the model is not acceptable with a MAPE of 39.8%. However, if we stratify patients according to VWD type, then the MAPE of the model for low VWF, type 1 and type 2 is respectively 39.5% and 33.6 and 56.9%. The stratification highlights the significant variability in the performance of the model across different patient subgroups, with the highest variability observed in patients with type 2 VWD, as evidenced by the highest MAPE. Moreover, when stratifying patients into baseline VWF:Act <0.30 and ≥0.30 IU/mL, then the MAPE is 51.6 and 33.5%. Thus, VWD type 1 patients with a VWF:Act baseline, before desmopressin testing ≥0.30 IU/mL displayed the best precision based on the MAPE.

The absolute difference, or in other words the difference between predicted VWF:Act and measured VWF:Act, is displayed in Figure S1. Figure S2 displays all PE against the baseline VWF:Act. Here, we observed a trend showing that patients with a baseline VWF:Act <0.30 IU/mL have a lower MPE compared to the other patients. In examining the absolute differences in IU/mL, all patients had a median absolute difference of 0.24 IU/mL, indicative of under-prediction. However, when categorized based on low VWF, type 1, and type 2, the median absolute differences were 0.44, 0.086, and -0.0049 IU/mL, respectively. Further stratification based on VWF:Act baseline levels of ≥0.30 and <0.30 IU/mL revealed median absolute differences of 0.34 and -0.18 IU/mL, respectively.

In terms of median absolute differences for peak levels across all patients, the value was 0.31 IU/mL. For groups with low VWF, type 1, and type 2, these differences were 0.54, 0.015, and -0.13 IU/mL, respectively, and 0.50 and -0.18 IU/mL for VWF:Act baseline ≥0.30 and <0.30 IU/mL, respectively. It should be noted that both type 1 and type 2 patients demonstrated an IQR of -0.32 to 0.49 IU/mL and -0.41 to 0.36 IU/mL, respectively, indicating substantial variability in the absolute differences of peak levels.

In summary, both type 1 and type 2 patients demonstrated satisfactory bias levels, indicating a balanced distribution of predictions both above and below the actual measurements. However, the precision of predictions for type 2 patients was notably poor, showing a significant variability in the model's estimates, whereas type 1 patients exhibited better precision. Patients with low VWF were generally under-predicted, as evidenced by the solely positive PE IQR and a positive median absolute difference at peak levels. Analysis stratified by baseline VWF:Act levels revealed that patients with baseline levels below 0.30 IU/mL were mostly over-predicted, as shown by a negative MPE and a negative median absolute difference at peak levels. Conversely, for patients with a baseline VWF:Act of ≥0.30 IU/mL, the model tended to under-predict.

Simulation-based diagnostics

Figure 2 displays simulation-based diagnostics illustrating the overall model performance. The pcVPC displayed the simulated VWF:Act levels and their variability across the population PK model compared to the measured VWF:Act levels within the independent validation dataset. The model-based simulations, accounting for the 90% prediction interval (PI), covered the measured VWF:Act levels mostly in the population PK model. However, a minor inconsistency was observed between the 50th and 5th percentiles of the observed data and the simulated intervals of the corresponding percentiles, represented by the solid line and the transparent blue areas, respectively. The primary inconsistency noted was that the median of the observed values is above the predicted values. In supplemental Figures 3 and 4, the pcVPC's are stratified on VWD type and baseline.
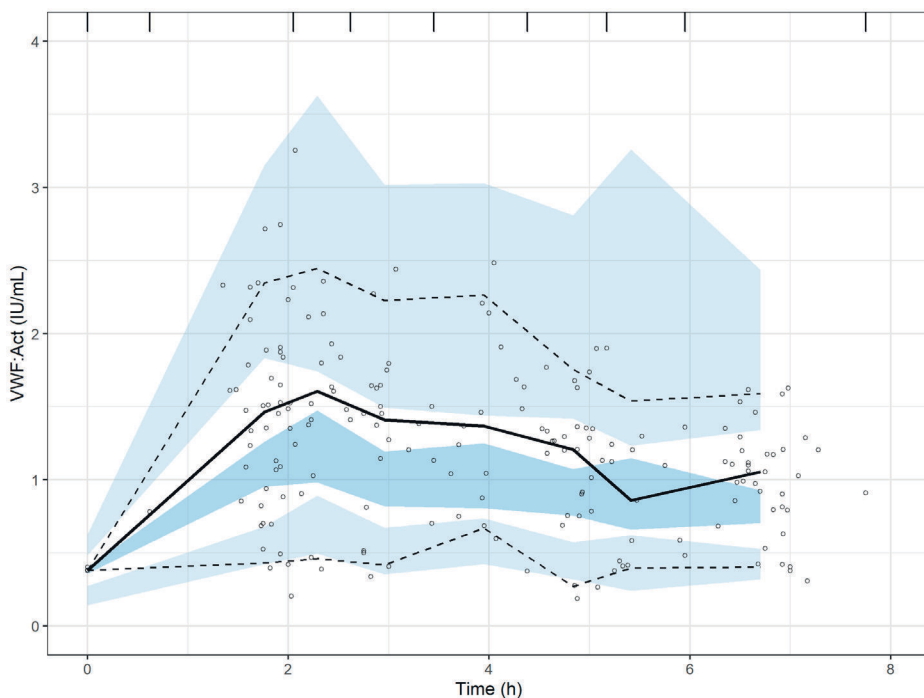
Figure 2. Prediction-corrected visual predictive check (pcVPC) plots of the independent dataset for the investigated population PK models of von Willebrand factor activity (VWF:Act) after desmopressin administration. Dots represent measured VWF:Act; the solid black line represents the 50th percentile of observed data; the dashed black lines represent the 5th and 95th percentiles of the population model. Shaded areas depict the model predicted 95% confidence intervals of the simulated percentiles.

Model predictability in clinical practice

Accurate prediction by the model, ensuring a predicted VWF peak level of ≥0.50, ≥0.80 or ≥1.0 IU/mL matches the measured peak VWF level, is important for clinical practice. Figure 3 illustrates the relationship between the measured VWF peak levels and their corresponding predicted values. Sixty-one peak samples were available in total.
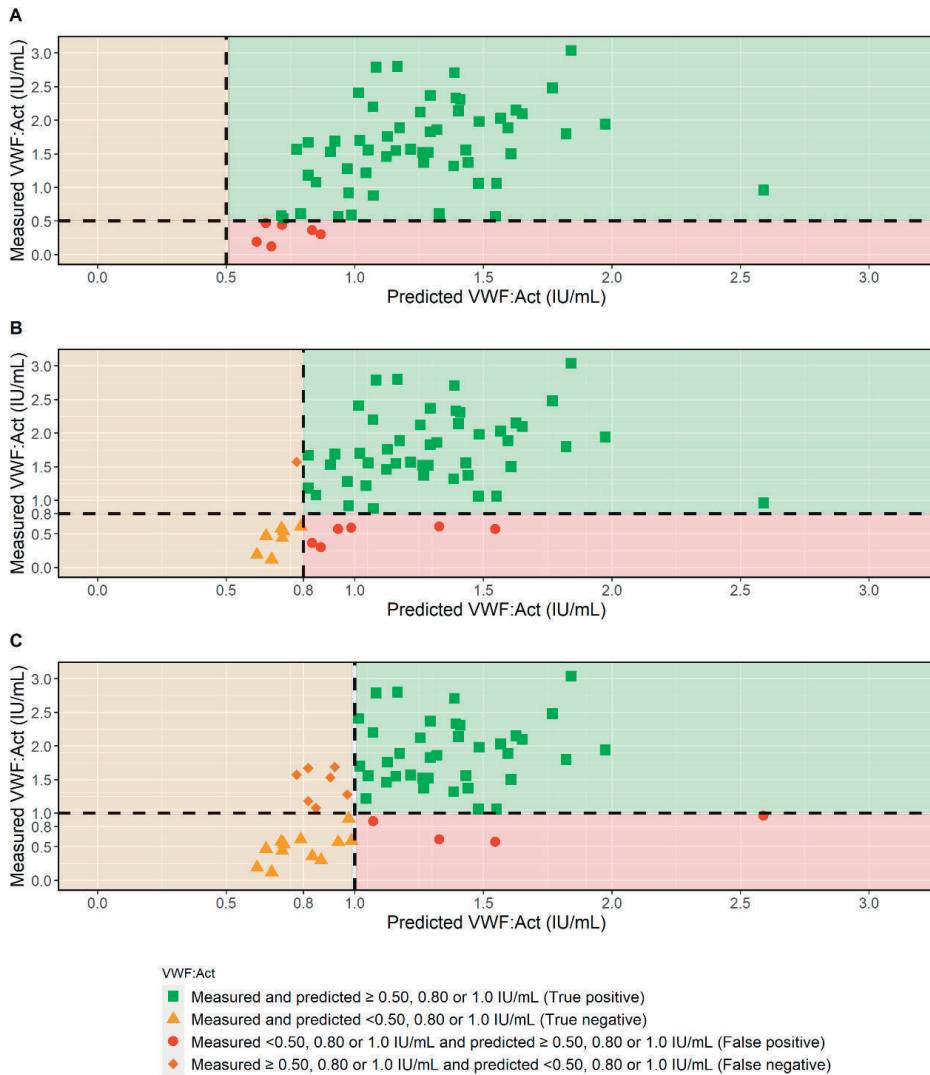
Figure 3. Predicted peak von Willebrand factor activity (VWF:Act) levels against measured peak VWF:Act levels. Dashed lines indicate the VWF:Act threshold level of 0.50 IU/mL (A), 0.80 IU/mL (B) or 1.0 IU/mL (C). Green shaded area represents measured and predicted VWF:Act levels above the threshold (True positive), while red shaded area represents measured VWF:Act levels below the threshold, but a predicted VWF:Act level above the threshold (True negative). Orange shaded areas represent measured and predicted VWF:Act level below the threshold (True negative), or measured above the threshold but predicted below the threshold (False negative).

When applying a threshold of ≥0.50 IU/mL, analyses show that 55/61 patients presented with VWF-Act levels exceeding 0.50 IU/mL for both measured and predicted values (true positive), while 6/61 patients displayed a measured VWF:Act <0.50 IU/mL, although the model predicted values ≥0.50 IU/mL (false negative).

When applying a threshold of ≥0.80 IU/mL, analyses show that 47/61 patients presented with VWF:Act levels exceeding 0.80 IU/mL for both measured and predicted values (true positive), while 7/61 samples displayed levels below this threshold for both measured and predicted values (true negative). The patients corresponding to these seven samples had the lowest baseline VWF:Act (median: 0.10 IU/mL, range: 0.04 – 0.16 IU/mL). Moreover, 6/61 samples displayed a measured VWF:Act <0.80 IU/mL, although the model predicted values >0.80 IU/mL (false negative). These particular patients had a relatively lower baseline VWF:Act before desmopressin administration (median: 0.17 IU/mL, range: 0.06 – 0.28 IU/mL) compared to the median baseline VWF:Act observed in the dataset (median: 0.33 IU/mL, range: 0.04 – 0.68 IU/mL). Additionally, 1/61 sample displayed a measured VWF:Act >0.80 IU/mL, while the predicted VWF:Act was <0.80 IU/mL (false negative).

When applying a threshold of ≥1.0 IU/mL, analyses show that 38/61 presented with VWF:Act levels exceeding 0.80 IU/mL for both measured and predicted values (true positive), while 12/61 samples displayed levels below this threshold for both measured and predicted values (true negative). Moreover, 4/61 samples displayed a measured VWF:Act <1.0 IU/mL, although the model predicted values ≥1.0 IU/mL (false positive). Additionally, 7/61 samples displayed a measured VWF:Act ≥1.0 IU/mL, while the predicted VWF:Act was <1.0 IU/mL (false negative).

The ROC analysis describes the ability of the model to predict a binary outcome, namely whether the VWF:Act will be above or below the target peak level threshold of 0.50, 0.80 or 1.0 IU/mL (Figure 4). Only a ROC analysis was performed for the threshold 0.80 and 1.0 IU/mL, as 0.50 IU/mL did not have any false positive or true negative values. The model showed good predictive performance with an area under the curve of 0.86 (sensitivity = 97%, specificity = 54%) and 0.80 (sensitivity = 84%, specificity = 75%) for predictions ≥0.80 and ≥1.0 IU/mL. The high sensitivity suggests that the model is good at identifying measured and predicted VWF:Act levels ≥0.80 and ≥1.0 IU/mL, missing only one and seven positive cases. However, while the model showed a high degree of sensitivity, the specificity indicated a considerable number of cases where VWF:Act levels measured below these thresholds were incorrectly predicted to exceed them, particularly for the ≥0.80 IU/mL threshold, suggesting a higher rate of false positives at this level.
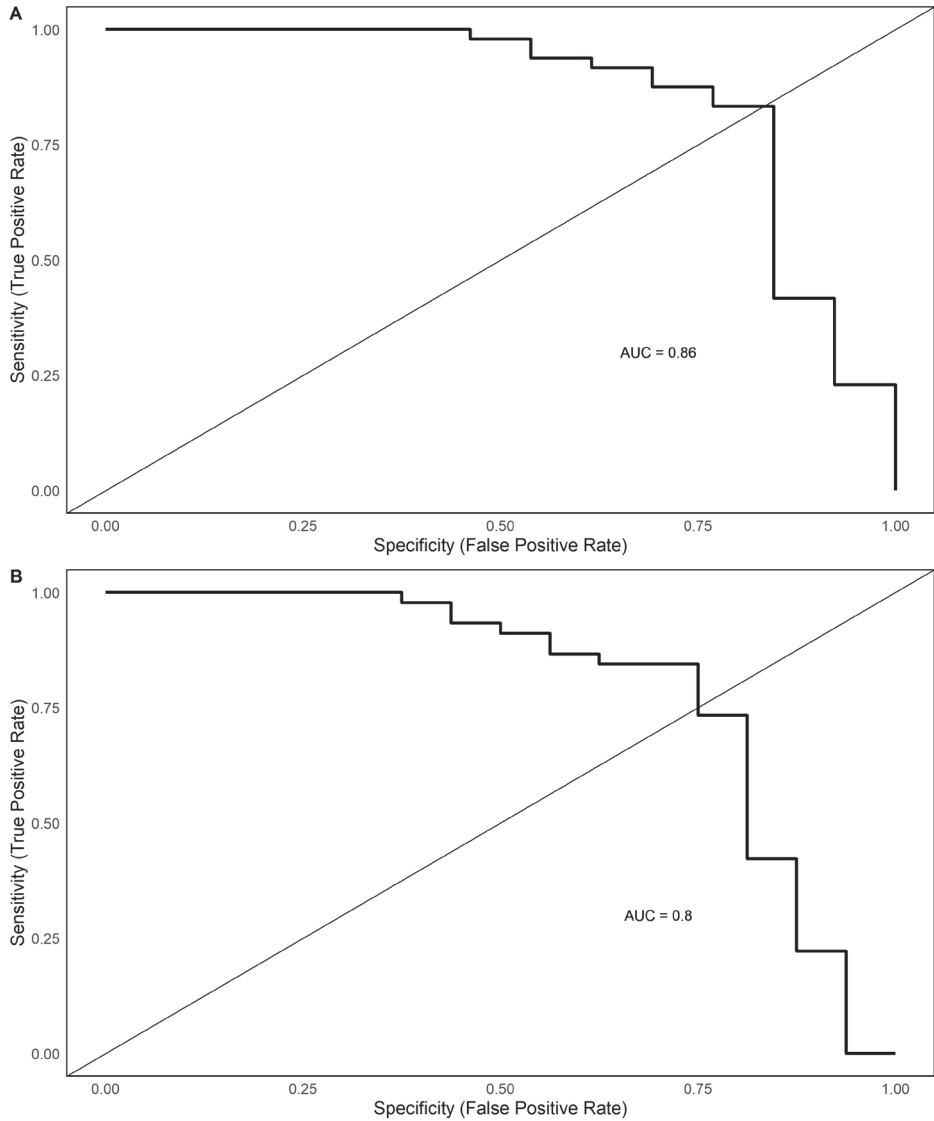
6

Figure 4. Receiver operating characteristic (ROC) curve for predicting the peak von Willebrand factor activity above or below the target peak level of 0.80 IU/mL (A) or 1.0 IU/mL (B). AUC: area under the curve

DISCUSSION

For VWD patients, assessing their response to desmopressin is critical to enable adequate prevention and treatment of bleeding with this easily applicable and less expensive drug. Performing desmopressin tests however is time consuming for both patients and medical staff. Eliminating the need for these tests would therefore be beneficial, but can only be realized if accurate prediction of desmopressin response is possible in each individual patient. Population PK modelling may be able to predict the individual response to desmopressin based on individual patient characteristics. Therefore, adequate predictive performance of such a population PK model must be validated. This study shows that the previously developed population PK model has adequate performance in terms of bias across the entire population, yet notable disparities emerge when categorizing by (sub)type of VWD. Patients with type 1 VWD exhibited the most accurate predictions in terms of both bias and precision. In contrast, type 2 patients experienced significant imprecision, indicated by considerable variability in predictions. Patients with low levels VWF generally demonstrated underestimations in their predictions, which from a clinical standpoint, could still be deemed acceptable. However, predictions for patients with a baseline VWF:Act less than 0.30 IU/mL tended to be overestimated, a situation considered clinically undesirable due to the higher than actual measurements predicted leading to potential bleeding risk for the patient when treated.

Our independent validation dataset represented a heterogeneous group of VWD patients e.g. VWD type age, and gender. Nevertheless, baseline VWF:Act before desmopressin administration was lower (median: 0.33 IU/mL) in our external independent dataset when compared to the previously developed population PK model (VWF:Act baseline before desmopressin administration mean: 0.50 IU/mL)[14]. Although the population PK model did not fulfill all performance criteria, certain sub-groups showed adequate bias and higher precision in their predictions. Particularly VWD type 1 demonstrated more reliable predictions. Conversely, patients with a VWF:Act baseline of <0.30 IU/mL displayed substantial over-prediction by the model, meaning that their predicted levels of VWF:Act were consistently higher than what was actually measured. This discrepancy could potentially be attributed to the original dataset used for development of the population PK model, in which patients had an atypical mean VWF:Act baseline of 0.50 IU/mL before desmopressin administration[14]. It is plausible that the previous developed population PK model by de Jager et al. inadequately captured patients with lower VWF:Act baselines, resulting in the observed over-prediction in this independent validation study. Furthermore, the study by de Jager et al. included fewer patients with low VWF levels compared to our independent validation dataset. Additionally, patients in our dataset were generally younger and had a slightly lower body weight on aver-

age. These variations in demographic and clinical characteristics might account for the differences in predictive outcomes. In addition, over-prediction may also be caused by unidentified covariates, which were then, of course, not taken into account in the published study but which may play a role in desmopressin responses of VWD patients. This aligns with previous findings indicating a significant variability in how patients respond to desmopressin[8,10].

Previously, it was noted that patients categorized as having low VWF levels, particularly those with historically lowest VWF levels ranging from 0.30 to 0.50 IU/mL, demonstrated a complete response to desmopressin[5,13]. While other VWD patients should perform a desmopressin test to confirm their response. This finding suggested that desmopressin testing might not be essential for low VWF patients. While the population PK model aimed to predict the response to desmopressin, the external validation revealed shortcomings in bias and precision. Intriguingly, the model exhibited an under-prediction in low VWF patients but an over-prediction in patients with a VWF:Act baseline <0.30 IU/mL. The current population PK model was not able to accurately predict VWF:Act levels post-intravenous desmopressin administration in patients with a VWF:Act baseline <0.30 IU/mL. Therefore, the necessity for desmopressin testing in VWD patients, especially in patients with a VWF baseline <0.30 IU/mL, remains unchanged.

VWD type 1 patients typically have a VWF:Act baseline <0.30 IU/mL. However, in our independent validation dataset, we encountered VWD type 1 patients with VWF:Act baseline levels as low as 0.05 IU/mL. Our validation analysis highlighted that the increase in VWF:Act is notably lower in patients with a baseline VWF:Act of <0.30 IU/mL, as observed by over-prediction of the model. The wide range of baseline VWF:Act levels observed in type 1 patients underscores the varied response to desmopressin administration, where the increase in VWF:Act is partially dependent on the baseline VWF:Act level. Thus, for accurate predictions of VWF:Act levels post-desmopressin administration using population PK modelling, further sub classification of VWD type 1 appears necessary. Previously, it has been demonstrated that the desmopressin response is influenced by genotype in type 1 VWD patients[8]. Moreover, Atiq et al. investigated the impact of desmopressin on VWF:Act among patients diagnosed with VWD type 1 and type 2 with various genetic variants in the VWF gene[20]. Notably, individuals with genetic variants in type 1 have substantially lower baseline VWF:Act levels and a reduced increase in VWF:Act following desmopressin administration compared to type 1 patients when genetic variants cannot be demonstrated. It is plausible that certain type 1 patients included in our independent validation dataset may have gene mutations, potentially explaining the lower response to desmopressin observed in this subgroup. Moreover, other studies have shown a large

variability in response after desmopressin administration in type 1 VWD patients[8,10]. This further underlies the importance of the characterization of type 1 VWD.

The external validation carried out in our study presents several limitations. Firstly, we have a lower number of patients (n = 61) and VWF:Act samples (n = 247) compared to the developed model. Specifically, our independent validation dataset included a limited number of patients with type 2 VWD, which limits the robustness of the results derived. Secondly, we did not have VWF:Act samples 24h post-desmopressin administration, therefore CL of VWF:Act could not be accurately described.The published population PK model by de Jager et al. mainly consisted of covariates implemented on the clearance (CL). Therefore, it is unfortunate that VWF:Act samples 24h post-desmopressin administration were not collected. Thirdly, our external validation mainly consisted of peak samples and a large variability in PE was observed. However, there were no covariates included in the population PK model that distinguished different VWF peak levels obtained for various sub-population within VWD, such as those related to the volume of distribution or bioavailability. These factors may be important in explaining the high PE seen across many patients. It is essential to incorporate clinically relevant covariates related to PK parameters, as the existing population PK model was not able to identify significant covariates affecting these parameters. Furthermore, accurately characterizing VWD types is crucial for enhancing the predictive performance of the population PK model. The current performance of the model is suboptimal across various VWD types, as indicated by inadequate predictive performance across one or more metrics. This suggests that the present approach of including covariates related to PK parameters in the model is insufficient. The characterization of VWD types is key to appropriately integrating these covariates into the model. Additionally, baseline VWF:Act before desmopressin administration is a critical factor, as it appears to be a significant indicator of desmopressin response across various studies[13]. Thus, it is imperative to revise the current population PK model to incorporate clinically relevant covariates that accurately reflect PK parameters.

In conclusion, the present study shows that the previously developed population PK model has adequate performance in terms of bias across the entire population, yet notable disparities emerge upon categorizing by types of VWD. Patients with type 1 VWD exhibited the most accurate predictions in terms of both bias and precision. However, the observation of over-prediction in patients with a VWF baseline below 0.30 IU/mL underscores the importance of still using a desmopressin test in these clinical settings to ensure effective treatment with desmopressin in VWD patients.

REFERENCES

1. Leebeek FWG, Eikenboom JCJ. Von Willebrand's Disease. Longo DL, ed. *N Engl J Med*. 2016;375(21):2067-2080. doi:10.1056/NEJMra1601561

2. Lenting PJ, Casari C, Christophe OD, Denis C V. von Willebrand factor: The old, the new and the unknown. *J Thromb Haemost*. 2012;10(12):2428-2437. doi:10.1111/jth.12008

3. de Wee EM, Sanders Y V., Mauser-Bunschoten EP, et al. Determinants of bleeding phenotype in adult patients with moderate or severe von Willebrand disease. *Thromb Haemost*. 2012;108(4):683-692. doi:10.1160/TH12-04-0244

4. James PD, Connell NT, Ameer B, et al. ASH ISTH NHF WFH 2021 guidelines on the diagnosis of von Willebrand disease. *Blood Adv*. 2021;5(1):280-300. doi:10.1182/BLOODADVANCES.2020003265

5. Lavin M, Aguila S, Schneppenheim S, et al. Novel insights into the clinical phenotype and pathophysiology underlying low VWF levels. *Blood*. 2017;130(21):2344-2353. doi:10.1182/blood-2017-05-786699

6. Franchini M, Focosi D. Targeting von Willebrand disease: the current status and future directions of management therapies. *Expert Rev Hematol*. 2023;16(11):871-878. doi:10.1080/17474086.2023.2268282

7. Connell NT, Flood VH, Brignardello-Petersen R, et al. Ash isth nhf wfh 2021 guidelines on the management of von willebrand disease. *Blood Adv*. 2021;5(1):301-325. doi:10.1182/BLOODAD-VANCES.2020003264

8. Castaman G, Lethagen S, Federici AB, et al. Response to desmopressin is influenced by the genotype and phenotype in type 1 von Willebrand disease (VWD): results from the European Study MCMDM-1VWD. *Blood*. 2008;111(7):3531-3539. doi:10.1182/blood-2007-08-109231

9. Revel-Vilk S, Schmugge M, Carcao MD, Blanchette P, Rand ML, Blanchette VS. Desmopressin (DDAVP) Responsiveness in Children with von Willebrand Disease. *J Pediatr Hematol Oncol*. 2003;25(11):874-879. doi:10.1097/00043426-200311000-00010

10. Federici AB, Mazurier C, Berntorp E, et al. Biologic response to desmopressin in patients with severe type 1 and type 2 von Willebrand disease: Results of a multicenter European study. *Blood*. 2004;103(6):2032-2038. doi:10.1182/blood-2003-06-2072

11. Castaman G. How I treat von Willebrand disease. *Thromb Res*. 2020;196(March):618-625. doi:10.1016/j.thromres.2020.07.051

12. De Wee EM, Leebeek FWG, Eikenboom JCJ. Diagnosis and management of von Willebrand Disease in the Netherlands. *Semin Thromb Hemost*. 2011;37(5):480-487. doi:10.1055/s-0031-1281032

13. Heijdra JM, Atiq F, Al Arashi W, et al. Desmopressin testing in von Willebrand disease: Lowering the burden. *Res Pract Thromb Haemost*. 2022;6(6):1-10. doi:10.1002/rth2.12784

14. De Jager NCB, Heijdra JM, Kieboom Q, et al. Population Pharmacokinetic Modeling of von Willebrand Factor Activity in von Willebrand Disease Patients after Desmopressin Administration. *Thromb Haemost*. 2020;120(10):1407-1416. doi:10.1055/s-0040-1714349

15. Aarons L, Ogungbenro K. Optimal design of pharmacokinetic studies. *Basic Clin Pharmacol Toxicol*. 2010;106(3):250-255. doi:10.1111/j.1742-7843.2009.00533.x

16. Sherwin CMT, Kiang TKL, Spigarelli MG, Ensom MHH. Fundamentals of Population Pharmacokinetic Modelling. *Clin Pharmacokinet*. 2012;51(9):573-590. doi:10.1007/bf03261932

17. Heijdra JM, Al Arashi W, Cnossen MH, et al. Is pharmacokinetic-guided dosing of desmopressin and von Willebrand factor-containing concentrates in individuals with von Willebrand disease or low von Willebrand factor reliable and feasible? A protocol for a multicentre, non-randomised, open label coho. *BMJ Open*. 2022;12(2):1-6. doi:10.1136/bmjopen-2021-049493

18.   Guo T, van Hest RM, Roggeveen LF, et al. External evaluation of population pharmacokinetic models of vancomycin in large cohorts of intensive care unit patients. *Antimicrob Agents Chemother*. 2019;63(5):1-9. doi:10.1128/AAC.02543-18

19.   Sheiner LB, Beal SL. Some suggestions for measuring predictive performance. *J Pharmacokinet Biopharm*. 1981;9(4):503-512. doi:10.1007/BF01060893

20.   Atiq F, Heijdra J, Snijders F, et al. Desmopressin response depends on the presence and type of genetic variants in patients with type 1 and type 2 von Willebrand disease. *Blood Adv*. 2022;6(18):5317-5326. doi:10.1182/bloodadvances.2021006757

21.   Cnossen MH, van Moort I, Reitsma SH, et al. SYMPHONY consortium: Orchestrating personalized treatment for patients with bleeding disorders. *J Thromb Haemost*. 2022;20(9):2001-2011. doi:10.1111/jth.15778

6

SUPPLEMENT

A population pharmacokinetic (PK) model describing von Willebrand factor activity (VWF:Act) levels after desmopressin administration in von Willebrand disease (VWD) was developed by de Jager et al[1]. Below the final PK parameters are displayed in table 1. The formulas of the PK parameters in the final model are displayed in equation 1-4

**Supplement table 1. Final population pharmacokinetics parameters by de Jager et al.**

Parameter	Final estimation
K_a (h^{-1})	1,830
Clearance (L/70 kg/h)	0.152
Volume of distribution (L/70 kg)	0.994
F	1
F virtual dosing	0.0780
Age on *F*	0.57
VWD type 1 on clearance	1
VWD type 2 on clearance	1.99
VWD type 2A on clearance	2.51
VWD type 2M on clearance	1.9
VWD type 2N on clearance	0.885
Low VWF activity on clearance	0.915
Sex on clearance	0.715
IIV clearance (%)	0.461
IIV volume of distribution (%)	0.0697
IIV *F* virtual dosing (%)	3.35
IIV *F* (%)	0.312 (60.5)
Additive residual variability (%)	0.0517
Proportional residual variability (%)	0.146

$$Clearance\ (CL)\ \left(\frac{L}{h}\right) = 0.152\ \times \frac{Body\ weight^{0.75}}{70}\ \times 1_{VWD\ type\ 1} \times 1.99_{VWD\ type\ 2} \times 2.51_{VWD\ type\ 2A} \times$$
$$1.90_{VWD\ type\ 2M} \times 0.885_{VWD\ tpye\ 2N} \times 0.915_{Low\ VWF\ activity} \times 0.715_{female}\ \times e^{\eta CL}$$

(Equation 1)

$$Volume\ of\ distribution\ (Vd)\ (L) = 0.994\ \times \frac{Body\ weight}{70} \times e^{\eta Vd}$$

(Equation 2)

$$F = \ 1 \times \frac{Age^{0.57}}{28}\ \times e^{\eta}$$

(Equation 3)

$$F_{virtual\ dosing} = 0.0714\ \times e^{\eta\ virtual\ dosing}$$

(Equation 4)
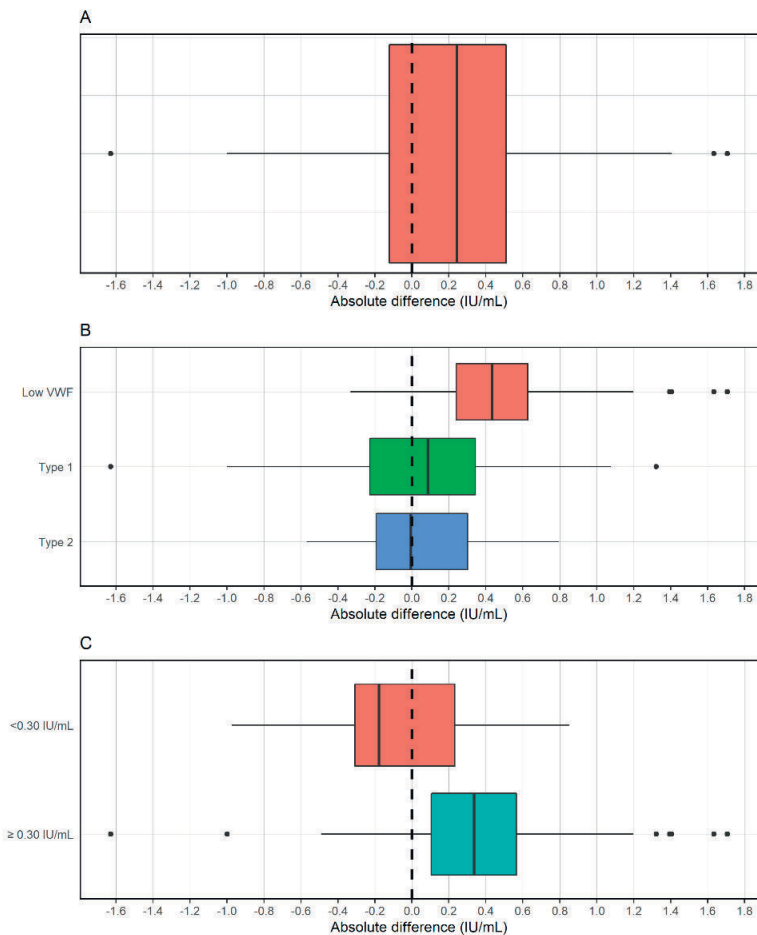
Supplement figure 1. Box plots of the absolute difference (IU/mL) for VWF:Act levels. A) Absolute difference of all patients, B) Absolute difference of patients stratified on von Willebrand disease type, C) Absolute difference of patients stratified on baseline VWF:Act <0.30 IU/mL or ≥0.30 IU/mL. Black dashed line are reference lines indicating an absolute different of 0 IU/mL. Absolute difference was calculated as: measured VWF:Act – predicted VWF:Act.
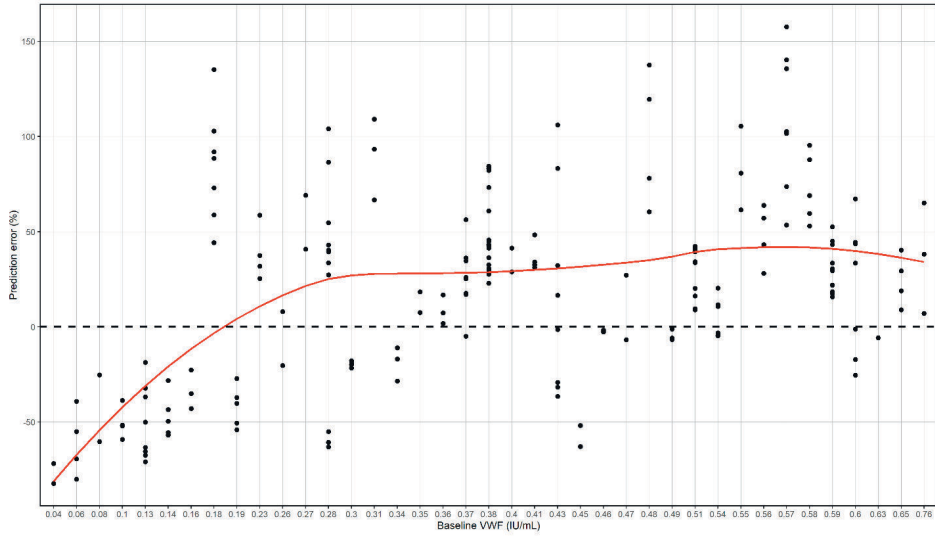
Supplement figure 2. Baseline von Willebrand factor activity (VWF:Act) against prediction error (PE%) The red line represents the smooth line (loess smooth). The dashed line represents the prediction error of 0%. Dots represent patients with a calculated PE where a VWF:Act level was measured.
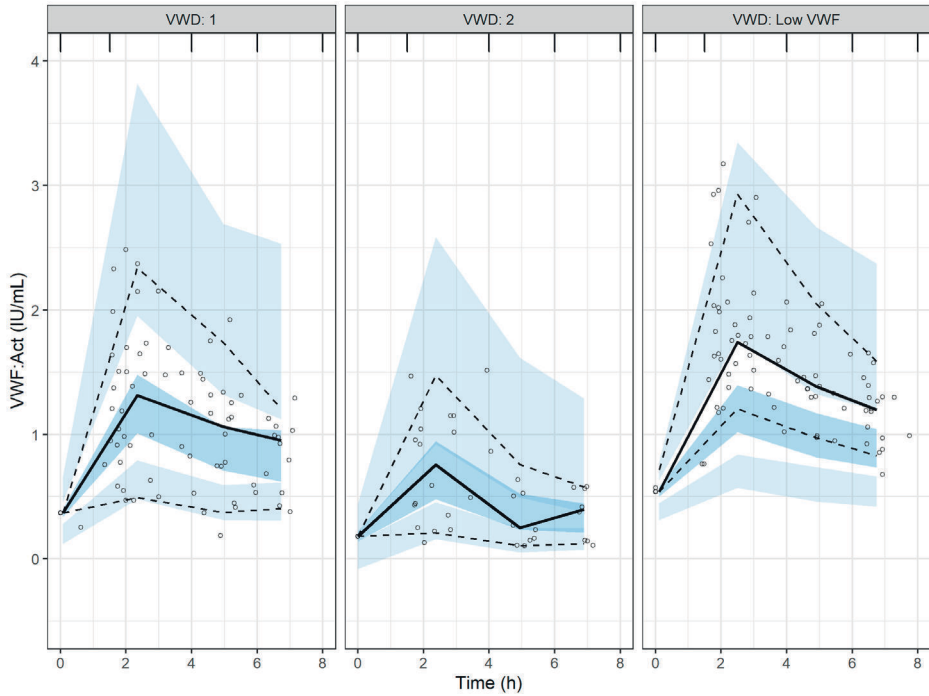
Supplement figure 3. Prediction-corrected visual predictive check (pcVPC) plots of the external dataset for the investigated population PK models of von Willebrand factor activity (VWF:Act) after desmopressin administration stratified into von Willebrand disease (VWD) type 1, 2 and low VWF. Dots represent measured VWF:Act; the solid black line represents the 50th percentile of observed data; the dashed black lines represent the 5th and 95th percentiles of the population model. Shaded areas depict the model predicted 95% confidence intervals of the simulated percentiles.
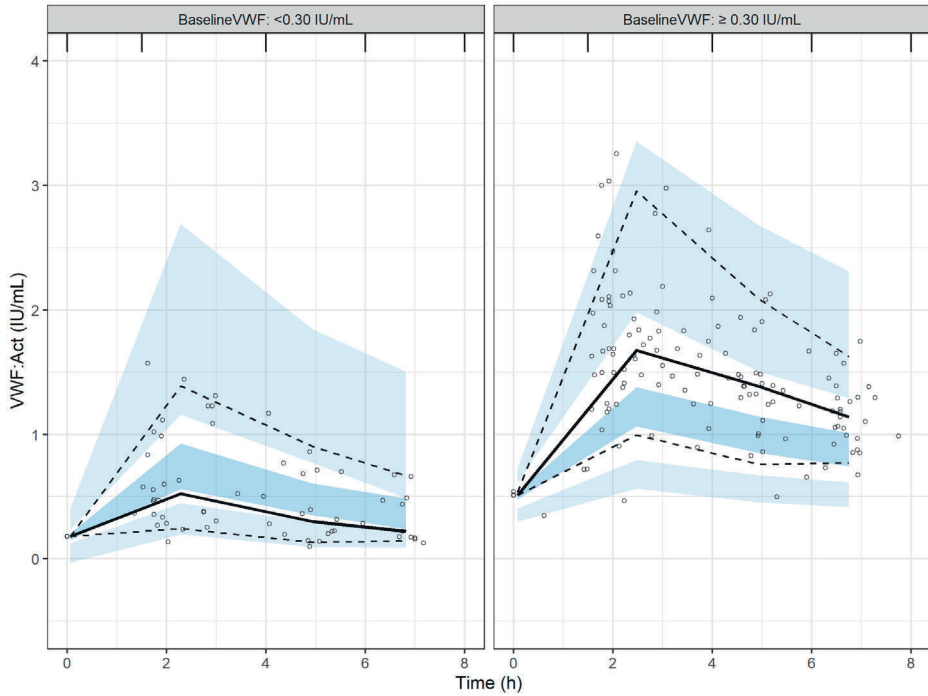
Supplement figure 4. Prediction-corrected visual predictive check (pcVPC) plots of the external dataset for the investigated population PK models of von Willebrand factor activity (VWF:Act) after desmopressin administration stratified into VWF:Act baseline of <0.30 or ≥0.30 IU/mL. Dots represent measured VWF:Act; the solid black line represents the 50th percentile of observed data; the dashed black lines represent the 5th and 95th percentiles of the population model. Shaded areas depict the model predicted 95% confidence intervals of the simulated percentiles.

SUPPLEMENTARY REFERENCES
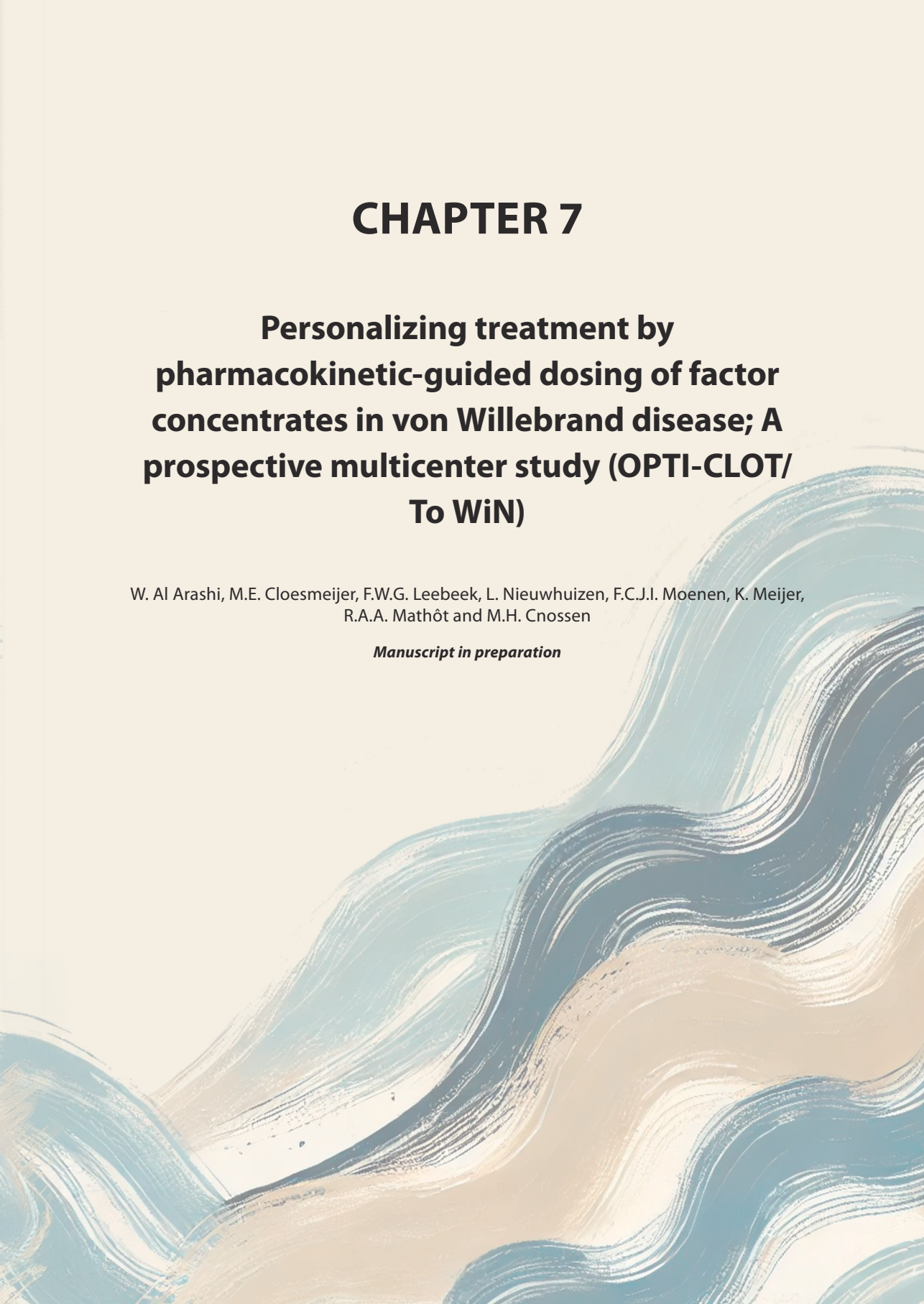
1. De Jager NCB, Heijdra JM, Kieboom Q, et al. Population Pharmacokinetic Modeling of von Willebrand Factor Activity in von Willebrand Disease Patients after Desmopressin Administration. *Thromb Haemost*. 2020;120(10):1407-16.

6

CHAPTER 7

Personalizing treatment by pharmacokinetic-guided dosing of factor concentrates in von Willebrand disease; A prospective multicenter study (OPTI-CLOT/To WiN)

W. Al Arashi, M.E. Cloesmeijer, F.W.G. Leebeek, L. Nieuwhuizen, F.C.J.I. Moenen, K. Meijer, R.A.A. Mathôt and M.H. Cnossen

Manuscript in preparation

ABSTRACT

Despite body weight-based dosing, there is still substantial interindividual variation in the Von Willebrand factor(VWF) and factor VIII(FVIII) levels after infusion of VWF/FVIII concentrate. Therefore, we aimed to investigate the reliability and feasibility of pharmacokinetic (PK)-guided dosing of a VWF/FVIII concentrate in patients with Von Willebrand disease (VWD) undergoing medical procedures.

Methods

A prospective multicenter intervention study was performed in VWD patients requiring Haemate P® during a medical procedure between April 8th 2019 until July 1st 2023. Dosing regimens based on individual PK parameters, obtained through a priori PK profile, were calculated using a population PK model. Predicted and measured VWF activity(VWF:Act) and factor VIII(FVIII:C) levels were compared to assess the predictive performance, aiming at a prediction error (PE) within ±25%.

Results

Twenty-nine VWD patients were included: 11 type 1 and 18 type 2 VWD. Medical procedures were classified as low 17/29 (59%) and medium bleeding risk 12/29 (41%). In total, 138/202 (65%) VWF:Act levels and 124/202 (61%) FVIII:C levels were within ± 25% of the predicted levels. The median PE [interquartile range] for VWF:Act peak and trough levels was 15%[8-26] and 23%[11-41], respectively. For FVIII:C peak and trough levels, it was 18% [9-30] and 21% [10-37]. The positive PE indicates the observed measurements were higher than the predictions. Four (14%) patients experienced minor bleeding complications. No cases of thrombosis occurred. Patients and physicians reported high satisfaction with PK-guided dosing.

Conclusion

This study shows promising results regarding the reliability and feasibility of PK-guided dosing in VWD patients undergoing medical procedures. However, due to the heterogeneity of VWD, more data is essential to optimize and refine further personalization of treatment by application of PK-guided dosing of VWF/FVIII concentrates.

INTRODUCTION

Von Willebrand disease (VWD) is the most common inherited bleeding disorder, affecting 0.6-1.3% of the population[1]. It results from defects in von Willebrand factor (VWF), causing mucocutaneous bleeding, hematomas, menorrhagia and bleeding during medical procedures. VWD is categorized into three types. Type 1 VWD, accounting for 70-80% of cases, involves a partial deficiency of VWF due to reduced synthesis, secretion or increased clearance. Type 2 VWD, accounting for 20% of cases, represents various qualitative defects in VWF and is divided into subtypes[2]. In type 2A, there is reduced VWF binding to platelets, while in type 2B VWF has an increased affinity for platelets. Both subtypes are characterized by low levels of high molecular weight VWF multimers (HMWM). In type 2M, reduced platelet binding is observed with normal HMWM and in type 2N a decreased affinity of VWF to FVIII is seen, resulting in lower FVIII:C levels. Finally, in type 3 VWD, accounting for <5%, extremely low circulating VWF levels are measured, resulting in severe VWD[3]. VWF serves as a chaperone protein for FVIII, protecting FVIII from proteolysis in the circulation. Therefore, patients with VWD, especially those with severe deficiencies, also present with lower FVIII:C levels.

The goal of treatment in VWD is to prevent or stop bleeding by increasing VWF and FVIII levels to adequate levels for hemostasis. This is achieved by administering desmopressin to stimulate the release of endogenous VWF and FVIII or by infusion of VWF-containing concentrates. The choice of treatment depends on VWD type, bleeding phenotype, severity and location of bleeding, and type of medical procedure. Desmopressin is an option for patients with type 1 and 2 who demonstrate an adequate response of VWF and FVIII following desmopressin testing[4]. Although, desmopressin is accessible and inexpensive, dosing frequency is limited due to tachyphylaxis. Various VWF-containing concentrates are available for VWD treatment with different VWF/FVIII ratios and HMWM content[5]. Dosing these concentrates is still based on body weight and guided by targeting of VWF and FVIII levels which are determined by bleeding severity or the type of medical procedure[3].

In a retrospective analysis, Hazendonk et al. reported that treatment with a specific VWF/FVIII concentrate (Haemate P®) was suboptimal in VWD patients undergoing medical procedures. Most VWF and FVIII trough levels exceeded predefined target levels (≥ 0.20 IU/mL), for type 1 (65% and 91%), type 2 (53% and 72% and type 3 VWD (57% and 93%), respectively. However some fell below target levels, with 16 to 38% of VWF:Act trough levels and 8 to 14% of FVIII:C trough levels observed to be lower which respectively may lead to an increased risk of thrombosis and/or bleeding, as well as unnecessary costs due to excessive dosing.

The inter-individual differences in response to VWF/FVIII concentrates can be explained by variation in pharmacokinetics (PK) between patients. Lethagen et. al, studied the use of an individual PK profile prior to surgery for optimal loading dosage of VWF/FVIII concentrate, focusing on the feasibility of this approach[6]. They reported that using a loading dose based on the VWF PK profile was feasible and resulted in excellent to good hemostasis in almost all patients[6]. In a similar study which focused on using prior PK profiling to guide dosing during surgery, Di Paola et al. observed high intra-individual variability between PK parameters obtained pre- and post-surgery, limiting its use for optimal perioperative dosing[7].

In a recent randomized controlled trial, we demonstrated that PK-guided dosing of FVIII concentrates in patients with hemophilia A improved the attainment of FVIII levels within the prescribed range[8]. Importantly, in this study, a preoperative PK profile was obtained and after the initiation of surgery, doses were iteratively adjusted daily. In VWD, PK-guided dosing based on this approach has not yet been studied. Therefore, the aim of this specific arm of our study is to investigate the reliability and feasibility of iteratively PK-guided dosing of VWF/FVIII concentrate in VWD patients undergoing medical procedures, focusing on a specific VWF/ FVIII concentrate in this publication.

METHODS

Study design

The OPTICLOT/To WiN study is a prospective, multicenter, intervention study that is ongoing in four hemophilia treatment centers in the Netherlands: Erasmus MC, University Medical Center Rotterdam; University Medical Center Groningen; Maxima Medisch Centrum and Maastricht University Medical Center. The study was approved by the Medical Ethics Committee of the Erasmus MC and registered at the Netherlands Trial Register "OMON", as NL-OMON54546 and in EudraCT as 2018-001631-46. The design of OPTICLOT/To WIN study has been described in an earlier publication[9].

Study population

The OPTICLOT/To WiN study consists of four interventions arms[9]. This article focuses on intervention arm B in which patients were treated with VWF-containing concentrates during medical procedures, applying PK guidance. We now report on the initial results using a specific VWF/ FVIII concentrate, Haemate P®, which is a plasma-derived factor concentrate containing VWF and FVIII with a VWF/FVIII ratio of 2.4:1[5]. Table 1 shows the inclusion and exclusion criteria of study, specifically for intervention arm B.

Table 1: Inclusion and exclusion criteria for OPTICLO/To WIN study, intervention group of Arm B, in which PK-guided dosing of VWF/FVIII concentrate was performed.

Inclusion criteria	Exclusion criteria
All ages	Any other known hemostatic abnormalities
Hemorrhagic symptoms or a family history of von Willebrand disease with historically lowest levels of VWF:Ag <0.60 IU/mL and/or VWF:Act <0.60 IU/mL and/or VWF:CB <0.60 m/L and/or FVIII:C <0.40 IU/mL;	Acquired VWD
Need for a medical procedure requiring replacement therapy	Presence of VWF antibodies (>0.2 BU)
Written patient informed consent	Withdrawal of informed consent

Abbreviations: VWD, von Willebrand disease; VWF, von Willebrand factor; FVIII:C, factor FVIII activity; VWF:Ag, von Willebrand factor antigen; VWF:Act, Von Willebrand factor activity; VWF:CB, Von Willebrand factor collagen binding activity; IU, International units; mL, millimeters

Study intervention

Figure 1 depicts the study design and interventions in arm B. Firstly, included patients underwent PK profiling, involving the infusion of a 25 IU/kg dose of the VWF/FVIII concentrate based on FVIII with blood sampling at T=0, T=10 (peak level) minutes, T=2 hours, T= 24 hours and T=48 hours. The treating physician established VWF:Act and/or FVIII:C target levels for patients during the medical procedure, based on guidelines and patient characteristics and determined the duration of treatment. The clinical pharmacologist provided first doses based on individual patient characteristics (VWD type, body weight and age), predefined target levels combined with type and severity of medical procedure and the individual PK profile. This PK-guided dosing advice was then discussed with the treating physician for approval. Secondly, during the medical procedure, PK-guided dosing was applied iteratively, with monitoring of factor levels to assess if targets were achieved, adjusting the dosing if necessary. Importantly, the treating physician was allowed to overrule the PK-guided dosing advice if another dose was preferred due to clinical reasons.

Blood sampling for factor levels was performed at baseline (before the medical procedure), after each infusion at T=10 minutes (peak level), after the medical procedure (post-procedure level) and at T≥ 12 hours after infusion (trough level). As this study was designed as a clinical study in a real word setting, exact timing of blood sampling for factor levels was not always possible. Peak level sampling deviations were allowed up to 30 minutes and for trough levels and other levels up to +/- 1 to 2 hours, with precise documentation of time points. At the end of study participation, the treating physician and patients received a questionnaire regarding their opinion on PK-guided dosing.
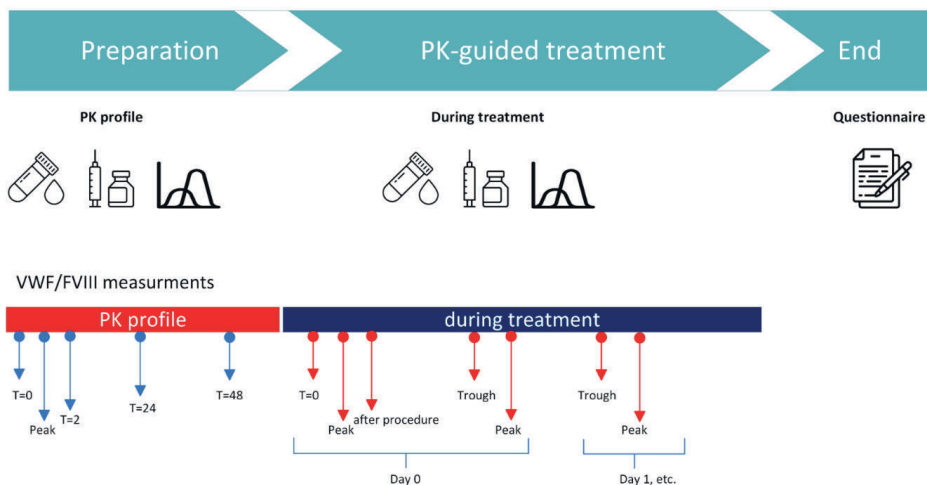
Figure 1: OPTCLOT/To WiN study design: intervention group arm B with VWF/FVIII concentrates
Abbreviation: VWF, Von Willebrand factor; FVIII, factor FVIII; PK, pharmacokinetic

Clinical and laboratory measurements

Data of patients, medical procedures and treatment characteristics were collected. Patient characteristics included age, most recent body weight, VWD type, historically lowest levels of VWF (including VWF:Activity (VWF:Act); VWF:Antigen (VWF:Ag), VWF:collagen binding activity (VWF:CB)), FVIII:C and ABO blood group. Type 1 VWD was defined as having a VWF:Act/VWF:Ag ratio >0.7, whereas type 2 VWD was categorized as VWF:Act/VWF:Ag ratio ≤0.7. Regarding medical procedures, type of procedure, estimated and actual duration, starting timepoint and ending time, bleeding risk and ASA classification were documented. As the estimated duration of the medical procedure was required for the calculation of the PK-guided dosing regimens, it was obtained from surgery schedules, or procedure appointments. Subsequently, the actual duration was documented after the procedure: if unavailable, the estimated duration was used instead. The bleeding risk of the medical procedure was classified as minor, medium or high according to Koshy et al.[10]. If classifications according to Koshy et al. were not feasible, the most probable bleeding risk was determined. Treatment characteristics were documented including treatment duration, timing, dosing and frequency of VWF/FVIII concentrate, mode of infusion (continuous or bolus infusion) of VWF/FVIII concentrate, co- medication with effects on hemostasis (tranexamic acid, low molecular weight heparin, non- steroidal anti- inflammatory drugs) and complications including bleeding and thrombosis.

Laboratory measurements were conducted according to locally certified protocols. Routine blood tests before a medical procedure included measurements of blood group, hemoglobin, platelets, liver function (alanine aminotransferase (ALT), aspartate aminotransferase (AST), gamma-glutamyl transferase (GGT), alkaline phosphatase, lactate dehydrogenase and albumin) and kidney function (urea and creatinine).

PK-guided dosing

Maximum a posteriori (MAP) Bayesian analysis, using the population PK (PopPK) model by Bukkems et al. for Haemate P® was applied to estimate the individual PK parameters for VWF:Act and FVIII:C based on the measurements of VWF:Act and FVIII:C levels during the individual PK profile[11]. The individual PK parameters were used to design a dosing advice for the medical procedure. In the applied population model the covariates of the PK parameters were: VWD type, estimated medical procedure duration and ASA score. Therefore, these were incorporated in the dosing calculations. Measurements of VWF:Act/FVIII:C collected both before and after the medical procedure were iteratively added into the model on a daily basis to assess modification of the dosing regimen for the subsequent day. Any adjustments to the dosing scheme were made if the model's predictions were below or significantly exceeded the target levels for VWF:Act/FVIII:C. The latter was not specified by specific cut-offs but rather discussed with treating physician if necessary.

Study outcomes

The primary endpoint of the study was the reliability of PK-guided dosing which was defined as the actual difference between predicted VWF:Act and FVIII:C and measured VWF:Act and FVIII:C levels, referred to as predictive performance. The relative prediction error (PE) (equation 1) and absolute error (AE) (equation 2) were used to assess the predictive performance. PE indicates the accuracy of the predictions, where a positive PE suggests that the observed levels are higher than predicted, and a negative PE indicates that the observed levels are lower than predicted. AE indicates the precision of the predictions, with a higher AE signifying greater deviation from the predicted levels. Importantly, the accepted or ideal AE or PE were not determined at the beginning of study because the study population was expected to be too heterogeneous. The goal was to determine the predictive performance by assessing both the PE and AE and to identify the percentages of levels within a range of ±25% of the predicted levels and to calculate the median PE. Clinically accepted AE was explored.

$$PE\ (\%) = \frac{Observed\ level - predicted\ level}{predicted\ level} \times 100\%$$

(equation 1)

$$AE\ \left(\frac{IU}{mL}\right) = |Observed\ level - predicted\ level|$$

(equation 2)

Secondary endpoints included the feasibility of PK-guided dosing, bleeding complications and incidence of thrombosis. Feasibility was defined as the satisfaction of the treating physician and patients as well as potential cost-reduction by application of PK-guided dosing. Satisfaction was measured by questionnaire. Physicians were asked four questions regarding their satisfaction with PK-guided dosing, the burden for the medical team and patient and if they would choose PK-guided dosing again. Patients were also asked four questions regarding satisfaction with PK-guided dosing, the burden of PK-guided dosing, their appreciation of being aware of their factor levels during treatment and whether they would recommend PK-guided dosing to other patients. All questions were rated on a scale from 1 and 10, and if rating included a half number, it was rounded off or up to a whole number. Cost effectiveness of PK-guided dosing was only assessed for the loading dose of VWF/FVIII concentrate on the day of the medical procedure in order to compare with body weight-based dosing. The latter was provided by the treating physician during the study preparation. Bleeding complications were categorized as minor or major. A minor bleeding complication was defined as additional treatment with a hemostatic drug. A major bleeding complication was defined as prolonged hospitalization not due to logistic issues (such as infusion not being possible at home), a need to repeat the medical procedure to ensure hemostasis and/or (permeant) morbidity due to the bleeding complication.

Statistical analysis

Descriptive data are presented as numbers with percentages for categorical variables and medians with an interquartile range (IQR) for continuous variables. In cases where data were not normally distributed, the non- parametric Mann- Whitney U test was used to compare groups and Wilcoxon Signed Rank test was used for related continues variables. A p-value of less than 0.05 was considered statistically significant.

RESULTS

A total of 29 patients completed the study and were analyzed. Eleven (38%) patients were included with type 1 VWD and 18 (62%) patients with type 2. Among patients with type 2 VWD, there were 11 (61%) with type 2A, three (17%) with type 2B, three (17%) with type 2M and one (5%) with type 2N. Patients with type 1 VWD had median historically lowest measured VWF:Ag and VWF:Act level of 0.29 IU/mL [0.11-0.46] and 0.12 IU/mL [0.09-0.17], respectively. For patients with type 2 VWD the median historically lowest measured VWF:Ag and VWF: Act level were respectively 0.34 IU/mL [0.11-0.50] and 0.11 IU/mL [0.08-0.16] IU/mL. The median historically lowest measured FVIII:C level was 0.30 IU/mL [0.13-0.47] IU/mL for patients with type 1 and 0.33 IU/mL [0.17-0.53] for patients with type 2 VWD.

Table 2: General characteristics of included study population.

	N (%) or median [interquartile range]	N (%) or median [interquartile range]	N (%) or median [interquartile range]
	Total	**Type 1**	**Type 2**
No. of patients	29	11 (38)	18 (62)
Female gender	23 (79)	9 (82)	14 (78)
Age, years	61 [49 – 69.5]	66 [54 – 78]	56.5 [40 – 67]
Body weight^, kg	73 [68 – 84.5]	80 [71 – 91]	73 [62.5 – 83.75]
Von Willebrand disease			
Lowest VWF/FVIII level, IU/mL			
VWF:Ag	0.29 [0.11 – 0.46]	0.25 [0.10-0.31]	0.34 [0.11-0.50]
VWF:Act	0.12 [0.09 – 0.17]	0.13 [0.10-0.24]	0.11 [0.08-0.16]
FVIII:C	0.31 [0.17 – 0.51]	0.30 [0.13-0.47]	0.33 [0.17-0.53]
VWF/FVIII level before treatment**, IU/mL			
VWF:Act	0.16 [0.09 – 0.53]	0.55 [0.14-0.69]	0.14 [0.06-0.29]
FVIII:C	0.56 [0.25 – 0.85]	0.74 [0.22-1.07]	0.39 [0.26-0.76]
Medical intervention			
Duration, min	40 [30 – 76]	41 [30-60]	35 [30-87]
Bleeding risk^			
Low	17 (59)	8 (73)	9 (50)
Medium	12 (41)	3 (27)	9 (50)
Treatment and complications			
Treatment duration, days	2 [1-5.5]	2 [1-2]	2 [1-6]
Bleeding complications^^			
Major	0	-	-
Minor	4 (14)	1 (9)	3 (17)
Thrombosis	0	-	-

Among patients with type 2 VWD, there were 11 (61%) with type 2A, three (17%) with type 2B, one (5%) with type 2N, and three (17%) with type 2M. *Measured or collected at time of PK profiling

**VWF/FVIII levels were taken on the day of medical intervention and before the infusion of Haemate P®

^ Based on a surgical risk score, adapted from Koshy et al., Blood; 1995

^^ Bleeding complication: major was defined as necessity of second surgical intervention, hemoglobin decrease ≥1.24 mmol/L and/or requiring red blood cell transfusion, or bleeding prolonging patient hospitalization; minor was defined only required additional haemostatic treatment without requiring second surgical intervention, red blood cell transfusion, or prolonging patient hospitalization. Abbreviations: No., number (percentages); Median, [IQR = Interquartile range 25%-75%]; kg, kilogram; VWF, von Willebrand factor; FVIII:C, factor VIII activity; VWF:Act, von Willebrand factor activity; VWF:Ag, von Willebrand factor antigen; IU/mL international units per milliliter;

7

Two (6%) of the 31 initially eligible patients did not complete the study. One patient with type 3 VWD was not treated with PK-guided dosing, as the treating physician preferred body weight-based dosing, considering the difference with the proposed PK-guided dose. The second patient with type 3 VWD experienced an allergic reaction during Haemate P® infusion. Table 2 shows the general baseline characteristics of the 29 patients included. Only age was shown to be significantly different between type 1 and 2 VWD patients, as patients with type 2 were significantly younger (p=0.019). All patients underwent PK profiling prior to their medical procedure. Most patients underwent PK profiling between 1 and 9 weeks before their medical procedure (n=23) and six patients underwent PK profiling between 28-69 weeks due to the type of medical procedure or scheduling circumstances.

Patients underwent various medical procedures, with dental interventions being the most frequent (n=7, 24%). Other medical procedures included colonoscopy (n=3), gastroscopy (n=3), gynecologic procedures (n=3), orthopedic surgery (n=3), dermatological procedures (n=2), urologic procedures (n=2), general surgery (n=2), eye surgery (n=1), cardiac procedure (n=1), a vaginal delivery (n=1) and an (minor) orthopedic procedure (n=1). The median duration of these medical procedures was 40 minutes [30-76]. The bleeding risk was classified as low in 17 (59%) procedures and medium in 12 (41%) procedures, with no significant difference between patients with type 1 and 2 VWD (p=0.27).

Treatment specifications and hemostatic complications

In total, 117 target levels were set by the treating physician, comprising 82 (70%) VWF:Act levels and 35 (40%) FVIII:C levels. The predefined target peak levels before the initiation of the medical procedure were as follows: >0.50 IU/mL(n=5), >0.80 IU/mL (n=13), >1.00 IU/mL (n=23) and >1.50 IU/mL (n=1). For subsequent trough levels during the medical procedure, predefined target levels were >0.3 IU/mL (n=6), >0.5 IU/mL (n=54) and >0.8 IU/mL (n=15). Sixteen patients (55%), only VWF:Act was applied as the target level, in 12 patients (41%) both VWF:Act and FVIII:C were used as target levels, and in one (4%) patient only FVIII:C was targeted.

The median treatment duration was two days [1-5.5]. The median dosage of the first infusion of Haemate P® was 30 IU/kg FVIII [23-40], for patients with type 1 was the median dosage 25 IU/kg FVIII [16-33] and patients with type 2 31 IU/kg FVIII [24-46] (p=0.84).

Four (14%) patients experienced minor bleeding complications. No major bleeding complications occurred and there were no cases of thrombosis. Table 3 shows the characteristics of patients with minor bleeding complications and provides more detailed information.

Table 3: Characteristics of patients with minor bleeding complication

Patient	VWD Type	Age (years)	Type of medical procedure	Treatment duration (days)	Day of complication	Bleeding complication	Additional treatment	Pre-procedure VWF:Act peak level (IU/mL)	Pre-procedure FVIII:C peak level (IU/mL)	Target levels achieved (yes/no)	Last VWF:Act trough level* (IU/mL)	Last FVIII:C trough level* (IU/mL)
1	2B	54	Dental procedure	1	Day 8 after treatment	Gingival bleeding	One day Haemate P®, and tranexamic acid	0.42	0.66	No Targeted VWF:Act peak 0.5	-	-
2	2A	31	Gynecology procedure	6	Day 9 after treatment	Vaginal bleeding	Tranexamic acid	1.21	1.07	No One trough target level not achieved at day 0 (0.66 IU/mL instead of 0.8)	0.42	0.88
3	2A	43	Gynecology procedure	2	Day 9 after treatment	Vaginal bleeding	Two days Haemate P®, tranexamic acid, and local intervention	1.35	1.17	Yes	0.23	0.63
4	1	74	Cardiac procedure	1	Day 2 of treatment	Hematoma at location of infusion	One day Haemate P®	1.31	1.29	Yes	1.07	1.47

Abbreviations: VWD, von Willebrand disease; VWF:Act, von Willebrand factor activity; FVIII:C, factor FVIII activity; IU, international units; ml, milliliters

7

Predictive performance

In total, 202 VWF:Act and FVIII:C levels were measured and predicted, comprising 29 (14%) baseline levels, 84 (42%) peak levels, 62 (31%) trough levels and 27 (13%) post-procedure level. Measured VWF:Act and FVIII:C levels are presented in Figure 2. Figure 3 illustrates the PE for VWF:Act and FVIII:C levels, specified for peak and trough levels and Table 4 shows the median PE (MPE) and median AE (MAE) for VWF:Act and FVIII: C, specified for peak and trough levels and each type of VWD.
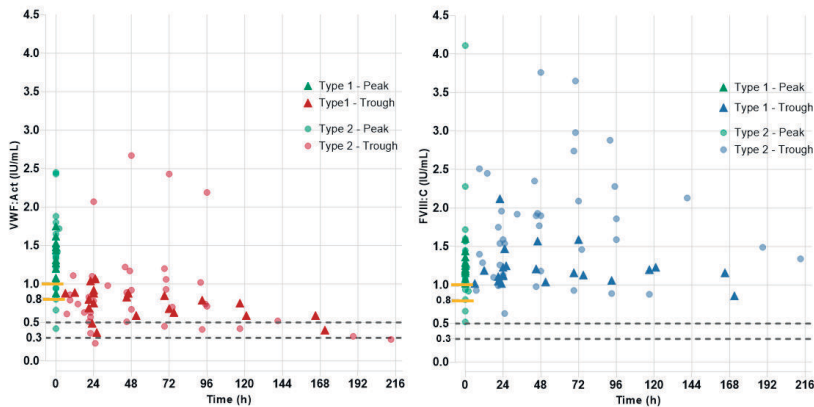

Figure 2: Measured factor levels during treatment. VWF:Act levels are shown in red and FVIII:C levels in blue. Time= 0 indicates the intial infusion of VWF/FVIII concetrate, with subsquently levels starting as peak levels and after the first peak levels only trough levels are presented. The yellow lines indicates predefined target peak levels and the dashed black lines indicate the target trough levels. Notably, both the target level of 0.8 IU/mL and 0.5 IU/mL were used both for peak and trough levels. *The four high VWF:Act trough levels between 24 and 96 hours were observed in one patient with type 2N who received continuous VWF/FVIII concentrate. Abbreviations: VWF:Act, von Willebrand activity; FVIII:C, factor VIII activity; VWF/FVIII concentrate, von Willebrand factor and factor VIII concentrate; IU, international units h, hour.

Von Willebrand factor activity

The MPE for VWF:Act peak levels was 14% [4-25] (n=84) and for VWF:Act trough levels was 21% [2-38] (n=62). No significant in the MPE was observed between VWD types (Table 4). The MAE for VWF:Act peak levels was 0.19 [0.07-0.31] (n=84) and for VWF:Act trough levels it was 0.16 [0.06-0.25] (n=62). Patients with type 2 VWD had significantly higher MAE compared to patients with type 1 VWD (0.20 [0.07-0.32] (n=40) versus 0.10 [0.05-0.18] (n=22); p=0.02). No significant differences in MPE and MAE were observed between medical procedures with low and moderate bleeding risk.

Overall, focusing on VWF:Act levels, 138 (65%) were within the rang ± 25% of the predicted levels. Among the VWF:Act peak levels, 61 (73%) fell within this range and 34 (55%) of the VWF:Act trough levels also fell within this range (Figure 3). For peak levels, 22 (26%) were above this range (≥ +25%) and one (1%) level was below this range (≤
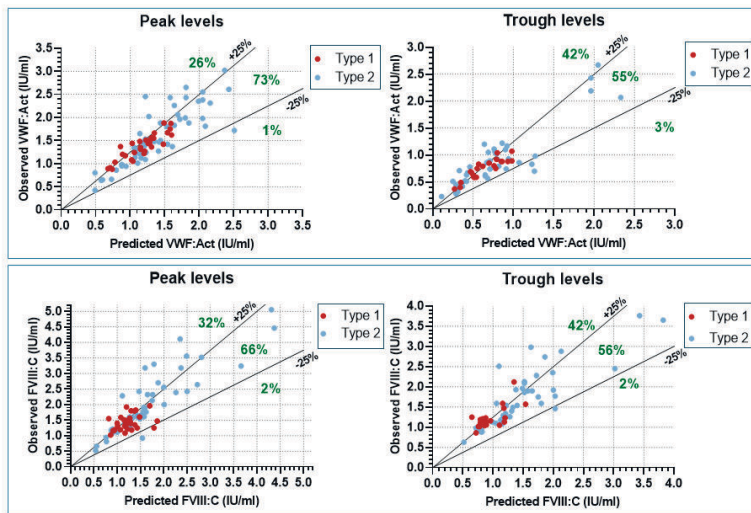
Figure 3: Predictive error for VWF:Act and FVIII:C levels, comparing predicted levels and measured levels. Factor levels are dived into peak and trough and levels. Peak levels represent all peak levels, which were taken during treatment. Through levels represent all trough levels, which were taken during the treatment with at least 12 hours (-/+ 1 hour) after a bolus infusion of VWF/FVIII concentrate (n=28 patients) or during continuous infusion (n=1 patient). Abbreviations: VWF:Act, von Willebrand activity; FVIII:C, factor VIII activity; VWF/FVIII concentrate, von Willebrand factor and factor VIII concentrate; IU, international units h, hour.

7

Table 4: The predictive performance as assessed by the prediction error (PE) and absolute error (AE).

		Median predictive error (MPE), % [IQR]				Median absolute error (MAE), IU/mL [IQR]			
		Total	Type 1 VWD	Type 2 VWD	P-value	Total	Type 1 VWD	Type 2 VWD	P-value
Peak	Total levels	n=84	n=32	n=52		n=84	n=32	n=52	
	VWF:Act	14 [4-25]	17 [9-26]	11 [1-25]	0.153	0.19 [0.07-0.31]	0.20 [0.13-0.27]	0.19 [0.07-0.35]	0.590
	FVIII:C	17 [6-29]	17 [8-30]	17 [5-27]	0.883	0.24 [0.13-0.42]	0.25 [0.14-0.40]	0.23 [0.10-0.56]	0.980
Trough	Total levels	n=62	n=22	n=40		n=62	n=22	n=40	
	VWF:Act	21 [2-38]	17 [5-36]	22 [-3-45]	0.757	0.16 [0.06-0.25]	0.10 [0.05-0.18]	0.20 [0.07-0.32]	0.020
	FVIII:C	21 [6-37]	32 [20-42]	14 [4-33]	0.024	0.25 [0.11-0.41]	0.27 [0.16-0.37]	0.22 [0.09-0.55]	0.780

Abbreviations: VWD, von Willebrand disease; VWF:Act, von Willebrand factor activity; FVIII:C, factor FVIII activity; IU, international units; ml; milliliters, IQR; interquartile range

-25%). For trough levels, 26 (42%) were above this range (≥ +25%) and two (3%) levels were below this range (≤ -25%).

For VWF:Act peak levels, 24 (29%) and 33 (39%) of levels had AE values ≤ 0.1 IU/mL and ≤ 0.15 IU/mL, respectively. In the case of VWF:Act trough levels, 14 (23%) and 23 (37%) of levels had AE values ≤ of 0.05 IU/mL and ≤ of 0.1 IU/mL, respectively. No significant differences were found between patients with type 1 and type 2 VWD.

Factor VIII activity

The MPE for FVIII:C peak levels was 17% [6-29] (n=84) and for trough levels it was 21% [6-37] (n=62) (Table 4). Patients with type 2 VWD had significantly lower MPE compared to patients with type 1 VWD (14% [4-33] (n=40) versus 32% [20-42] (n=22); p=0.024). No significant difference was observed in the MPE between medical procedures with low and moderate bleeding risk.
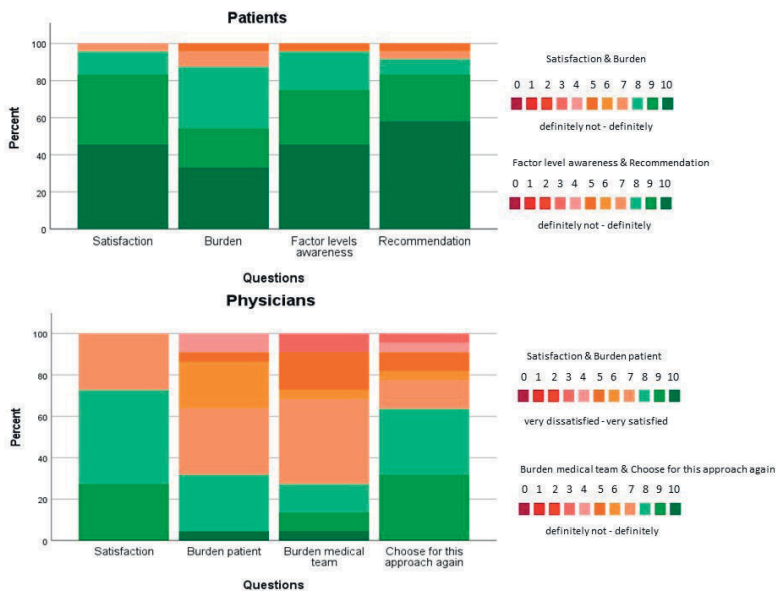
Figure 4: The outcome questionnaires for patients and physicians to assess the feasibility of PK-guided dosing. For patients, the questions focused on their satisfaction with PK-guided dosing, the burden it placed on them, the importance of knowing their factor levels during treatment and whether they would recommend PK-guided dosing to other patients. Physicians were asked about their satisfaction with PK-guided dosing, the burden for the medical team and the patient and whether they would choose for PK-guided dosing again. Responses were rated on a scale ranging from very dissatisfied (1-0) to very satisfied (10) with intermediate categories including dissatisfied (2-3), somewhat dissatisfied (4-5), somewhat satisfied (6-7), satisfied (8-9) and from definitely not (0-1) to definitely (9-10), with intermediate categories including probably not (2-4), neutral (5-6), probably yes (7-8).

The MAE for FVIII:C peak levels was 0.24 IU/mL [0.13-0.42] (n=84) and for FVIII:C trough levels it was 0.25 IU/mL [0.11-0.41] (n=62). No significant difference was observed in the MAE between VWD types (Table 4). The MAE for FVIII:C peak levels was significantly lower in patients undergoing medical procedures with low bleeding risk compared to those with moderate bleeding risk (0.17 [0.08-0.30] and 0.29 [0.14-52], respectively; p=0.03).

Overall, focusing on FVIII:C levels, 124 (61%) were within ± 25% between predicted and measured levels. Among FVIII:C peak levels, 55 (66%) levels were within this range and 35 (56%) of trough levels also fell within this range (Figure 3). For peak levels, 27 (32%) were above this range (≥ +25%) and two (2%) levels were below this range (≤ -25%). For trough levels, 26 (42%) were above this range (≥ +25%) and one (2%) level was below this range (≤ -25%).

For FVIII:C peak levels, 17 (20%) and 30 (36%) of levels had AE values ≤ 0.1 IU/mL and ≤ 0.15 IU/mL, respectively. In case of FVIII:C trough levels, 6 (10%) and 13 (21%) of levels had AE values ≤ of 0.05 IU/mL and ≤ of 0.1 IU/mL, respectively. No significant differences in MPE were observed between VWF:Act and FVIII:C. The MAE for VWF:Act level was significantly lower compared to MAE for FVIII:C level, which applies for peak (p=0.021) as well as trough (<0.001) levels.

PK-guided and body weight-based dosing

In 23 (79%) patients, information regarding the potential body weight-based dosage for the first infusion was available. The median differences between PK-guided and body weight-based dosing of the loading dose (the first infusion) was -3 IU/kg FVIII [-14-4], which was not significant (p=0.31). Four patients (17%) required similar doses, 12 (53%) patients required lower doses with PK guidance and seven (30%) patients needed higher doses with PK guidance when compared to body weight-based dosing. No significant differences were found between loading doses in patients with type 1 and 2 VWD based on body weight-based and PK-guided dosing.

Patients and treating physicians' satisfaction

Figure 4 shows the patient- and physician reported outcomes of the questionnaire regarding the feasibility and satisfaction with PK-guided dosing. Twenty-four (83%) patients completed the questionnaire and 23 (79%) physicians. All patients reported high satisfaction with PK-guided dosing, rating their satisfaction between 7 and 10 on a 10-point Likert scale. Physicians also reported high satisfaction, rating their satisfaction between 7 and 9. Regarding the study burden, patients were satisfied and scored between 7 and 10. Physicians were less satisfied, scoring between 4 to 10 score for the patient burden and reported varying scores regarding the burden on the medical team.

DISCUSSION

This prospective study reports promising results regarding the reliability and feasibility of PK-guided dosing in patients with VWD who require VWF/FVIII concentrate during medical procedures, by applying an individual PK profile and a previously developed PopPK model with iterative daily dosing adjustments.

The primary study outcome, i.e. reliability, was defined by predictive performance, assessed using PE (%) to define accuracy, and AE (IU/mL) to define precision between measured and predicted factor levels. Our results show that observed VWF:Act levels were underpredicted, as indicated by the positive PE and relatively accurate: VWF peak levels by 14 % [4-25] and VWF trough levels by 21% [2-38]. In the ideal situation PE is not significantly different from zero. However, the majority of VWF:Act levels, including 73% of peak VWF:Act levels and 55% of trough levels, were within ±25% prediction range. This chosen prediction range means that all levels within the range are acceptable and levels exceeding +25% indicate overtreatment and levels below -25% indicate undertreatment according to predefined levels set by treating physician, the majority according to guidelines. Importantly, only 1% of peak and 3% of trough levels were below -25%. These results are beneficial as this minimizes risk of undertreatment while increasing safety. Moreover, the choice of a ±25% prediction range is common practice to assess predictive performance and it aligns with the findings by Bukkems et al., where the residual error of the PopPK model was reported to be 27% for VWF:Act. Interestingly, this residual error reflects the variability caused by intra-patient PK and the imprecision of the applied assay[11]. The results in our study for FVIII:C levels are also more of less similar regarding underprediction and levels within ±25% prediction, although there were fewer FVIII:C levels within this range compared to VWF:Act levels. Additionally, undertreatment was also less common in our prospective study, with only 2% of both peak and trough FVIII:C levels below -25%.

Overall, underprediction and overprediction, i.e. lower predictive performance, could be explained by errors in Bayesian modeling in general, as well as discrepancies in data used to develop the PopPK model, such as differences in population and assays for VWF:Act and FVIII:C, for both peak and trough levels. Moreover, the applied PopPK model shows that VWF clearance decreases when procedures are of longer duration[11]. Since estimated duration was used for predictions, which in some cases was significantly different from the actual duration of the procedure, this discrepancy may have affected the predictions. This results in lower predictive performance, with VWF:Act levels typically underpredicted when the actual procedure duration is shorter than estimated.

Type 2 VWD patients had a significantly lower median PE for FVIII trough levels compared to type 1 VWD patients, indicating more accurate predictions for FVIII trough levels in type 2 (14% [4-33] versus 32% [20-42]). In contrast, type 1 patients had a significantly lower median AE for VWF:Act trough levels compared to type 2 VWD patients, suggesting higher imprecision of the predictions in type 2 VWD patients. These differences are difficult to explain but may be resolved by further refining the PopPK model with data from more patients.

Overall, the PE and AE of FVIII:C levels were slightly higher compared to those of VWF:Act levels, indicating lower predictive performance. The significantly higher MAE suggests lower precision, which could be attributed to the following factors. As known, FVIII:C levels depend on VWF levels. Although the PopPK model by Bukkems et al, described this VWF-FVIII interaction, predicting FVIII:C levels remain challenging due to these interactions. Additionally, in VWD patients, except for type 2N, endogenous FVIII is not directly affected and FVIII:C levels are able to increase due to stress, as experienced during medical procedures. This endogenous increase is difficult to predict.

In the retrospective study by Hazendonk et al. most observed VWF:Act and FVIII:C trough levels exceeded predefined target levels (≥ 0.20 IU/mL) in VWD patients undergoing medical procedures and receiving VWF/FVIII concentrate, which was dosed according to body weight[12]. Our approach resulted in fewer VWF:Act trough levels exceeding predefined target levels (40% for type 1 and 50% for type 2) compared to the findings reported by Hazendonk et al. (65% for type 1 and 53% in type 2). In contrast, all FVIII trough levels in our study exceed the predefined target level ≥ 0.20IU/mL, highlighting the challenge of predicting FVIII levels[12]. Notably, Hazendonk et al. included more patients with type 1 VWD and more major surgeries, therefore comparisons should be made with caution. Despite our approach leading to relatively fewer exceeding levels, there is still a high proportion of VWF and FVIII levels exceeding the predefined target levels (≥ 0.20 IU/mL), suggesting that the precision of our predictions is not yet sufficient. This issue could potentially be resolved by enriching the PopPK model with more data.

No major bleeding occurred and only four (14%) patients experienced minor bleeding. Furthermore, no thrombosis was diagnosed in our study population. Although FVIII:C trough levels (median 1.31 [1.11-1.91] were high in our study population, they did not reach extremely high levels. According to a systematic review, thrombosis due to factor concentrate treatment is rare (prevalence of 3.6 per 1000 patients) and typically associated with prolonged FVIII:C trough levels ≥2.00 IU/mL or with FVIII:C trough levels ≥1.50 IU/mL along with other thrombotic risk factor[13].

Regarding the feasibility of PK-guided dosing, both patients and physicians were satis-fied with this approach. Although treating physicians reported some concerns regard-ing the burden of PK guidance of dosing on patients and the medical team, the patients did not perceive the increased blood sampling as burdensome. Furthermore, PK-guided dosing showed no advantage of cost-reduction over body weight-based dosing for the loading dose. Due to our study design, only the loading dose could be compared. This aligns with the findings by van Moort et. al, which showed no lower consumption of FVIII concentrate in the PK-guided intervention arm compared to standard dose arm with body weight-based dosing in a randomized controlled trial[8]. Importantly, their findings are based on the FVIII consumption during the entire treatment period up to 14 days after initiation of replacement therapy.

Our study is not the first to examine the benefits of PK-guided dosing in VWD. However, our approach differs from that of Lethagen et al. and Di Paola et al. as we not only as-sessed a PK profile before the medical procedure to calculate the dosing regimen but also applied iterative daily dosing adjustments. This approach allowed us to optimize treatment and manage changes in the PK parameters of VWF and FVIII throughout the duration of treatment[6,7]. In addition to this strength, our study depicts a real-word condition with no restrictions regarding study population or medical procedure, making it easier to translate our findings into clinic practice.

Our study has some limitations. First, the PopPK model by Bukkems et al. primarily con-sisted of patients with type 1 and type 2A VWD, complicating predictions for other VWD types. However, due to the heterogeneous nature of VWD and low prevalence of sub-types within type 2 and type 3 VWD, it will always remain challenging to include enough representative patients. Therefore, we underline the importance of multicenter settings in such studies. Second, our results suggest that the clearance of VWF:Act declines over time during treatment. However the current PopPK model does not describe time dependent PK of VWF:Act and should therefore be refined. Third, due to the real-world setting of our study, missing data was inevitable, especially in the questionnaires. Finally, although patients were satisfied with PK-guided dosing and did not report burdened by blood sampling, the results could be biased as the study likely included patients less affected by frequent blood sampling. The requirement for a prior PK profile is especially burdensome. Although this PK profile is essential to calculate PK parameters, it should also be practical and patient friendly to minimize the number of blood samples needed. Future studies should focus on this.

In conclusion, the study results show that the predictive performance of a PK-guided approach for the treatment of VWD patients undergoing medical procedures with a spe-

cific VWF/FVIII concentrate is reliable, mainly demonstrating underprediction, making it clinically safe. Further data collection within this ongoing prospective study will lead to the enrichment of existing PopPK model, further improving the precision of predictions as well as construction of PopPK models for other VWF containing concentrates.

7

REFERENCES

1. Rodeghiero, F., Castaman, G., & Dini, E. (1987). Epidemiological Investigation of Rodeghiero, F., Castaman, G., & Dini, E. (1987). Epidemiological Investigation of the Prevalence of von Willebrand's Disease. Blood, 69(2), 454-459. https://doi.org/https://doi.org/10.1182/blood.V69.2.454.454

2. Sadler, J. E., Budde, U., Eikenboom, J. C. J., Favaloro, E. J., Hill, F. G. H., Holmberg, L., Ingerslev, J., Lee, C. A., Lillicrap, D., Mannucci, P. M., Mazurier, C., Meyer, D., Nichols, W. L., Nishino, M., Peake, I. R., Rodeghiero, F., Schneppenheim, R., Ruggeri, Z. M., Srivastava, A., . . . The Working Party On Von Willebrand Disease, C. (2006). Update on the pathophysiology and classification of von Willebrand disease: a report of the Subcommittee on von Willebrand Factor. Journal of Thrombosis and Haemostasis, 4(10), 2103-2114. https://doi.org/https://doi.org/10.1111/j.1538-7836.2006.02146.x

3. Leebeek, F. W., & Eikenboom, J. C. (2016). Von Willebrand's Disease. N Engl J Med, 375(21), 2067-2080. https://doi.org/10.1056/NEJMra1601561

4. Heijdra, J. M., Atiq, F., Al Arashi, W., Kieboom, Q., Wuijster, E., Meijer, K., Kruip, M., Leebeek, F. W. G., Cnossen, M. H., & Group, O. C. S. (2022). Desmopressin testing in von Willebrand disease: Lowering the burden. Res Pract Thromb Haemost, 6(6), e12784.

5. Heijdra, J. M., Cnossen, M. H., & Leebeek, F. W. G. (2017). Current and Emerging Options for the Management of Inherited von Willebrand Disease. Drugs, 77(14), 1531-1547. https://www.ncbi.nlm.nih.gov/pmc/articles/PMC5585291/pdf/40265_2017_Article_793.pdf

6. Lethagen, S., Kyrle, P. A., Castaman, G., Haertel, S., Mannucci, P. M., & Group, H. P. S. S. (2007). von Willebrand factor/factor VIII concentrate (Haemate P) dosing based on pharmacokinetics: a prospective multicenter trial in elective surgery. J Thromb Haemost, 5(7), 1420-1430.

7. Di Paola, J., Lethagen, S., Gill, J., Mannucci, P., Manco-Johnson, M., Bernstein, J., Nichols, W. L., & Bergman, G. E. (2011). Presurgical pharmacokinetic analysis of a von Willebrand factor/factor VIII (VWF/FVIII) concentrate in patients with von Willebrand's disease (VWD) has limited value in dosing for surgery. Haemophilia, 17(5), 752-758.

8. van Moort, I., Preijers, T., Bukkems, L. H., Hazendonk, H., van der Bom, J. G., Laros-van Gorkom, B. A. P., Beckers, E. A. M., Nieuwenhuizen, L., van der Meer, F. J. M., Ypma, P., Coppens, M., Fijnvandraat, K., Schutgens, R. E. G., Meijer, K., Leebeek, F. W. G., Mathôt, R. A. A., Cnossen, M. H., & group, O.-C. s. (2021). Perioperative pharmacokinetic-guided factor VIII concentrate dosing in haemophilia (OPTI-CLOT trial): an open-label, multicentre, randomised, controlled trial. Lancet Haematol, 8(7), e492-e502.

9. Heijdra, J. M., Al Arashi, W., de Jager, N. C. B., Cloesmeijer, M. E., Bukkems, L. H., Zwaan, C. M., Leebeek, F. W. G., Mathôt, R. A. A., Cnossen, M. H., & Group, O.-C. S. (2022). Is pharmacokinetic-guided dosing of desmopressin and von Willebrand factor-containing concentrates in individuals with von Willebrand disease or low von Willebrand factor reliable and feasible? A protocol for a multicentre, non-randomised, open label cohort trial, the OPTI-CLOT: to WiN study. BMJ Open, 12(2), e049493.

10. Koshy, M., Weiner, S. J., Miller, S. T., Sleeper, L. A., Vichinsky, E., Brown, A. K., Khakoo, Y., & Kinney, T. R. (1995). Surgery and anesthesia in sickle cell disease. Cooperative Study of Sickle Cell Diseases. Blood, 86(10), 3676-3684.

11. Bukkems, L. H., Heijdra, J. M., de Jager, N. C. B., Hazendonk, H., Fijnvandraat, K., Meijer, K., Eikenboom, J. C. J., Laros-van Gorkom, B. A. P., Leebeek, F. W. G., Cnossen, M. H., & Mathôt, R. A. A. (2021). Population pharmacokinetics of the von Willebrand factor-factor VIII interaction in patients with von Willebrand disease. Blood Adv, 5(5), 1513-1522.

12.   Coppola, A., Franchini, M., Makris, M., Santagostino, E., Di Minno, G., & Mannucci, P. M. (2012). Thrombotic adverse events to coagulation factor concentrates for treatment of patients with haemophilia and von Willebrand disease: a systematic review of prospective studies. Haemophilia, 18(3), e173-e187. https://doi.org/https://doi.org/10.1111/j.1365-2516.2012.02758.x

13.   Hazendonk HCAM, Heijdra JM, de Jager NCB, Veerman HC, Boender J, van Moort I, Mathôt RAA, Meijer K, Laros-van Gorkom BAP, Eikenboom J, Fijnvandraat K, Leebeek FWG, Cnossen MH; "OPTI-CLOT" and "WIN" study group. Analysis of current perioperative management with Haemate® P/Humate P® in von Willebrand disease: Identifying the need for personalized treatment. Haemophilia. 2018 May;24(3):460-470. doi: 10.1111/hae.13451.

7

CHAPTER 8

A novel population pharmacokinetic model for the von Willebrand factor-factor VIII interaction for von Willebrand patients requiring replacement therapy for medical procedures

M.E. Cloesmeijer, W. Al Arashi, J.M. Heijdra, F. W.G. Leebeek, L. Nieuwhuizen, F.C.J.I. Moenen, K. Meijer, M.H. Cnossen[*] and R.A.A. Mathôt[*]

*Both are last authors

ABSTRACT

Aims

During a medical procedure, von Willebrand disease (VWD) patients can be treated with von Willebrand factor (VWF)/factor VIII (FVIII) concentrate(s) to protect patients from bleeding. Previously, a population pharmacokinetic (PK) model was developed that described the PK of VWF: Activity (VWF:Act) and FVIII after infusion of Haemate P® in a medical procedure setting. The aim of this study was to validate this model and update the PK parameters using new independent data.

Methods

Data were obtained from the prospective OPTICLOT/ To WiN study, in which VWF/FVIII-concentrate (Haemate P®) doses were iteratively adjusted on basis of the observed VWF:Act and FVIII activity levels peri-operatively. The predictive performance of the previously reported model was assessed by calculating the median prediction error (MPE) and median absolute prediction error (MAPE) to determine bias and precision. Moreover, the predictive performance was assessed using prediction-corrected visual predictive check (pcVPC) and goodness-of-fit(GOF) plots. Subsequently, a new population PK model was developed by using nonlinear mixed-effects modelling (NONMEM).

Results

Thirty patients were enrolled in the OPTICLOT/ To WiN study. A total of 702 (350 VWF:Act and 352 FVIII) samples were available for analysis. First, we assessed the predictive performance of a previously developed population PK model for the observed VWF:Act and FVIII levels. The MPE for VWF:Act and FVIII was respectively, -15.1% and -9.62%, while the MAPE for VWF:Act and FVIII was respectively, 41.1% and 31.7%. Based on the outcomes of the pcVPC, GOF plots and MPE and MPE, there was room for model improvement. In the new model activity versus time profiles were adequately described. During the medical procedure, VWF:Act CL declined over time from a typical value of 513 mL/h/70 kg to 297 mL/h/70 kg at 48 hours post-treatment initiation; inter-individual variability was 49%. Increased VWF:Act levels were associated with reduced FVIII CL. This phenomenon was described with an inhibitory maximum effect model, identifying a half-maximum effect at 0.90 IU/mL VWF:Act. This interaction notably decreases FVIII CL from 513 to 257 mL/h/70kg.

Conclusion

In this study, a previously developed population PK model for VWF:Act and FVIII was tested and updated. The updated model adequately described the time dependent PK of VWF:Act and the effect of VWF:Act on FVIII PK. The new model allows individualization of dosing regimens and thereby potentially enhances treatment efficacy.

INTRODUCTION

Von Willebrand disease (VWD)is an inherited bleeding disorder characterized by quantitative or qualitative defects in von Willebrand factor (VWF), a protein that plays a crucial role in primary hemostasis and platelet adhesion to injured blood vessel walls[1]. Patients with VWD experience bleeding due to a deficiency or dysfunction of VWF, which results in defects in primary hemostasis since VWF is essential for platelet adhesion and aggregation. VWF also acts as a carrier protein for FVIII, protecting it from degradation in circulation and therefore increasing its half-life. Deficiencies and defects in VWF lead to impaired platelet plug formation. VWD is divided into different subtypes[2]. Type 1 is characterized by a partial quantitative deficiency of VWF, while type 2 (A, B, M, N) demonstrate qualitative defects in VWF function. Lastly, in type 3 a severe deficiency or absence of VWF is observed.

The dynamic interplay between von VWF:Act and FVIII levels plays a critical role in maintaining hemostasis, both to mediate platelet adhesion to sites of vascular injury[3] and to stabilize FVIII presence. Given the complexity of these interactions and the variability in patient responses, understanding the pharmacokinetics (PK) of VWF:Act and FVIII, including factors influencing their clearance (CL), becomes imperative to optimize treatment strategies. Bukkems et al. previously developed a VWF-FVIII interaction population PK model during medical procedures, focusing on the administration of VWF-FVIII concentrate (Haemate P®)[4]. Their study, however, exclusively used retrospective data from historical medical procedures. We aimed to construct a new VWF-FVIII interaction population PK model based on newly acquired prospective data, including data from both pre- and post-procedure phases. Our aim is to enhance predictive accuracy and describe the dynamics of VWF and FVIII interactions in patients with VWD across various clinical scenarios.

METHODS

Patients

Data of patients diagnosed with VWD or low VWF (historically lowest VWF antigen or VWF activity level of 0.30–0.50 IU/mL) were selected from the OPTI-CLOT: To WiN study This is a multicenter, multi-arm procedure, non-randomized, open label intervention study[5]. which is described extensively in an earlier publication. The study was approved by the Medical Ethics Committee of the Erasmus MC, University Medical Center Rotterdam, the Netherlands, and and to EudraCT with number 2018-001631-46. The study was conducted according to good clinical practice guidelines and the Declaration of

Helsinki, and in accordance with the Dutch Medical Research Involving Humans Act. All patients provided written informed consent[5].

Data from 30 patients participating in Arm B of the OPTI-CLOT: To WiN trial was used. All patients underwent varying medical procedures requiring treatment with VWF/FVIII-containing concentrate to prevent bleeding. Patients were recruited from Hemophilia Treatment Centers in the Netherlands between April 1st 2019 and July 1st 2023. In the pre-medical procedure, patients received a test dose of VWF/FVIII-containing concentrate to establish the individual PK profile. Blood sampling for VWF:Act and FVIII was performed before the administration of the VWF/FVIII-containing concentrate to determine endogenous VWF:Act and FVIII baseline. Afterwards, samples were taken approximately 10 minutes, 2-6 hours, 24 hours and 48 after administration. On the day of the medical procedure, samples were collected prior to treatment administration. Following treatment administration, samples were immediately obtained to assess peak VWF/FVIII levels, and another sample was collected after finalization of the medical procedure. If patients required treatment with VWF/FVIII-containing concentrate for multiple days after the procedure, additional samples were taken before and after each administration of the treatment during the course of the treatment.

Predictive performance and population modelling

This prospectively collected data was used to investigate the predictive performance of a previously developed model by Bukkems et al. In NONMEM software (7.4., ICON, Hanover, MD, United States)[6] the option MAXEVAL=0 was used to obtain population and individual Bayesian predictions (goodness of fit (GOF) plots). These predictions were plotted versus the observed activity levels. Furthermore, a prediction corrected visual predictive check (pcVPC) was performed. The predictive performance of the previously reported model by Bukkems et al. was also assessed by calculating the median prediction error (MPE) (equation 1) and median absolute prediction error (MAPE) (equation 2) to determine bias and precision. With an acceptable MPE of +/- 20% and a MAPE of less than 30%[18].

$$PE\ (\%) = \frac{C_{observation} - C_{prediction}}{C_{prediction}} \times 100\ \%$$

(Equation 1)

(Equation 2)

$$MAPE\ (\%) = median\ of\ |PE|$$

A novel population PK model was developed using prospective data. The population PK model was developed in NONMEM software as well and further evaluated using PsN and R studio[7,8]. Development of the model was performed in three steps (i) a structural model including inter-individual variability, (ii) residual error model and (iii) covariate analysis.

Details of model development are provided in the supplementary files. Turnover models were used to describe the change of endogenous of VWF:Act and FVIII levels over time. First, separate models of VWF:Act and FVIII were developed, afterwards the models were combined and the interaction between VWF:Act and FVIII was modelled. An inhibitory maximal effect (I_{max}) function of VWF:Act levels on the FVIII CL was included. This function was used to describe the decrease of FVIII CL with higher levels of VWF:Act.

Model evaluation

Goodness of fit (GOF) plots were applied to evaluate the performance of all models. The precision of the parameter estimates was expressed as relative standard error (RSE %) and confidence intervals (CI). A RSE value < 30% for fixed effects and < 50% for random effects were considered acceptable[9]. For assessment of the robustness of the parameter estimates a bootstrap using 1000 new data sets from the original dataset was used. Moreover, prediction-corrected visual predictive checks (pcVPC) were performed.

Simulations

Simulations were performed based on the final PK model to evaluate the clinical significance of time-dependent CL on the levels of VWF:Act and FVIII and FVIII CL dependency on VWF:Act. The aim was to maintain VWF:Act levels above 0.50 IU/mL during the initial three days post medical procedure[10]. For these simulations, a typical patient profile of VWD type 2A from the population PK model was selected. The typical patient had a VWF:Act baseline of 0.14 IU/mL and body weight of 70 kg.

8

RESULTS

Data from 30 patients were available of which characteristics are displayed in Table 1. Seven males and 23 females were included, the median age was 63 years (interquartile range (IQR) 49 – 69), body weight 73 kg (68 – 83). Most patients had type 1 VWD (n=11), followed by type 2A (n=11), 2B (n=4), 2M (n=2), 2N (n=1) and type 3 VWD (n=1).

Predictive performance

In our study, a total of 702 samples were collected, with 298 samples taken before the medical procedure (pre-procedure) and 404 samples taken post-procedure. All samples were above the limit of quantification of the assays. Our initial analysis focused on assessing the predictive performance of a previously developed population PK model for VWF:Act and FVIII levels. We performed a pcVPCs using both data pre- and post-medical procedure. In supplementary figure 1 the pcVPCs of pre-medical procedure are displayed. We observed that 95th and median percentiles of the observed data do

Table 1. Patient characteristics

Characteristic	N=30 Number or median (interquartile range)	Range
Male/female	7/23	
Age, years	63 (48 – 69)	28 – 79
Body weight, kg	73 (68 – 83)	55 – 119
Von Willebrand disease type		
Type 1	11	
Type 2A,B M, N	11, 4, 2, 1	
Type 3	1	
Lowest VWF:Act, IU/mL	0.11 (0.07 – 0.18)	0.04 – 0.90
Lowest FVIII, IU/mL	0.30 (0.16 – 0.46)	0.06 – 0.97
Endogenous baseline VWF:Act, IU/mL	0.17 (0.08 – 0.32)	0.04 – 1.89
Endogenous baseline FVIII, IU/mL	0.58 (0.30 – 0.85)	0.08 – 1.43
Surgery information		
No. of surgeries	30	
Duration of surgery, min	52.5 (30 – 90)	5 – 240
Severity of surgery		
Minor	18	
Major	12	
ASA classification		
I	7	
II	20	
III	3	
Dose information		
FVIII dose in IU/kg during PK profile	25 (24 – 26)	20 – 56
FVIII dose in IU/kg during perioperative setting	31 (24 – 48)	12 – 63

not fall within the prediction areas for both VWF:Act and FVIII. This suggests that the model does not accurately capture the variability of the data for the pre- procedure circumstances. In supplementary figure 2 the pcVPCs of the for the of post- procedure phase are displayed. Again, the 95th and median percentiles of the observed data are outside the prediction area for VWF:Act, whereas for FVIII the observed data are mostly within the prediction area. This indicates better model alignment with observed data post-procedure for FVIII but not for VWF:Act. Importantly, despite the discrepancies noted above, most of all observed data fall within the prediction areas. Supplementary figures 3 and 4 display the GOF plots, also using both pre- and post- procedure data.

Moreover, the MPE for VWF:Act and FVIII was respectively, -15.1% and -9.62%, while the MAPE for VWF:Act and FVIII was respectively, 41.1% and 31.7%. While the bias is

acceptable with less than +/- 20%, the precision is not acceptable, as the precision is above 30%. Thus, the outcomes of the pcVPCs, GOF plots, MPE and MAPE indicate there is room for model refinement or adjustment, especially to better capture the dynamics of VWF:Act across different conditions and improve the fit for FVIII pre-procedure.

Development of a new population PK model

A novel population PK model was developed, describing VWF:Act and FVIII levels using both data pre- and post-medical procedures. A schematic overview of the models is displayed in figure 1. A two-compartment model was the best fit for VWF:Act, whereas a one-compartment model was found to be the best fit for FVIII levels. Key to both models was the application of a turnover model, which was used to describe the endogenous levels of VWF:Act and FVIII in each patient. A turnover model describes the dynamic process of synthesis, distribution, and elimination of a VWF:Act and FVIII within the body. It accounts for the rates at which the VWF:Act and FVIII is produced and cleared. On both VWF:Act and FVIII, IIV was included in on the CL, central volume of distribution (V1) and the baseline levels.

Following the development of the novel PK model for VWF:Act and FVIII, the relationship between VWF:Act levels and CL of FVIII was further explored to understand the dynamic interplay between these factors. An inhibitory maximum effect (I_{max}) model was used to quantify the influence of VWF:Act levels on FVIII CL. This inclusion led to a significant improvement in model performance ($p < 0.01$). The analysis revealed that at a VWF:Act level of 0.90 IU/mL, the half-maximum effect (IC_{50}) of the inhibitory effect on FVIII CL was achieved. This interaction was further characterized by a marked reduction in FVIII CL, from an initial rate of 513 mL/h/70kg with a (virtual) VWF:Act level of 0 IU/mL to 257 mL/h/70 kg, upon achieving the IC_{50} VWF:Act level of 0.90 IU/mL. This finding dem-
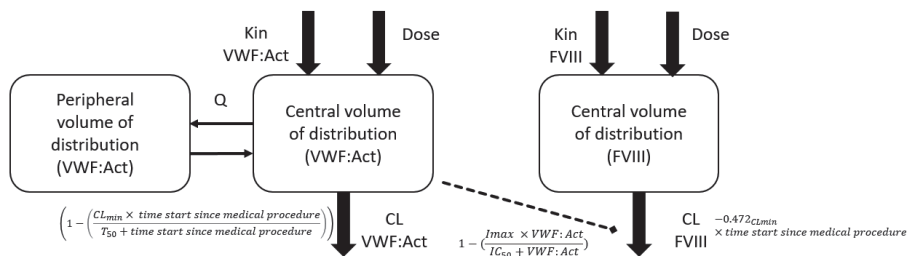
8

Figure 1. Schematic overview of the population pharmacokinetic model describing the interaction between von Willebrand factor activity (VWF:Act) and factor VIII (FVIII) and the time dependent CL functions on VWF:Act and FVIII. An Imax function was used to describe the inhibitory effect of the VWF:Act levels on the clearance of FVIII. CL: clearance, Kin: zero-order production rate of endogenous VWF:Act or FVIII, Q: inter-compartmental clearance.

onstrates a substantial decrease in FVIII CL as a function of increasing VWF:Act levels, highlighting the critical influence of VWF:Act on the CL of FVIII.

Covariate analysis

During the medical procedure, the CL of VWF:Act decreased non-linearly over time. The time-dependent CL was modelled by a sigmoid Imax function. A typical CL was estimated to be 513 mL/h/70 kg, and this CL decreased further over time. After 24- and 48-hours treatment initiation, the CL was approximately 328 and 297 mL/h/70 kg, respectively. Even with the inhibitory model of VWF:Act on FVIII CL, the CL of FVIII continued to decrease over time, following a linear trend post-medical procedure. This decrease in FVIII CL occurred independently of the VWF:Act levels, indicating that the reduction in CL was consistent regardless of the presence or absence of VWF:Act. A sigmoid function was also tested, but did not result in a significantly better model fit. CL decreased linearly with 0.475 mL/h/70kg per hour. At the start of the medical procedure, the typical FVIII CL is 476 mL/h/70 kg, While the FVIII CL 24 hours after treatment initiation is approximately 465 mL/h/70 kg (approximately 3% lower). This CL continues to decrease over time, with the value further reducing to approximately 453 mL/h/70 kg (approximately 5% lower) 48-hour post-treatment initiation. All the aforementioned FVIII CL values were calculated in the absence of VWF:Act levels. IIV was also tested on the time-dependent CL parameters (CL_{min}) for both VWF:Act and FVIII, but this resulted in large shrinkage or imprecise parameter estimations. The time-dependent CL of VWF:Act and FVIII during medical procedure is illustrated in supplement figure 5.

In the covariate analysis, VWD type was identified as a significant covariate affecting the baseline von Willebrand Factor Activity (VWF:Act). For type 1 VWD patients and type 2N, the typical baseline VWF:Act was estimated to be 0.388 IU/mL. However, for individuals with VWD types 2A, 2B, and 2M, the baseline VWF:Act was estimated to be 0.14 IU/mL, while for VWD type 3 the VWF:Act baseline was 0.0981 IU/mL.

The GOF plots of the final model demonstrate that the model describes VWF:Act and FVIII levels adequately (Figure 2 and 3). The pcVPC shows similar adequate model performance (Figure 4). Finally, the estimates and 95% confidence intervals of the bootstrap confirm robustness of the model (Table 2).

Simulations to illustrate the clinical relevancy of time-dependent clearance

Simulations were performed to evaluate the clinical significance of time-dependent CL on the levels of VWF:Act and FVIII. For these simulations, a typical patient profile from the population PK model was selected. The results are presented in figure 5. In the set-
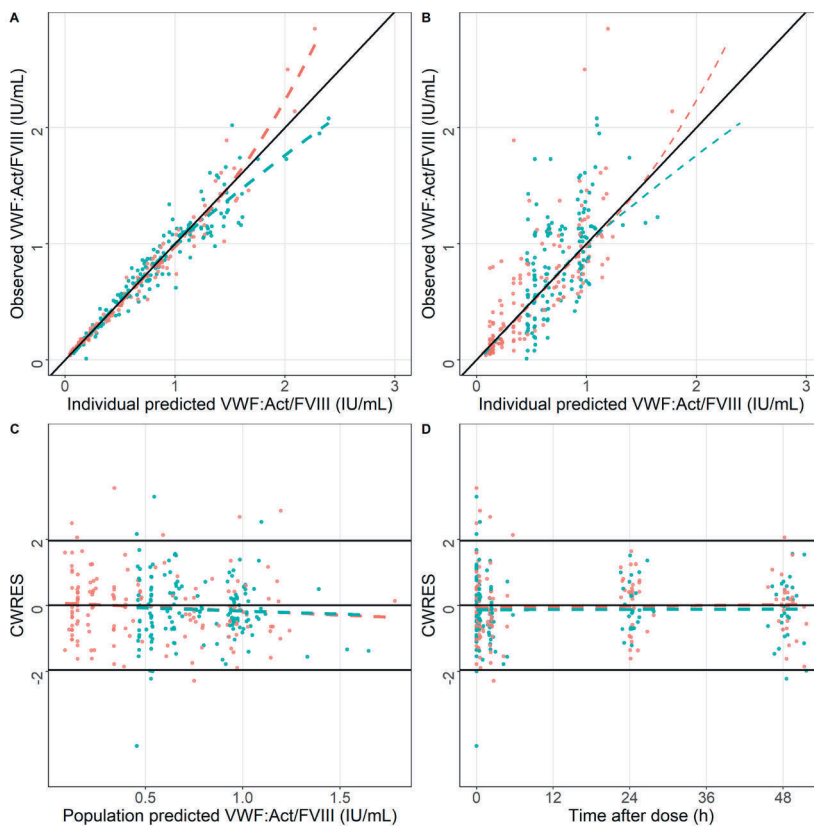
Figure 2. Goodness-of-fit (GOF) plots of the final interaction pharmacokinetic model of von Willebrand factor activity (VWF:Act) and factor VIII (FVIII) before medical procedure. Red dots represent VWF:Act, blue dots represent FVIII. A) Individual predicted (IPRED) vs observed concentrations, B) Population predicted (PRED) vs observed concentrations, C) Conditional weighted residuals (CWRES) vs PRED, D and H) Time after administration vs CWRES. The solid line is the line of identity. The dashed line represents the loess smooth line.

ting observed pre-medical procedure, depicted in Figure 5A, an initial dose of 2500 IU was administered at T=0 hours, followed by additional 1750 IU doses every 12 hours up to T=60 hours. This regimen maintained VWF:Act trough levels at 0.51, 0.52, and 0.52 IU/mL at T=24, 48, and 72 hours, respectively, for the typical patient. Conversely, figure 5B illustrates the time period while the medical procedure was ongoing where a time-dependent decrease in CL was incorporated in the model. Using the same dosing scheme, VWF:Act trough levels increased to 0.69, 0.88, and 0.98 IU/mL at T=24, 48, and 72 hours, respectively, indicating VWF accumulation due to reduced CL over time. This suggests that a reduced dosage could achieve the target VWF:Act levels of >0.50 IU/mL, as shown in figure 5c. Here, an initial dose of 2500 IU was followed by 1000 IU doses at T=12 and 24 hours, and 750 IU doses at T=36, 48, and 60 hours, achieving VWF:Act trough levels of 0.54, 0.53, and 0.53 IU/mL at T=24, 48, and 72 hours, respectively.

Table 2: Final population pharmacokinetic parameter estimates and bootstrap results

Parameter	Final model estimations (RSE%) [Shrinkage %]	Bootstrap Medan value [95% CI]
CL VWF:Act (L/h/70 kg)	513 (10)	513 [422 – 630]
V1 VWF:Act (L/70 kg)	4820 (5)	4774 [4307 – 5246]
Q VWF:Act (L/h/70 kg)	667 (41)	697 [177 – 1655]
V2 VWF:Act (L/h/70 kg)	998 (28)	1026 [598 – 2024]
Baseline VWF:Act VWD type 1 and 2N (IU/mL)	0.387 (14)	0.383 [0.306 – 0.500]
CL FVIII (L/h/70 kg)	476 (30)	489 [306 – 820]
V1 FVIII (L/h/70 kg)	3470 (6)	3433 [3150 – 3844]
Baseline FVIII (IU/mL)	0.441 (15)	0.443 [0.336 – 0.569]
IC50 VWF:Act (IU/mL)	0.900 (35)	0.914 [0.478 – 1.62]
Covariates		
Baseline VWF:Act VWD type 2A, B, M	0.140 (18)	0.358 [0.254 – 0.534]
Baseline VWF:Act VWD type 3 on	0.0981 (23)	0.254 [0.166 – 0.317]
CL_{min} VWF:Act (during medical procedure)	0.511 (7)	0.510 [0.443 – 0.592]
T_{50} of CL_{min} VWF:Act (h)	10.1 (35)	9.70 [1.58 – 16.5]
Decrease CL FVIII per hour (during medical procedure)	-0.472 (44)	-0.482 [-0.994 to -0.106]
Inter-individual variability (CV%)		
VWF:Act CL	49.2 (14) [5]	47.6 [31.7 – 66.5]
VWF:Act V1	30.6 (23) [4]	28.9 [17.4 – 43.9]
VWF:Act baseline	82.7 (12) [0]	79.9 [56.5 – 110]
FVIII CL	73.4 (19) [9]	75.8 [46.1 – 131]
FVIII V1	13.9 (25) [36]	13.0 [5.06 – 20.0]
FVIII baseline	59.8 (2) [0]	57.8 [35.6 – 83.3]
Correlation inter-individual variability CL – V1 VWF:Act	76.1	
Correlation inter-individual variability baseline VWF:Act – CL FVIII	78.9	
Residual variability		
Proportional error VWF:Act (%)	13.4 (9)	13.2 [11.0 – 15.7]
Proportional error FVIII (%)	17.6 (10)	17.2 [14.2 – 20.2]

CI: confidence interval, CL: clearance, CV: coefficient of variation calculated as $\sqrt{(e^{(\omega^2)}-1)} \times 100$, FVIII: factor VIII, RSE: relative standard error, V1: central volume of distribution, V2: peripheral volume of distribution, VWF:Act: von Willebrand factor activity, Q: intercompartmental clearance.

Applied formulas to calculate typical PK parameters

$$CL\ VWF = \theta_{cl} \times \left(\frac{Body\ weight}{70}\right)^{0.75} \times \left(1 - \left(\frac{CL_{min} \times time\ start\ since\ medical\ procedure}{T_{50} + time\ start\ since\ medical\ procedure}\right)\right);$$

$$V1\ VWF = \theta_V \times \left(\frac{Body\ weight}{70}\right)^1;$$

$$Q\ VWF = \theta_{CL} \times \left(\frac{Body\ weight}{70}\right)^{0.75};$$

$$V2\ VWF = \theta_V \times \left(\frac{Body\ weight}{70}\right)^1;$$

$$Baseline\ VWF\ VWD\ type\ 1\ and\ 2N = \theta_{Baseline\ VWD\ type\ 1\ and\ 2N};$$

$$Baseline\ VWF\ VWD\ type\ 2A,\ B\ and\ M = \theta_{Baseline\ VWD\ type\ 2A,B\ and\ M};$$

$$Baseline\ VWF\ VWD\ type\ 3 = \theta_{Baseline\ VWD\ type\ 3};$$

$$CL\ FVIII = \theta_{CL} \times \left(\frac{Body\ weight}{70}\right)^{0.75} - 0.472_{CLmin} \times time\ start\ since\ medical\ procedure;$$

$$V1\ FVIII = \theta_V \times \left(\frac{Body\ weight}{70}\right)^1;$$

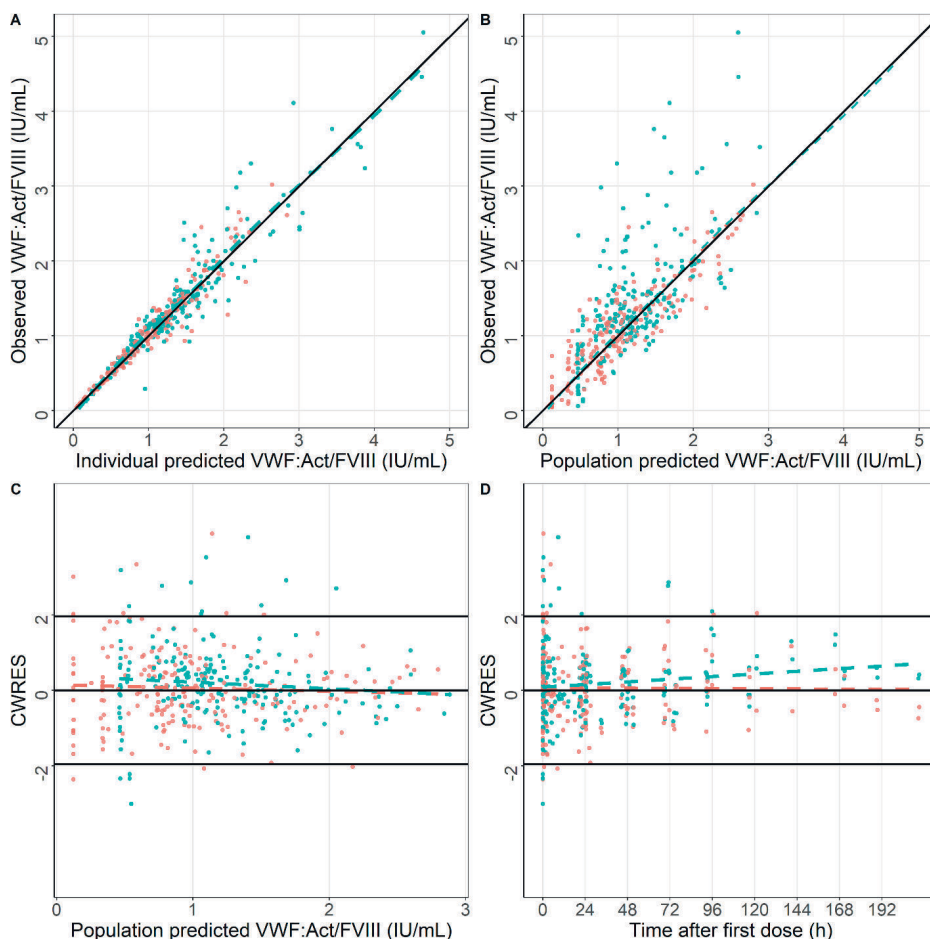$$Baseline\ FVIII = \theta_{Baseline\ FVIII}$$

Figure 3. Goodness-of-fit plots of the final interaction pharmacokinetic model of von Willebrand factor activity (VWF:Act) and factor VIII (FVIII) during/after medical procedure. Red dots represent VWF:Act, blue dots represent FVIII. A) Individual predicted (IPRED) vs observed concentrations, B) Population predicted (PRED) vs observed concentrations, C) Conditional weighted residuals (CWRES) vs PRED, D and H) Time after administration vs CWRES. The solid line is the line of identity. The dashed line represents the loess smooth line.

Figure 5 also explores the impact of time-dependent CL on FVIII levels. In the setting pre-medical procedure was initiated (figure 5A), FVIII trough levels remained relatively stable throughout the following days, averaging about 1.15 IU/mL. However, during the medical procedure with accounted time-dependent CL (figure 5B), FVIII trough levels began at 1.15 and rose to 1.54 IU/mL at T=24 and T=72 hours. When applying the adjusted lower dosing regimen during the medical procedure setting (figure 5C), simulated FVIII trough levels were lower, at 0.97, 0.94, and 0.91 IU/mL at T=24, 48, and 72 hours, respectively.
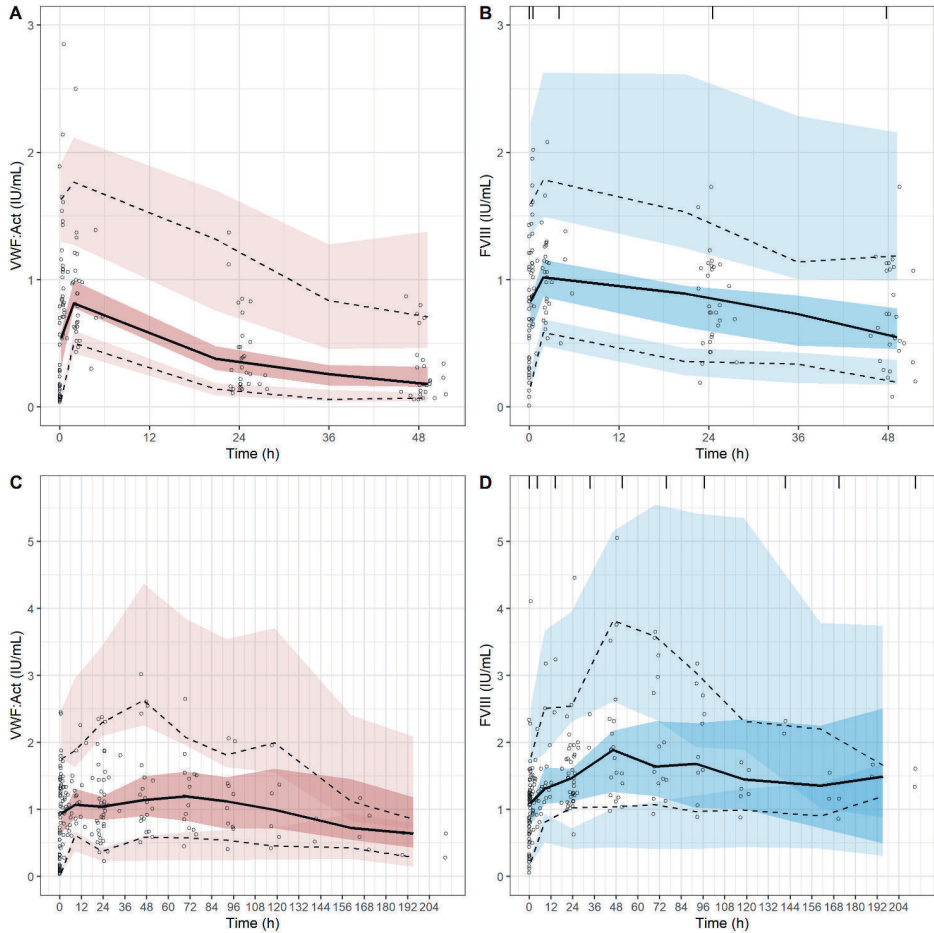
Figure 4. Prediction-corrected Visual Predictive Check (pcVPC) for von Willebrand factor activity (VWF:Act) and factor VIII (FVIII) of the novel population pharmacokinetic model. A and B) pcVPC of VWF:Act and FVIII levels before medical procedure. C and D) pcVPC of VWF:Act and FVIII levels during medical procedure. The solid lines represent the median and the 5th and 95th percentiles of the observed data, while the shaded areas show the 90% prediction intervals for the median and percentiles based on simulations from the final model. Circles represent individual observed data points.
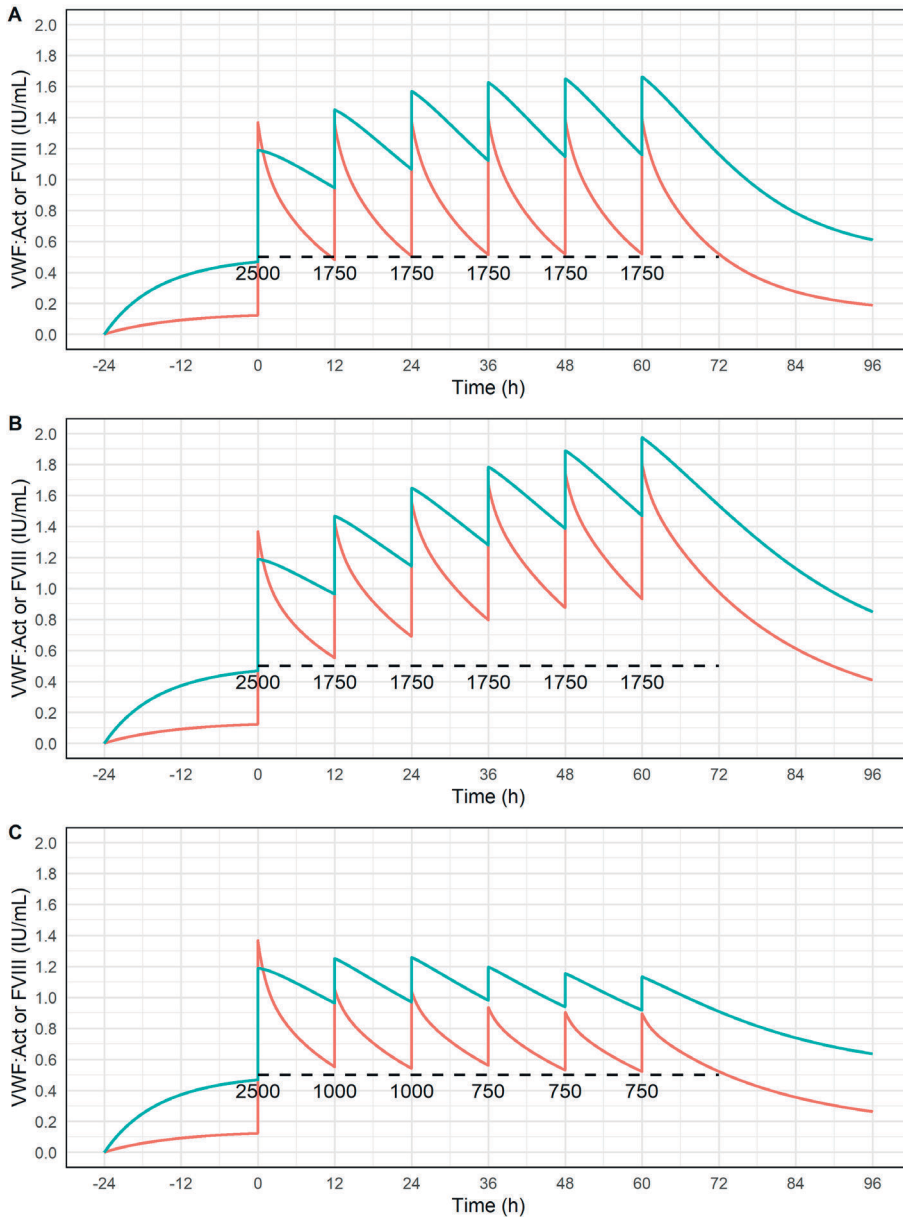
Figure 5. Impact of time-dependent clearance on von Willebrand factor activity (VWF:Act) and factor VIII (FVIII) levels. Simulations of a typical patient with von Willebrand disease were performed to illustrate the impact of time-dependent clearance on VWF:Act and FVIII levels. Red lines indicate the predictions for VWF:Act, while blue lines show the predictions for FVIII. Dashed horizontal lines indicate the target levels of >0.50 IU/mL for both VWF:Act and FVIII. Dosages administered in international units (IU) of FVIII are shown below these dashed lines. A) displays a typical simulated patient in the preoperative setting without time-dependent clearance effects on VWF:Act and FVIII. B) displays a typical simulated patient during medical procedure, incorporating time-dependent clearance effects on both factors. C) demonstrates that during medical procedure, achieving target levels (>0.50 IU/mL) required lower dosages compared to before medical procedure, based on simulations.

DISCUSSION

This study presents the development of a novel population PK model describing the complex interaction of VWF:Act and FVIII before and after a medical procedure, highlighting the significant dynamics in the CL of both coagulation factors especially during the post-procedure period. Notably, our findings reveal a discernible pattern of (non)-linear reduction in the CL of VWF:Act and FVIII over time in the post-medical procedure setting, a phenomenon not observed in the pre-medical procedure phase. This suggests a potential for reduction of this specific VWF-FVIII concentrate dosage while maintaining target levels, optimizing treatment and minimizing bleeding risks during medical procedures.

In the perioperative setting, our analyses revealed patterns of CL dynamics for VWF:Act and FVIII. While the CL of VWF:Act decreased non-linearly over time, following a sigmoidal pattern, the CL of FVIII exhibited a linear decrease. The clinical relevance of these findings lies in the impact on dosing regimens and treatment optimization. As the CL of VWF:Act and FVIII decrease over time, higher plasma levels of these factors are attained. Consequently, in patients receiving treatment with longer durations, lower dosages may be sufficient to achieve target plasma levels of VWF:Act and FVIII due to the prolonged presence of these factors resulting from the lower CL over time. This highlights the importance of considering the changes in CL dynamics when optimizing dosing strategies in the perioperative setting. Additionally, Hazendonk et al., observed an accumulation of VWF:Act and FVIII levels during medical procedures involving the use of the same VWF-FVIII concentrate (Haemate P®) as in our model in a retrospective study[11]. This accumulation aligns with our observation of a decreased CL of VWF:Act and FVIII in the perioperative setting. The study by Hazendonk et al. provides a valuable parallel to our current studies, reinforcing the concept that the CL of these coagulation factors undergoes significant alterations in response to therapeutic procedures. A reason for the decrease in CL over time could be due to saturation of CL pathways as FVIII and VWF are cleared from circulation through receptor-mediated pathways. For FVIII, the low-density lipoprotein receptor-related protein 1 (LRP1) plays a major role in the CL of FVIII, and it is also likely involved in the the CL of VWF:Act[12,13]. While ADAMTS13 is not a receptor but an enzyme, it is crucial for the cleavage of large VWF multimers in the circulation into smaller, less active forms[13]. The administration of Haemate P® may lead to a saturation of these CL pathways, particularly at higher or sustained levels. As the treatment continues and endogenous production is supplemented by the treatment, the CL pathways may become increasingly saturated, leading to a decrease in CL rates over time. The novel model underscores the clinical relevance of incorporating time-dependent CL in the PK of VWF:Act and FVIII, particularly in the perioperative setting. They suggest that dosage

adjustments based on dynamic CL changes can effectively maintain target factor levels, optimizing patient care while potentially reducing the risk of excessive coagulation factor accumulation. However, it may also be possible due to increase in endogenous productions of factor levels.

An additional critical consideration stemming from our findings, is the implication of sustained high levels of VWF:Act and FVIII. Prolonged levels (>2.50 IU/ml) of these factors can elevate the risk of thrombosis[14–16]. This potential for thrombotic complications highlights an essential advantage of reducing the dosage of VWF-FVIII concentrates in the perioperative setting. By optimizing the dosing regimen to maintain target levels without excessive accumulation, we not only preserve the therapeutic efficacy but also mitigate the thrombosis risk. Reducing thrombotic risk through dose adjustment could be important when incorporating PK insights into clinical decision-making processes.

Our study had some limitations. In the analysis, we integrated data from a previously developed model by Bukkems et al. into our analysis [data not shown]. The rationale behind this approach was to obtain a larger dataset encompassing a broader patient population, thereby enhancing the robustness and generalizability of the model. However, we encountered challenges during the model development process, when combining the data from the previous model with our current dataset. Despite efforts to integrate the datasets, the combined model was instable. This instability may be attributed to differences in data quality, study design, and patient characteristics between the two datasets. Notably as stated earlier, the dataset from the previous model comprised retrospective data, whereas our current dataset was derived from a prospective study. Prospective data collection offers several advantages, including standardized data collection protocols, more stringent quality control measures, ensuring data accuracy. In contrast, retrospective data may be subject to inherent limitations such as incomplete or inconsistent documentation, variability in data collection practices over time, and potential biases introduced during data extraction and analysis.

Secondly, the disparity in sample sizes between the two datasets also influenced the stability of the combined model. The previous dataset, which included 118 patients, provided a larger and more diverse sample compared to our current dataset, which comprised of only 30 patients. Consequently, PK parameter estimations tended to be biased towards the larger dataset, potentially overshadowing the contributions of our prospective data. Thirdly, there is an under-representation of certain VWD subtypes, specifically type 2B, 2N, 2M, and type 3, within our dataset. The scarcity of data on these subtypes in our model currently limits the applicability of our findings to the broader

8

VWD patient population. The absence of substantial data from these patient groups hampers our ability to fully understand the PK dynamics and treatment responses in these VWD subtypes. Lastly, the applicability of our model is specific to Haemate P®, which possesses a von VWF-FVIII ratio of 2.4:1. This specificity raises concerns about the management of prolonged high FVIII levels, a situation that might be inevitable due to its inclusion in VWF-FVIII concentrates, even for patients who already possess adequate endogenous FVIII levels. This characteristic of Haemate P® underscores a critical challenge in treatment strategies, particularly for individuals who might not require additional FVIII supplementation and demonstrate FVIII accumulation. Therefore, while Haemate P® is effective in addressing deficiencies of both VWF and FVIII, its fixed ratio presents a limitation that necessitates patient-specific management to mitigate the risk of inducing excessively high FVIII levels.

In conclusion, our study provides valuable insights into the PK of VWF:Act and FVIII by a novel model describing the interaction of VWF:Act and FVIII levels in pre- and post-medical procedure settings. The observed differences in PK pre- and post-medical procedure phases allow for iterative dose adjustments to individualize dosing regimens. However, this interim analysis shows that continued data collection is essential to further understand and anticipate the dynamics of replacement therapy in VWD patients. We believe this approach will facilitate optimized therapeutic strategies, enhancing treatment efficacy.
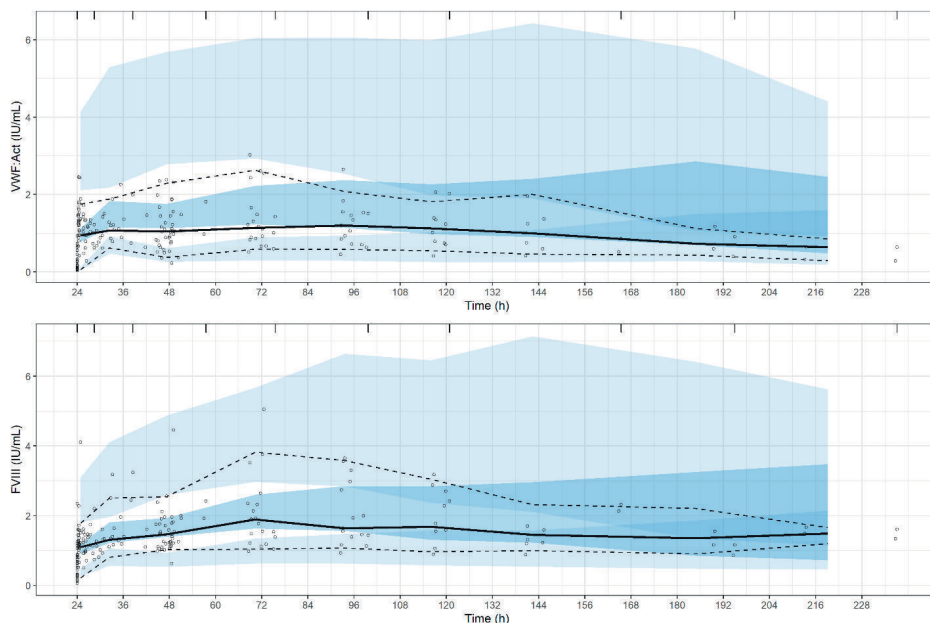
REFERENCES

1.   Leebeek FWG, Eikenboom JCJ. Von Willebrand's Disease. Longo DL, editor. *N Engl J Med*. 2016;375(21):2067-80.

2.   James PD, Connell NT, Ameer B, et al. ASH ISTH NHF WFH 2021 guidelines on the diagnosis of von Willebrand disease.*Blood Adv*. 2021;5(1):280-300.

3.   Kiouptsi K, Reinhardt C. Physiological Roles of the von Willebrand Factor-Factor VIII Interaction. *Subcell Biochem*. 2020;94:437-64.

4.   Bukkems LH, Heijdra JM, de Jager NCB, et al. Population pharmacokinetics of the von Willebrand factor-factor VIII interaction in patients with von Willebrand disease.*Blood Adv*. 2021;5(5).

5.   Heijdra JM, Al Arashi W, Cnossen MH, et al. Is pharmacokinetic-guided dosing of desmopressin and von Willebrand factor-containing concentrates in individuals with von Willebrand disease or low von Willebrand factor reliable and feasible? A protocol for a multicentre, non-randomised, open label coho.*BMJ Open*. 2022;12(2):1-6.

6.   Bauer RJ. NONMEM Tutorial Part I: Description of Commands and Options, With Simple Examples of Population Analysis.*CPT Pharmacometrics Syst Pharmacol*. 2019;8(8):525-37.

7.   Keizer RJ, Karlsson MO, Hooker A. Modeling and simulation workbench for NONMEM: Tutorial on Pirana, PsN, and Xpose.*CPT Pharmacometrics Syst Pharmacol*. 2013;2(6):1-9.

8.   Lindbom L, Ribbing J, Jonsson EN. Perl-speaks-NONMEM (PsN) - A Perl module for NONMEM related programming.*Comput Methods Programs Biomed*. 2004;75(2):85-94.

9.   Nguyen THT, Mouksassi MS, Holford N, et al. Model evaluation of continuous data pharmacometric models: Metrics and graphics.*CPT Pharmacometrics Syst Pharmacol*. 2017;6(2):87-109.

10.   Connell NT, Flood VH, Brignardello-Petersen R, et al. Ash isth nhf wfh 2021 guidelines on the management of von willebrand disease.*Blood Adv*. 2021;5(1):301-25.

11.   Hazendonk HCAM, Heijdra JM, de Jager NCB, et al. Analysis of current perioperative management with Haemate® P/Humate P® in von Willebrand disease: Identifying the need for personalized treatment.*Haemophilia*. 2018;24(3):460-70.

12.   Saenko EL, Yakhyaev A V., Mikhailenko I, et al. Role of the low density lipoprotein-related protein receptor in mediation of factor VIII catabolism.*J Biol Chem*. 1999;274(53):37685-92.

13.   Lenting PJ, Van Schooten CJM, Denis C V. Clearance mechanisms of von Willebrand factor and factor VIII.*J Thromb Haemost*. 2007;5(7):1353-60.

14.   Kamphuisen PW, Eikenboom JCJ, Rosendaal FR, et al. High factor VIII antigen levels increase the risk of venous thrombosis but are not associated with polymorphisms in the von Willebrand factor and factor VIII gene.*Br J Haematol*. 2001;115(1):156-58.

15.   Martinelli I. von Willebrand factor and factor VIII as risk factors for arterial and venous thrombosis. *Semin Hematol*. 2005;42(1):49-55.

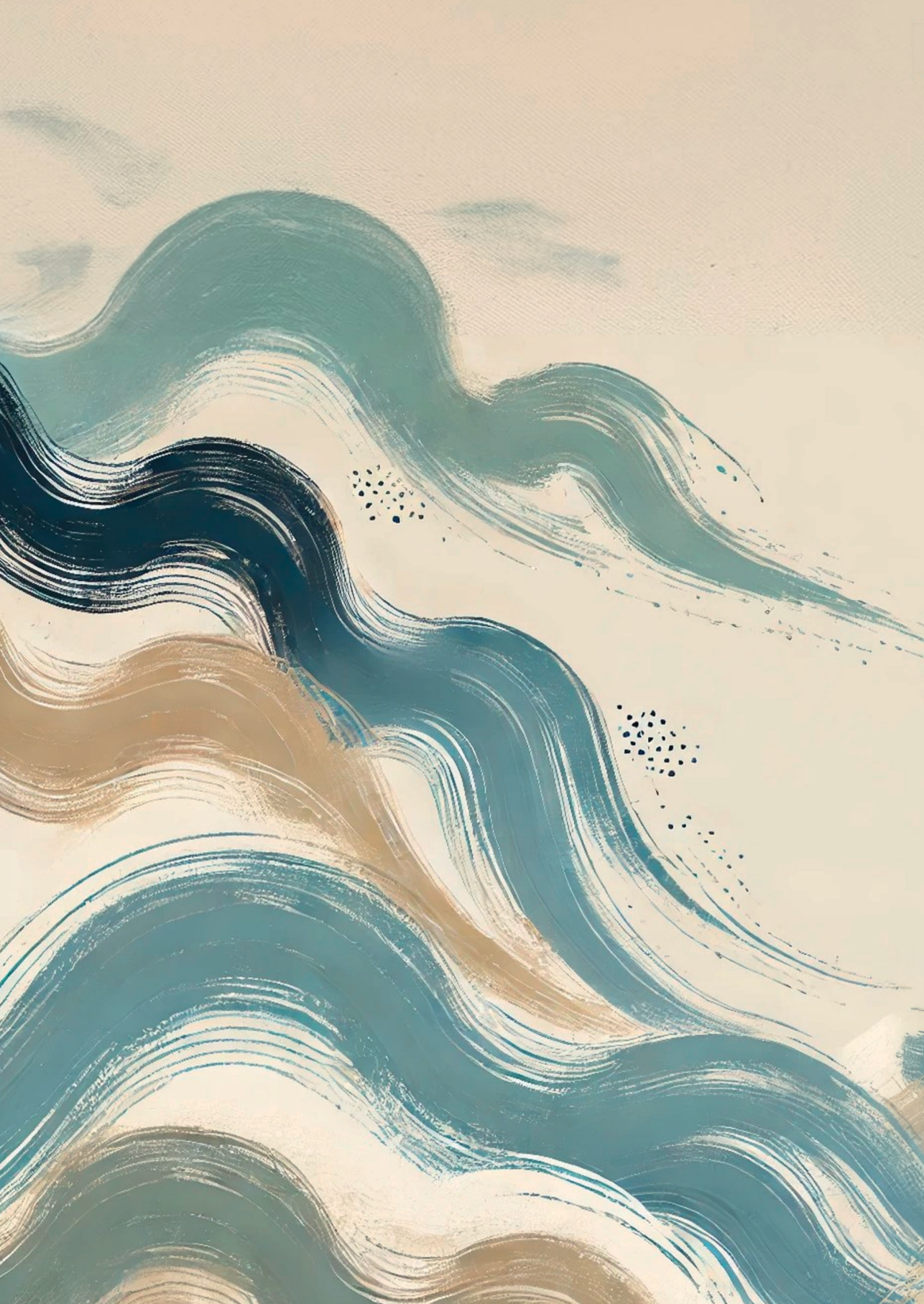16.   Berntorp E. Thrombosis in patients with hemorrhagic disorders.*Minerva Med*. 2013;104(2):169-73.

8
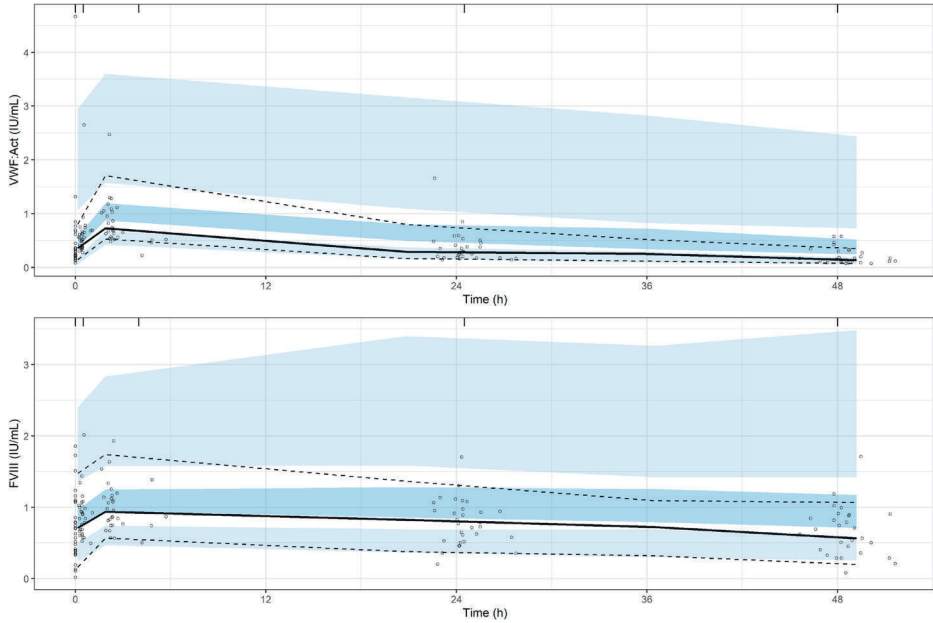
SUPPLEMENT

Supplement figure 1. Predictive Check (pcVPC) using pre-medical intervention data for von Willebrand factor activity (VWF:Act) and factor VIII (FVIII) population pharmacokinetic model by Bukkems et al. The solid lines represent the median and the 5th and 95th percentiles of the observed data, while the shaded areas show the 90% prediction intervals for the median and percentiles based on simulations from the final model. Circles represent individual observed data points, corrected for prediction discrepancies due to covariate and dosing differences. The divergence of observed percentiles from the predictive intervals, with solid lines lying outside the shaded areas, highlights discrepancies between the model predictions and the observed data, suggesting a potential misspecification in the model's predictive performance.

Supplement figure 2: Prediction-corrected Visual Predictive Check (pcVPC) using post-medical intervention data for von Willebrand factor activity (VWF:Act) and factor VIII (FVIII) population pharmacokinetic model by Bukkems et al. The solid lines represent the median and the 5th and 95th percentiles of the observed data, while the shaded areas show the 90% prediction intervals for the median and percentiles based on simulations from the final model. Circles represent individual observed data points, corrected for prediction discrepancies due to covariate and dosing differences. The divergence of observed percentiles from the predictive intervals, with solid lines lying outside the shaded areas, highlights discrepancies between the model predictions and the observed data, suggesting a potential misspecification in the model's predictive performance.
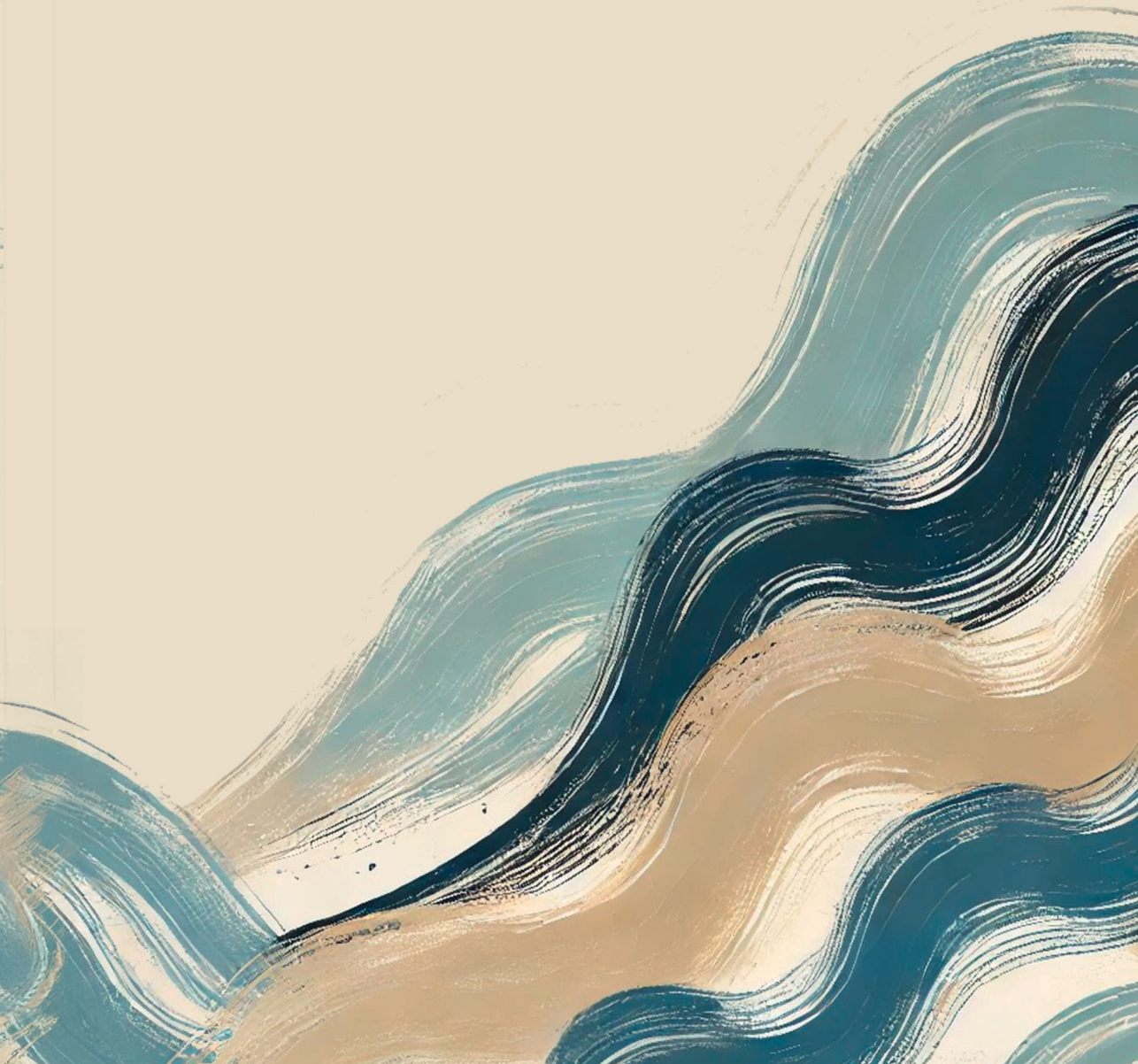
8

PART III

Applying artificial intelligence in pharmacometrics
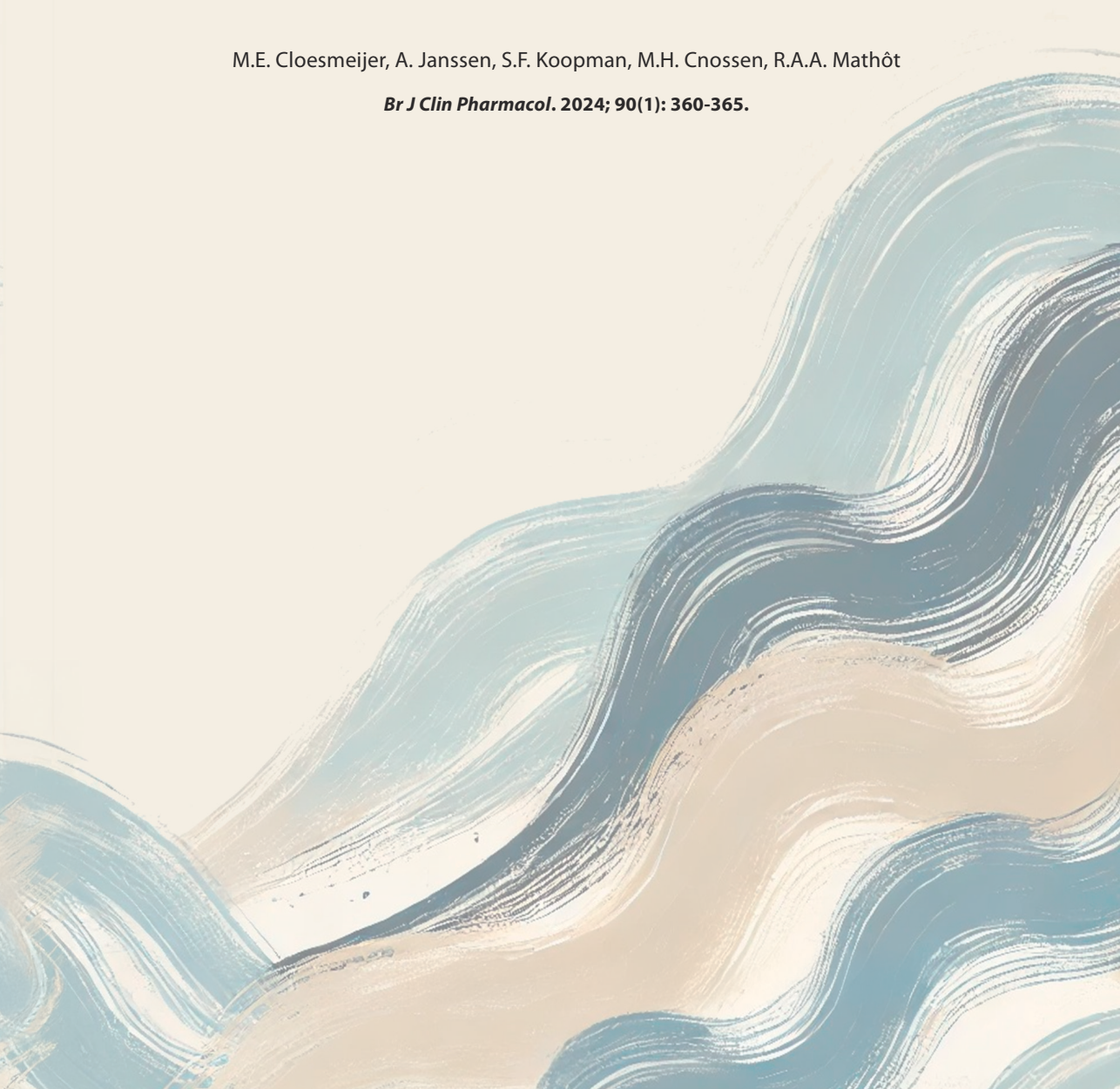
CHAPTER 9

ChatGPT in pharmacometrics?
Potential opportunities and limitations

M.E. Cloesmeijer, A. Janssen, S.F. Koopman, M.H. Cnossen, R.A.A. Mathôt

ABSTRACT

The potential of using ChatGPT in pharmacometrics was explored in this study, with a focus on developing a population pharmacokinetic (PK) model for standard half-life factor VIII. Our results demonstrated that ChatGPT can be utilized to accurately obtain typical PK parameters from literature, generate a population PK model in R, and develop an interactive Shiny application to visualize the results. ChatGPT's language generation capabilities enabled the development of R codes with minimal programming knowledge and helped to identify as well fix errors in the code. While ChatGPT presents several advantages, such as its ability to streamline the development process, its use in pharmacometrics also has limitations and challenges, including the accuracy and reliability of AI-generated data, the lack of transparency and reproducibility regarding codes generated by ChatGPT. Overall, our study demonstrates the potential of using ChatGPT in pharmacometrics, but researchers must carefully evaluate its use for their specific needs.

INTRODUCTION

Over the years, the use of artificial intelligence (AI) in medical research has shown great promise in enhancing drug discovery, identifying new treatment targets, and predicting disease outcomes[1]. AI is an umbrella term encompassing several advanced technologies, such as machine learning, natural language processing, and deep learning. These methods facilitate the extraction of patterns and insights from vast amounts of data. A recent exciting development in AI research has been the public release of ChatGPT[2], developed by OpenAI. The model architecture behind ChatGPT (GPT; Generative Pre-trained Transformer[3]) has shown to be very capable of achieving strong natural language understanding, while its accessible graphical user interface has resulted in widespread adoption.

Large Language Models (LLMs) such as ChatGPT are trained on an enormous corpus of text in order to generative responses to queries[4]. By devoting considerable human time labeling the quality of generated responses and re-training the model to produce the best responses, ChatGPT has suprised many by producing fluent and accurate responses to human inquiries. Aside from the public interest in the use of ChatGPT, there have also been suggestions to using the model to assist students and researchers by editing text, answering questions, writing code, and finding relevant literature given a query[5–8].

There already exist several publications discussing the potential impact of LLMs on a wide range of different research fields[9–11]. It however remains unknown if tools like ChatGPT can also support researchers from relatively small research fields, potentially underrepresented in the training data. In this work, we investigate if ChatGPT can be used to assist during the development of population pharmacokinetic (PK) models. As an use-case, we use ChatGPT to generate R code for predicting in vivo drug concentrations of standard half-life factor VIII (FVIII) concentrates in patients with haemophilia A[12]. Next, we query ChatGPT to generate an interactive R shiny application that can be used for the interpretation of the model and the selection of optimal doses to reach certain target FVIII levels. Based on this use-case, we aim to show that researchers unfamiliar with programming in R can nonetheless produce usable code for data analysis and discuss its limitations.

METHODS

Data collection and model development

We used the official implementation of ChatGPT v3.5 (https://chat.openai.com; OpenAI; 2023 May 24 version) to send and receive answers to queries. We wanted to make a population PK model for standard half-life FVIII in R and visualize the results by using a Shiny application. First, a simple query ("in R, make an one-compartment pharmacokinetic model for FVIII") was used and the output generated by ChatGPT was evaluated. Based on the generated R code, follow-up queries were used to extend the functionalities of the PK model:

Population PK modelling
1) In R, can you make an one-compartment pharmacokinetic model for FVIII using the package "desolve"? In the R code, use a CL of 2.5 dL/h and a V of 40 dL
2) Can you use a dose of 1000 IU(International units)?
3) Can you add allometric body weight scaling on the PK parameters?
4) Can you also include inter-individual variability on the PK parameters?

Population PK simulations
5) Can you simulate a population of 50 subjects?
6) Can you display every subject into one plot?
7) How can I reproduce this population for the simulation?
8) In the plot, can you display a prediction interval of the FVIII levels for the simulated population? Add a shaded area for the prediction interval in the plot.

Shiny application

9) Can you display the results in a shiny application?

10) Define a slider input for dose (250 to 4000 IU, steps of 250IU) and body weight (40 to 100kg, steps of 1kg).

11) Also, add as a slider a target FVIII level (ranging from 30 to 100 IU/dL with steps of 10 IU/dL). The app should also print the probability of reaching the target FVIII level at time 0 in this whole population.

The full queries are available at: https://chat.openai.com/share/5bd2a0fb-1662-4baa-88a2-2a7a44b31e1f. Answers to the above queries were regenerated multiple times to investigate the reproducibility of responses by ChatGPT.

RESULTS

Developing a population PK model using ChatGPT

First, we asked ChatGPT to make an one-compartment pharmacokinetic model for FVIII in R and regenerate the responses. Each time, we obtained different R codes with different R packages used to develop the PK model. Furthermore, we encountered several errors while executing some of the generated R codes. A short overview of the output is displayed in figure 1.

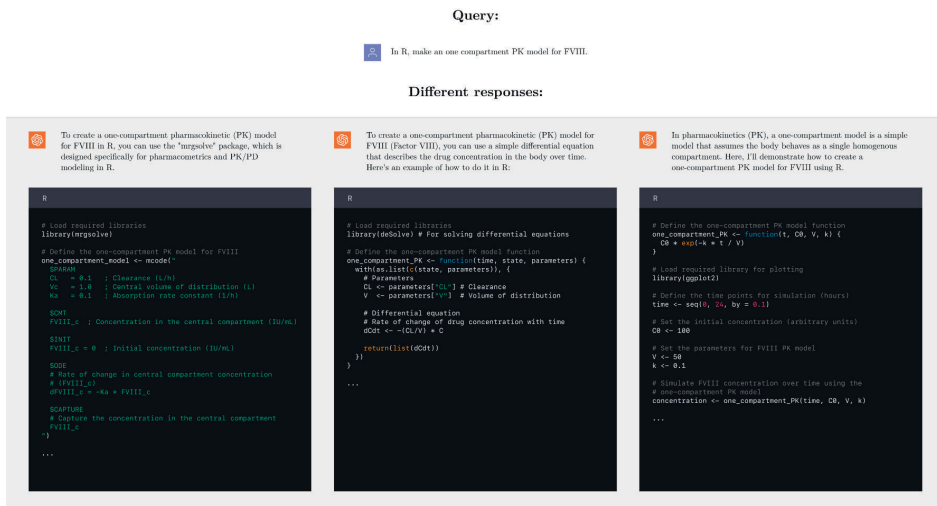**Figure 1. Example of variability in responses from ChatGPT when asking simple queries.** Original conversations can be obtained from https://chat.openai.com/share/340f6b7a-324c-4d07-ba2c-adb85337520b, https://chat.openai.com/share/0b992845-cebd-40f8-81a9-e7753a83eb2a, and https://chat.openai.com/share/cbd18eca-aea9-4cea-a99d-6707ae42cd7b.
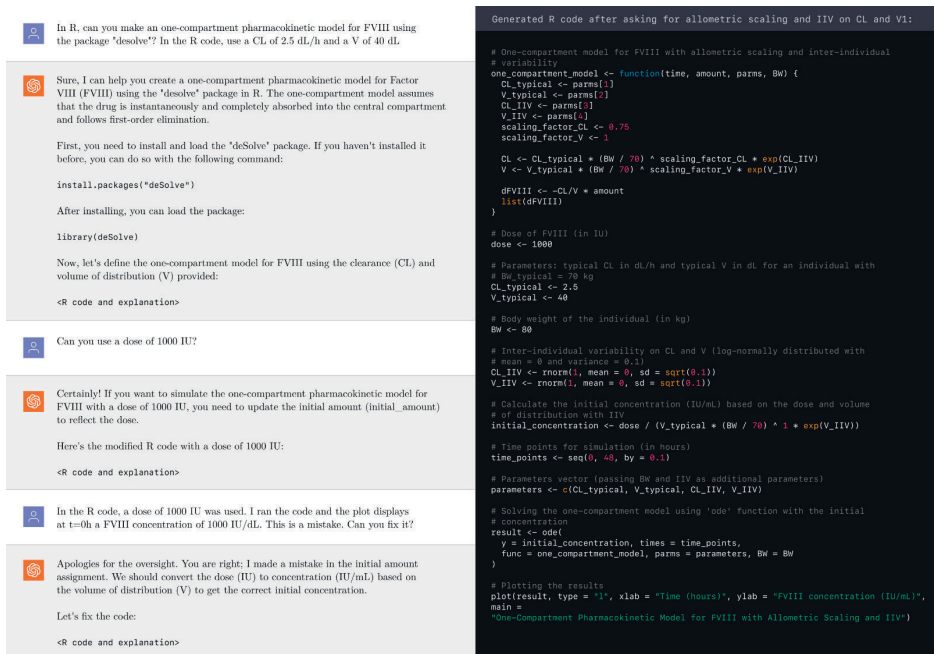
Figure 2. Example of conversation-wise development of population PK model using ChatGPT. Excerpt of our conversation with ChatGPT with the goal of iteratively developing a population PK model for factor VIII. ChatGPT produces usable code with detailed explanations and correctly resolves code errors when prompted. Full conversation can be obtained from https://chat.openai.com/share/5bd2a0fb-1662-4baa-88a2-2a7a44b31e1f

Next, more detailed queries were used in a step-wise manner to generate a population PK model by ChatGPT. Some of the output is displayed in figure 2. We then iteratively asked ChatGPT to add components to the model. ChatGPT understood how to normalize the PK parameters to body weight using allometric scaling and add inter-individual variability. Some of the code generated by ChatGPT resulted in errors. For example, after requesting ChatGPT to use a dose of 1000 IU, the initial concentration of FVIII was incorrect. We promptly asked ChatGPT to correct the error, in which ChatGPT successfully corrected the initial concentration. Other errors occurred, however ChatGPT demonstrated its problem-solving capabilities by providing revised R codes and solutions to address these issues. Not only did ChatGPT often produce functional code, it also provided explanation on each section of the code. Afterwards we asked ChatGPT to develop a shiny application to visualize FVIII levels. The Shiny application allowed the adjustment of patient body weight (from 40 to 100 kg with steps of 1 kg) and within the desired dosing interval (between 250 and 4000 IU). A shaded area displayed the 95% prediction interval. ChatGPT was able to successfully generate a Shiny application that can simulate population FVIII levels over time, with realistic predictions[13] (figure 3). The R code is displayed in supplement 1.
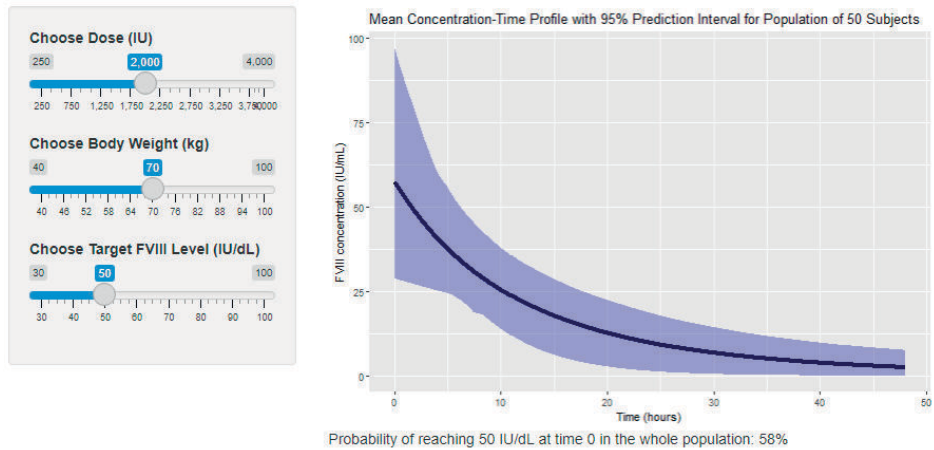
Figure 3. Generated Shiny application for simulating population factor VIII (FVIII) levels. The figure shows the simulated FVIII levels over 48 hours in a population. The black solid line represents the mean FVIII prediction, the shaded areas display the 95% prediction interval. The probability of reaching the target FVIII level at time = 0h in the population is printed.

What it cannot do

While ChatGPT was successful in generating the model and Shiny application, reruns of the prompts often resulted in different outcomes. In some of these, the R code resulted in an error. To assess the impact of different querying approaches, a comparison was made between simple query and step-wise queries. The results revealed that the reproducibility of outcomes was higher when employing step-wise queries. However, even with this approach, achieving exact replication of R code based on a given query was difficult. Nonetheless, more similar R code was produced through step-wise querying. Moreover, ChatGPT was successful in generating R code for single dose simulations, but struggled to provide appropriate code for simulating multiple doses of FVIII. Therefore, caution must be exercised when using R codes generated by ChatGPT in pharmacometrics. We also asked ChatGPT to produce NONMEM code for the same model. Although the produced code did resemble a NONMEM control stream, the produced file contained multiple errors and redundancies and failed to run.

DISCUSSION

We show that ChatGPT has the ability to generate functional R code for predicting drug concentration using a population PK model as well to develop an interactive Shiny application to visualize model predictions.

ChatGPT generated an one-compartment population PK model in R and updated the code based on user specifications. By using ChatGPT to develop a Shiny application in R, users inexperienced with R shiny can easily produce web applications for interpreting their models. Both applications show how ChatGPT can be used without extensive coding or programming knowledge. This can significantly reduce development time and effort, while potentially improving user experience of such applications. Another advantage of using ChatGPT for programming is its ability to assist developers in identifying and fixing errors in their code. ChatGPT can suggest possible solutions for errors and other coding mistakes, which helps inexperienced users to debug their code[14,15]. This feature can help streamline the development process and improve the overall quality of R code.

There are also some limitations and challenges to the use of ChatGPT for applications related to pharmacometrics. ChatGPT is a stochastic model, meaning that generating responses to the same query multiple times may yield different results. This variability can be influenced by factors such as model randomness, potential biases in the training data, but most importantly input phrasing. During our analysis, we observed that using a simple query yielded different outcomes. For instance, ChatGPT generated R code using packages such as mrgsolve or deSolve to generate a PK model. To address this, we incorporated step-wise queries with specific instructions to use the deSolve package. Additionally, we employed more detailed queries to develop the model and Shiny application, resulting in higher success rates and improved reproducibility. Therefore, it is important to employ careful phrasing of queries in order to produce the desired results. To enhance reproducibility, it is recommended to document the specific inputs used and the code generated by ChatGPT. This documentation can help ensure that the exact same conditions are used in subsequent runs or when sharing the code with others. By providing detailed information about the inputs and code, other researchers or users can attempt to reproduce the results. Moreover, the generated code by ChatGPT may contain errors and therefore the code may not provide the intended results. Often errors may resolved by regenerating the R code by ChatGPT or by copying the error from the R console as a follow-up query into ChatGPT. Code generated by ChatGPT should be thoroughly reviewed and validated to ensure its correctness and completeness. This involves testing the code, comparing the results with expected outcomes, and verifying

9

that it aligns with established pharmacometric principles and practices. Unfortunately, this might be difficult for the potential target audience of those learning to code.

Next, the accuracy and reliability of AI-generated data may be affected by biases and knowledge gaps in the training data or the complexity of the query, for example when asking to produce code for more complex biological systems[16,17]. ChatGPT often appears very confident in its responses. However, when responding with queries such as "there was an error in the code", it is quick to acknowledge the previous response as incorrect, even if it was not. Additionally, the lack of transparency and interpretability of AI algorithms may raise ethical concerns and limit their widespread adoption[18,19].

Another limitation to consider is that in our tests, ChatGPT was unable to generate functional NONMEM control streams. This was unfortunate as NONMEM is considered to be the gold standard in pharmacometrics research, and the identification of errors in these streams can greatly support students learning to use it[20]. This may be due to the limited availability of publicly available control streams, making it difficult for ChatGPT to learn from and generate accurate and reliable code for NONMEM models.

In conclusion, the integration of ChatGPT in pharmacometrics has the potential to streamline the development process and improve the user experience for pharmacometrics researchers. We deem it unlikely that ChatGPT will replace pharmacometricians in its current state. ChatGPT does have great value with respect to aiding researchers in finding and explaining information, generating and helping to debug code, and the education of new generations of pharmacometricians. As ChatGPT continues to evolve and improve, it has the potential to become an even more valuable tool in the field of pharmacometrics. It is likely that other pharmacometricians will find new and innovative ways to integrate it into their workflows and further enhance its capabilities in the field of pharmacometrics.

REFERENCES

1. Bohr A, Memarzadeh K. *The Rise of Artificial Intelligence in Healthcare Applications*.; 2020. doi:10.1016/B978-0-12-818438-7.00002-2

2. Gordijn B, Have H ten. ChatGPT: evolution or revolution? *Med Heal Care Philos*. 2023;26(1):1-2. doi:10.1007/s11019-023-10136-0

3. Radford A, Narasimhan K, Salimans T, Sutskever I, others. Improving language understanding by generative pre-training. Published online 2018.

4. Floridi L, Chiriatti M. GPT-3: Its Nature, Scope, Limits, and Consequences. *Minds Mach*. 2020;30(4):681-694. doi:10.1007/s11023-020-09548-1

5. Taecharungroj V. "What Can ChatGPT Do?" Analyzing Early Reactions to the Innovative AI Chatbot on Twitter. *Big Data Cogn Comput*. 2023;7(1):35. doi:10.3390/bdcc7010035

6. Liévin V, Hother CE, Winther O. Can large language models reason about medical questions? Published online 2022:1-33. doi:https://doi.org/10.48550/arXiv.2207.08143

7. Kashefi A, Mukerji T. ChatGPT for Programming Numerical Methods. Published online 2023:1-51. http://arxiv.org/abs/2303.12093

8. Temsah O, Khan SA, Chaiah Y, et al. Overview of Early ChatGPT's Presence in Medical Literature: Insights From a Hybrid Literature Review by ChatGPT and Human Experts. *Cureus*. 2023;15(4). doi:10.7759/cureus.37281

9. Dahmen J, Kayaalp ME, Ollivier M, et al. Artificial intelligence bot ChatGPT in medical research: the potential game changer as a double-edged sword. *Knee Surgery, Sport Traumatol Arthrosc*. 2023;31(4):1187-1189. doi:10.1007/s00167-023-07355-6

10. Zhu JJ, Jiang J, Yang M, Ren ZJ. ChatGPT and Environmental Research. *Environ Sci Technol*. Published online 2023:1-4. doi:10.1021/acs.est.3c01818

11. Sallam M. The Utility of ChatGPT as an Example of Large Language Models in Healthcare Education, Research and Practice: Systematic Review on the Future Perspectives and Potential Limitations. *medRxiv*. Published online 2023:2023.02.19.23286155. http://medrxiv.org/content/early/2023/02/21/2023.02.19.23286155.abstract

12. Franchini M, Mannucci P. Past, present and future of hemophilia: a narrative review. *Orphanet J Rare Dis*. 2012;7(1):24. doi:10.1186/1750-1172-7-24

13. Bukkems LH, Preijers T, Van Spengler MWF, Leebeek FWG, Cnossen MH, Mathôt RAA. Comparison of the Pharmacokinetic Properties of Extended Half-Life and Recombinant Factor VIII Concentrates by in Silico Simulations. *Thromb Haemost*. 2021;121(6):731-740. doi:10.1055/s-0040-1721484

14. Ahmad A, Waseem M, Liang P, Fehmideh M, Aktar MS, Mikkonen T. Towards Human-Bot Collaborative Software Architecting with ChatGPT. Published online 2023:1-7. http://arxiv.org/abs/2302.14600

15. Biswas S. Role of ChatGPT in Computer Programming. *Mesopotamian J Comput Sci*. Published online 2023:8-16. doi:10.58496/mjcsc/2023/002

16. Borji A. A Categorical Archive of ChatGPT Failures. Published online 2023:1-41. http://arxiv.org/abs/2302.03494

17. Mann DL. Artificial Intelligence Discusses the Role of Artificial Intelligence in Translational Medicine: A JACC: Basic to Translational Science Interview With ChatGPT. *JACC Basic to Transl Sci*. 2023;8(2):221-223. doi:10.1016/j.jacbts.2023.01.001

18. Editorials N. Tools such as ChatGPT threaten transparent science; here are our ground rules for their use. *Nature*. 2023;613:612.

9

19.   Biswas S. ChatGPT and the Future of Medical Writing. *Radiology*. 2023;307(2):3-5. doi:10.1148/radiol.223312

20.   Keizer RJ, Karlsson MO, Hooker A. Modeling and simulation workbench for NONMEM: Tutorial on Pirana, PsN, and Xpose. *CPT Pharmacometrics Syst Pharmacol*. 2013;2(6):1-9. doi:10.1038/psp.2013.24

21.   Alexander SPH, Kelly E, Mathie A, et al. THE CONCISE GUIDE TO PHARMACOLOGY 2019/20: Introduction and Other Protein Targets. *Br J Pharmacol*. 2019;176(S1):S1-S20. doi:10.1111/bph.14747

SUPPLEMENT

Final R code of the population PK model for factor VIII and Shiny application

```
# Install and load required packages
if (!requireNamespace("shiny", quietly = TRUE)) {
 install.packages("shiny")
}
library(shiny)
library(ggplot2)
library(dplyr)
library(deSolve)

# Set the seed for reproducibility
set.seed(123)

# One-compartment model for FVIII with allometric scaling and inter-individual variability
one_compartment_model <- function(time, amount, parms, BW) {
 CL_typical <- parms[1]
 V_typical <- parms[2]
 CL_IIV <- parms[3]
 V_IIV <- parms[4]
 scaling_factor_CL <- 0.75
 scaling_factor_V <- 1

 CL <- CL_typical * (BW / 70) ^ scaling_factor_CL * exp(CL_IIV)
 V <- V_typical * (BW / 70) ^ scaling_factor_V * exp(V_IIV)
 dFVIII <- -CL/V * amount
 list(dFVIII = dFVIII) # Ensure that the result is always a list
}

# Parameters: typical CL in dL/h and typical V in dL for an individual with BW_typical = 70 kg
CL_typical <- 2.5
V_typical <- 40

# Body weight of the individuals (in kg) for the population
BW_population <- rnorm(50, mean = 70, sd = 10)

# Inter-individual variability on CL and V (log-normally distributed with mean = 0 and variance = 0.1) for
        the population
CL_IIV_population <- rnorm(50, mean = 0, sd = sqrt(0.1))
V_IIV_population <- rnorm(50, mean = 0, sd = sqrt(0.1))

# Time points for simulation (in hours)
time_points <- seq(0, 48, by = 0.1)
```

```
# Shiny App UI
ui <- fluidPage(
 titlePanel("FVIII Concentration-Time Profiles for Population of 50 Subjects"),
 sidebarLayout(
 sidebarPanel(
 sliderInput("dose", "Choose Dose (IU)", min = 250, max = 4000, value = 1000, step = 250),
 sliderInput("body_weight", "Choose Body Weight (kg)", min = 40, max = 100, value = 70, step = 1),
 sliderInput("target_fviii", "Choose Target FVIII Level (IU/dL)", min = 30, max = 100, value = 50, step = 10)
 ),
 mainPanel(
 plotOutput("fviii_plot"),
 textOutput("probability_text")
 )
 )
)

# Shiny App Server
server <- function(input, output) {

 # Create reactive expression for the simulation
 fviii_simulation <- reactive({
 dose <- input$dose
 BW <- input$body_weight

 # Perform Monte Carlo simulations for each subject in the population
 results_population <- vector("list", length = length(BW_population))
 initial_concentrations <- numeric(length = length(BW_population)) # Store initial concentrations for
         each subject
 for (i in 1:length(BW_population)) {
 BW <- BW_population[i]
 CL_IIV <- CL_IIV_population[i]
 V_IIV <- V_IIV_population[i]

 # Calculate the initial concentration (IU/mL) based on the dose and volume of distribution with IIV
 initial_concentration <- dose / (V_typical * (BW / 70) ^ 1 * exp(V_IIV))

 # Parameters vector (passing BW and IIV as additional parameters)
 parameters <- c(CL_typical, V_typical, CL_IIV, V_IIV)

 # Solving the one-compartment model using 'ode' function with the initial concentration
 result <- ode(y = initial_concentration, times = time_points, func = one_compartment_model, parms =
         parameters, BW = BW)

 # Store the results for the current subject
  results_population[[i]] <- data.frame(time = result[, 1], concentration = result[, 2], subject =
        paste("Subject", i))
```

```
# Store the initial concentration for this subject
initial_concentrations[i] <- result[1, 2]
}

# Combine the results for all subjects into a single data frame
all_results <- do.call(rbind, results_population)
all_results <- all_results %>%
group_by(time) %>%
summarize(mean_concentration = mean(concentration),
lower_ci = quantile(concentration, 0.025),
upper_ci = quantile(concentration, 0.975))

# Calculate the probability of reaching the target FVIII level at time 0 for the whole population
prob_reaching_target <- mean(initial_concentrations >= input$target_fviii)
return(list(all_results = all_results, prob_reaching_target = prob_reaching_target))
})

# Create the plot
output$fviii_plot <- renderPlot({
all_results <- fviii_simulation()$all_results
ggplot(data = all_results, aes(x = time, y = mean_concentration)) +
geom_line(color = "black", size = 1.5) +
geom_ribbon(aes(ymin = lower_ci, ymax = upper_ci), fill = "blue", alpha = 0.3) +
labs(x = "Time (hours)", y = "FVIII concentration (IU/mL)", title = "Mean Concentration-Time Profile with
        95% Prediction Interval for Population of 50 Subjects")
})

# Display the probability of reaching target FVIII level at time 0 for the whole population
output$probability_text <- renderText({
prob_reaching_target <- fviii_simulation()$prob_reaching_target
 paste("Probability of reaching", input$target_fviii, "IU/dL at time 0 in the whole population:",
        scales::percent(prob_reaching_target))
})
}

# Run the Shiny App
shinyApp(ui, server)
```

9

PART IV

General discussion and summaries

CHAPTER 10

General discussion

GENERAL DISCUSSION

The application of pharmacometrics in the clinical management of inborn bleeding disorders represents a significant advancement in personalization of treatment, offering new insights into the optimal use of drugs like FVIII and FIX concentrates, VWF/FVIII concentrates and desmopressin. Importantly, pharmacometrics can 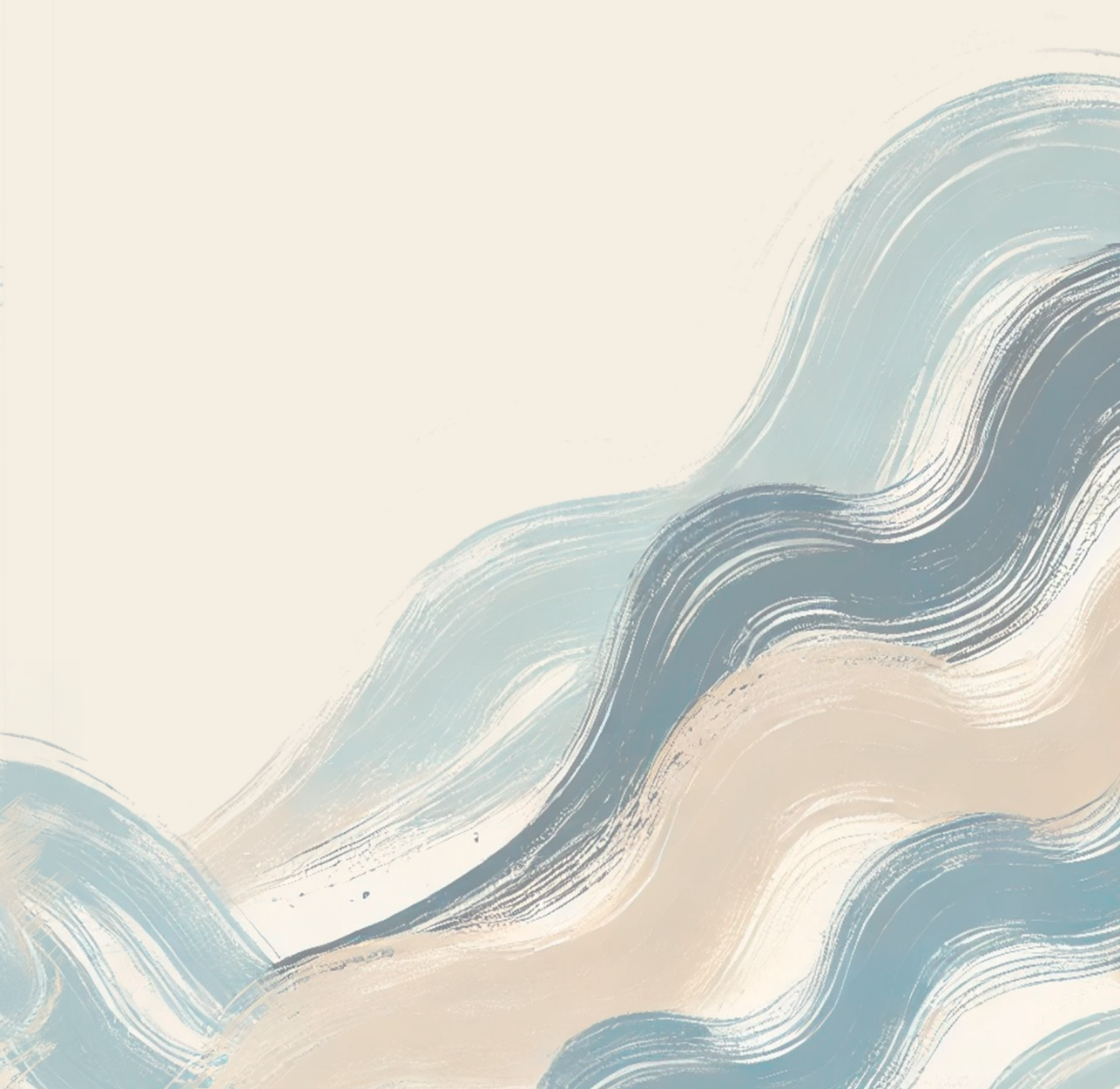also be applied for upcoming novel drugs and dosing strategies. This thesis provides a comprehensive exploration of pharmacokinetic, pharmacodynamic and physiologically based pharmacokinetic modelling techniques across various contexts of hemophilia and von Willebrand Disease (VWD), highlighting the role of pharmacometrics in the treatment of bleeding disorders. In addition to pharmacometrics, this thesis incorporates machine learning and artificial intelligence techniques to aid in developing pharmacometric models, addressing areas where traditional methodologies fall short in data analysis. The promising integration of these techniques underlines the importance of this multidisciplinary approach, merging different scientific domains to advance treatment strategies within this field. The findings from each chapter contribute to a deeper understanding of the drug dynamics and patient response variability, displaying the potential for pharmacometric approaches to optimize treatment strategies for these complex conditions.

Interconnectivity between methodological approaches in pharmacometrics

The methodological approaches throughout the chapters of this thesis showcase the dynamic use of pharmacometrics in a new advancement of personalized treatment for inborn bleeding disorders. In conjunction with these methodological approaches, in this general discussion the findings are placed within a broader context that includes biomolecular mechanisms and clinical relevance. This comprehensive approach not only enhances our understanding of drug behavior and patient variability but also bridges the gap between theoretical models and practical, clinical applications, underscoring the significance of pharmacometrics in advancing patient-specific therapy in the field of bleeding disorders.

Bridging methodologies for personalized treatment
A common theme in this thesis is the use of pharmacometrics to personalize treatment for patients with hemophilia and VWD. The incorporation of machine learning, as detailed in **chapter 2** on F8 missense variants and desmopressin response, further emphasizes the interaction of pharmacometrics and machine learning. This approach allows for a understanding of the complex relationships between genetic F8 missense variants and desmopressin response, surpassing the capabilities of traditional pharmacometric methods. One of the key benefits of incorporating machine learning is its

10

ability to efficiently handle and analyze the extensive diversity of F8 missense variants. Given the abundance and complexity of F8 missense variants, traditional pharmaco-metric approaches may struggle with the analysis or require an impractical amount of time to reach similar conclusions. Machine learning, however, can rapidly process and interpret large amounts of datasets, identifying patterns and correlations that might not be immediately apparent through traditional methods[1,2]. The F8 missense variants and its desmopressin response were further analyzed by also considering the bio-molecular mechanisms for biological plausibility of inclusion of F8 missense variants.

Further expanding in new advances in pharmacometrics, AI, including tools like Chat-GPT, has been increasingly used in various scientific areas. In **chapter 9,** ChatGPT was able to extract pharmacokinetic estimates from the literature, while building population pharmacokinetic models, and visualizing the results through interactive applications. The ability of artificial intelligence to navigate vast amounts of data, identify relevant information, and assist in model construction represents a shift in how researchers ap-proach pharmacometric analysis. ChatGPT has demonstrated remarkable capabilities in streamlining the model development process, from initial data gathering to the final presentation of results.

Novel integration of physiologically based pharmacokinetic modelling
A standout contribution of this thesis is the novel integration of physiologically based pharmacokinetic modelling, particularly in the context of recombinant factor IX Fc fusion protein (rFIXFc) and recombinant factor IX (rFIX) in **chapter 4**. Physiologically based phar-macokinetic modelling is an exceptional technique due to its ability to provide a detailed and mechanistic understanding of drug distribution[3], especially in areas not directly ac-cessible through conventional pharmacokinetic studies, such as drug behavior prediction in the extravascular space. This is particularly crucial for the management of hemophilia B, where the efficacy of treatment depends not just on the levels of coagulation factors within the plasma compartment but also on their presence and activity in extravascular space[4]. By incorporating the binding mechanisms of rFIXFc and rFIX to extravascular type 4 collagen, physiologically based pharmacokinetic models provide invaluable insights into how these treatments exert their hemostatic effects beyond the plasma compartment, highlighting their true therapeutic potential in hemophilia B treatment. The exploration of physiologically based pharmacokinetic modelling within the context of bleeding dis-orders is novel. Prior to this work, only a handful of studies have explored applying physi-ologically based pharmacokinetic models to understand the pharmacokinetics of drugs used for treating bleeding disorders[5,6]. The novelty of this approach lies in its utilization of a more mechanistic approach to better describe the observed pharmacokinetics. Further-more, it may also transform how therapies are developed and optimized for hemophilia

B and potentially other bleeding disorders. By providing a mechanistic framework that can predict drug behavior across various biological compartments, physiologically based pharmacokinetic modelling may possibly open new pathways for personalized medicine.

The methodological interconnectivity showcased in this thesis not only advances our understanding of pharmacokinetics and pharmacodynamics in bleeding disorders but also highlights the impact of integrating machine learning and artificial intelligence into pharmacometric research. Our findings gain deeper physiological insights from the population pharmacokinetic, pharmacodynamic, and physiologically based pharmacokinetic models, which incorporate bio-molecular mechanisms. While machine learning has the ability to analyze complex correlations in large datasets and artificial intelligence's contribution in model development. The synergy of these diverse methodologies—each with its unique strengths—exemplifies the potential of interdisciplinary collaboration in refining and personalizing treatment strategies. This harmonious integration influences the future direction of personalized treatment strategies.

Impact on personalized treatment

Personalization of dosing regimens can be carried out *a priori* by using covariates alone, to predict subpopulation pharmacokinetics, or *a posteriori* by using pharmacokinetic-guided dosing to predict the individual pharmacokinetics. Figure 1 displays an example of this workflow.
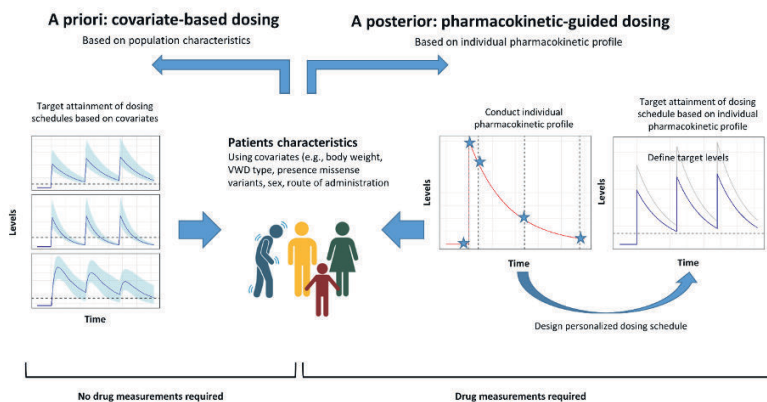

Figure 1. Example of a workflow for individualized dosing using population pharmacokinetic modelling. Dose personalization can be carried out *a priori* using covariates alone, for example for dose predictions based on body weight or age or *a posteriori* using pharmacokinetic-guided dosing to predict the individual pharmacokinetics.

A priori: on basis of patient characteristics

Various methods are available to implement personalized treatments in patients. One method is to distinguish between specific patient characteristics, i.e. *covariates*. These covariates can be included in a population pharmacokinetic model, to explain the inter-individual variability in the response of the drug between patients. To tailor treatments effectively, understanding how various covariates contribute to drug response variability is crucial. Key covariates such as body weight and age play a significant role in these approaches[7].

Various population pharmacokinetic models have been developed for desmopressin for example. These models are important for understanding the variability in drug responses among patients by incorporating covariates on the pharmacokinetic parameters. Previous research has displayed the importance of the following covariates in the response of desmopressin: VWD type and sex on the clearance, age on the response of desmopressin[8], most recent FVIII level on the baseline FVIII levels, clearance and volume of distribution[9].

In this thesis, we have continued to further investigate which covariates are important to explain the inter-individual variability of desmopressin response. **Chapter 2** on the effects of F8 missense mutations on desmopressin response in non-severe hemophilia A patients, exemplifies the critical role of genetic factors in treatment efficacy. By incorporating genetic variability into population pharmacokinetic models, it becomes possible to predict which patients are likely to respond adequately to desmopressin treatment based on their specific F8 variants, gene variant of F8. This approach facilitates the selection of the most effective treatment strategies, minimizing trial and error and reducing the risk of adverse events. Typically, an effective response to desmopressin is characterized by achieving peak FVIII levels above 0.50 IU/mL[10]. Understanding the specific F8 missense variant in a patient could allow for the prediction of desmopressin efficacy without the need for preliminary testing, potentially broadening its application in clinical practice. Currently, preferences often lean towards the more expensive coagulation factor concentrates for managing bleeding episodes or preparing for surgery, despite desmopressin being a viable alternative when desmopressin response is tested as adequate.

In **chapter 5,** we focus on the pharmacokinetic-pharmacodynamic relationships between desmopressin concentration and VWF:Act in patients with VWD. This chapter introduces a dosing of 0.3 mcg/kg with a capped dose recommendation of 30 mcg. This cap ensures that patients achieve therapeutic benefits despite lower dosing according to body weight. This recommendation emerges from findings that higher doses of

desmopressin than 30 mcg do not further increase VWF:Act release from the vascular endothelial cells. It is noteworthy, however, that different recommendations exist in the literature regarding the optimal capped dose for desmopressin. For example, Siew et al recommended a capped dose of 15 mcg[11]. Whereas the 2021 ASH/ISTH/NHF/WFH VWD guidelines suggested a capped dose of 20 mcg[12]. Our research, supported by population pharmacometric modelling, indicates that using the latter recommendation could lead to suboptimal treatment for individuals over 50 kg.

Intravenous administration of desmopressin is favored for its rapid therapeutic onset, although subcutaneous and intranasal routes are also viable options[13,14]. The use of intranasal administration is common, but it should be realized that there is a notable variability in patient response. Following desmopressin administration, both FVIII and VWF:Act levels are increased. Our preliminary findings suggest that the choice of administration route—intravenous or subcutaneous—does not significantly impact the increase in VWF:Act levels in patients with VWD. This study was not yet included in this thesis. Nonetheless, for patients with hemophilia A, data show a difference in the response of FVIII levels, with subcutaneous and intranasal routes exhibiting lower increases compared to intravenous administration. Therefore, patients with hemophilia A may need to be cautious in selecting an administration route, especially when aiming to achieve specific peak FVIII levels. However, fortunately a test dose is required to evaluate if the response to desmopressin is adequate. With the use of a population pharmacokinetic model, a test dose may not be longer necessary for every patient, as the response can be predicted a priori. Though, it is crucial that the population pharmacokinetic model demonstrates adequate predictive performance for predicting desmopressin response, before eliminating the need for a desmopressin test.

Within the scope of this thesis, several predictive performances using an external validation dataset were performed. External validation is crucial for as it verifies the ability of the model to predict drug concentration in an independent patient population. In **chapter 6,** we focused on the response of desmopressin on VWF:Act levels in VWD. This analysis revealed a tendency for the model to overestimate the response in patients with an VWF:Act baseline below 0.30 IU/mL, pre-desmopressin administration. Accurate predictions for this patient subgroup are particularly important, given their significant need for precise therapeutic management. While VWD patients with a VWF:Act baseline ranging between 0.30-0.50 IU/mL are typically expected to respond adequately to desmopressin[15], those with lower baseline levels are generally advised to undergo desmopressin testing to determine their individual response[12]. Based on the outcomes of this predictive performance analysis, it is recommended that patients with a VWF:Act baseline below 0.30 IU/mL should still undergo a desmopressin response test, in order

10

to verify adequate desmopressin testing. This underscores the importance of not only developing a population pharmacokinetic model but also validating it with an external dataset.

The necessity for external validation becomes especially critical in light of the research undertaken within this thesis, where a population pharmacokinetic model was developed to incorporate F8 missense variants, aiming to predict desmopressin response in hemophilia A patients (**chapter 2**). In order to translate modelling efforts into practical applications that can genuinely benefit patient care, ensuring the model's predictive performance is adequate. This requirement for external validation stems from the model's potential clinical impact—providing a tool that could eliminate the need for traditional desmopressin testing by predicting drug response based on genetic makeup. Consequently, before applying a population pharmacokinetic model incorporating F8 missense variants in hemophilia A in clinical settings or practice, external validation is essential to ensure its reliability and accuracy in patient care.

A posteriori: on basis of levels

In addition to desmopressin, VWF/FVIII concentrates, such as Haemate P® with a VWF/FVIII ratio of 2.4 to 1, are used in the management of VWD when desmopressin fails to adequately increase VWF/FVIII levels. This thesis utilizes a previously developed population pharmacokinetic model describing the interaction between VWF and FVIII using Haemate P®[16]. While pharmacokinetic-guided dosing has been used in hemophilia[17–20], its implementation in VWD represents a novel approach. Through pharmacokinetic-guided dosing, minimal blood samples pre- and post-administration are analyzed to derive VWF/FVIII levels, when applied to the population pharmacokinetic model, yield individualized pharmacokinetic parameters such as clearance and volume of distribution. This enables the design of more optimal dosing recommendations.

This research investigates the feasibility and reliability of pharmacokinetic-guided dosing in the perioperative management of VWD, highlighting several benefits over traditional body weight dosing in **chapter 7.** Most patients had a predefined target VWF:Act and FVIII level at ≥0.80-1.0 IU/mL at the start of the medical intervention, while some patients had a target level of ≥0.50 IU/mL. Nearly all patients achieved these predefined target levels. In contrast, the study conducted by Hazendonk et al. utilized body weight-based dosing post medical intervention, resulting in significantly higher VWF and FVIII levels, often exceeding 2.00 IU/mL[21]. While this approach effectively prevents bleeding, it raises concerns due to the potential risks associated with elevated coagulation factor levels, including thrombosis and other thromboembolic events. For those requiring further treatment post-initial medical intervention, the target levels were adjusted to a

range of 0.30 – 0.50 IU/mL, and once again, nearly all patients were able to meet these target levels.

Primarily, pharmacokinetic-guided dosing achieves more accurate attainment of target VWF:Act levels, addressing the significant variability observed in previous studies that employed body weight dosing[21]. Additionally, it provides precise predictions of VWF:Act levels on the day of surgery. Importantly, maintaining VWF:Act and FVIII levels within a therapeutic range is crucial; excessively high levels (>2.00 IU/mL) pose a risk of thrombotic complications[22]. Pharmacokinetic-guided dosing mitigates this risk by optimizing dosage to avoid excessively high coagulation factor levels. However, managing FVIII levels presents a challenge, especially since FVIII is a component of Haemate P®. Furthermore, pharmacokinetic-guided dosing enhances treatment efficiency. Other studies applying pharmacokinetic-guided dosing during medical intervention also reported better target attainment compared to standard (body weight) dosing[23]. Van Moort et al. reported perioperative pharmacokinetic-guidance of FVIII concentrate dosing leads to an improvement in target attainment, however the consumption was similar compared to standard treatment[24]. Body weight-based approaches can lack precision, often necessitating adjustments based on trial and error. In contrast, pharmacokinetic-guided dosing uses pharmacokinetic insights for more accurate dosing, improving outcomes for patients who may otherwise be at risk of under- or overtreatment. The personalized dosing advice generated through this method enables physicians to monitor VWF:Act and FVIII levels over time, facilitating timely adjustments to maintain desired levels or administer additional doses as needed. Overall, the adoption of pharmacokinetic-guided dosing in VWD, particularly in the context of surgical interventions, signifies a step towards more individualized and effective treatment strategies, underscoring the value of pharmacokinetic models in optimizing patient care.

Based on the clinical data of **chapter 7**, we developed a novel population pharmacokinetic model of the interaction of VWF:Act FVIII levels. The model presented in **chapter 8** was built using data from the OPTICLOT/To WiN study, where VWF/FVIII concentrate doses were adjusted according to observed activity levels during medical procedures. Notably, VWF:Act clearance decreased from 513 mL/h/70 kg at the start to 297 mL/h/70 kg after 48 hours. Additionally, increased VWF:Act levels were found to inhibit FVIII clearance, described by an inhibitory maximum effect model with a half-maximum effect at 0.90 IU/mL VWF:Act and reducing FVIII clearance from 513 to 257 mL/h/70 kg. The implications of decreasing clearance over time for VWF:Act and FVIII are substantial, as they suggest that lower doses may be required over time to maintain therapeutic levels, reducing the risk of overdose and associated complications.

10

Limitations and Future Directions

*Implementation of pharmacokinetic-guided dosing of von Willebrand disease in
clinical practice*

Implementing pharmacokinetic-guided dosing for VWD in clinical settings is currently
uncommon. However, our findings indicate that pharmacokinetic-guided dosing im-
proves the target VWF:Act levels in perioperative settings, as the variability in VWF:Act
levels is lower compared to body weight based dosing[21]. Despite its benefits, there are
several challenges associated with the application of pharmacokinetic-guided dosing
for VWD. For instance, in our study, participants were required to undergo an extensive
pharmacokinetic profiling process prior to their surgery. This involved administering a
test dose of Haemate P®, followed by collecting a series of five blood samples over two
days. These procedures necessitated considerable time investments from both the pa-
tients and the healthcare staff, including those administering the medication, collecting
and analyzing the blood samples, all of which took place within a hospital setting.

Previous research has shown pre-surgical pharmacokinetics of patient is different com-
pared to its pharmacokinetics during surgery[25]. Therefore, pre-surgical pharmacokinet-
ics might have limited usage in personalized dosing during surgical procedures. Rather
than conducting a full pharmacokinetic profile before surgery, a more practical and
time-efficient approach could involve using body weight-based dosing on the day of
the medical intervention. By collecting blood samples both before and after administer-
ing the dose, clinicians can assess VWF:Act and FVIII levels to investigate the initial thera-
peutic response. Subsequently, pharmacokinetic-guided dosing strategies could be
implemented from the first day post-surgery onwards, utilizing the data gathered on the
day of the operation to inform any necessary dose adjustments. Previous perioperative
studies have documented considerable variability in both peak and post-administration
levels of VWF:Act and FVIII when using Haemate P® based on body weight dosing[26,27].
This underscores the importance of monitoring VWF:Act and FVIII levels post adminis-
tration, particularly for patients undergoing treatment over several days. Such assess-
ments enable adjustments for both under-treatment and over-treatment. Consequently,
utilizing pharmacokinetic-guided dosing post-surgery emerges as a viable strategy in
optimizing treatment. This method aligns with practices observed in the administration
of antibiotics, where therapeutic drug monitoring is utilized to refine dosing regimens
based on the samples[28–30].

A challenge in expanding the use of pharmacokinetic-guided dosing for VWD is the
limited availability of population pharmacokinetic models. Currently, only population
pharmacokinetic models of Haemate (plasma derived VWF/FVIII; ratio 2.4:1) and desmo-

pressin are available for VWD[8,16]. However, there are other VWF-containing concentrates that are used, such as Wilate®[31] (plasma derived VWF/FVIII; ratio 1:1), Vonvendi®[32] (recombinant VWF, only VWF-containing concentrate), Wilfactin®[33] (plasma derived pure VWF concentrate) etc. For pharmacokinetic-guided dosing to be fully integrated into the management of VWD, it is necessarily to develop and validate population pharmacokinetic models for these and other VWF-containing treatments. This approach would ensure that clinicians can tailor dosing strategies across all of available concentrates.

Relating pharmacokinetics to bleeding risks in von Willebrand disease patients

Bleeding risks are described using population pharmacokinetic-pharmacodynamic models in hemophilia A patients[34]. Contrastingly, assessments of bleeding risks in VWD patients have not been as extensively modeled. Generally, individuals with VWD exhibit an overall more moderate bleeding tendency compared to those with hemophilia. Yet, a specific subset of VWD patients, particularly those with Type 3 VWD, experience severe clinical manifestations similar to those observed in severe hemophilia, including joint and gastrointestinal bleedings[35,36]. Such patients frequently receive prophylactic treatments. Currently, these prophylactic regimens are primarily determined based on the body weight of the patient, however there are a few clinical trials assessing the long-term benefits of prophylaxis in VWD at this moment[37]. In hemophilia, pharmacokinetic-guided dosing is increasingly used to achieve more precise FVIII or FIX target levels. Looking ahead, it is conceivable that type 3 VWD patients might similarly benefit from pharmacokinetic-guided dosing strategies. By correlating the pharmacokinetic profile of a patient with their bleeding risk, it may be possible to refine and personalize prophylactic treatments for those with type 3 VWD, enhancing the overall effectiveness of their management.

Implementation of clinical relevant covariates in population pharmacokinetic and pharmacodynamic models

10

Determining the practical application of population pharmacokinetic or pharmacodynamic models is crucial in model development. The intended use of the model significantly influences its design and complexity. For instance, if the objective is merely to describe the drug concentration over time or to estimate the of inter-individual variability of pharmacokinetic parameters, a basic population model incorporating typical pharmacokinetic or pharmacodynamic parameters with inter-individual variability might suffice. However, when aiming to apply these models in a clinical context to generate precise predictions tailored to individual patient characteristics, the selection of covariates becomes critical[7].

Firstly, any covariate incorporated into the model must be readily measurable or obtainable from the patient for whom the model prediction is required. This ensures that the model can be practically applied in a clinical setting without necessitating additional, potentially complex assessments. Secondly, it is important to include covariates into the model that are crucial for accurate predictions[38]. For example, during the external validation of a model predicting desmopressin response on VWF:Act levels in VWD patients in **chapter 6**, numerous covariates were included on the clearance. Nonetheless, it was the prediction of peak VWF:Act levels following desmopressin administration that was the most clinical significance. Given inaccurate peak VWF:Act level predictions for specific VWD sub-populations using the external dataset, a more effective strategy might involve included covariates on the volume of distribution or bioavailability. Such adjustments could better reflect variations in peak VWF:Act levels, enhancing the predictive accuracy of the model and clinical utility.

Developing physiological-based pharmacokinetic models for the remaining FIX-concentrates

The development of a physiologically based pharmacokinetic model for recombinant factor IX Fc fusion protein (rFIXFc) and recombinant factor IX (rFIX) within this thesis marks a significant advance in our understanding of hemophilia B treatment, by describing the interaction with type IV collagen in the extravascular space. Yet, there are more variants of FIX concentrates on the market, such as rFIX linked to albumin (rFIX-FP®) or PEGylated rFIX (N9-GP®), each presenting a unique pharmacokinetic profile[39]. Literature shows that these pharmacokinetic variations influence the proportion of FIX concentrates that distributes into extravascular spaces, which, in turn, may affect bleeding episodes in patients[40]. It is suggested that the efficiency with which a FIX concentrate permeates the extravascular spaces directly correlates with its efficacy in reducing bleeding episodes[41].

By extending the application of physiological-based pharmacokinetic models to a broader range of FIX concentrates, we can quantify the FIX levels in both the bloodstream and extravascular compartments. This approach enables a comparative analysis of FIX ratios between these two spaces, providing deeper insights into the pharmacokinetic behaviors of various FIX concentrates. Such models hold the potential to understand how each FIX concentrate accesses and functions within the extravascular spaces. Next, we can compare the extravascular distribution of different FIX concentrates. This will not only enhance our understanding of the pharmacokinetic properties of these treatments but also clarify their implications for hemostasis in the extravascular spaces. By quantifying the extravascular distribution profiles of each FIX concentrate, we may understand which FIX concentrates are most likely to reduce bleeding episodes effectively.

Furthermore, these insights can inform you about the development of new FIX concentrates designed to maximize extravascular access and efficacy. As we deepen our comprehension of the critical factors influencing the performance of FIX concentrates in the extravascular space, we can refine treatment strategies to offer patients more reliable and efficient hemostatic control.

Other roles of physiological-based pharmacokinetic within bleeding disorders

Within the context of bleeding disorders, the use of physiologically based pharmacokinetic modelling represents a promising field with multiple potential applications. This novel approach may significantly enhance our understanding and management of these disorders, particularly in specific populations such as infants, pregnant women, and the elderly[42,43]. These groups often exhibit unique physiological characteristics that can alter pharmacokinetics, making them distinct from the adult population typically included in population pharmacokinetic analyses. Due to these differences, directly extrapolating pharmacokinetic data from adults to these atypical populations will lead to inaccurate pharmacokinetic profiles, highlighting the need for tailored pharmacokinetic predictions. Physiologically based pharmacokinetic modelling addresses this gap by allowing the physiological properties to be adjusted to reflect the specific conditions of these underrepresented groups.

Furthermore, physiologically based pharmacokinetic modelling extends its utility by offering a mechanistic approach to pharmacokinetic prediction that exceeds the capabilities of more traditional population pharmacokinetic modelling. For instance, in this thesis, we explore the interaction between VWF and FVIII using a population pharmacokinetic model developed with NONMEM. While NONMEM provides valuable insights, it encounters limitations in handling complex models and a large number of parameters, particularly when attempting to incorporate detailed molecular mechanisms. Physiologically based pharmacokinetic modelling could potentially fill this gap by facilitating a more detailed understanding of the molecular interactions between VWF and FVIII. This approach not only allows for the exploration of how VWF binds to FVIII but also enhances our understanding of the molecular dynamics at play.

10

Possibilities within pharmacokinetic-pharmacodynamic guided dosing in hemophilia

Notably, the OPTI-CLOT study group within the SYMPHONY consortium recently completed a large prospective study on pharmacokinetic-guided prophylaxis dosing in hemophilia [44]. Traditionally, dosing in hemophilia, whether for routine prophylaxis or in perioperative setting, largely depends on maintaining specific coagulation factor levels—FVIII for hemophilia A and FIX for hemophilia B, as determined by the treating

hematologist. Commonly, target trough levels are established at >0.01 or 0.03 IU/mL for prophylaxis, and 0.30-0.50 IU/mL for post-surgical management[45]. However, it is observed that patients can exhibit varying bleeding tendencies even at similar trough levels, indicating a bleeding phenotype not solely predictable by coagulation factor levels alone[46,47].

This discrepancy underscores the potential limitation of relying solely on coagulation factor levels to predict bleeding risks. Research indicates that coagulation factor levels do not always directly correlate with bleeding episodes[40], suggesting the need for alternative markers to distinguish between different bleeding phenotypes. In **chapter 3** a promising approach involves integrating thrombin and plasmin generation with coagulation factor levels to provide a more comprehensive assessment of the global hemostatic effect[48,49]. The pharmacokinetic-pharmacodynamic model previously developed, which incorporates these markers, has shown promise in predicting bleeding risks and could be further validated in prospective studies.

Adopting a pharmacokinetic-pharmacodynamic guided dosing strategy, incorporating both coagulation factor levels and thrombin and plasmin generation, could lead to personalized regimens that more accurately reflect individual hemostatic profiles. For instance, patients with comparable pharmacokinetic profiles of coagulation factor levels might receive different dosing regimens based on their thrombin and plasmin generation rates. However, this more complex but real world approach, introduces several challenges. It requires additional measurements, increasing the workload for hemophilia treatment centers. Moreover, the centers must be equipped with the necessary assays for thrombin and plasmin generation measurements, which are not commonly used. Importantly, the developed model displayed significant inter-individual variability and residual error in thrombin and plasmin generation, complicating the implementation of pharmacokinetic-pharmacodynamic guided dosing. These factors highlight the complexities of utilizing thrombin and plasmin generation in combination with coagulation factor levels for hemophilia management and necessitate further exploration to establish guidelines and optimize treatment protocols.

Conclusion

In conclusion, the studies in this thesis support the application of pharmacometrics in the management of bleeding disorders. Through the utilization of various pharmacometric tools, we have been able to further personalize and optimize treatment regimens, showcasing the potential of these methodologies in clinical applications. For the future, it is crucial to consider which additional steps are necessary to further integrate pharmacokinetic-guided dosing into clinical practice, particularly for conditions such as

VWD. Moreover, we should also evaluate how artificial intelligence and machine learning can further aid in our model development. Lastly, the exploration of physiologically based pharmacokinetic modelling in other bleeding disorders represents an interesting expansion for the application of pharmacometrics.

10

REFERENCES

1.   van Gelder T, Vinks AA. Machine Learning as a Novel Method to Support Therapeutic Drug Management and Precision Dosing. *Clin Pharmacol Ther*. 2021;110(2):273-276. doi:10.1002/cpt.2326

2.   Janssen A, Bennis FC, Mathôt RAA. Adoption of Machine Learning in Pharmacometrics: An Overview of Recent Implementations and Their Considerations. *Pharmaceutics*. 2022;14(9):1-26. doi:10.3390/pharmaceutics14091814

3.   Zhuang X, Lu C. PBPK modeling and simulation in drug research and development. *Acta Pharm Sin B*. 2016;6(5):430-440. doi:10.1016/j.apsb.2016.04.004

4.   Stafford DW. Extravascular FIX and coagulation. *Thromb J*. 2016;14(Suppl 1). doi:10.1186/s12959-016-0104-2

5.   Pestel S, Chung D, Rezvani-Sharif A, et al. A Quantitative Systems Pharmacology (QSP) Model to Compare the Non-Clinical Biodistribution and Efficacy between Recombinant Factor IX (rIX) Therapies. *Blood*. 2021;138(Supplement 1):4240-4240. doi:10.1182/blood-2021-145878

6.   Xia B, Katragadda S, Teutonico D, Macha S, Demissie M, Benson C. A Physiologically Based Pharmacokinetic (PBPK) Model for Adults to Characterize BIVV001 Activity, a New Class of Factor VIII (FVIII) with High Sustained Factor Activity. *Blood*. 2020;136(Supplement 1):18-19. doi:10.1182/blood-2020-138894

7.   Joerger M. Covariate pharmacokinetic model building in oncology and its potential clinical relevance. *AAPS J*. 2012;14(1):119-132. doi:10.1208/s12248-012-9320-2

8.   De Jager NCB, Heijdra JM, Kieboom Q, et al. Population Pharmacokinetic Modeling of von Willebrand Factor Activity in von Willebrand Disease Patients after Desmopressin Administration. *Thromb Haemost*. 2020;120(10):1407-1416. doi:10.1055/s-0040-1714349

9.   Schütte LM, Van Hest RM, Stoof SCM, et al. Pharmacokinetic modelling to predict FVIII:C response to desmopressin and its reproducibility in nonsevere haemophilia a patients. *Thromb Haemost*. 2018;118(4):621-629. doi:10.1160/TH17-06-0390

10. Loomans JI, Kruip MJHA, Carcao M, et al. Desmopressin in moderate hemophilia a patients: A treatment worth considering. *Haematologica*. 2018;103(3):550-557. doi:10.3324/haematol.2017.180059

11. Siew DA, Mangel J, Laudenbach L, Schembri S, Minuk L. Desmopressin responsiveness at a capped dose of 15µg in type 1 von Willebrand disease and mild hemophilia A. *Blood Coagul Fibrinolysis*. 2014;25(8):820-823. doi:10.1097/MBC.0000000000000158

12. Connell NT, Flood VH, Brignardello-Petersen R, et al. Ash isth nhf wfh 2021 guidelines on the management of von willebrand disease. *Blood Adv*. 2021;5(1):301-325. doi:10.1182/BLOODADVANCES.2020003264

13. Rodeghiero F, Castaman G, Mannucci PM. Prospective multicenter study on subcutaneous concentrated desmopressin for home treatment of patients with von Willebrand disease and mild or moderate hemophilia A. *Thromb Haemost*. 1996;76(5):692-696.

14. Rose EH, Aledort LM. Nasal spray desmopressin (DDAVP) for mild hemophilia A and von Willebrand disease. *Ann Intern Med*. 1991;114(7):563-568. doi:10.7326/0003-4819-114-7-563

15. Lavin M, Aguila S, Schneppenheim S, et al. Novel insights into the clinical phenotype and pathophysiology underlying low VWF levels. *Blood*. 2017;130(21):2344-2353. doi:10.1182/blood-2017-05-786699

16. Bukkems LH, Heijdra JM, de Jager NCB, et al. Population pharmacokinetics of the von Willebrand factor-factor VIII interaction in patients with von Willebrand disease. *Blood Adv*. 2021;5(5). doi:10.1182/BLOODADVANCES.2020003891

17. Hazendonk H, Fijnvandraat K, Lock J, et al. A population pharmacokinetic model for perioperative dosing of factor VIII in hemophilia a patients. *Haematologica*. 2016;101(10):1159-1169. doi:10.3324/haematol.2015.136275

18. Hazendonk HCAM, van Moort I, Mathôt RAA, et al. Setting the stage for individualized therapy in hemophilia: What role can pharmacokinetics play? *Blood Rev*. 2018;32(4):265-271. doi:10.1016/j.blre.2018.01.001

19. Goedhart TMHJ, Janssen A, Mathôt RAA, Cnossen MH. The road to implementation of pharmacokinetic-guided dosing of factor replacement therapy in hemophilia and allied bleeding disorders. Identifying knowledge gaps by mapping barriers and facilitators. *Blood Rev*. 2023;61(May):101098. doi:10.1016/j.blre.2023.101098

20. Lissitchkov T, Rusen L, Georgiev P, et al. PK-guided personalized prophylaxis with Nuwiq® human-cl rhFVIII in adults with severe haemophilia A. *Haemophilia*. 2017;23(5):697-704. doi:10.1111/hae.13251

21. Hazendonk HCAM, Heijdra JM, de Jager NCB, et al. Analysis of current perioperative management with Haemate® P/Humate P® in von Willebrand disease: Identifying the need for personalized treatment. *Haemophilia*. 2018;24(3):460-470. doi:10.1111/hae.13451

22. Bugnicourt JM, Roussel B, Tramier B, Lamy C, Godefroy O. Cerebral venous thrombosis and plasma concentrations of factor VIII and von Willebrand factor: A case control study. *J Neurol Neurosurg Psychiatry*. 2007;78(7):699-701. doi:10.1136/jnnp.2006.103465

23. Richter DC, Frey O, Röhr A, et al. Therapeutic drug monitoring-guided continuous infusion of piperacillin/tazobactam significantly improves pharmacokinetic target attainment in critically ill patients: a retrospective analysis of four years of clinical experience. *Infection*. 2019;47(6):1001-1011. doi:10.1007/s15010-019-01352-z

24. van Moort I, Preijers T, Bukkems LH, et al. Perioperative pharmacokinetic-guided factor VIII concentrate dosing in haemophilia (OPTI-CLOT trial): an open-label, multicentre, randomised, controlled trial. *Lancet Haematol*. 2021;8(7):e492-e502. doi:10.1016/S2352-3026(21)00135-6

25. Di Paola J, Lethagen S, Gill J, et al. Presurgical pharmacokinetic analysis of a von Willebrand factor/factor VIII (VWF/FVIII) concentrate in patients with von Willebrand's disease (VWD) has limited value in dosing for surgery. *Haemophilia*. 2011;17(5):752-758. doi:10.1111/j.1365-2516.2011.02583.x

26. Thompson AR, Gill JC, Ewenstein BM, et al. Successful treatment for patients with von Willebrand disease undergoing urgent surgery using factor VIII/VWF concentrate (Humate-P®). *Haemophilia*. 2004;10(1):42-51. doi:10.1046/j.1351-8216.2003.00809.x

27. Lethagen S, Kyrle PA, Castaman G, et al. von Willebrand factor/factor VIII concentrate (Haemate® P) dosing based on pharmacokinetics: A prospective multicenter trial in elective surgery. *J Thromb Haemost*. 2007;5(7):1420-1430. doi:10.1111/j.1538-7836.2007.02588.x

28. De Waele JJ, Carrette S, Carlier M, et al. Therapeutic drug monitoring-based dose optimisation of piperacillin and meropenem: A randomised controlled trial. *Intensive Care Med*. 2014;40(3):380-387. doi:10.1007/s00134-013-3187-2

29. de Velde F, Mouton JW, de Winter BCM, van Gelder T, Koch BCP. Clinical applications of population pharmacokinetic models of antibiotics: Challenges and perspectives. *Pharmacol Res*. 2018;134(May):280-288. doi:10.1016/j.phrs.2018.07.005

30. Mabilat C, Gros MF, Nicolau D, et al. Diagnostic and medical needs for therapeutic drug monitoring of antibiotics. *Eur J Clin Microbiol Infect Dis*. 2020;39(5):791-797. doi:10.1007/s10096-019-03769-8

31. Berntorp E, Windyga J. Treatment and prevention of acute bleedings in von Willebrand disease - Efficacy and safety of Wilate®, a new generation von Willebrand factor/factor VIII concentrate. *Haemophilia*. 2009;15(1):122-130. doi:10.1111/j.1365-2516.2008.01901.x

10

32. Franchini M, Mannucci PM. Von Willebrand factor (Vonvendi®): the first recombinant product licensed for the treatment of von Willebrand disease. *Expert Rev Hematol*. 2016;9(9):825-830. doi: 10.1080/17474086.2016.1214070

33. Goudemand J, Scharrer I, Berntorp E, et al. Pharmacokinetic studies on Wilfactin, a von Willebrand factor concentrate with a low factor VIII content treated with three virus-inactivation/removal methods. *J Thromb Haemost*. 2005;3(10):2219-2227. doi:10.1111/j.1538-7836.2005.01435.x

34. Bukkems LH, Versloot O, Cnossen MH, et al. Association between Sports Participation, Factor VIII Levels and Bleeding in Hemophilia A. *Thromb Haemost*. 2023;123(3):317-325. doi:10.1055/a-1983-0594

35. Lethagen S. Clinical experience of prophylactic treatment in von Willebrand disease. *Thromb Res*. 2006;118(SUPPL. 1):10-12. doi:10.1016/j.thromres.2006.01.021

36. Berntorp E. Prophylaxis and treatment of bleeding complications in von Willebrand disease type 3. *Semin Thromb Hemost*. 2006;32(6):621-625. doi:10.1055/s-2006-949667

37. Miesbach W, Berntorp E. Translating the success of prophylaxis in haemophilia to von Willebrand disease. *Thromb Res*. 2021;199(December 2020):67-74. doi:10.1016/j.thromres.2020.12.030

38. Tunblad K, Lindbom L, McFadyen L, Jonsson EN, Marshall S, Karlsson MO. The use of clinical irrelevance criteria in covariate model building with application to dofetilide pharmacokinetic data. *J Pharmacokinet Pharmacodyn*. 2008;35(5):503-526. doi:10.1007/s10928-008-9099-z

39. Preijers T, Bukkems L, van Spengler M, Leebeek F, Cnossen M, Mathôt R. In silico comparison of pharmacokinetic properties of three extended half-life factor IX concentrates. *Eur J Clin Pharmacol*. 2021;77(8):1193-1200. doi:10.1007/s00228-021-03111-2

40. Mann DM, Stafford KA, Poon MC, Matino D, Stafford DW. The Function of extravascular coagulation factor IX in haemostasis. *Haemophilia*. 2021;27(3):332-339. doi:10.1111/hae.14300

41. Leuci A, Enjolras N, Marano M, et al. Extravascular factor IX pool fed by prophylaxis is a true hemostatic barrier against bleeding. *J Thromb Haemost*. 2024;22(3):700-708. doi:https://doi.org/10.1016/j.jtha.2023.11.023

42. Dallmann A, Solodenko J, Ince I, Eissing T. Applied Concepts in PBPK Modeling: How to Extend an Open Systems Pharmacology Model to the Special Population of Pregnant Women. *CPT Pharmacometrics Syst Pharmacol*. 2018;7(7):419-431. doi:10.1002/psp4.12300

43. Stader F, Penny MA, Siccardi M, Marzolini C. A Comprehensive Framework for Physiologically-Based Pharmacokinetic Modeling in Matlab. *CPT Pharmacometrics Syst Pharmacol*. 2019;8(7):444-459. doi:10.1002/psp4.12399

44. Goedhart TMHJ, Bukkems LH, Coppens M, et al. Design of a Prospective Study on Pharmacokinetic-Guided Dosing of Prophylactic Factor Replacement in Hemophilia A and B (OPTI-CLOT TARGET Study). *TH Open*. 2022;06(01):e60-e69. doi:10.1055/a-1760-0105

45. Kempton CL. Prophylaxis in hemophilia: how much is enough? *Blood*. 2021;137(13):1709-1711. doi:10.1182/blood.2020009603

46. Santagostino E, Mancuso ME, Tripodi A, et al. Severe hemophilia with mild bleeding phenotype: molecular characterization and global coagulation profile. *J Thromb Haemost*. 2010;8(4):737-743. doi:10.1111/J.1538-7836.2010.03767.X

47. Lim MY. How do we optimally utilize factor concentrates in persons with hemophilia? *Hematology*. 2021;2021(1):206-214. doi:10.1182/hematology.2021000310

48. Dargaud Y, Negrier C, Rusen L, et al. Individual thrombin generation and spontaneous bleeding rate during personalized prophylaxis with Nuwiq® (human-cl rhFVIII) in previously treated patients with severe haemophilia A. *Haemophilia*. 2018;24(4):619-627. doi:10.1111/hae.13493

49.   Valke LLFG, Bukkems LH, Barteling W, et al. Pharmacodynamic monitoring of factor VIII replace-
        ment therapy in hemophilia A: Combining thrombin and plasmin generation. *J Thromb Haemost*.
        2020;18(12):3222-3231. doi:10.1111/jth.15106

10

CHAPTER 11

Summary/Samenvatting
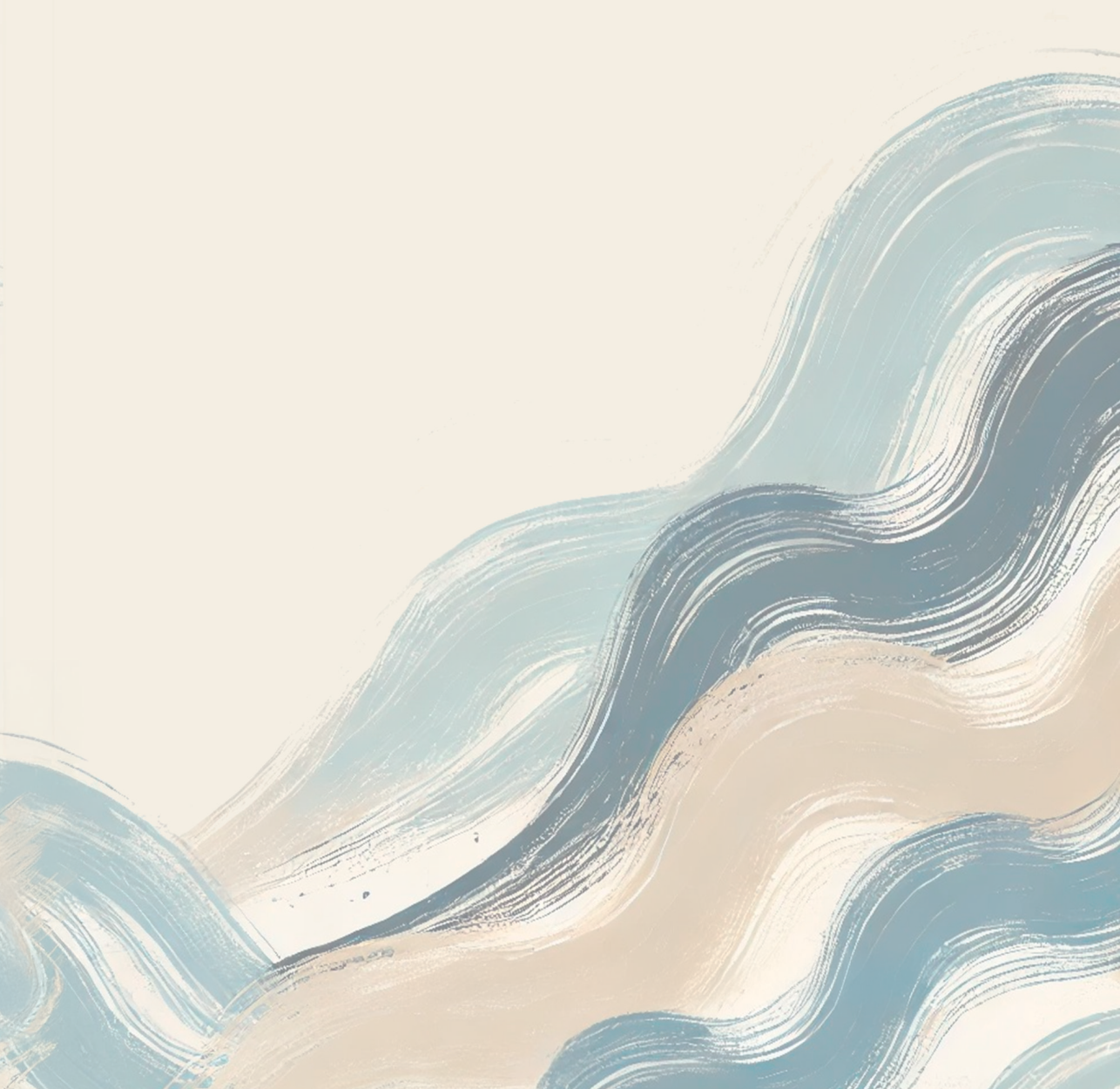
SUMMARY

The studies presented in this thesis focus on the treatment optimization of patients with inborn bleeding disorders, such as hemophilia and von Willebrand disease (VWD), by using various pharmacometric modelling techniques to personalize dosing

In **chapter 1**, we introduce the thesis content, outlining the dynamic use of pharmacometrics in the personalized treatment of inborn bleeding disorders. In pharmacometric analyses mathematical models are used to describe and predict drug behavior in the body. Hemophilia and VWD are inborn bleeding disorders characterized by deficiencies in specific coagulation factors. Hemophilia, particularly types A and B, involves deficiencies in factor VIII (FVIII) and factor IX (FIX), respectively, leading to bleeding episodes if not managed properly. VWD results from a deficiency or dysfunction of von Willebrand factor (VWF), essential for platelet adhesion and stabilization of factor VIII in the bloodstream. Low VWF levels increase the risk of prolonged bleeding and poor wound healing, complicating surgical procedures and leading to excessive blood loss.

Traditional treatments for these conditions involve regular administration of factor concentrates based on body weight to prevent bleeding. During surgical interventions, these concentrates are also used to ensure proper blood clotting. However, individual responses to these treatments vary widely due to genetic differences, pharmacokinetics (how the body absorbs, distributes, metabolizes, and excretes the drug), and other patient-specific factors. This variability necessitates a more personalized approach to treatment, achievable through pharmacometrics.

Besides applying traditional pharmacometric techniques to bleeding disorders, we also explore the integration of artificial intelligence (AI) to enhance model development and data analysis. Using AI can streamline the development process, improve the accuracy of pharmacometric models, and facilitate more effective personalization of treatment regimens. This thesis explores pharmacometrics across three parts: hemophilia, VWD, and the integration of AI in pharmacometrics.

11

Part I: Pharmacometrics in Hemophilia

The first part of this thesis focuses on the application of pharmacometrics in hemophilia, aiming to optimize and personalize treatment regimens. In **chapter 2**, the journey of exploring pharmacometrics in hemophilia begins with understanding the variability in patient responses to desmopressin, particularly in non-severe hemophilia A patients. This study employs a machine learning approach, specifically Shapley Additive Explanations (SHAP), to unravel the effects of F8 missense mutations on desmopressin response.

Data from 1,441 patients across multiple centers from the INSIGHT study revealed that specific F8 variants significantly influence FVIII peak levels post-desmopressin administration. By integrating various patient characteristics such as F8 variants, route of administration, and body weight, the study reduced response variability, highlighting the complexity of individual responses and the potential for tailored treatments based on genetic profiles.

Chapter 3 builds on the foundation of personalized treatment by using pharmacokinetic-pharmacodynamic modelling for FVIII replacement therapy. The study assesses the predictive performance of an existing model by examining its ability to relate FVIII doses to thrombin and plasmin generation parameters. Thrombin generation is a key step in the coagulation cascade, while plasmin generation is involved in clot breakdown or fibrinolysis. By dosing based on thrombin and plasmin generation levels, rather than solely on FVIII levels, we can better assess the overall hemostatic balance of the patient. Findings indicated the need for model refinement, particularly in predicting FVIII levels and plasmin generation. The refined model demonstrated improved accuracy.

Expanding the scope to hemophilia B, **chapter 4** introduces a physiologically-based pharmacokinetic model for recombinant FIX-Fc fusion protein (rFIXFc). The model predicts the concentration-time profiles and binding dynamics of rFIXFc to type IV collagen in the extravascular space. The findings of the study suggest that extravascular rFIXFc plays a crucial role in hemostasis, with significantly higher area under the curve values compared to plasma. This model provides a deeper understanding of rFIXFc distribution in the extravascular space.

Part II: Pharmacometrics in von Willebrand Disease

The second part of this thesis extends the application of pharmacometrics to von Willebrand disease (VWD), another inherited bleeding disorder. In **chapter 5**, the relationship between desmopressin dose, plasma concentration, and von Willebrand factor activity (VWF:Act) in type 1 VWD patients is quantified. Using a population pharmacokinetic-pharmacodynamic model, the study demonstrates that a one-compartment model best describes desmopressin kinetics, with increases in VWF:Act post desmopressin administration. The current dosing guidelines for desmopressin in VWD recommend an intravenous dose of 0.3 mcg/kg. Our study supports these guidelines and further suggests a dosing cap of 30 mcg in patients over 100 kg to prevent excessive dosing. The simulations provide evidence for effective desmopressin use in managing VWD and also indicate that the current guidelines are sufficient.

Further refining VWD treatment, **chapter 6** validates a previously developed population pharmacokinetic model for VWF:Act post desmopressin administration. Using an external dataset from the OPTICLOT/To-WiN study, the predictive performance of the model is evaluated. While the model showed adequate bias, precision was insufficient, particularly in patients with low baseline VWF:Act levels (<0.30 IU/mL). The implications of these model predictions suggest that patients with low baseline VWF:Act levels might experience over-prediction of VWF:Act response, potentially leading to suboptimal management of their condition. This validation underscores the necessity of desmopressin testing in clinical settings to ensure accurate VWF:Act predictions and effective treatment outcomes.

Continuing the exploration of VWF/FVIII concentrates, **chapter 7** investigates the reliability and feasibility of pharmacokinetic-guided dosing in VWD patients in the OPTICLOT/TO-WiN study. The study compares predicted and measured VWF:Act and FVIII levels, demonstrating that pharmacokinetic-guided dosing achieves target levels more precisely than bodyweight-based dosing. Despite some discrepancies, the findings support the potential for pharmacokinetic-guided dosing to enhance personalized treatment, though further data is needed to optimize dosing regimens fully.

Chapter 8 concludes part II by updating the previous pharmacokinetic model for VWF and FVIII in **chapter 7**. The updated model accurately describes time-dependent pharmacokinetic profiles post medical procedures of both VWF:Act and FVIII levels and the interaction between VWF:Act levels and FVIII clearance. This refined model enables individualized dosing regimens, enhancing treatment efficacy and supporting the dynamic use of pharmacometrics in managing VWD.

Part III: Applying Artificial Intelligence in pharmacometrics

The third and final part of this thesis explores the integration of artificial intelligence in pharmacometrics, highlighting its potential to aid in model development and data analysis in personalized medicine. In **chapter 9,** the use of ChatGPT in developing a population pharmacokinetic model for FVIII is examined. By using the language generation capabilities of ChatGPT, the study successfully obtains pharmacokinetic parameters, generates R code, and creates an interactive application. While highlighting the advantages of artificial intelligence in streamlining model development, the chapter also addresses challenges related to data accuracy and code transparency. This exploration underscores the potential of artificial intelligence in advancing pharmacometrics, albeit with careful consideration of its limitations.

11

Each chapter contributes uniquely to the overarching theme of utilizing pharmaco-metrics for personalized treatment in inherited bleeding disorders: **Chapters 2, 3, and 4 illustrate** the application of pharmacometrics in hemophilia, demonstrating how genetic and pharmacokinetic factors can inform individualized treatment regimens. **Chapters 5, 6, 7, and 8** extend these principles to VWD showcasing the refinement and validation of pharmacokinetic-pharmacodynamic models to enhance treatment precision and efficacy. **Chapter 9** introduces the innovative use of AI, exemplifying how artificial intelligence can improve pharmacometric research and model development. Collectively, these chapters illustrate the advancement of personalized medicine via dynamic pharmacometric approaches, with the goal of improving clinical outcomes for patients with inherited bleeding disorders.

SAMENVATTING

De studies gepresenteerd in dit proefschrift richten zich op de optimalisatie van de behandeling van patiënten met aangeboren bloedingstollingsstoornissen, zoals hemofilie en de ziekte van von Willebrand (VWD), door het gebruik van verschillende farmacometrische modelleertechnieken om de dosering te personaliseren.

In **hoofdstuk 1** introduceren we de inhoud van het proefschrift, waarin het dynamisch gebruik van farmacometrie om de behandeling van erfelijke bloedingsstoornissen te personaliseren wordt beschreven. Farmacometrie maakt gebruik van wiskundige modellen om het verloop van de concentratie van het gebruikte medicijn en het bij behorende effect in het lichaam te beschrijven en te voorspellen. Hemofilie en VWD zijn aangeboren bloedstollingsstoornissen die ontstaan door een tekort aan specifieke stollingsfactoren. Hemofilie A en B worden veroorzaakt door respectievelijk een tekort aan factor VIII (FVIII) en factor IX (FIX). Dit leidt tot (spontane) bloedingen doordat het lichaam niet in staat is tot adequate stolling. VWD wordt veroorzaakt door een tekort of defect van von Willebrand factor (VWF). VWF is essentieel voor de plaatjesadhesie en aggregatie en stabilisatie van factor VIII in de bloedbaan. Lage VWF-spiegels leiden ook tot bloedingen, wat chirurgische ingrepen compliceert en leidt tot overmatig bloedverlies indien niet adequaat behandeld.

Traditionele behandelingen voor deze bloedstollingsstoornissen bestaan uit regelmatige toedieningen van stollingsfactorconcentraten of desmopressine op basis van lichaamsgewicht om bloedingen te voorkomen. Dit kan preventief of profylactisch worden gedaan, dan wel acuut (on demand) rondom bloedingen of ter preventie van bloedingen rondom medische ingrepen. De concentraties in het bloed na toediening variëren echter sterk door verschillen in diverse bekende en onbekende patiënt karakteristieken, waaronder farmacokinetiek een belangrijke is. Farmacokinetiek is gedefinieerd als hoe het lichaam het geneesmiddel absorbeert, distribueert, metaboliseert en uitscheidt. Deze variabiliteit vereist een meer gepersonaliseerde benadering van de behandeling, waarbij farmacometrie kan worden toegepast om de relatie tussen dosis, concentratie en effect (en de variatie daarin tussen patiënten) te kwantificeren.

11

Naast het toepassen van traditionele farmacometrische technieken op bloedstollingsstoornissen, onderzoeken we in onze studies ook de integratie van kunstmatige intelligentie (AI) om de farmacometrische modelontwikkeling en data-analyse te verbeteren. Het gebruik van AI kan het ontwikkelingsproces stroomlijnen, de nauwkeurigheid van modellen verbeteren en een effectievere personalisatie van behandelingsregimes mo-

gelijk maken. Dit proefschrift verkent de toepassing van farmacometrie in drie gebieden: bij behandeling van hemofilie en VWD en met de integratie van AI.

Deel I: Farmacometrie in hemofilie

Het eerste deel van dit proefschrift richt zich op de toepassing van farmacometrie in hemofilie, met als doel behandelingsregimes te optimaliseren en personaliseren. In **hoofdstuk 2** wordt farmacometrie gebruikt om de variabiliteit tussen patiënten m.b.t. desmopressine respons zoals gemeten d.m.v. factor VIII (en VWF) waardes te beschrijven en begrijpen, met name bij patiënten niet-ernstige hemofilie A. Deze studie maakt gebruik van een specifieke machine learning-techniek, Shapley Additive Explanations (SHAP), om de effecten van F8-missense varianten op de respons van desmopressine te begrijpen. Gegevens van 1441 patiënten uit meerdere centra toonden aan dat specifieke F8-varianten significant van invloed zijn op de piek spiegels van factor VIII na toediening van desmopressine. Door verschillende patiëntkenmerken zoals F8-varianten, toedieningsroute en lichaamsgewicht te includeren, konden wij de variabiliteit in respons deels verklaren.

Hoofdstuk 3 bouwt hierop voort door gebruik te maken van farmacokinetisch-farmacodynamisch modelleren van een standard halfwaarde tijd (SHL) factor VIII concentraat. In deze studie werd het vermogen om met een bestaand model, de factor VIII-doses te relateren aan trombine- en plasminogeen parameters in het bloed gemeten d.m.v. een specifieke test, onderzocht. De generatie van trombine is een cruciale stap in het bloedstollingsproces, terwijl plasminogeen betrokken is bij het afbreken van bloedstolsels tijdens de fibrinolyse. Door te doseren op basis van trombine- en plasminogeenwaarden in plaats van alleen op factor VIII-spiegels, kan hypothetisch de algehele hemostatische balans van de patiënt beter beoordeeld worden. De bevindingen van deze analyse gaven aan dat verbetering van het model nodig was, met name m.b.t. het voorspellen van factor VIII-spiegels en plasminogeen. Een nieuw ontwikkeld model beschreef de relaties nauwkeuriger.

In **hoofdstuk 4** is een fysiologisch gebaseerd farmacokinetisch model ontwikkeld voor recombinant FIX-Fc fusie-eiwit (rFIXFc) dat gebruikt wordt voor de behandeling van hemofilie B. Het model voorspelt de concentratie-tijdprofielen en bindingsdynamiek van rFIXFc aan type IV-collageen in de extravasculaire ruimte. De bevindingen van de studie suggereren dat extravasculair rFIXFc een cruciale rol speelt in hemostase, met aanzienlijk hogere concentraties en dus blootstelling in de extravasculaire ruimte in vergelijking met plasma. Dit model biedt meer inzicht in de distributie van rFIXFc in het lichaam en het belang van de extravasculaire ruimte bij de hemostase.

Deel II: Farmacometrie in de ziekte van von Willebrand

In het tweede deel van deze thesis wordt farmacometrie toegepast bij onderzoek in patiënten met VWD. In **hoofdstuk 5** wordt de relatie tussen dosering van desmopressine, de concentratie in plasma en von Willebrand factor activiteit in bloed (VWF:Act) bij type 1 VWD-patiënten gekwantificeerd. Met behulp van een populatie farmacokinetisch-farmacodynamisch model toont de studie aan dat een één-compartimentmodel het beste de farmacokinetiek van desmopressine beschrijft, weergegeven als een stijging van VWF:Act activiteit na toediening van desmopressine. De huidige doseringsrichtlijnen voor desmopressine bij VWD adviseren een intraveneuze dosis van 0,3 mcg/kg. Onze studie ondersteunt deze richtlijnen en suggereert verder dat een doseringslimiet van 30 mcg bij patiënten met een lichaamsgewicht boven de 100 kg kan worden gehanteerd om overdosering te voorkomen. De simulaties onderbouwen dit meer effectievere gebruik van desmopressine bij de behandeling van VWD en geven ook aan dat de huidige richtlijnen adequaat zijn.

Hoofdstuk 6 beschrijft de validatie van een eerder ontwikkeld populatie farmacokinetisch model voor VWF spiegels (<0,30 IU/mL). Op basis van deze modelvoorspellingen kan gesteld worden dat voor patiënten met lagere baseline VWF:Act spigels mogelijk een te hoge VWF:Act respons wordt voorspeld, wat kan leiden tot suboptimale behandeling. Deze validatie onderstreept de noodzaak van het testen van de desmopressine respons in de kliniek om nauwkeurige VWF:Act voorspelling en effectieve behandeling te kunnen waarborgen.

In het volgende **hoofdstuk 7** wordt prospectieve OPTICLOT/TO-WiN studie beschreven waarin de betrouwbaarheid en haalbaarheid van farmacokinetisch gestuurd doseren van een VWF/FVIII concentraat wordt onderzocht bij VWD-patiënten. In deze studie worden de voorspelde en gemeten VWF:Act en FVIII speigels vergeleken, waarbij blijkt dat door toepassing van farmacokinetisch gestuurd doseren de streefwaarden nauwkeuriger worden bereikt dan door dosering op basis van lichaamsgewicht. Ondanks enkele discrepanties ondersteunen de bevindingen dat farmacokinetisch gestuurd doseren de potentie heeft om een meer gepersonaliseerde behandeling te bewerkstelligen. Echter, verdere studies nodig zijn om de doseringsregimes volledig te optimaliseren.

11

Deel II wordt afgesloten met **hoofdstuk 8** waarin het eerder gepubliceerde farmacokinetische model voor VWF:Act en FVIII wordt herzien en uitgebreid met nieuwe gegevens uit de OPTICLOT/To-WiN studie zoals beschreven in **hoofdstuk 7**. Het herziene model beschrijft nauwkeurig de tijdsafhankelijke farmacokinetiek van VWF en FVIII en de relatie tussen de VWF:Act spiegel in het bloed en de FVIII klaring. Dit verfijnde model

verbetert de geïndividualiseerde doseringsregimes en is een voorbeeld van de toepassing van farmacometrie bij optimalisatie van behandeling van patiënten met VWD.

Deel III: Kunstmatige Intelligentie in de farmacometrie

In het derde en laatste deel van deze thesis wordt de integratie van kunstmatige intelligentie in farmacometrie verkent, waarbij de potentiële voordelen voor ontwikkeling van modellen en analyse van data worden benadrukt. In **hoofdstuk 9** wordt het gebruik van ChatGPT bij de ontwikkeling van een populatie farmacokinetisch model voor FVIII onderzocht. Door gebruik te maken van de taalgeneratiecapaciteiten van ChatGPT, worden succesvol farmacokinetische parameters uit de literatuur verkregen, worden R-code gegenereerd en een interactieve applicatie gecreëerd. De voordelen van kunstmatige intelligentie bij het stroomlijnen van modelontwikkeling worden in het hoofdstuk benadrukt, maar ook de uitdagingen met betrekking tot gegevensnauwkeurigheid en codetransparantie worden genoemd. Deze verkenning onderstreept het potentieel van toepassing van kunstmatige intelligentie binnen de farmacometrie.

Elk hoofdstuk draagt op een unieke manier bij aan het overkoepelende thema van dit proefschrift: het gebruik van farmacometrie voor gepersonaliseerde behandeling bij de aangeboren bloedstollingsstoornissen. **Hoofdstukken 2, 3 en 4** illustreren de toepassing van farmacometrie in hemofilie, waarbij wordt aangetoond hoe genetische en farmacokinetische factoren geïndividualiseerde behandelingsregimes kunnen informeren. In de **hoofdstukken 5, 6, 7 en 8** worden farmacometrische principes uitgebreid naar VWD, waarbij farmacokinetisch-farmacodynamische modellen worden verfijnd en gevalideerd met als doel de precisie en effectiviteit van de behandeling te verbeteren. **Hoofdstuk 9** introduceert het innovatieve gebruik van kunstmatige intelligentie, waarbij wordt aangetoond hoe kunstmatige intelligentie farmacometrisch onderzoek en modelontwikkeling kan aanvullen.

In zijn totaal, illustreren de hoofdstukken in dit proefschrift de vooruitgang van gepersonaliseerde behandeling via dynamische farmacometrische benaderingen, met als doel het verbeteren van behandelingen voor patiënten met aangeboren bloedingstollingsstoornissen.

APPENDICES
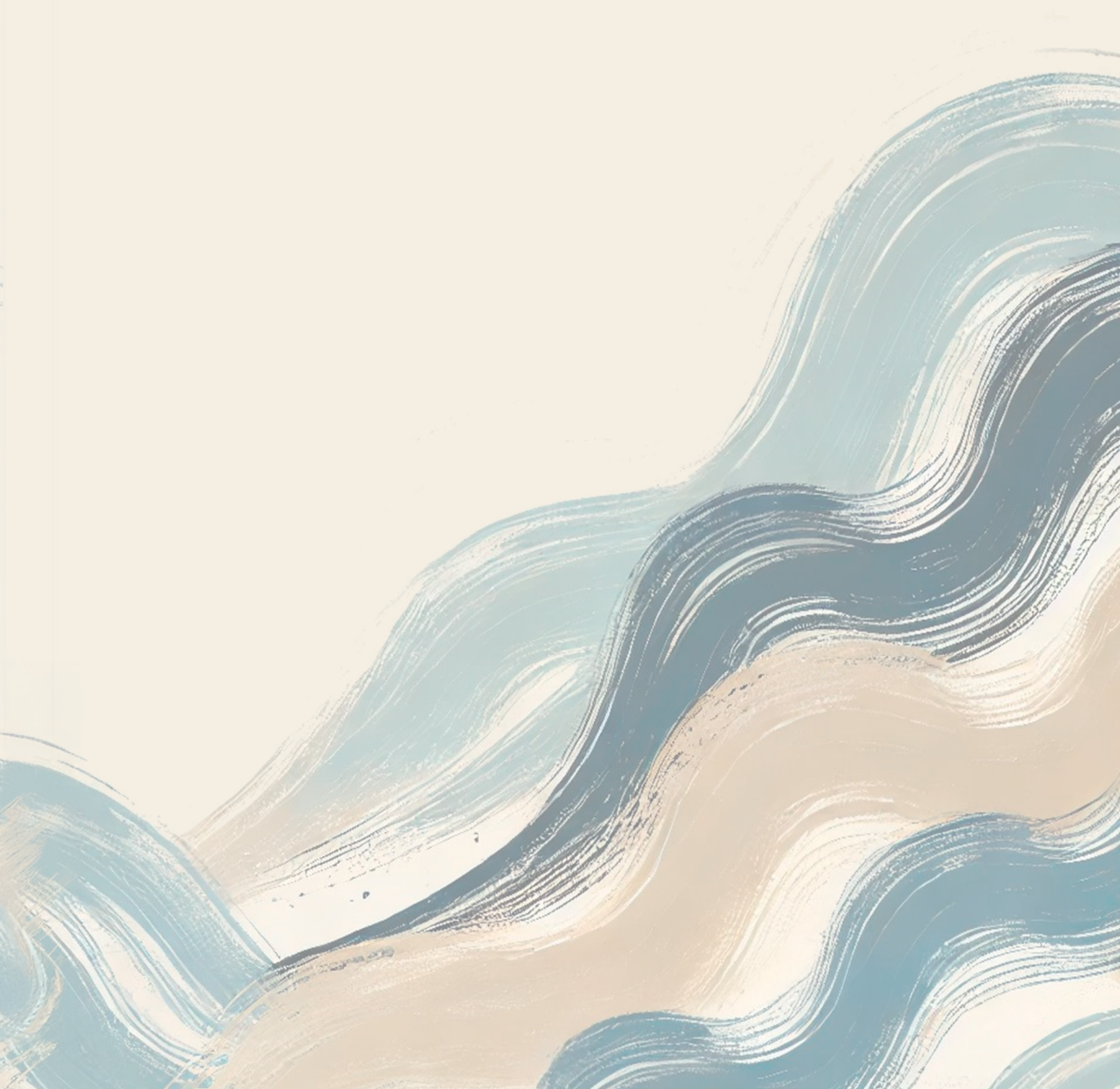
LIST OF PUBLICATIONS

This thesis

Cloesmeijer ME, Janssen A, Koopman SF, Cnossen MH, Mathôt RAA; SYMPHONY consortium. ChatGPT in pharmacometrics? Potential opportunities and limitations. Br J Clin Pharmacol. 2024 Jan;90(1):360-365. doi: 10.1111/bcp.15895. Epub 2023 Sep 6. PMID: 37621112.

Heijdra JM, **Cloesmeijer ME**, de Jager NCB, Leebeek FWG, Kruip MHJA, Cnossen MH, Mathôt RAA; OPTI-CLOT/ To WiN study group and SYMPHONY consortium. Quantification of the relationship between desmopressin concentration and Von Willebrand factor in Von Willebrand disease type 1: A pharmacodynamic study. Haemophilia. 2022 Sep;28(5):814-821. doi: 10.1111/hae.14582. Epub 2022 May 8. PMID: 35526239.

Cloesmeijer ME, Sjögren E, Koopman SF, Lenting PJ, Cnossen MH, Mathôt RAA; OPTI-CLOT study group and SYMPHONY consortium. PBPK modeling of recombinant factor IX Fc fusion protein (rFIXFc) and rFIX to characterize the binding to type 4 collagen in the extravascular space. CPT Pharmacometrics Syst Pharmacol. 2024 Sep 16. doi: 10.1002/psp4.13159. Epub ahead of print. PMID: 39285704.

Valke LLFG, **Cloesmeijer ME**, Mansouritorghabeh H, Barteling W, Blijlevens NMA, Cnossen MH, Mathôt RAA, Schols SEM, van Heerde WL. Pharmacokinetic-Pharmacodynamic Modelling in Hemophilia A: Relating Thrombin and Plasmin Generation to Factor VIII Activity After Administration of a VWF/FVIII Concentrate. Eur J Drug Metab Pharmacokinet. 2024 Mar;49(2):191-205. doi: 10.1007/s13318-024-00876-6. Epub 2024 Feb 17. PMID: 38367175; PMCID: PMC10904421.

Cloesmeijer ME, del Castillo Alferez J, Janssen A, Loomans J, van Hest RM, Cnossen MH, Mathôt RAA; SYMPHONY consortium. The effects of F8 missense variants on desmopressin response in non-severe hemophilia A patients investigated using machine learning.

Cloesmeijer ME, Al Arashi W, Heijdra JM, Leebeek FWG, Nieuwhuizen L, Moenen FCJI, Cnossen MH, Mathôt RAA; SYMPHONY consortium. Predictive performance of a population pharmacokinetic model of desmopressin response to assess the necessity of desmopressin testing in von Willebrand disease.

Al Arashi W, **Cloesmeijer ME**, Leebeek FWG, Nieuwhuizen L, Moenen FCJI, Meijer K, Cnossen MH, Mathôt RAA; SYMPHONY consortium. Personalizing treatment by pharma-

cokinetic-guided dosing of factor concentrates in von Willebrand disease: A prospective multicenter study (OPTI-CLOT/To WiN).

Cloesmeijer ME, Al Arashi W, Heijdra JM, Leebeek FWG, Nieuwhuizen L, Moenen FCJI, Meijer K, Cnossen MH, Mathôt RAA; SYMPHONY consortium. A novel population pharmacokinetic model for the von Willebrand factor-factor VIII interaction for von Willebrand patients requiring replacement therapy for medical procedures. I

Other

Heijdra JM, Al Arashi W, de Jager NCB, **Cloesmeijer ME**, Bukkems LH, Zwaan CM, Leebeek FWG, Mathôt RAA, Cnossen MH; OPTI-CLOT Study Group. Is pharmacokinetic-guided dosing of desmopressin and von Willebrand factor-containing concentrates in individuals with von Willebrand disease or low von Willebrand factor reliable and feasible? A protocol for a multicentre, non-randomised, open label cohort trial, the OPTI-CLOT: to WiN study. BMJ Open. 2022 Feb 15;12(2):e049493. doi: 10.1136/bmjopen-2021-049493. PMID: 35168962; PMCID: PMC8852670.

Cloesmeijer ME, van den Oever HLA, Mathôt RAA, Zeeman M, Kruisdijk-Gerritsen A, Bles CMA, Nassikovker P, de Meijer AR, van Steveninck FL, Arbouw MEL. Optimising the dose of clonidine to achieve sedation in intensive care unit patients with population pharmacokinetics. Br J Clin Pharmacol. 2020 Aug;86(8):1620-1631. doi: 10.1111/bcp.14273. Epub 2020 Mar 29. PMID: 32150285; PMCID: PMC7373711.

Cloesmeijer ME, van Esdonk MJ, Lynn AM, Smits A, Tibboel D, Daali Y, Olkkola KT, Allegaert K, Mian P. Impact of enantiomer-specific changes in pharmacokinetics between infants and adults on the target concentration of racemic ketorolac: A pooled analysis. Br J Clin Pharmacol. 2021 Mar;87(3):1443-1454. doi: 10.1111/bcp.14547. Epub 2020 Oct 9. PMID: 32901947; PMCID: PMC9328374.

PHD PORTFOLIO

M.E. Cloesmeijer
PhD period: April 2020 – April 2024
PhD supervisors: prof.dr. R.A.A. Mathôt
prof. dr. M.H. Cnossen

General courses	Year	EC
The Amsterdam UMC World of Sciences	2020	0.7
Practical Biostatistics	2020	1.4
Advanced Topics in Biostatistics	2022	2.1
BROK (basis cursus regelgeving klinisch onderzoek)	2022	1.5
Scientific writing	2021	1.5
Project management	2022	0.6
Workshops	**Year**	**EC**
Simcyp Focused Workshop: Biologics	2021	3.0
Educational Pharmacometrics Summer Symposium	2023	0.3
(Inter)national conferences	**Year**	**EC**
Pharmacometrics Benelux Network meeting (PNB) (3x)	2022-2023	0.5
European Association of Haemophilia and Allied disorders congress (EAHAD) (3x)	2021-2023	2.0
International Society on Thrombosis and Haemostasis congress (ISTH) (2x)	2021-2022	2.0
Population Approach Group Europe congress (PAGE) (3x)	2021-2023	1.8
Voorjaarsdag Nederlandse Vereniging voor Klinische Farmacologie en Biofarmacie (NVKFB)	2023	0.5
Figon: The Dutch Medicines Days (DMD)	2023	0.5
Poster presentations	**Year**	**EC**
Quantifying the Concentration-effect Relation of Desmopressin on the von Willebrand Factor Activity in Patients with von Willebrand Disease (PAGE)	2021	0.5
Physiologically-based pharmacokinetic modelling of recombinant factor IX Fc fusion protein (rFIXFc) and recombinant FIX (rFIX) to characterize extravasation and binding to type 4 collagen (PAGE)	2023	0.5
Pharmacokinetic-pharmacodynamic modelling in hemophilia A: relating thrombin and plasmin generation to factor VIII activity after administration of VWF/FVIII (NVKFB)	2023	0.5
Oral presentations	**Year**	**EC**
Quantifying the Concentration-effect Relation of Desmopressin on the von Willebrand Factor Activity in Patients with von Willebrand Disease (ISTH)	2020	0.5
The effect of F8 missense mutation and route of administration on desmopressin response in nonsevere hemophilia A using population PK modelling. (EAHAD)	2023	0.5
Pharmacokinetic-pharmacodynamic modelling in hemophilia A: relating thrombin and plasmin generation to factor VIII activity after administration of VWF/FVIII (NVKFB)	2023	0.5
Physiologically-based pharmacokinetic modelling of recombinant factor IX Fc fusion protein (rFIXFc) and recombinant FIX (rFIX) to characterize extravasation and binding to type 4 collagen (FIGON)	2023	0.5

Appendices

Other	Year	EC
NONMEM monthly meeting	2020-2024	3.0
SYMPHONY/OPTICLOT bimonthly meeting	2020-2024	3.0
SYMPHONY yearly General Assembly	2020-2024	0.3
Supervising	**Year**	**EC**
Master student: Development of a population pharmacokinetic model of Von Willebrand Factor activity after IV/SC desmopressin treatment in Von Willebrand Disease patients.	2023-2024	1.0

DANKWOORD

Na vier jaar promotieonderzoek voelt het vreemd om dit hoofdstuk van mijn leven af te sluiten. Het waren jaren vol pieken- en dalen, maar vooral met veel pieken. Ik ben enorm dankbaar voor de kans om onderzoek te doen binnen het vakgebied dat mijn grootste interesse heeft. Ik ben trots op het resultaat dat dit proefschrift mag zijn geworden, evenals op de waardevolle samenwerkingen die de verschillende projecten mogelijk hebben gemaakt. Allereerst wil ik de patiënten bedanken voor hun deelname aan de studies. Zonder jullie betrokkenheid was dit proefschrift nooit tot stand gekomen.

Beste **Ron, prof. dr. Mathôt,** in 2018 kwam ik bij jou voor het eerst aan als master-student. Je was al opzoek naar een stagair voor project over farmacokinetiek van clonidine. Met veel enthousisme en plezier heb ik mijn stage bij jou afgerond en 2 jaar later begon ik bij jou als promovendi onder het SYMPHONY consortium. Het begin van mijn PhD-traject was apart. Het was middenin corona tijdperk en we mochten niet of minimaal op locatie werken. Desondanks is alles toch goed gekomen. In deze jaren heb ik veel geleerd. Ik waardeer enorm alle tijd die je ingestoken hebt in mij. Oprecht vond ik heel fijn dat je altijd klaarstond voor mij. Dat ik altijd tussendoor nog even een meeting kan inplannen. Of als het niet helemaal ging volgens mijn plan, wist je toch mij doorheen te staan door jouw optisme.

Beste, **Marjon, prof. dr. Cnossen**, Ik herinner me nog goed de eerste keer dat we elkaar ontmoetten tijdens de SYMPHONY-sollicitaties. Ik kreeg meteen de indruk dat je een open en warm persoon was, en die indruk bleek gedurende mijn PhD-traject volledig te kloppen. Hoewel we elkaar door de omstandigheden, zoals de coronapandemie en mijn werkplek in Amsterdam, niet altijd regelmatig in persoon zagen, wist ik altijd dat ik je kon bereiken wanneer dat nodig was. Bedankt voor je steun gedurende deze periode. Ik heb veel geleerd van jouw klinische expertise. Soms voelt modelleren als een reeks cijfers en complexe berekeningen, maar jouw klinische kennis zorgde ervoor dat mijn modellen een duidelijke klinische relevantie kregen.

Graag wil ik de commissie, **prof. dr. Touw, prof. dr. van Hasselt, prof. dr. Dijkgraaf, prof. dr. Fijnvandraat, prof. dr. Meijers, dr. van Hest,** bedanken voor het beoordelen van mijn manuscript.

Assos. Prof. dr. Erik Sjorgen, thank you for the collaboration on the PBPK factor IX project! I always had an interest in applying PBPK modelling. I learned a lot of PBPK modelling using PK-Sim because of you. I appreciate all the time you dedicated to this project.

Aan de **Ronderzoekers, Laura, Amadou, Steffie, Alex en Sjoerd**, hoewel we in ons hok helaas (toen) geen direct zonlicht hadden, was het altijd gezellig met jullie. Bedankt voor alle waardevolle discussies, de leuke conferentiereizen, en vooral ook voor het geduld om naar mijn geklaag over van alles en nog wat te luisteren. Bedankt ook aan alle apothekers van Amsterdam UMC voor de mooie tijd die we hebben doorbracht. Ook aan de andere kant van de Amstel, **Medhat**. Dank je voor al onze interessante pharmacometrics discussies! Heel veel succes met het afronden van jouw PhD!

I would also like to thank all the members of the SYMPHONY consortium, it was nice to hear all the different disciplines within bleeding disorders, and not just PK-PD modelling of bleeding disorders. It even led to a very nice collaboration with **Jessica del Castillo**. Thank you for the nice collaboration we had with the RISE study!

Daarnaast wil ik alle andere OPTI-CLOTTERS, **Lorenzo, Jessica, Tine, Caroline,** en **Wala**, hartelijk bedanken voor de fijne samenwerking en de tweemaandelijkse meetings. Wala, bedankt voor jouw harde inzet in de To-WiN studie. Zonder jou, hadden we nooit zoveel patienten kunnen includeren. Succes met het afronden van jouw PhD!

Lars, dank voor de fijne samenwerking. Nadat Laura haar PhD had afgerond, heb ik het stokje van haar overgenomen om het PK-PD model verder uit te werken. Het was een groot plezier om samen aan dit project te werken en ons artikel hierover te publiceren.

Ik wil ook een aantal mensen bedanken voor mijn PhD traject, waardoor ik in staat was om waardevolle ervaring op te bouwen in pharmacometrics en dat ook verder toe te passen in mijn PhD.

Paola, jij hebt me voor het eerst laten kennismaken met NONMEM en R. Hoewel ik met beide programma's nog nooit had gewerkt, had ik de motivatie om ze te leren. Dankzij jouw begeleiding werd mijn eerste masterproject zelfs gepubliceerd. Bedankt dat je me de kans gaf om zelfstandig een manuscript te schrijven en te publiceren!

Beste **Huub, Maurits,** bedankt dat ik mijn tweede masterstage bij jullie mocht doen. Het was een mooie samenwerking tussen het Deventer Ziekenhuis en Amsterdam UMC, samen met Ron. Ik ben erg blij met het resultaat en dat ik mijn eerder opgedane kennis kon toepassen binnen jullie project. Dit project is ook gepubliceerd, en ik ben jullie dankbaar dat jullie mij de kans hebben gegeven om dit te mogen doen!

Also, thanks to my FFXIV static, and especially my raid buddies **Oulan, Kou, Kami, Leb**. Thank you for getting through the corona time during my PhD, where I was able to some

other focus beside my PhD. Instead, we had weeklong frustrations at each savage tier. Thank you for all the fun times before and let's do another savage tier in future!

Anushka, mijn basisschool vriendin sinds groep 1-2. Ons eerste baantje was een krantenwijk die we samen gingen doen en aan het einde van het jaar gingen we met onze "nieuwjaarskaartjes" langs de deuren. Ik denk dat mensen ons vooral geld gaven omdat niemand echt interesse had in onze drie minuten durende nieuwjaarswensen… Nu, bijna twintig jaar later, ziet ons werk er heel anders uit. Dank je wel voor je steun tijdens mijn PhD en voor alle videocalls die we hadden tijdens mijn pauzes.

Aja, we kennen elkaar al 20+ jaar. Het begon op het Comenius College en daarna zijn we ook samen naar het Libanon Lyceum gegaan om het VWO te doen en uiteindelijk zijn we ook terecht gekomen om in Amsterdam te wonen. We hebben zoveel meegemaakt in de afgelopen jaren, vooral al onze food tours. Het begon al op de middelbare school dat we naar Londen gingen, speciaal om te eten. Bedankt voor al je steun, alle gezellige reisjes en vriendschap van de afgelopen jaren!

Anouk, we kennen elkaar al sinds het Libanon Lyceum. Samen met Aja hadden we altijd onze food tours, en niet voor niets heet onze WhatsApp-groep "De eetclub." Ook tijdens de (korte) periode dat je op het AMC was, bracht je altijd gezelligheid met je mee. Dank je wel voor je vriendschap en de vele fijne gesprekken.

Arwin, Priscilla, mijn BFW maatjes. Zonder jullie zou mijn studietijd een stuk minder leuk zijn geweest. Het is maar goed dat ik (heel awkward) op de tweede(?) dag naast jullie kwam zitten. Vanaf dat moment gingen we vaak samen buiten eten, en het werd onze traditie om na elk tentamen een etentje te plannen. Ons studentenleven draaide eigenlijk om de vraag: "Waar gaan we nu eten?" Dankzij jullie heb ik mijn studietijd echt doorstaan, inclusief al die treinreizen met vertraging of annulering.

Niesha dank je dat jij mijn paranimf wilde zijn voor deze speciale dag. Dankje dat ik altijd bij jou voor alles terecht kan komen en voor alle leuke lunch trips naar Belgie en PH, 5G, TB, BK etc.

Wing bedankt dat jij mijn andere paranimf wilde worden, ondanks je nu helemaal in het noorden van Duitsland woont. Nog even en dan ben jij ook klaar met jouw PhD! Dank je dat je altijd klaar voor me stond.

Lieve, **Zuster Gretha,** u kent mij vanaf mijn geboorte al en u heeft zoveel betekend voor onze familie. Ik ben u enorm dankbaar voor alles wat u voor ons heeft gedaan,

Lieve **zus** en ook jouw gezin, **Tim, Jazz en Noa.** Dank je voor alle steun tijdens mijn PhD. Dit is nou uiteindelijk het resultaat waar ik al die jaren aan heb gewerkt! Wie had ooit gedacht dat ik hier zou staan. Ondanks onze twee heel verschillende persoonlijkheden, hebben we altijd veel begrip voor elkaar, en dat brengt ons dichterbij. Ik ben zo dankbaar dat jij mijn zus bent!

Lieve **papa**, helaas kon je niet heel aanwezig zijn bij ons, desondanks heb je veel invloed op ons gebracht. Zonder jou kon ik dit allemaal nooit bereiken. Bedankt voor alles.

Lieve **mama**, ik heb veel respect voor hoe je ons hebt opgevoed. Door jouw steun en hulp heb ik mezelf kunnen ontwikkelen, en zonder jou had ik nooit gestaan waar ik nu sta. Ik ben je ontzettend dankbaar voor alles wat je voor ons hebt gedaan. Bedankt dat je altijd zo'n zorgzame en liefdevolle moeder bent geweest.

Special mention to **Rhea**, thank you for your emotional support. With our similar shared hobbies, we understand each other perfectly. Thank you, my partner, **Mahir.** Thank you for supporting me through everything. Both in the ups and downs of my PhD and also personally. Even when I doubt myself, you continue to believe in me and my abilities. I feel incredibly fortunate to have you by my side. I am looking forward to doing all the amazing adventures and journeys that lie ahead of us.

ABOUT THE AUTHOR

Michael Cloesmeijer (1992) was born and raised in Rotterdam. After he completed his secondary education, earning his VWO diploma, he pursued a bachelor's and master's degree in Bio-Pharmaceutical Sciences at Leiden University. During his master's studies, he developed an interest in pharmacometrics and clinical pharmacology, leading him to undertake two research internships in this research area. His projects focused on the enantiomer-specific pharmacokinetics in infants versus adults and optimizing clonidine dosing for sedation in intensive care unit patients using population pharmacokinetics.

With a growing interest for clinical pharmacology and pharmacometrics, he sought to advance his expertise in the field by enrolling as a PhD student at the Amsterdam UMC under the supervision of Prof. Dr. R.A.A. Mathôt and Prof. Dr. M.H. Cnossen, as part of the SYMPHONY consortium. During his PhD, he further developed his skills in pharmacometrics modelling, focusing on optimizing therapeutic outcomes in bleeding disorders.

Following the completion of his PhD and gaining several years of experience in clinical pharmacology and pharmacometrics, he transitioned to the field of preclinical pharmacology. He joined Genmab as a quantitative translational pharmacology scientist, where he focuses on modelling to support first-in-human dosage decisions.